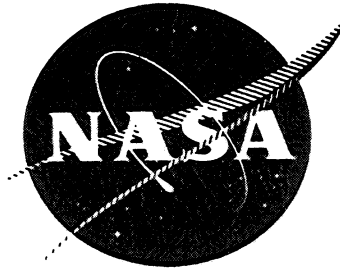


N71-25460

NASA CR-82862

GE R71 AEG 149



TASK IV STAGE DATA AND PERFORMANCE REPORT

FOR

CASING TREATMENT INVESTIGATIONS

VOLUME I

EVALUATION OF RANGE AND DISTORTION TOLERANCE FOR HIGH MACH NUMBER TRANSONIC FAN STAGES

By

W.A. Tesch

GENERAL ELECTRIC COMPANY
Aircraft Engine Group
Cincinnati, Ohio 45215

CASE FILE
COPY

Prepared For

NATIONAL AERONAUTICS AND SPACE ADMINISTRATION

May, 1971

NASA Lewis Research Center
Contract NAS3-11157
Charles H. Voit Project Manager

TASK IV STAGE DATA AND PERFORMANCE REPORT

FOR

CASING TREATMENT INVESTIGATIONS

VOLUME I

**EVALUATION OF RANGE AND DISTORTION TOLERANCE
FOR HIGH MACH NUMBER TRANSONIC FAN STAGES**

By

W.A. Tesch

GENERAL ELECTRIC COMPANY

Aircraft Engine Group

Cincinnati, Ohio 45215

Prepared For

NATIONAL AERONAUTICS AND SPACE ADMINISTRATION

May, 1971

NASA Lewis Research Center

Contract NAS3-11157

Charles H. Voit Project Manager

ABSTRACT

Two high-tip-speed compressor stages were tested with various rotor tip casing treatment configurations under conditions of undistorted inlet flow, tip-radial distortion and circumferential distortion. The first stage consisted of a 1400 ft/sec tip speed medium-aspect-ratio rotor plus a stator vane row; the second stage had a 1500 ft/sec tip speed medium-aspect-ratio rotor and a stator vane row. This second stage was tested both with and without zero-turning inlet guide vanes. Overall performance and stall margin were determined for each stage configuration and inlet condition at 70, 90, and 100% of design speed. Extensive surveys of flow conditions were made for the case of circumferential distortion. In addition, blade element data were obtained when testing with undistorted and radial distortion inlet conditions.

Undistorted inlet tests of the 1400 ft/sec tip speed stage indicated an increase in design speed stall margin from 0.213 to values ranging from 0.255 to 0.290 with the addition of casing treatment. The circumferential-grooves casing treatments, which gave 0.04 to 0.05 improvements in stall margin, had less than one point in efficiency penalty; the skewed-slots casing treatments gave some of the largest stall margin gains (0.077) with an efficiency penalty of less than two percentage points. With the zero-turning inlet guide vanes installed, the 1500 ft/sec tip speed stage design speed stall margin rose from 0.129 to 0.320 with the inclusion of the blade-angle-slots casing treatment. Similar stall margin gains were obtained with the inlet guide vanes deleted.

Volume I contains the techniques and procedure used to acquire the data and an analysis and discussion of the test results; Volume II, NASA CR-82867, contains tabulations of blade element and circumferential distortion flow survey data.

LIST OF ILLUSTRATIONS

<u>Figure</u>		<u>Page</u>
1 (a)	Honeycomb Casing Treatment Used In The Task IV Program.	87
1 (b)	Circumferential-Grooves Casing Treatment Configurations Used In The Task IV Program.	88
1 (c)	Skewed-Slot Casing Treatment Configurations Used In The Task IV Program.	89
1 (d)	Blade-Angle-Slot Casing Treatment Configurations Used In The Task IV Program.	90
2	Meridional Sectional View of Task II Stage Test Vehicle.	91
3	Schematic Diagram of House Compressor Test Facility.	92
4 (a)	Tip-Radial Distortion Screen.	93
4 (b)	Circumferential Distortion Screen.	94
5 (a)	Meridional View Showing Instrumentation Locations.	95
5 (b)	Circumferential Development Showing Instrumentation Locations.	96
6	Fixed and Traverse Instrumentation Used In The Task IV Program.	97
7	Relationship Between Flow Function and Meridional Mach No. Used For Transferring Traverse Measurements To Blade Edges.	99
8 (a)	Task I Stage Undistorted Inlet Performance Map; Honeycomb #1 Casing Treatment.	100
8 (b)	Task I Stage Undistorted Inlet Performance Map; Honeycomb #2 Casing Treatment.	101
8 (c)	Task I Stage Undistorted Inlet Performance Map; Circumferential-Grooves #1 Casing Treatment.	102
8 (d)	Task I Stage Undistorted Inlet Performance Map; Circumferential-Grooves #2 Casing Treatment.	103
8 (e)	Task I Stage Undistorted Inlet Performance Map; Circumferential-Grooves #3 Casing Treatment.	104

LIST OF TABLES (Concluded)

VOLUME II

<u>Table</u>		<u>Page</u>
XXV	Task II Stage Circumferential Distortion Flow Survey Data; 100% Speed; Near Stall; Without Inlet Guide Vanes; Without Casing Treatment.	501
XXVI	Task II Stage Circumferential Distortion Flow Survey Data; 100% Speed; Maximum Flow; Without Inlet Guide Vanes; Without Casing Treatment.	510

LIST OF ILLUSTRATIONS (Continued)

<u>Figure</u>		<u>Page</u>
8 (f)	Task I Stage Undistorted Inlet Performance Map; Skewed-Slots #1 Casing Treatment.	105
8 (g)	Task I Stage Undistorted Inlet Performance Map; Skewed-Slots #2 Casing Treatment.	106
8 (h)	Task I Stage Undistorted Inlet Performance Map; Skewed-Slots #3 Casing Treatment.	107
8 (i)	Task I Stage Undistorted Inlet Performance Map; Skewed-Slots #4 Casing Treatment.	108
8 (j)	Task I Stage Undistorted Inlet Performance Map; Blade-Angle-Slots #1 Casing Treatment.	109
8 (k)	Task I Stage Undistorted Inlet Performance Map; Blade-Angle-Slots #2 Casing Treatment.	110
9	Task II Rotor Inlet Static-Pressure As Measured By a 4-Parameter Combination Probe and a Static-Pressure Wedge Probe.	111
10	Task II Rotor Incidence Angle As Calculated From Measurements By a 4-Parameter Combination Probe and a Static-Pressure Wedge Probe.	112
11 (a)	Task I Stage Radial Distortion Performance Map, Honeycomb #1 Casing Treatment.	113
11 (b)	Task I Stage Radial Distortion Performance Map; Honeycomb #2 Casing Treatment.	114
11 (c)	Task I Stage Radial Distortion Performance Map; Circumferential-Grooves #1 Casing Treatment.	115
11 (d)	Task I Stage Radial Distortion Performance Map; Circumferential-Grooves #2 Casing Treatment.	116
11 (e)	Task I Stage Radial Distortion Performance Map; Circumferential-Grooves #3 Casing Treatment.	117
11 (f)	Task I Stage Radial Distortion Performance Map; Skewed-Slots #1 Casing Treatment.	118

LIST OF ILLUSTRATIONS (Continued)

<u>Figure</u>		<u>Page</u>
11 (g)	Task I Stage Radial Distortion Performance Map; Skewed-Slots #3 Casing Treatment.	119
11 (h)	Task I Stage Radial Distortion Performance Map; Skewed-Slots #4 Casing Treatment.	120
11 (i)	Task I Stage Radial Distortion Performance Map; Blade-Angle-Slots #1 Casing Treatment.	121
11 (j)	Task I Stage Radial Distortion Performance Map; Blade-Angle-Slots #2 Casing Treatment.	122
12	Task I Stage Circumferential Distortion Performance Map; Skewed-Slots #2 Casing Treatment.	123
13 (a)	Task I Stage Circumferential Distortion Profiles of Flow Conditions at 100% Speed Near Stall at Plane 0.95.	124
13 (b)	Task I Stage Circumferential Distortion Profiles of Flow Conditions at 100% Speed Near Stall at Plane 1.51.	126
13 (c)	Task I Stage Circumferential Distortion Profiles of Flow Conditions at 100% Speed Near Stall at Plane 2.20.	128
14 (a)	Task I Rotor Blade Element Data, 5% Immersion, 100% Speed, Undistorted Inlet.	130
14 (b)	Task I Rotor Blade Element Data, 10% Immersion, 100% Speed, Undistorted Inlet.	132
14 (c)	Task I Rotor Blade Element Data, 30% Immersion, 100% Speed, Undistorted Inlet.	134
14 (d)	Task I Rotor Blade Element Data, 90% Immersion, 100% Speed, Undistorted Inlet.	136
14 (e)	Task I Rotor Blade Element Data, 95% Immersion, 100% Speed, Undistorted Inlet.	138
15	Radial Distribution of Task I Rotor Adiabatic Efficiency (at 100% Speed, Undistorted Inlet, Intermediate Flow) With Casing Treatments Honeycomb #2, Circumferential-Grooves #2, Skewed-Slots #2 and Blade-Angle-Slots #1.	140

LIST OF ILLUSTRATIONS (Continued)

<u>Figure</u>		<u>Page</u>
16 (a)	Task II Stage Undistorted Inlet Performance Map Illustrating the Effects of Casing Treatment With Inlet Guide Vanes Installed.	141
16 (b)	Task II Stage Undistorted Inlet Performance Map Illustrating the Effects of Casing Treatment Without Inlet Guide Vanes Installed.	142
16 (c)	Task II Stage Undistorted Inlet Performance Map Illustrating the Effects of Inlet Guide Vanes With Casing Treatment Installed.	143
16 (d)	Task II Stage Undistorted Inlet Performance Map Illustrating the Effects of Inlet Guide Vanes Without Casing Treatment Installed.	144
17 (a)	Task II Rotor Inlet Axial Velocity With and Without Inlet Guide Vanes; 100% Speed Intermediate Flow, Undistorted Inlet (Solid Casing).	145
17 (b)	Task II Rotor Incidence Angle With and Without Inlet Guide Vanes; 100% Speed Intermediate Flow, Undistorted Inlet (Solid Casing).	146
17 (c)	Task II Rotor Adiabatic Efficiency With and Without Inlet Guide Vanes; 100% Speed Intermediate Flow, Undistorted Inlet (Solid Casing).	147
17 (d)	Task II Rotor Inlet Absolute Flow Angle With and Without Inlet Guide Vanes; 100% Speed Intermediate Flow, Undistorted Inlet (Solid Casing).	148
18	Stator Contribution to Task II Stage Adiabatic Efficiency Before and After Task I Rotor Failure.	149
19 (a)	Task II Stage Radial Distortion Performance Map Illustrating The Effects of Casing Treatment With Inlet Guide Vanes Installed.	150
19 (b)	Task II Stage Radial Distortion Performance Map Illustrating The Effects of Casing Treatment Without Inlet Guide Vanes Installed.	151
19 (c)	Task II Stage Radial Distortion Performance Map Illustrating The Effects of Inlet Guide Vanes With Casing Treatment Installed.	152

LIST OF ILLUSTRATIONS (Continued)

<u>Figure</u>		<u>Page</u>
20 (a)	Task II Stage Circumferential Distortion Performance Map Illustrating The Effects of Casing Treatment With Inlet Guide Vanes Installed.	154
20 (b)	Task II Stage Circumferential Distortion Performance Map Illustrating The Effects of Casing Treatment Without Inlet Guide Vanes Installed.	155
20 (c)	Task II Stage Circumferential Distortion Performance Map Illustrating The Effects of Inlet Guide Vanes With Casing Treatment Installed.	156
20 (d)	Task II Stage Circumferential Distortion Performance Map Illustrating The Effects of Inlet Guide Vanes Without Casing Treatment Installed.	157
21 (a)	Task II Stage Circumferential Distortion Profiles of Flow Conditions at 100% Speed Near Stall With Inlet Guide Vanes and With Casing Treatment Installed at Plane 0.18.	158
21 (b)	Task II Stage Circumferential Distortion Profiles of Flow Conditions at 100% Speed Near Stall With Inlet Guide Vanes and With Casing Treatment Installed at Plane 0.95.	159
21 (c)	Task II Stage Circumferential Distortion Profiles of Flow Conditions at 100% Speed Near Stall With Inlet Guide Vanes and With Casing Treatment Installed at Plane 1.51.	161
21 (d)	Task II Stage Circumferential Distortion Profiles of Flow Conditions at 100% Speed Near Stall With Inlet Guide Vanes and With Casing Treatment Installed at Plane 2.20.	163
22 (a)	Task II Stage Circumferential Distortion Profiles of Flow Conditions at 100% Speed Near Stall Without Inlet Guide Vanes and With Casing Treatment Installed at Plane 0.95.	166
22 (b)	Task II Stage Circumferential Distortion Profiles of Flow Conditions at 100% Speed Near Stall Without Inlet Guide Vanes and With Casing Treatment Installed at Plane 1.51.	168

LIST OF ILLUSTRATIONS (Continued)

<u>Figure</u>		<u>Page</u>
22 (c)	Task II Stage Circumferential Distortion Profiles of Flow Conditions at 100% Speed Near Stall Without Inlet Guide Vanes and With Casing Treatment Installed at Plane 2.20.	170
23 (a)	Task II Stage Circumferential Distortion Profiles of Flow Conditions at 100% Speed Near Stall Without Inlet Guide Vanes and Without Casing Treatment Installed at Plane 0.95.	172
23 (b)	Task II Stage Circumferential Distortion Profiles of Flow Conditions at 100% Speed Near Stall Without Inlet Guide Vanes and Without Casing Treatment Installed at Plane 1.51.	174
23 (c)	Task II Stage Circumferential Distortion Profiles of Flow Conditions at 100% Speed Near Stall Without Inlet Guide Vanes and Without Casing Treatment Installed at Plane 2.20.	176
24	Task II Circumferential Distortion IGV Inlet and Rotor Inlet Flow Angles at 100% Speed Near Stall With and Without Inlet Guide Vanes.	178
25 (a)	Task II Circumferential Distortion Inlet Guide Vane Wakes at 100% Speed, Near Stall; Undistorted Flow Region.	180
25 (b)	Task II Circumferential Distortion Inlet Guide Vane Wakes at 100% Speed, Near Stall; Entering Distortion Screen Shadow.	181
25 (c)	Task II Circumferential Distortion Inlet Guide Vane Wakes at 100% Speed, Near Stall; Distorted Flow Region.	182
25 (d)	Task II Circumferential Distortion Inlet Guide Vane Wakes at 100% Speed, Near Stall, Leaving Distortion Screen Shadow.	183
26	Task II Circumferential Distortion IGV Inlet and Rotor Inlet Flow Angles at 100% Speed Maximum Flow With and Without Inlet Guide Vanes.	184

LIST OF ILLUSTRATIONS (Concluded)

<u>Figure</u>		<u>Page</u>
27 (a)	Task II Circumferential Distortion Inlet Guide Vane Wake Survey at 100% Speed, Maximum Flow; Undistorted Flow Region.	186
27 (b)	Task II Circumferential Distortion Inlet Guide Vane Wake Survey at 100% Speed, Maximum Flow; Entering Distorted Flow Region.	187
27 (c)	Task II Circumferential Distortion Inlet Guide Vane Wake Survey at 100% Speed, Maximum Flow; Distorted Flow Region.	188
27 (d)	Task II Circumferential Distortion Inlet Guide Vane Wake Survey at 100% Speed, Maximum Flow; Leaving Distorted Flow Region.	189

TABLE OF CONTENTS

VOLUME II

<u>Section</u>	<u>Page</u>
APPENDIX B - DUPLICATE LISTING OF TASK I AND TASK II STAGE TEST DATA	197
APPENDIX C - LISTING OF TASK I STAGE UNDISTORTED INLET BLADE ELEMENT DATA	231
APPENDIX D - LISTING OF TASK I STAGE RADIAL DISTORTION BLADE ELEMENT DATA	301
APPENDIX E - LISTING OF TASK I STAGE CIRCUMFERENTIAL DISTORTION FLOW SURVEY DATA	363
APPENDIX F - LISTING OF TASK II STAGE UNDISTORTED INLET BLADE ELEMENT DATA	383
APPENDIX G - LISTING OF TASK II STAGE RADIAL DISTORTION BLADE ELEMENT DATA	415
APPENDIX H - LISTING OF TASK II STAGE CIRCUMFEREN- TIAL DISTORTION FLOW SURVEY DATA	437
DISTRIBUTION LIST	519

TABLE OF CONTENTS

VOLUME I

<u>Section</u>		<u>Page</u>
I	SUMMARY	1
II	INTRODUCTION	3
III	APPARATUS AND PROCEDURE	5
	1. Test Compressor Stages	5
	2. Casing Treatment Configurations	6
	3. Test Facility	8
	4. Inlet Distortion Equipment	8
	5. Instrumentation	9
	a. Task I Stage Instrumentation	9
	b. Task II Stage Instrumentation	10
	6. Data Reduction Methods	11
	a. Overall Performance Data Program	12
	b. Blade Element Data Program	14
	c. Circumferential Distortion Data Program	15
	7. Test Procedure	16
	a. Undistorted Inlet and Radial Distortion Testing	17
	b. Circumferential Distortion Testing	18
IV	RESULTS AND DISCUSSION	19
	1. Task I Stage Results	19
	a. Undistorted Inlet Test Results	19
	b. Radial Distortion Test Results	20
	c. Circumferential Distortion Test Results	21
	d. Analysis and Discussion	23
	2. Task II Stage Results	25
	a. Undistorted Inlet Test Results	25
	b. Radial Distortion Test Results	27
	c. Circumferential Distortion Test Results	28
	d. Analysis and Discussion	28
V	CONCLUSIONS	31
	APPENDIX A - SYMBOLS	33
	REFERENCES	37
	TABLES	39
	FIGURES	87

LIST OF TABLES

VOLUME I

<u>Table</u>		<u>Page</u>
I	Summary of Stage Design Specifications and Performance.	39
II (a)	Summary of Instrumentation Used for Task I Stage Testing.	40
II (b)	Summary of Instrumentation Used for Task II Stage Testing	41
III	Summary of Blade Element Data Reduction Constants.	42
IV	Summary of Task I Stage Undistorted Inlet Test Data.	47
V	Summary of Task I Stage Radial Distortion Test Data.	58
VI	Summary of Task I Stage Circumferential Distortion Test Data.	68
VII (a)	Summary of Task I Stage Undistorted Inlet Performance.	69
VII (b)	Summary of Task I Stage Radial Distortion Performance.	70
VII (c)	Summary of Task I Stage Circumferential Distortion Performance.	71
VII (d)	Corrected Task I Rotor Casing Treatment Efficiency Penalty.	72
VII (e)	Variations of Maximum Flow at 100% Speed During Task I Stage Casing Treatment Tests.	73
VIII	Summary of Task II Stage Undistorted Inlet Test Data.	74
IX	Summary of Task II Stage Radial Distortion Test Data.	78
X	Summary of Task II Stage Circumferential Distortion Test Data.	81
XI (a)	Summary of Task II Stage Undistorted Inlet Performance.	84
XI (b)	Summary of Task II Stage Radial Distortion Performance.	85
XI (c)	Summary of Task II Stage Circumferential Distortion Performance	86

LIST OF TABLES (Continued)

VOLUME II

<u>Table</u>		<u>Page</u>
XII	Symbols for Blade Element Output.	232
XIII	Task I Stage Undistorted Inlet Blade Element Data.	235
XIV	Task I Stage Radial Distortion Blade Element Data.	302
XV	Task I Stage Circumferential Distortion Flow Survey Data; 100% Speed; Maximum Flow; Skewed-Slots #2 Casing Treatment.	364
XVI	Task I Stage Circumferential Distortion Flow Survey Data; 100% Speed; Near Stall; Skewed-Slots #2 Casing Treatment.	373
XVII	Task II Stage Undistorted Inlet Blade Element Data.	384
XVIII	Task II Stage Radial Distortion Blade Element Data.	416
XIX	Task II Stage Circumferential Distortion Flow Survey Data; 100% Speed; Near Stall; With Inlet Guide Vanes and Casing Treatment.	438
XX	Task II Stage Circumferential Distortion Flow Survey Data; 100% Speed; Maximum Flow; With Inlet Guide Vanes and Casing Treatment.	450
XXI	Task II Stage Circumferential Distortion Flow Survey Data; 70% Speed; Intermediate Flow; With Inlet Guide Vanes and Casing Treatment.	462
XXII	Task II Stage Circumferential Distortion Flow Survey Data; 100% Speed; Near Stall; Without Inlet Guide Vanes; With Casing Treatment.	474
XXIII	Task II Stage Circumferential Distortion Flow Survey Data; 100% Speed; Maximum Flow; Without Inlet Guide Vanes; With Casing Treatment.	483
XXIV	Task II Stage Circumferential Distortion Flow Survey Data; 70% Speed; Intermediate Flow; Without Inlet Guide Vanes; With Casing Treatment.	492

SECTION I

SUMMARY

This report presents the results of Task IV of the NASA program under Contract NAS3-11157. Tests utilized the NASA Task I and Task II compressor stages of Contract NAS3-11157 with rotor tip casing treatment under distorted and undistorted inlet flow conditions. The Task I Stage consisted of a 1400-ft/sec tip speed rotor having a design total-pressure ratio of 1.636 and an aspect ratio of 2.5, together with accompanying stators. The Task II Stage consisted of a 1500-ft/sec tip speed rotor having a design pressure ratio of 1.686 and an aspect ratio of 2.36; this stage utilized the Task I stators and was tested both with and without zero-turning guide vanes.

Testing was performed using the Task I Stage with undistorted inlet flow and tip-radial inlet flow distortion for each of eleven casing treatment configurations. Failure of the Task I rotor blades during circumferential distortion testing necessitated use of the Task II Stage for the completion of the program. The Task II Stage was tested with undistorted, tip-radial and circumferential inlet flow distortion in three configurations involving the inclusion/exclusion of inlet guide vanes and casing treatment. Only one casing treatment configuration was used for testing of the Task II Stage. Overall performance and stall limits for all inlet flow conditions and stage configurations were determined at 70, 90, and 100% speeds. In the case of circumferential distortion, extensive radial and circumferential flow surveys were made. Radial flow surveys and blade element data were also obtained for the undistorted and radial distortion condition.

Undistorted inlet tests of the 1400 ft/sec tip speed stage indicated an increase in design speed stall margin from 0.213 to values ranging from 0.255 to 0.290 with the addition of casing treatment. The circumferential-grooves casing treatments, which gave 0.04 to 0.05 improvements in stall margin, had less than one point in efficiency penalty; the skewed slots casing treatments gave some of the largest stall margin gains, 0.077, with an efficiency penalty

of less than two percentage points. With the zero-turning inlet guide vanes installed, the 1500 ft/sec tip speed stage design speed stall margin rose from 0.129 to 0.320 with the inclusion of the blade-angle-slots casing treatment. Similar stall margin gains were obtained with the inlet guide vanes deleted.

SECTION I

SUMMARY

This report presents the results of Task IV of the NASA program under Contract NAS3-11157. Tests utilized the NASA Task I and Task II compressor stages of Contract NAS3-11157 with rotor tip casing treatment under distorted and undistorted inlet flow conditions. The Task I Stage consisted of a 1400-ft/sec tip speed rotor having a design total-pressure ratio of 1.636 and an aspect ratio of 2.5, together with accompanying stators. The Task II Stage consisted of a 1500-ft/sec tip speed rotor having a design pressure ratio of 1.686 and an aspect ratio of 2.36; this stage utilized the Task I stators and was tested both with and without zero-turning guide vanes.

Testing was performed using the Task I Stage with undistorted inlet flow and tip-radial inlet flow distortion for each of eleven casing treatment configurations. Failure of the Task I rotor blades during circumferential distortion testing necessitated use of the Task II Stage for the completion of the program. The Task II Stage was tested with undistorted, tip-radial and circumferential inlet flow distortion in three configurations involving the inclusion/exclusion of inlet guide vanes and casing treatment. Only one casing treatment configuration was used for testing of the Task II Stage. Overall performance and stall limits for all inlet flow conditions and stage configurations were determined at 70, 90, and 100% speeds. In the case of circumferential distortion, extensive radial and circumferential flow surveys were made. Radial flow surveys and blade element data were also obtained for the undistorted and radial distortion condition.

Undistorted inlet tests of the 1400 ft/sec tip speed stage indicated an increase in design speed stall margin from 0.213 to values ranging from 0.255 to 0.290 with the addition of casing treatment. The circumferential-grooves casing treatments, which gave 0.04 to 0.05 improvements in stall margin, had less than one point in efficiency penalty; the skewed slots casing treatments gave some of the largest stall margin gains, 0.077, with an efficiency penalty

of less than two percentage points. With the zero-turning inlet guide vanes installed, the 1500 ft/sec tip speed stage design speed stall margin rose from 0.129 to 0.320 with the inclusion of the blade-angle-slots casing treatment. Similar stall margin gains were obtained with the inlet guide vanes deleted.

SECTION II

INTRODUCTION

The need to reduce the size and weight of gas turbines for advanced military and commercial aircraft has led to the use of high-tip-speed fan and compressor stages. The Task IV portion of NASA Contract NAS3-11157 was designed to investigate the effect of rotor-tip casing treatment on the efficiency, stall margin, and distortion tolerance of high-tip-speed stages. The Task IV program utilized both the NASA Task I and Task II compressor stages. The Task I Stage consisted of a 1400-ft/sec tip speed rotor having a design total-pressure ratio of 1.636 and an aspect ratio of 2.5, together with accompanying stators. The Task II Stage consisted of a 1500-ft/sec tip speed rotor having a design pressure ratio of 1.686 and an aspect ratio of 2.36; this stage utilized the Task I stators and was tested both with and without zero-turning guide vanes. References 1 and 2 document the design of these stages. Task I performance is presented in Reference 3; Task II performance with and without inlet flow distortion is presented in References 4 and 5, respectively.

Casing treatment configurations evaluated were the honeycomb, circumferential-groove, skewed-slot, and blade-angle-slot types. Variations in the geometries of the casing treatments resulted in a total of eleven configurations tested. References 6 and 7 present results of previous investigations into the performance of compressor stages with rotor-tip casing treatment.

The Task I Stage performance was determined for each casing treatment configuration with undistorted and tip radial distortion inlet flow conditions. However, fatigue failure of the Task I rotor precluded completing the planned program with the Task I Stage. As a result, the remainder of the program was performed with the Task II Stage. Task II Stage performance was determined for undistorted, tip radial distortion and circumferential distortion for three configurations: with inlet guide vanes and casing treatment, without inlet guide vanes and with casing treatment, and without inlet guide vanes and without casing treatment. The performance of the Task II Stage with inlet

guide vanes and a conventional solid casing was available from the previously completed Task II portion of the Contract, as documented in References 4 and 5. The blade-angle-slot configuration was used in all tests with the Task II Stage utilizing casing treatment.

This report has been prepared in two volumes; the first volume summarizes apparatus, procedure, and results, while the second, NASA CR-82867, contains the output of the blade element and circumferential distortion data reduction programs.

SECTION III

APPARATUS AND PROCEDURE

1. TEST COMPRESSOR STAGES

The basic design requirement for the Task I Stage was to provide a stator to match the flow conditions leaving Rotor 1B, a high-performance 1400 ft/sec tip speed rotor previously tested as an isolated blade row. The results of these tests are given in Reference 8. The Task I Stage test vehicle employed much of the existing hardware from earlier Rotor 1B testing, including rotor blades and inlet ducting. New hardware included the stator vanes, stator hub region flowpath parts, and a special inlet section for distortion testing.

The design of Rotor 1B is described in Reference 2. This 1400 ft/sec tip speed rotor had an inlet hub:tip radius ratio of 0.5, a tip solidity of 1.3, and an aspect ratio of 2.5 with radially-constant chord length. Design tip diffusion factor was 0.35, and design tip inlet relative Mach number was 1.43. The tip blade section shapes were the multiple-circular-arc type with zero leading edge camber. A part-span shroud was located approximately at 40% span from the tip; below the part-span shroud, the blade section shapes were double-circular-arc type.

Additional details of the Task I Stage design are given in Reference 1. Table I is a summary of Task I Stage blade row design parameters and predicted performance. The rotor and stator were matched at a stage design condition of 219.4 lbs/sec weight flow at 100% corrected rotor speed. The performance of the Task I Stage was characterized by a peak adiabatic efficiency of 0.850 with a 1.624 pressure ratio at a corrected weight flow of 217.2 lbs/sec and a stall margin of 0.213 at 100% design speed. Estimated running clearance at 100% corrected speed was 0.027 - 0.034 inch.

The new stator vanes were designed to be compatible with the rotor exit absolute air angles measured at Rotor 1B test data Reading 52, Reference 2, the Task I Stage design point. The stator had double-circular-arc type

vane sections at the outer part of the blade which blended into arbitrarily-shaped hub sections designed especially for low-suction-surface Mach numbers. Stator hub solidity was 2.155, and aspect ratio was 2.065 with a radially-nonconstant chord varying from 3.184 inches at the hub to 3.65 inches at the tip. Additional stator design details are given in Reference 1 and in Table I of this report.

The Task II Stage used for this program consisted of a 1500 ft/sec tip speed rotor, variable-geometry inlet guide vanes, and variable-stagger stators. The inlet guide vanes were used only in the zero-turning position, and the variable-stage stators were set in their nominal position. Table I is a summary of Task II Stage blade row design parameters and predicted performance. Additional details of the Task II Stage design are given in Reference 1.

The 1500 ft/sec tip speed Task II rotor had an inlet hub:tip ratio of 0.5, a tip solidity of 1.40, and an aspect ratio of 2.5 with a nonlinear chord distribution varying from 3.601 inches at the tip to 3.361 inches at the hub. Design tip diffusion factor was 0.368 with a design inlet relative Mach number of 1.526. The rotor tip design total pressure ratio was 1.686. Estimated running clearance at 100% corrected speed was 0.0167 inch.

The inlet guide vane was derived from an uncambered NACA Series 65 airfoil with a maximum thickness:chord ratio of 10%. The vane was made in two parts to accomplish camber variation. The nose part (whose chord was 20.43% of the total chord) was fixed in the axial direction, while the rear flap could be rotated to vary the trailing edge angle. The solidity, based on the sum of the nose and flap chords, ranged from 1.299 at the tip to 1.788 at the hub. The IGV was used only in the zero-turning position for the Task IV program.

2. CASING TREATMENT CONFIGURATIONS

During the undistorted and radial distortion testing of the Task I Stage, eleven casing treatment configurations were evaluated. These casing treatments were based on geometrical variations of four basic configurations:

honeycomb, circumferential-grooves, skewed-slots, and blade-angle-slots. Figure 1 illustrates the eleven configurations.

The honeycomb configurations, Figure 1(a), had hexagonal cells angled 70° from radial in the direction of rotor rotation. The cells, 1.26 inches deep, were open in back to a plenum chamber. A variation to this configuration was accomplished by sealing the back of the honeycomb cell structure from the plenum.

Figure 1(b) illustrates the circumferential-groove casing treatment configurations. The basic configuration consisted of seven grooves 0.125 inch wide, 0.375 inch deep, and at 0.0625 inch separation. The first groove was placed 0.375 inch aft of the rotor tip leading edge. The first variation of this configuration eliminated the aft two grooves and increased the depth of the remaining five grooves to 0.75 inch. A final configuration consisted of five forward grooves with a depth of 0.1875 inch.

The third type of casing treatment evaluated was the skewed-slot configuration shown in Figure 1(c). The basic geometry had two bands of 300 axial slots each, 0.56 inch deep by 0.125 inch wide by 0.762 inch long, tilted from radial by 60° in the direction of rotor rotation. The forward band of slots was located at the rotor tip leading edge and was separated 0.125 inch from the rear band of slots. The axial length of each band of slots was reduced 50% for the second and third skewed-slot configurations by filling the front half of the forward slots and the rear half of the rear slots flush with the casing flowpath. The second configuration retained the original-depth slots, while the third configuration possessed half-depth slots. A final skewed-slot configuration retained the reduced length and original-depth rear slots; the forward slots were configured into two bands of short, original-depth slots by insertion of a 0.125 inch web.

The blade-angle-slot casing treatment configurations are shown in Figure 1(d). The original configuration consisted of 300 radial slots, 0.125 inch wide by 0.60 inch deep by 1 inch axial length, staggered at an angle of 60° from axial. The leading edge of the slots was 0.32 inch aft of the rotor

tip leading edge. The alterations made to obtain the second blade-angle-slot configuration consisted of reducing the number of slots to 150 by filling every other slot.

Figure 2 presents a meridional view of the test vehicle, including details of the casing treatment insert installation.

3. TEST FACILITY

Performance tests were conducted in General Electric's House Compressor Test facility in Lynn, Massachusetts. The test compressor drew atmospheric air through two banks of filters. The first filter bank was intended to remove 22% of the particles larger than 3-5 microns (dust spot test), and the second filter bank was intended to remove 90-95% of the remaining particles down to the same size. The air then passed through a coarse-wire inlet screen, into the bellmouth, and then through the compressor. In the exit assembly, the compressor discharge flow was split into two concentric streams. The inner air stream was passed into an exit pipe containing a flow straightener and a venturi flowmeter and then was exhausted to the atmosphere. The outer air stream passed through a sliding cylindrical throttle valve into a collector. Two pipes, each of which contained a flow straightener and a venturi flowmeter, then discharged the outer stream to the atmosphere. Power to drive the test compressor was provided by a high-pressure, noncondensing steam turbine rated at 15,000 horsepower. A schematic layout of the test facility is shown in Figure 3.

4. INLET DISTORTION EQUIPMENT

The Task IV inlet distortion screens were the same types used in Tasks I and II distortion testing. Both radial and circumferential distortions were tested. The radial distortion screen, shown in Figure 4(a), covered the outer 40% of the annulus area, while the circumferential screen, shown in Figure 4(b), spanned a 90° arc from hub to tip. Both screens were made of 20-mesh 0.016-inch diameter wire, giving an open area of 46%.

The support screen, which spanned the entire annulus and to which the

inlet guide vane total-pressure wake rakes, shown at the 10, 50, and 90% immersions for testing inlet guide vanes and casing treatment.

used for Task II Stage testing differed from those in that 4-parameter combination probes were used instead of wedge and cobra probes. Since the inlet guide vanes, an additional combination of inlet guide vane at Plane 0.18.

Probes were also used during stall testing with

programs were used to reduce the test data. A program computed average fluid properties at measured by fixed instruments and calculated performance parameters such as total-pressure ratio. Blade Element Data Program calculated vector performance parameters for seven streamline sections.

This program reduced data from both fixed and above two computer programs were used primarily for undistorted inlet and radial inlet flow circumferential Distortion Data Program was used to reduce data at numerous circumferential, radial, and meridional inlet flow distortion testing.

The program also calculated overall performance parameters determined by special circumferential/meridional data were obtained from both fixed and undistorted circumferential positions of the

that were common to all three data reductions. It was determined that the radial position and meridional positions in which data were recorded were fixed at

rotated 360° past the inlet for testing. The support structure consisted of 1/4-inch-diameter wire, and was designed to separate

the inlet diameter forward of the inlet section approximately 1/2 inch and support screen remained in the distorted inlet, in order to

elements provided for each phase of testing. These instruments, and of instrumentation schematics, Fig-

number and pitch angle data reduction calculations. These were accounted for. Fixed-inlet or Mach number effects, but small enough to be neglected.

inlet from fixed instrumentation at 11 positions on design streamlines and 95% of annulus height. Pressure forward of the distorted static rakes located at inlet was measured with 24 chromel-alumel thermocouples. The inlet screen was obtained by two

7-element total pressure distortion rakes located at Plane 0.18 in the 30° and 195° circumferential positions. Figure 6(a) illustrates one of these rakes. State exit conditions were measured at Plane 2.20 with seven 14-element total-pressure and total-temperature wake rakes. An example of these rakes can be seen in Figure 6(b). Discharge static pressures were measured by eight hub and eight casing static taps at the exit plane.

For blade element data, the inlet total conditions were obtained in the same manner as for overall performance data. The rotor inlet conditions for each immersion at Plane 0.95 were based on measurements of total pressure, total temperature, static pressure, and flow angle from a combination probe. Figure 6(c) shows an enlarged photograph of the combination probe-sensing element. At the rotor exit/stator inlet station, Plane 1.51, the total pressure, total temperature and flow angle were obtained at each immersion from a cobra probe. Figure 6(d) shows the cobra probe head. One 8° wedge probe, designated T-4 in Figures 5(a) and 5(b), was used to measure static pressure at this location. This probe is illustrated in Figure 6(e). Exit total temperatures and total pressures for the stator were obtained from the fixed wake rakes used to determine overall performance. Static pressures and flow angles were measured at each immersion with an angle-seeking wedge probe, designated T-11 in Figures 5(a) and 5(b).

For tests with circumferential inlet flow distortion, traverse data were recorded at the 10, 50, and 90% immersions by the traverse probes instead of the usual seven immersions.

Three hot wire anemometer probes at the 10, 50, and 90% immersions at Plane 1.51 were used during all stall tests to signal the initiation of rotating stall cells. For all other testing, the hot wires were removed from the airstream. Figure 6(f) illustrates one of these probes.

b. TASK II STAGE INSTRUMENTATION

All fixed overall performance instrumentation used for testing of the Task II Stage was identical to that used when testing the Task I Stage. In

addition, three 14-element inlet guide vane total-pressure wake rakes, shown in Figure 6(g), were installed at the 10, 50, and 90% immersions for testing of the Task II Stage with inlet guide vanes and casing treatment.

Traverse instrumentation used for Task II Stage testing differed from that used in Task I Stage tests in that 4-parameter combination probes were used at Planes 1.51 and 2.20 instead of wedge and cobra probes. Since the Task II Stage was tested with inlet guide vanes, an additional combination probe was required ahead of the inlet guide vane at Plane 0.18.

The hot wire anemometer probes were also used during stall testing with the Task II Stage.

6. DATA REDUCTION METHODS

Three separate computer programs were used to reduce the test data. The Overall Performance Data Program computed average fluid properties at each measuring station from data measured by fixed instruments and calculated overall stage and rotor performance parameters such as total-pressure ratio and adiabatic efficiency. The Blade Element Data Program calculated vector diagram and blade element performance parameters for seven streamline sections of both the rotor and the stator. This program reduced data from both fixed and traversing instruments. The above two computer programs were used primarily to reduce data obtained during undistorted inlet and radial inlet flow distortion testing. A special Circumferential Distortion Data Program was used to calculate vector diagram data at numerous circumferential, radial, and axial locations during circumferential inlet flow distortion testing. This data reduction computer program also calculated overall performance data from average fluid properties determined by special circumferential/radial mass-averaging methods. Input data were obtained from both fixed and traverse instruments at twelve different circumferential positions of the distortion screen.

Several assumptions were made that were common to all three data reduction programs. First, it was assumed that the radial position and meridional slope angle of each stream surface on which data were recorded were fixed at

the design value for all operating conditions. Second, all mass-averaging calculations used to determine average total temperature and total pressure were formulated in terms of enthalpy and entropy. Finally, the real gas properties of dry air were used in all thermodynamic calculations.

Additional details of the data reduction methods used appear in the following sections.

a. OVERALL PERFORMANCE DATA PROGRAM

Average test-vehicle inlet conditions ahead of the inlet distortion screen were taken as the arithmetic average of the Plane 0.01 thermocouple and total-pressure rake readings. With radial inlet flow distortion, the average stage inlet total-temperature was calculated as mentioned above, but inlet total-pressure was radially mass-averaged from readings of the two distortion rakes located at Plane 0.18, between the distortion screen and the inlet guide vanes. The static pressure used in the mass-averaging procedure was determined at each of the seven radial instrument positions by linear interpolations versus radius between arithmetically-averaged hub and casing wall static pressure values. Total pressure at each radial position was taken as the arithmetic average of the values given by the two inlet distortion rakes. An approximate value of average inlet total pressure was also calculated by this program for the case of circumferential inlet flow distortion. At each radial instrument position, the pressure reading from the Plane 0.18 rake located in the 270° undistorted region was weighted three times as heavily as that from the rake located in the 90° distorted region when calculating the local average pressure with circumferential distortion. These were then mass-averaged radially, as in the case of radial inlet flow distortion. With either inlet distortion, Plane 0.18 flow angles were assumed to be zero degrees, or axial.

Average stage exit total pressure and total temperature were calculated from data measured by the Plane 2.20 wake rakes. A simultaneous radial and circumferential mass-averaging procedure was used to properly account for variations of measured properties across the stator spacing as well as

radially. The static pressure required at each of the seven radial measurement positions was again obtained by linear interpolation between average wall static pressure values. In addition to overall fluid properties at Plane 2.20, the data reduction program also calculated average total temperature and total pressure at each radial position by mass-averaging circumferentially across each wake rake. Flow angles at Plane 2.20 were assumed to equal zero degrees plus or minus any stator stagger adjustment. These methods of obtaining discharge conditions were believed to offer excellent accuracy for axisymmetric flow fields expected with radially-distorted inlet conditions, but to be only approximate for circumferential distortion testing. In order to calculate more accurate total properties with circumferential distortion at each specific discharge wake rake radial and circumferential location, the static pressure associated with each particular wake rake was interpolated from reading of hub and casing wall static taps located at the same circumferential position as the wake rake.

Rotor exit total pressure at each of the seven radial measurement positions was taken as the arithmetic average of the three highest readings on each stage exit wake rake. Total temperature at each radial position was assumed equal to the stage exit value. Average total pressure at the rotor exit station was calculated by a radial mass-averaging procedure which used a weight flow at each radial position calculated from stage exit properties and flow angles.

The rotor inlet total pressure at each immersion at Plane 0.95 for the present test was determined using a table of inlet guide vane loss coefficients versus inlet Mach number and guide vane turning angle. These loss coefficients were obtained during undistorted inlet testing of the Task II Stage as discussed in Reference 4. The inlet Mach number was calculated using the distortion rake total pressure reading and a static pressure obtained from a linear interpolation between arithmetically-averaged casing and hub static pressures. The average rotor inlet total pressure was calculated using a radial mass-averaging procedure, assuming the flow angle at the rotor inlet, Plane 0.95, equal to the inlet guide vane camber angle.

The average total temperatures and total pressures at the stage inlet, rotor inlet, rotor exit, and stage exit measurement stations were used to calculate overall performance parameters for the stage as a whole and for the rotor as an isolated blade row. In addition, the Overall Performance Data Program output gave local average total temperature and total pressure at seven radial positions at each measuring station which could be used as input data to the other data reduction computer programs.

b. BLADE ELEMENT DATA PROGRAM

Blade element and vector diagram data were obtained for the rotor, stator, and inlet guide vane during undistorted and radial distortion tests. Traverse probe measurements were obtained at seven immersions at the inlet and exit stations to each blade row. Circumferential uniformity was assumed for all such traverse data.

When the thermodynamic properties were determined at seven radial positions at each measuring plane, they were transferred along streamlines to the leading and trailing edges of each blade row. As mentioned, the slopes, radii, and streamtube convergence along streamlines between measurement plane and blade edge were assumed to remain fixed at the design values for all flow conditions. The tangential velocity was obtained at the edges of the blades by applying the condition of constant moment of angular momentum along each streamline. The calculated meridional Mach number at the measurement plane was used to determine the meridional Mach number at the blade edge from the streamtube convergence relationship illustrated in Figure 7. This method was a good approximation when the radius change between the blade edge and the measurement plane was small. However, since there was appreciable swirl velocity at the rotor trailing edge, large radius changes would adversely affect the approximate results. Table III gives the constants used in these computations for both rotor and stator. With the measured total conditions assumed to be constant along the design streamlines, and the tangential velocities and meridional Mach numbers determined at blade edges in the above manner, the velocities, Mach numbers, and all vector diagram components were

determined at the edges of each blade row.

Calculated blade element performance parameters included diffusion factor, static-pressure-rise coefficient, total-pressure-loss coefficient and loss parameter, adiabatic and polytropic efficiency, plus total-temperature and total-pressure ratios. Values of rotor and stator total pressure loss coefficient, loss parameter and blade element efficiency were calculated by using total temperature and rotor exit total pressure measured by the stage exit wake rakes rather than using the combination probe measurements at Plane 1.51.

c. CIRCUMFERENTIAL DISTORTION DATA PROGRAM

With the nonaxisymmetric flow produced by circumferential inlet flow distortions, special procedures were required to determine the circumferential variation of vector diagram parameters and to calculate overall performance from fluid properties that had been mass-averaged circumferentially as well as radially. At certain operating conditions, compressor speed and weight flow were maintained constant, and the distortion screen was rotated to twelve different circumferential positions. Both fixed and traverse instruments were read at each screen position.

Stage exit total temperatures and total pressures, measured at Plane 2.20 by wake rakes, were obtained in the form of local mass-averaged values at 10, 30, 50, 70, and 90% immersions at each screen position by processing the fixed instrument data through the Overall Performance Data Program. Stage exit static pressure and flow angle were measured by traverse probes at Plane 2.20 immersed to the 10, 50, and 90% immersions at each screen position. At the stage inlet, rotor inlet, and rotor exit planes, the total pressures, static pressures, and flow angles were also measured at three immersions by the traverse probes. Rotor exit total temperatures were also obtained from the Plane 1.51 probe.

These data were then input to the Circumferential Distortion Data Program. Input data were first corrected for variations in atmospheric conditions by applying temperature and pressure correction factors θ and δ as determined

from the Plane 0.01 data listed in the output of the Overall Performance Data Program for the appropriate screen position. The stage inlet temperature was then assumed constant, equal to 518.688°R . Radial interpolations versus radius were used with the data from the traverse probes to determine fluid properties at the 30 and 70% immersions where traverse data were not recorded. The circumferential position of each instrument, and thus of each item of measured data, relative to the distortion screen centerline was then determined; finally, by linear interpolation versus circumferential position, a value of total temperature, total pressure, static pressure, and flow angle was deduced at twelve standard circumferential positions and five radial positions at each of Planes 0.18, 0.95, 1.51, and 2.20.

These four fluid conditions, plus the assumption of design streamline slope angle, were sufficient to calculate all vector diagram components at each of the standard points in the flow field. In addition to calculating vector diagram data, the Circumferential Distortion Data Program also used this extensive set of data to calculate an average value of total temperature and total pressure at each measuring station. These were obtained by a mass-averaging procedure which accounted for circumferential as well as radial variations. These average fluid properties were then used to calculate overall performance for the stage and for the rotor as an isolated blade row.

7. TEST PROCEDURE

Testing of the NASA Task I Stage was performed at 70, 90, and 100% of design speed with each casing treatment configuration with undistorted inlet and tip-radial distortion. The second skewed-slot casing treatment configuration, which offered substantial stall margin gains accompanied with low peak efficiency losses, was then tested on the Task I Stage with circumferential distortion. Failure of the Task I rotor during this circumferential distortion test rendered the rotor and casing treatment unsalvageable. Therefore, the Task II Stage was substituted for the remainder of the Task IV tests. The first blade-angle-slot casing treating configuration, which offered similar performance to the second skewed-slot configuration, was used in all testing of the Task II Stage.

ing was also performed at 70, 90, and 100% of rotor distorted inlet flow, tip radial distortion, and circum- both with and without zero-turning inlet guide vanes casing treatment.

f each test run was concerned with defining the stall ular stage configuration and inlet flow distortion. stall point, the discharge throttle was closed until wire anemometer signals indicated that rotating stall the rotor. Three shielded hot-wire anemometers were 50, and 90% positions at Plane 1.51 and oscillograph d which showed the radial extent of the stalled region. was then reset to a position close to the stall limit and e data were recorded.

ce was obtained whenever the vehicle was stalled, and the ng weight flow was obtained by recording the ICPAC flow ll was detected. The true stalling weight flow was orrelation of ICPAC flow versus actual weight flow using uring overall performance testing.

ATED INLET AND RADIAL DISTORTION TESTING

g both the Task I and Task II Stages, after the stall limits and radially-distorted inlet flow had been established, over- data were recorded at 70, 90, and 100% of design rotor speed charge throttle settings.

rall performance testing of the Task I and Task II Stages with let and radial inlet flow distortion, blade element traverses hed using the traverse probes previously mentioned and indi- s II(a) and II(b). Blade element traverses were performed

—
nstantaneous Compressor Performance Analysis Computer) is an circuit which senses weight flow and pressure ratio, and which plots ties nearly instantaneously to provide an approximate on-line performance map.

at 100% speed for maximum, intermediate, and near-stalling weight flow conditions. At the conclusion of each blade element traverse, the probes were retracted out of the airstream and overall performance data was recorded. A supplementary set of traverses was performed with a static pressure wedge probe substituted for the Plane 0.95 combination probe when testing the Task II Stage with undistorted inlet flow and configured without inlet guide vanes and with a conventional solid casing.

b. CIRCUMFERENTIAL DISTORTION TESTING

Circumferential distortion overall performance testing of the Task I and Task II Stages was similar to that with undistorted inlet and radial distortion. Once the stall points had been identified for 70, 90, and 100% of design rotor speed, performance data were obtained for various flow conditions. In addition to overall performance testing, detailed radial and circumferential flow surveys were made. These surveys were performed using the distortion screen rotation capability and the traverse probes. Task I Stage screen rotation tests were performed at 100% speed maximum and near-stall flow conditions at discharge throttle settings identical to the original Task I screen rotation tests which used the Task I Stage with a conventional solid casing (Reference 3). Task II Stage screen rotation tests were performed at 100% speed for maximum and near-stall flow conditions and at 70% speed for an intermediate flow condition. The discharge throttle settings were duplicated from original Task II testing (Reference 5) for all but the near-stall condition at 100% speed. For each operating condition, at each of twelve circumferential distortion screen positions spaced every 30°, overall performance data were recorded and traverse data were obtained at immersion positions of 10, 50, and 90%. At each screen position, following the traverse test, the probes were retracted out of the airstream and overall performance data were recorded. These data were processed using the Circumferential Distortion Data Program as discussed in the Data Reduction Methods section.

SECTION IV
RESULTS AND DISCUSSION

1. TASK I STAGE TEST RESULTS

a. UNDISTORTED INLET TEST RESULTS

A listing of the stage overall performance readings obtained for each casing treatment configuration with undistorted inlet flow is given in Table IV. The stage overall performance maps are shown in Figures 8(a) - 8(k).* The solid lines on these maps indicate the performance of the Task I Stage with the conventional solid casing. The operating line shown on the performance maps indicates a constant discharge valve setting for which the design point of the conventional Task I Stage is reached at 100% speed. The undistorted inlet stall lines are also indicated on the performance maps.

The stalling performance of the Task I Stage with each casing treatment configuration was summarized by calculating values of stall margin. Stall margin was defined by the usual equation:

$$\text{Stall Margin} = \left[\left(\frac{P_{2.20}/P_{0.18}}{W/\theta/\delta} \right)_{\text{stall}} \left(\frac{P_{2.20}/P_{0.18}}{W/\theta/\delta} \right)_{\text{op. line}}^{-1.0} \right]$$

Table VII(a) contains a listing of the stall margin values and peak stage adiabatic efficiencies for 70, 90, and 100% of rotor design speed for each casing treatment configuration. The Task I Stage with a conventional solid casing had a stall margin of 0.213 and a peak efficiency of 0.850 at 100% speed. Two of the better casing treatment configurations, Skewed-Slot #2 and Blade-Angle-Slot #1, had stall margins of 0.290 and 0.262 and peak stage efficiencies of 0.841 and 0.845, respectively, at 100% speed.

* Figures 8(b), (d), (g) and (i) indicate the configurations responsible for the greatest increase in stall margin.

The output from the Blade Element Data Program is presented in Table XIII in Volume II. Additional presentation of blade element data was not performed due to the inability of the rotor inlet combination probe to accurately measure static pressure. Figure 9 presents rotor inlet static pressure measurements taken with a static-pressure wedge probe and with a combination probe, together with the associated hub and casing wall static pressure measurements. Figure 10 presents rotor inlet incidence angles calculated from static pressure data obtained with both probes. These measurements were taken during Task IV tests using the Task II Stage without inlet guide vanes and with a conventional solid casing at identical discharge valve settings at 100% speed. From Figure 9, it can be seen that while static pressure data obtained with the wedge probe agree well with wall static pressures and with the design expectation, the static pressure levels measured by the combination probe appear to be quite low, particularly in the lower-annulus region. Although the static pressure measurement of the combination probe is believed to be unreliable, the blade element data are tabulated in Table XIII of Volume II for comparative purposes.

b. RADIAL DISTORTION TEST RESULTS

The distortion screen used to produce the tip radial distortion is shown in Figure 4(a). The severity of the distortion pattern was indicated by the value of the distortion parameter: $(P_{\max.} - P_{\min.})/P_{\max.} = 0.141$ at 100% design speed near the limit of stall-free operation.

A listing of stage overall performance readings for each casing treatment configuration obtained with radial distortion is given in Table V. The stage overall performance maps are presented in Figures 11(a) - 11(j). The solid lines on these maps indicate the performance of the Task I Stage with radial distortion and with a conventional solid casing. The radial distortion stall lines are indicated on the performance maps for each casing treatment configuration. Rotating stalls were encountered at all speeds. Oscillograph traces obtained from shielded hot-wire anemometers indicated

that the rotating stall cells were most severe at the tip and were very weak at the hub in all instances.

Table VII(b) contains values of stall margin and peak adiabatic efficiency obtained for each casing treatment configuration with radial distortion at 70, 90, and 100% of design speed. Values for the Skewed-Slot #2 casing treatment configuration with radial distortion have not been included since failure of the filler material used to modify the original casing treatment to this configuration invalidated the test results.

Table XIV of Volume II contains detailed velocity diagram data and blade element performance parameters calculated by the Blade Element Data Program. Plots of the blade element data have not been presented for reasons of the measurement inaccuracy previously mentioned.

c. CIRCUMFERENTIAL DISTORTION TEST RESULTS

Circumferential distortion testing of the Task I Stage was accomplished with the Skewed-Slot #2 casing treatment configuration. This configuration was selected as a result of its encouraging undistorted inlet performance, as seen in Table VII(a).

The distortion screen used to produce the circumferential distortion is shown in Figure 4(b). A value for the distortion parameter was calculated for the near-stall condition at 100% design speed $(P_{\max.} - P_{\min.})/P_{\max.} = 0.111$. The nominal distortion screen centerline position used for overall performance readings was 195° from top center in order to align the center of the distortion pattern with one of the inlet distortion rakes.

Table VI contains a listing of the overall performance data obtained with circumferential inlet distortion. Figure 12 presents the compressor stage performance map using adjusted overall performance data. The solid lines indicate the performance of the Task I Stage with circumferential distortion and a conventional solid casing. The circumferential distortion

stall lines are indicated on the performance map, Figure 12. As in the radial distortion case, the rotating stall cells were most severe at the rotor tip and weakest at the hub.

Due to the limited sampling of data for single readings taken with the distortion screen in the nominal position, the Overall Performance Data Program calculated somewhat unreliable average values of fluid properties and overall performance parameters for circumferentially-distorted flow. In order to obtain data more representative of actual flow conditions, overall performance and traverse data were obtained at twelve screen positions for a single operating point as described in the Test Procedure Section. The screen rotation test data were processed using the Circumferential Distortion Data Program to obtain circumferentially, as well as radially, mass-averaged stage inlet and exit total pressures and stage exit total temperatures.

A correlation was then made between the average properties determined by the Circumferential Distortion Data Program and the corresponding properties obtained from the single overall performance reading at the nominal distortion screen position. A set of average correction factors for all Task IV circumferential distortion testing was then obtained for stage pressure ratio and discharge total temperature. These corrections were then applied to the readings for which no screen rotation tests were performed, and new overall performance parameters were calculated. Table VI and Figure 12 reflect the adjusted overall performance values.

Table VII(c) lists values of stall margin and adjusted peak efficiency obtained during circumferential distortion testing at 70, 90, and 100% of design speed.

Figure 13 presents the circumferential profiles of flow conditions at each measuring plane for the near-stall condition at 100% speed. Data are presented for the 10, 50, and 90% immersions with a distortion screen center-line position of 180° from top center. A detailed listing of fluid properties and velocity diagram data obtained from screen rotation tests is given

in Tables XV and XVI in Volume II.

d. ANALYSIS AND DISCUSSION

Undistorted inlet test results indicated that the Honeycomb #2, Circumferential-Grooves #2, Skewed-Slots #2 and Blade-Angle-Slots #1 configuration of each type of casing treatment were the most effective in improving the Task I Stage stall performance. From the summary of the Task I Stage undistorted inlet performance, Table VII(a), some conclusions may be stated as to the effect of casing treatment geometry. Casing treatments with the greatest depth, such as Circumferential-Grooves #2 and Skewed-Slots #2, provided more stall margin than those with a shallower depth. Similarly, a shorter axial length produced benefits both in stall margin and peak efficiency, as evidenced by the short Skewed-Slots #2 and #3 configurations. However, the test program did not permit the determination of the optimum axial length or depth. From the performance of Blade-Angle-Slots #1 and #2, it appears that the performance gains were a function of the casing treatment cavity volume; i.e., the greater volume produced larger performance gains. Again no extensive investigations were made of this effect.

It is noteworthy that significant improvements in stall margin were obtained using non-plenum casing treatment configurations. The non-plenum Honeycomb #2 configuration exhibited greater stall margin improvement with less efficiency penalty than the plenum-type Honeycomb #1 configuration. In addition, a qualitative comparison of the performance of the remaining non-plenum casing treatment configurations tested in the Task I Stage with the results given in References 6 and 7, which were investigations concerned with plenum-type casing treatments, indicated a plenum was not a necessary requirement for increased stall margin.

In an effort to better understand the effects of the casing treatment on the flow, blade element data from the best configuration of each casing treatment type were examined. Figures 14(a) - (e) present total and static-

pressure ratios, total-temperature ratio, and adiabatic efficiency versus discharge throttle valve position for the Honeycomb #2, Circumferential-Grooves #2, Skewed-Slots #2 and Blade-Angle-Slots #1 casing treatments. The solid casing configuration, also presented in Figure 14, had a 100% speed stalling discharge throttle equal to 4.60. Results at the 30% and 90% immersions, Figures 14(c) and 14(d), indicate that the casing treatment was not responsible for any significant departures from the performance with the solid casing configuration in the mid-span region of the annulus. Data at the 50% and 70% immersions also did not indicate any noticeable departure from the solid casing operating characteristics and are not presented. The outer two immersions, shown in Figures 14(a) and 14(b), indicate the flow in this region received a slightly higher work input. Corresponding increases in pressure ratio can be seen at the 5% immersion but not at 10%. Figure 14 indicates that, in general, the stall margin increases were due to increased weight flow range along the same blade element characteristics as in operation without casing treatment.

At the 5% immersion, the efficiency both with and without casing treatment was essentially the same. However, flow at the 10% immersion did not show an increased pressure ratio and a 0.02 to 0.04 drop in adiabatic efficiency occurred at this immersion. This efficiency penalty at 10% immersion was believed to be the result of casing treatment effects. Conversely, Figure 14(e) shows that the 95% immersion operated at higher total-pressure ratios with casing treatment for the same work input.

Figure 15 illustrates the efficiency distribution versus radial position for the 100% speed intermediate-flow condition. A 0.04 to 0.06 efficiency gain at the 95% immersion, due to pressure ratio increases, can be seen. This increase in hub efficiency is not believed to be a direct result of the utilization of casing treatment. In order to determine a more representative casing treatment efficiency penalty, the Task IV efficiencies were recalculated replacing the 90% and 95% immersion Task IV data with Task I Stage solid casing data. These results are presented in Table VII(d) for the eleven configurations

at a discharge throttle setting of 9 at 100% speed. The first column of Table VII(d) contains the efficiency difference without any data editing between the Task I rotor with the solid casing and the eleven configurations of the Task IV program. Column two presents the change in Task IV efficiency when the Task IV total-pressure and total-temperature ratios were replaced with Task I Stage solid casing data for the 90% and 95% immersions. The resulting efficiency penalties, based on edited data, due only to casing treatment effects are listed in the final column. The efficiency penalties increased approximately 0.003 when the hub efficiency increases were neglected.

Examination of the stage performance maps, Figures 8(a) - 8(k), indicates that some configurations had lower airflow at 100% speed at the fully open throttle setting. Several configurations experienced airflow reductions of as much as 2% of the Task I Stage solid casing level. Results from an investigation to determine whether this might be an effect of casing treatment were inconclusive. Table VII(e) compares airflow as inferred from bellmouth and flow nozzle measurements with flow indications at the rotor leading edge measurement plane for seven high-flow and four low-flow configurations. Considering the consistency of the results at the rotor leading edge plane, it is believed that the indications of flow shifts represent uncertainty in measurement, rather than a systematic result in some casing treatment configurations.

2. TASK II STAGE TEST RESULTS

a. UNDISTORTED INLET TEST RESULTS

A listing of Task II Stage overall performance readings obtained for each vehicle configuration with undistorted inlet flow is given in Table VIII. The stage performance maps are shown in Figure 16(a) - 16(d). The solid lines on Figures 16(a) and 16(d) indicate the performance of the Task II Stage with a conventional solid casing and with the inlet guide vanes at the zero-turning

setting. The solid lines on Figures 16(b) and 16(c) indicate the Task II Stage performance without inlet guide vanes or casing treatment, and with the inlet guide vanes and casing treatment, respectively. The operating line indicates a constant discharge valve setting for which the design point of the conventional Task II Stage is reached at 100% speed. Figure 16(a) indicates the effect of the casing treatment on the Task II Stage performance when configured with the inlet guide vanes. Figure 16(b) presents a similar comparison but without the inlet guide vanes installed. The effect of the inlet guide vanes on Task II Stage performance with the casing treatment installed is presented in Figure 16(c); a similar comparison is made in Figure 16(d), but with the test vehicle in the solid casing configuration.

The stall lines are indicated on the performance maps, Figures 16(a) - 16(d). Oscillograph traces obtained from shielded hot-wire anemometers indicated that the rotating stall cells were most severe at the tip and were very weak at the hub.

Table XI(a) contains a listing of stall margins and peak adiabatic efficiencies obtained at 70, 90, and 100% design speed for each vehicle configuration, including the original solid casing Task II Stage. The Blade-Angle-Slots #1 casing treatment gave an undistorted inlet Task II Stage stall margin value of 0.320, an increase of 0.191 over the solid casing value, when tested at design speed with the inlet guide vanes installed. With the inlet guide vanes deleted, the 100% speed stall margin increased from 0.182 with a solid casing to a value of 0.360 with casing treatment installed. In comparison, the effects of the inlet guide vanes were much less than the benefits due to casing treatment. As in the Task I Stage, the Task II Stage casing treatment efficiency penalties were never greater than two points.

Figures 17(a) - 17(d) present radial distributions of rotor inlet axial velocity, incidence angle, absolute flow angle, and adiabatic efficiency for the Task II solid casing configuration with and without inlet guide vanes. These figures indicate that the zero-turning inlet guide vanes were not

responsible for departures from the design intent and did not significantly affect the rotor inlet conditions. Differences in the data seen in these figures are most likely due to small differences in rotor speed or inlet flow blockage.

As a result of the Task I rotor failure, there was some concern as to whether the damage to the stators was severe enough to affect their performance. Figure 18 illustrates the stator contribution to the Task II Stage efficiency before and after failure of the Task I rotor. The figure indicates that the Task I rotor failure had no significant effect on the stator performance.

The output from the Blade Element Data Program is presented in Table XVII in Volume II. Graphical presentation of blade element data was not performed due to the inability of the rotor inlet combination probe to accurately measure static pressure.

b. RADIAL DISTORTION TEST RESULTS

The value of the distortion parameter for radial distortion testing with the Task II Stage was 0.151 at 100% speed near stalling flow. A listing of stage overall performance readings with radial distortion for each Task II Stage configuration is given in Table IX. The stage overall performance maps are presented in Figures 19(a) - 19(d). The radial distortion stall lines are indicated on the performance maps. As in the undistorted inlet testing, rotating stall cells were most severe at the rotor tip and weakest at the hub.

Table XI(b) contains stall margin and peak efficiency values for each Task II Stage configuration tested with radial distortion at 70, 90, and 100% speed. Table XVIII of Volume II contains the detailed velocity diagram data and blade element performance parameters for radial distortion tests calculated by the Blade Element Data Program.

c. CIRCUMFERENTIAL DISTORTION TEST RESULTS

The distortion screen used for this testing was the same as used for the Task I Stage circumferential distortion test. The distortion parameter for the 100% speed, near-stall condition equalled 0.128. Table X contains a listing of the overall performance obtained with circumferential inlet distortion. Figures 20(a) - 20(d) present compressor stage performance maps, using adjusted overall performance data. The adjustment of the overall performance data was accomplished as described in the Task I Stage circumferential distortion test results section. Table XIV and Figures 20(a) - 20(d) give adjusted overall performance values.

The circumferential distortion stall lines are indicated on the performance maps, Figures 20(a) - 20(d). Table XI(c) presents stall margin and peak efficiency values obtained for circumferential distortion testing of each vehicle configuration at 70, 90, and 100% of design speed. As in previous tests, rotating stall cells were most severe at the rotor tip and weakest at the hub.

Figures 21 - 23 present circumferential profiles of flow conditions at each measuring plane for each of the three Task II Stage configurations for the near-stall condition at 100% speed. Data are presented for the 10, 50, and 90% immersions. A detailed listing of fluid properties and vector diagram data for all screen rotation tests performed is given in Tables XIX - XXVI of Volume II.

d. ANALYSIS AND DISCUSSION

One of the primary objectives of the Task II Stage testing was to determine the effectiveness of the inlet guide vanes to act as flow straighteners with circumferential inlet flow distortion. Figure 24 presents the absolute

flow angles ahead of the guide vanes and at the rotor inlet for the 100% speed near-stall condition with circumferential distortion. Data are given both with and without inlet guide vanes at the 10, 50, and 90% immersions. From Figure 24 it can be seen that, at the near-stall condition, the inlet guide vanes reduced the peak preswirl angle but were not very effective in reducing the level of the counterswirl angles. However, the use of guide vanes appeared to aid in the reestablishment of the nominal flow direction after the peak flow angle region (circumferential location 220° - 360°) compared to the configuration without inlet guide vanes. The inlet guide vane wakes at four different circumferential positions relative to the inlet distortion pattern are shown in Figure 25. These data indicate that the inlet guide vanes were not stalled at the stage near-stall condition and were not responsible for the 25° variation in flow angle seen at the inlet guide vane inlet.

Figure 26 presents the absolute flow angles ahead of the guide vanes and at the rotor inlet for the maximum-flow condition at design speed. The flow angle levels measured ahead of the guide vanes appear to have 10° negative bias. This is believed to be due to a malfunction of the combination probe at plane 0.18. The inlet guide vanes were effective in straightening the flow at this operating condition. Both the peak preswirl and counterswirl levels were reduced and the axial flow direction was reestablished more rapidly (circumferential location 240° - 360°) with inlet guide vanes installed. The inlet guide vane wakes at this condition, shown in Figure 27, were largest at the edges of the distortion pattern, but again did not indicate any stalling of the inlet guide vanes.

SECTION V

CONCLUSIONS

The primary purpose of the Task IV phase of NASA Contract NAS3-11157 was to determine the effects of several casing treatment configurations on the performance of the Task I and Task II Stages. Secondly, it was desired to evaluate the influence of inlet guide vanes on the Task II Stage performance. Conclusions reached from the results of the Task IV program were as follows:

1. Increases in stall margin were obtainable with simple casing treatment geometries, such as the Circumferential-Grooves and Blade-Angle-Slots, which seem practical for use on production-type gas turbine engines.
2. Of the more practical configurations tested, the best Circumferential-Grooves configuration demonstrated a 0.065 gain in stall margin with undistorted inlet with a negligible efficiency loss at design speed. The best Blade-Angle-Slots configuration exhibited a 0.054 gain in stall margin with a 0.005 loss in efficiency at the same conditions. However, the Blade-Angle-Slots casing treatment was superior to the Circumferential-Grooves insert at part-speed with undistorted inlet and at all speeds with radial inlet distortion. The greatest stall margin gain, 0.077, was obtained with the Skewed-Slots configuration with an indicated efficiency penalty of 0.009.
3. All casing treatment configurations but one were of a non-plenum type and produced significant stall margin increases, indicating that circumferential or axial flow recirculations are not required for increased stall margin.
4. Blade element data, obtained between 5% and 95% immersion, proved inconclusive as to the cause of the stall margin increase but demonstrated the increases were obtained through operation at lower flows along the same characteristics as found in solid casing configurations rather than along new characteristics. Thus, it is believed that the flow phenomena responsible for the stall margin increases were extremely localized at the rotor tip.

5. The effects of the zero-turning inlet guide vanes on stall margin in the Task II Stage were approximately an order of magnitude less than the casing treatment effects. When operating at design speed with undistorted inlet, the inlet guide vanes were responsible for 0.04 loss in stall margin.
6. When subjected to circumferential inlet distortion, the zero-turning inlet guide vanes were seen to be relatively ineffective in eliminating the inlet swirl. The probable cause for the re-establishment of the distortion pattern at the rotor inlet was felt to be the large axial spacing between the inlet guide vanes and the rotor.

APPENDIX A - SYMBOLS

Symbol	Description	Units
A	Annulus or Streamtube Area	in. ²
C	Chord Length of Cylindrical Section	in.
C _h	Enthalpy-Equivalent Static-Pressure-Rise Coefficient, ie for Rotor: $C_h = \frac{2gJc_p t_1 \left[\left(\frac{p_2}{p_1} \right)^{\frac{\gamma-1}{\gamma}} - 1 \right] - (U_2^2 - U_1^2)}{V_1'^2}$	---
C _p	Static-Pressure-Rise Coefficient, ie for Rotor: $C_p = \frac{p_2 - p_1}{p_1' - p_1}$	---
c _p	Specific Heat at Constant Pressure, 0.2399 Btu/lb-°R	
D	Diffusion Factor: $D_{\text{Rotor}} = 1 - \frac{V_2'}{V_1'} + \frac{r_2 V_{\theta_2} - r_1 V_{\theta_1}}{2\bar{r} \sigma V_1'}$ $D_{\text{IGV/Stator}} = 1 - \frac{V_2}{V_1} + \frac{r_1 V_{\theta_1} - r_2 V_{\theta_2}}{2\bar{r} \sigma V_1}$	---
g	Acceleration Due to Gravity, 32.174 ft/sec ²	
i	Incidence Angle; Difference Between Flow Angle and Camber Line Angle at Leading Edge in Cascade Projection	deg
i _{ss}	Suction Surface Incidence Angle, Difference Between Flow Angle and Leading Edge Suction Surface	deg
J	Mechanical Equivalent of Heat, 778.161 ft-lb/Btu.	
K _{bl}	Effective Area Coefficient Due to Wall Boundary Layer Blockage	---
M	Mach Number	---
N	Rotational Speed	rpm

APPENDIX A - SYMBOLS (Continued)

Symbol	Description	Units
P	Total or Stagnation Pressure	psia
p	Static Pressure	psia
r	Radius	in.
\bar{r}	Mean Radius, Average of Streamline Leading and Trailing Edge Radii	in.
T	Total or Stagnation Temperature	°R
t	Static Temperature	°R
U	Rotor Speed	ft/sec
V	Air Velocity	ft/sec
W	Weight Flow	lbs/sec
Z	Displacement Along Compressor Axis	in.
β	Flow Angle; Angle Whose Tangent is the Ratio of Tangential to Axial Velocity	deg
$\Delta\beta$	Flow Turning Angle, $\Delta\beta = \beta_1 - \beta_2$	deg
γ	Ratio of Specific Heats	---
γ°	Blade-Chord Angle (Stagger), Angle in Cascade Projection Between Blade Chord and Axial Direction	deg
δ	Pressure Correction, $P_{\text{Actual}}/14.696 \text{ psia}$	
δ°	Deviation Angle, Difference Between Flow Angle and Camber Angle at Trailing Edge in Cascade Projection	deg
ϵ°	Slope of Meridional Streamline	deg
η	Efficiency	
θ	Temperature Correction, $T_{\text{Actual}}/518.7^\circ\text{R}$	
θ°	Circumferential Position From Top Center	deg

APPENDIX A - SYMBOLS (Continued)

Symbol	Description	Units
K°	Angle Between Tangent to Blade Meanline and the Axial Direction	deg
σ	Solidity, Ratio of Chord to Blade Spacing	---
$\bar{\omega}$	Total Pressure Loss Coefficient	---
	Rotor: $\bar{\omega}' = \frac{P_2'_{id} - P_2'}{P_1' - P_1}$, IGV/Stator: $\bar{\omega} = \frac{P_1 - P_2}{P_1 - p_1}$	
$\frac{\bar{\omega} \cos \beta_2}{2\sigma}$	Total Pressure Loss Parameter	---
Subscripts		
ad	Adiabatic	
an	Annulus	
d	Downstream Measurement Station (Table III)	
e	Edge of Blade (Figure 7)	
id	Ideal	
j	Immersion	
m	Meridional Direction	
p	Polytropic	
s	Measurement Station (Figure 7)	
ss	Suction Surface	
t	Tip at Station 1.0	
u	Upstream Measurement Station (Table III)	
z	Axial Direction	
θ	Tangential Direction	

APPENDIX A - SYMBOLS (Concluded)

Subscripts	Description
1	Leading Edge
2	Trailing Edge
0.01	Measurement Station Designation, Vehicle Inlet
0.18	Measurement Station Designation, IGV Inlet
0.95	Measurement Station Designation, Rotor Inlet
1.51	Measurement Station Designation, Stator Inlet
2.20	Measurement Station Designation, Stage Discharge

Superscripts	Description
'	Relative to Rotor
*	Critical Flow Condition

Table VII(e). Variations of Maximum Flow at 100% Speed During Task I Stage Casing Treatment Tests.

Configuration	Discharge Nozzle Flow	Bellmouth Flow	Flow Function $W/\sqrt{RT_T}/P_{TA}$ At Plane 0.95*	Average Axial Velocity At Plane 0.95**
Honeycomb #1	220.78	218.90	2.920	795.6
Honeycomb #2	220.42	221.20	2.936	802.7
Skewed-Slots #1	219.60	220.38	2.912	805.8
Skewed-Slots #3	221.54	222.23	N/A	804.0
Skewed-Slots #4	220.10	221.12	2.912	802.9
Blade-Angle- Slots #1	221.70	222.12	2.904	796.3
Blade-Angle- Slots #2	220.61	220.78	2.920	804.7
Average of High Flows	220.68	220.96	2.917	801.7
Circumferential Grooves #1	216.76	217.24	2.896	805.8
Circumferential Grooves #2	217.33	217.93	2.908	798.5
Circumferential Grooves #3	217.90	219.02	2.900	793.9
Skewed-Slots #2	216.31	217.04	2.896	797.9
Average of Low Flows	217.08	217.81	2.900	799.0
<p>* Based on edited total pressure at Plane 0.18 and wall static pressure at Plane 0.95</p> <p>** Based on blade element traverse data at Plane 0.95</p>				

Table VIII. Summary of Task II Stage Undistorted Inlet Test Data.

a. With Inlet Guide Vanes and Blade Angle Slots #1 Casing Treatment.

Reading Number	Percent Design Speed	Discharge Valve Setting	Inlet Corrected Weight Flow, Lbs/Sec	Stage Total-Pressure Ratio	Stage Adiabatic Efficiency	Type Point**
418	70	30	170.4	1.195	.763	OP
419	70	23.3*	117.0	1.317	.698	OP
420	70	15	164.1	1.245	.828	OP
421	70	10	155.4	1.277	.833	OP
422	70	6	145.4	1.301	.816	OP
423	90	30	207.3	1.309	.690	OP
424	90	2.5	162.9	1.577	.716	OP
425	90	15	205.4	1.416	.791	OP
426	90	10	201.4	1.503	.826	OP
427	90	9	200.2	1.529	.838	OP
428	100	30	222.9	1.365	.664	OP
429	100	8	218.9	1.705	.821	OP
430	100	30	224.1	1.371	.665	BE (p. 384)
431	100	9	220.6	1.675	.825	BE (p. 387)
432	100	4	192.6	1.791	.737	BE (p. 390)

* - Indicates discharge valve position with inner annulus discharge pipe closed.
 ** - OP - Overall Performance Reading
 BE - Blade Element Performance Reading

Table VII(c). Summary of Task I Stage Circumferential Distortion Performance.

Casing Treatment Configuration	70% Design Speed		90% Design Speed		100% Design Speed	
	Stall Margin	Peak η_{ad}	Stall Margin	Peak η_{ad}	Stall Margin	Peak η_{ad}
Task I Solid Casing	.242	.837	.149	.827	.090	.800
Skewed-Slots #2	.354	.833	.209	.838	.140	.828

Table VII(d). Corrected Task I Rotor Casing Treatment Efficiency Penalty,
100% Speed, Discharge Throttle = 9.

Configuration	Indicated Rotor Efficiency Penalty*	Task IV Efficiency Loss Due To Edited Data**	Corrected Rotor Efficiency Penalty
Honeycomb #1	.016	.003	.019
Honeycomb #2	.003	.002	.005
Circumferential Grooves #1	.002	.002	.004
Circumferential Grooves #2	-.006	.004	-.002
Circumferential Grooves #3	-.002	.004	.002
Skewed-Slots #1	.016	.002	.018
Skewed-Slots #2	.007	.002	.009
Skewed-Slots #3	.003	.004	.007
Skewed Slots #4	.016	.002	.018
Blade-Angle-Slots #1	.007	.003	.010
Blade-Angle-Slots #2	.008	.001	.009
<p>* Overall Performance Calculations of η (Task I Solid Casing) - η (Task IV)</p> <p>** Task IV 90% and 95% Immersion Data Replaced with Task I Rotor Solid Casing Data</p>			

Table VII (a). Summary of Task I Stage Undistorted Inlet Performance.

Casing Treatment Configuration	70% Design Speed		90% Design Speed		100% Design Speed	
	Stall Margin	Peak η_{ad}	Stall Margin	Peak η_{ad}	Stall Margin	Peak η_{ad}
Task I Solid Casing	.293	.895	.208	.873	.213	.850
Honeycomb #1	.379	.874	.286	.857	.277	.835
Honeycomb #2	.379	.872	.275	.868	.290	.845
Circumferential-Grooves #1	.312	.873	.233	.872	.264	.851
Circumferential-Grooves #2	.326	.873	.238	.877	.278	.857
Circumferential-Grooves #3	.307	.875	.208	.877	.256	.854
Skewed-Slots #1	.441	.853	.284	.856	.260	.832
Skewed-Slots #2	.357	.879	.279	.865	.290	.841
Skewed-Slots #3	.338	.880	.208	.868	.267	.848
Skewed-Slots #4	.391	.887	.265	.858	.255	.835
Blade-Angle-Slots #1	.387	.870	.256	.867	.262	.845
Blade-Angle-Slots #2	.349	.870	.246	.865	.258	.846

Table VII (b). Summary of Task I Stage Radial Distortion Performance.

Casing Treatment Configuration	70% Design Speed		90% Design Speed		100% Design Speed	
	Stall Margin	Peak η_{ad}	Stall Margin	Peak η_{ad}	Stall Margin	Peak η_{ad}
Task I Solid Casing	.060	.838	.033	.826	.035	.800
Honeycomb #1	.233	.830	.173	.822	.150	.797
Honeycomb #2	.190	.845	.138	.825	.117	.796
Circumferential-Grooves #1	.110	.845	.078	.830	.095	.808
Circumferential-Grooves #2	.117	.848	.093	.834	.084	.813
Circumferential Grooves #3	.105	.838	.069	.833	.108	.808
Skewed-Slots #1	.194	.850	.207	.827	.163	.793
Skewed-Slots #2						
Skewed-Slots #3	.134	.845	.087	.820	.094	.795
Skewed-Slots #4	.157	.840	.168	.824	.141	.796
Blade-Angle-Slots #1	.188	.835	.172	.813	.146	.789
Blade-Angle-Slots #2	.127	.823	.121	.823	.120	.790

Table V. Summary of Task I Stage Radial Distortion Test Data (Continued).

j. Blade Angle Slotted Insert #2 Casing Treatment.

Reading Number	Percent Design Speed	Discharge Valve Setting	Inlet Corrected Weight Flow, Lbs/Sec	Stage Total-Pressure Ratio	Stage Adiabatic Efficiency	Type Point**
343	70	30	165.7	1.199	.805	OP
344	70	15	156.1	1.242	.814	OP
345	70	12.5	152.2	1.254	.820	OP
346	70	10	148.0	1.265	.823	OP
347	70	7	140.0	1.275	.812	OP
348	90	30	201.9	1.313	.731	OP
349	90	15	198.3	1.408	.796	OP
350	90	12.5	195.7	1.438	.823	OP
351	90	10	191.9	1.472	.816	OP
352	90	7	182.3	1.511	.800	OP
353	100	30	214.7	1.367	.679	BE (p. 356)
354	100	11	212.1	1.572	.789	BE (p. 358)
355	100	7.4	203.2	1.650	.780	BE (p. 360)
356	100	9	208.7	1.617	.787	OP
357	100	15	213.9	1.486	.764	OP
<p>** - OP - Overall Performance Reading BE - Blade Element Performance Reading</p>						

Table VI. Summary of Task I Stage Circumferential Distortion Test Data.

Skewed Slots #2 Casing Treatment.

Reading Number	Percent Design Speed	Discharge Valve Setting	Inlet Corrected Weight Flow, Lbs/Sec	Stage Total-Pressure Ratio	Stage Adiabatic Efficiency	Type Point*	Distortion Screen Pos. From TDC
358	70	98.5	163.6	1.181	.751	OP	195
359	70	50	163.6	1.184	.755	OP	195
360	70	30	162.6	1.197	.785	OP	195
361	70	10	144.5	1.260	.831	OP	195
362	70	5	130.1	1.277	.778	OP	195
363	70	2	118.0	1.279	.719	OP	195
364	90	50	201.4	1.305	.740	OP	195
365	90	15	194.8	1.410	.834	OP	195
366	90	11	188.0	1.454	.838	OP	195
367	90	7.5	176.8	1.486	.816	OP	195
368	90	6	169.8	1.495	.795	OP	195
369	100	50	216.4	1.367	.728	OP	195
370	100	13	209.7	1.532	.825	OP	195
371	100	9.6	202.4	1.583	.822	OP	195
372	100	7.3	192.2	1.611	.788	OP	195
373	100	17	213.4	1.473	.805	OP	195
399	100	8	196.6	1.597	.797	OP	195
374	100	9.6	202.2	1.584	.828	OP	195
387	100	50	214.9	1.366	.730	OP	195
374-386	100	9.6	202.2	1.581	.805	SRT	195-165 (p. 377)
387-398	100	50	214.9	1.374	.728	SRT	195-165 (p. 364)

* - OP - Overall Performance Reading
SRT- Screen Rotating Test (12 Circumferential Distortion Screen Positions in 30° Intervals from 195° TDC)

Table V. Summary of Task I Stage Radial Distortion Test Data (Continued).

h. Skewed Slotted Insert #4 Casing Treatment.

Reading Number	Percent Design Speed	Discharge Valve Setting	Inlet Corrected Weight Flow, Lbs/Sec	Stage Total-Pressure Ratio	Stage Adiabatic Efficiency	Type Point**
19	70	30	165.8	1.200	.81	OP
20	70	12.5	153.4	1.256	.828	OP
21	70	5.9	137.1	1.283	.795	OP
22	70	10	149.1	1.268	.840	OP
23	70	15	156.3	1.244	.824	OP
24	90	30	202.5	1.321	.724	OP
25	90	15	199.4	1.422	.797	OP
26	90	10	193.6	1.490	.822	OP
27	90	5.6	178.2	1.545	.797	OP
28	90	8	188.0	1.521	.816	OP
29	100	30	216.0	1.374	.692	BE (p. 344)
30	100	11	212.7	1.583	.785	BE (p. 346)
31	100	9	209.1	1.637	.793	OP
32	100	7	203.5	1.684	.785	BE (p. 348)
33	100	15	214.5	1.504	.764	OP
34	70	10	149.8	1.269	.835	OP
<p>** - OP - Overall Performance Reading BE - Blade Element Performance Reading</p>						

Table V. Summary of Task I Stage Radial Distortion Test Data (Continued).

i. Blade Angle Insert #1 Casing Treatment.

Reading Number	Percent Design Speed	Discharge Valve Setting	Inlet Corrected Weight Flow, Lbs/Sec	Stage Total-Pressure Ratio	Stage Adiabatic Efficiency	Type Point**
270	70	30	165.5	1.199	.809	OP
271	70	15	156.2	1.242	.836	OP
272	70	10	147.6	1.266	.823	OP
273	70	4.5	131.6	1.279	.787	OP
275	90	15	197.5	1.406	.801	OP
276	90	10	190.5	1.465	.812	OP
277	90	5.5	174.4	1.515	.784	OP
278	90	30	201.2	1.315	.730	OP
279	100	30	214.2	1.367	.685	BE (p. 350)
280	100	7	201.7	1.658	.782	BE (p. 352)
281	100	11	212.0	1.568	.789	BE (p. 354)
282	100	15	213.4	1.488	.769	OP
283	70	10	147.5	1.264	.827	OP

** - OP - Overall Performance Reading
BE - Blade Element Performance Reading

Table V. Summary of Task I Stage Radial Distortion Test Data (Continued).

f. Skewed Slotted Insert #1 Casing Treatment.

Reading Number	Percent Design Speed	Discharge Valve Setting	Inlet Corrected Weight Flow, Lbs/Sec	Stage Total-Pressure Ratio	Stage Adiabatic Efficiency	Type Point**
100	70	30	166.7	1.199	.806	OP
101	70	4.5	134.4	1.291	.794	OP
102	70	8	144.2	1.281	.833	OP
103	70	12.5	155.2	1.256	.846	OP
104	70	15	158.4	1.244	.850	OP
105	90	30	203.1	1.315	.723	OP
106	90	5.2	177.5	1.548	.785	OP
107	90	12	197.5	1.457	.821	OP
108	90	10	194.6	1.488	.828	OP
109	90	8	188.1	1.519	.815	OP
110	100	30	215.7	1.369	.689	OP
111	100	6.5	202.2	1.690	.782	BE (p. 332)
112	100	9	209.9	1.634	.792	BE (p. 334)
113	100	11	212.6	1.576	.791	OP
114	100	15	214.8	1.493	.764	OP
115	100	30	215.3	1.370	.693	BE (p. 336)
<p>** - OP - Overall Performance Reading BE - Blade Element Performance Reading</p>						

Table V. Summary of Task I Stage Radial Distortion Test Data (Continued).

g. Skewed Slotted Insert #3 Casing Treatment.

Reading Number	Percent Design Speed	Discharge Valve Setting	Inlet Corrected Weight Flow, Lbs/Sec	Stage Total-Pressure Ratio	Stage Adiabatic Efficiency	Type Point**
245	70	30	165.3	1.198	.759	OP
246	70	15	155.4	1.239	.821	OP
247	70	10	148.1	1.264	.847	OP
248	70	6.5	138.0	1.276	.800	OP
249	90	30	202.0	1.316	.736	OP
250	90	15	199.0	1.415	.797	OP
251	90	10	191.9	1.478	.820	OP
252	90	8	186.5	1.505	.808	OP
253	100	30	215.9	1.373	.706	BE (p. 338)
254	100	11	211.8	1.578	.791	BE (p. 340)
255	100	8.2	207.0	1.646	.794	BE (p. 342)
256	100	15	214.5	1.498	.772	OP

** - OP - Overall Performance Reading
BE - Blade Element Performance Reading

Table V. Summary of Task I Stage Radial Distortion Test Data (Continued).

d. Circumferential Grooved Insert #2 Casing Treatment.

Reading Number	Percent Design Speed	Discharge Valve Setting	Inlet Corrected Weight Flow, Lbs/Sec	Stage Total-Pressure Ratio	Stage Adiabatic Efficiency	Type Point**
147	70	30	165.3	1.196	.795	OP
148	90	30	200.4	1.307	.734	OP
149	100	8.5	207.2	1.633	.813	BE (p. 320)
150	100	30	213.3	1.360	.706	BE (p. 322)
151	100	9.5	209.2	1.608	.812	BE (p. 324)
152	100	11	210.9	1.572	.806	OP
153	100	15	212.8	1.487	.781	OP
154	90	8	186.9	1.498	.826	OP
155	90	10	191.9	1.473	.834	OP
156	90	12	196.2	1.443	.832	OP
157	90	9	189.3	1.488	.833	OP
158	70	15	157.6	1.243	.848	OP
159	70	12.5	153.6	1.252	.846	OP
160	70	9	145.4	1.267	.833	OP
161	70	7.5	141.2	1.270	.821	OP
** - OP - Overall Performance Reading BE - Blade Element Performance Reading						

Table V. Summary of Task I Stage Radial Distortion Test Data (Continued).

e. Circumferential Grooved Insert #3 Casing Treatment.

Reading Number	Percent Design Speed	Discharge Valve Setting	Inlet Corrected Weight Flow, Lbs/Sec	Stage Total-Pressure Ratio	Stage Adiabatic Efficiency	Type Point**
214	70	30	163.5	1.197	.810	OP
215	70	7.7	139.0	1.266	.811	OP
216	70	10	145.7	1.261	.835	OP
217	70	12.5	151.8	1.250	.837	OP
218	70	15	155.6	1.238	.834	OP
219	90	30	198.5	1.309	.743	OP
220	90	12	193.6	1.439	.830	OP
221	90	10	190.7	1.465	.832	OP
222	90	8	183.6	1.489	.823	OP
223	100	30	211.9	1.363	.705	BE (p. 326)
224	100	9	204.9	1.608	.808	BE (p. 328)
225	100	8.5	205.1	1.620	.805	OP
226	100	11	207.6	1.563	.806	BE (p. 330)
227	100	15	211.3	1.488	.789	OP

** - OP - Overall Performance Reading
BE - Blade Element Performance Reading

Table V. Summary of Task I Stage Radial Distortion Test Data (Continued).

b. Honeycomb Insert #2 Casing Treatment.

Reading Number	Percent Design Speed	Discharge Valve Setting	Inlet Corrected Weight Flow, Lbs/Sec	Stage Total-Pressure Ratio	Stage Adiabatic Efficiency	Type Point**
48	70	30	165.3	1.196	.797	OP
49	90	30	201.2	1.308	.731	OP
50	100	30	214.3	1.362	.703	OP
51	100	7.5	204.3	1.649	.786	BE (p. 308)
52	100	9	207.5	1.617	.797	BE (p. 310)
53	100	30	214.4	1.364	.708	BE (p. 312)
54	90	10	191.4	1.469	.825	OP
55	90	6.5	179.6	1.506	.797	OP
56	70	12.5	151.3	1.251	.844	OP
57	70	5	132.3	1.275	.777	OP
58	70	8	143.6	1.270	.819	OP
** - OP - Overall Performance Reading BE - Blade Element Performance Reading						

Table V. Summary of Task I Stage Radial Distortion Test Data (Continued).

c. Circumferential Grooved Insert #1 Casing Treatment.

Reading Number	Percent Design Speed	Discharge Valve Setting	Inlet Corrected Weight Flow, Lbs/Sec	Stage Total-Pressure Ratio	Stage Adiabatic Efficiency	Type Point**
82	70	30	165.1	1.196	.800	OP
83	70	12	150.6	1.251	.843	OP
84	70	8	140.7	1.266	.821	OP
85	90	30	199.7	1.307	.741	OP
86	90	10	191.0	1.465	.831	OP
87	90	8.5	186.6	1.486	.827	OP
88	100	30	212.9	1.360	.712	OP
89	100	8.5	206.5	1.619	.808	OP
90	100	9	207.1	1.611	.811	BE (p. 314)
91	100	11	209.7	1.563	.804	BE (p. 316)
92	100	15	212.1	1.485	.778	BE (p. 318)
93	100	30	213.2	1.363	.710	OP
94	90	15	197.7	1.401	.817	OP
95	90	12	194.3	1.437	.825	OP
96	70	15	157.2	1.238	.843	OP
97	70	10	147.1	1.258	.838	OP

** - OP - Overall Performance Reading
BE - Blade Element Performance Reading

Table IV. Summary of Task I Stage Undistorted Inlet Test Data (Concluded).

k. Blade Angle Slotted Insert #2 Casing Treatment.

Reading Number	Percent Design Speed	Discharge Valve Setting	Inlet Corrected Weight Flow, Lbs/Sec	Stage Total-Pressure Ratio	Stage Adiabatic Efficiency	Type Point**
325	70	30	167.2	1.181	.788	OP
326	70	18.5	162.8	1.210	.838	OP
327	70	13.5	156.8	1.236	.867	OP
328	70	10	152.0	1.256	.869	OP
329	70	8	144.3	1.267	.853	OP
330	70	5	135.1	1.279	.81	OP
331	70	0.8	116.2	1.285	.737	OP
332	90	30	204.7	1.293	.729	OP
333	90	15	203.6	1.39	.837	OP
334	90	10	197.2	1.469	.865	OP
335	90	8	190.7	1.503	.858	OP
336	90	3.8	164.5	1.521	.777	OP
337	90	5	175.5	1.53	.812	OP
338	100	30	220.6	1.355	.696	BE (p. 295)
339	100	9	214.6	1.63	.846	BE (p. 297)
340	100	4.3	184.2	1.688	.757	BE (p. 299)
341	100	7	206.9	1.68	.826	OP
342	100	11	218.1	1.565	.831	OP
<p>* - Indicates discharge valve position with inner annulus discharge pipe closed. ** - OP - Overall Performance Reading BE - Blade Element Performance Reading</p>						

Table V. Summary of Task I Stage Radial Distortion Test Data.

a. Honeycomb Insert #1 Casing Treatment.

Reading Number	Percent Design Speed	Discharge Valve Setting	Inlet Corrected Weight Flow, Lbs/Sec	Stage Total-Pressure Ratio	Stage Adiabatic Efficiency	Type Point**
22	70	30	164.8	1.178	.722	OP
23	70	15	158.1	1.240	.823	OP
24	70	4	129.6	1.275	.758	OP
25	70	7	141.2	1.277	.814	OP
26	90	30	202.0	1.309	.725	OP
27	90	5.5	176.5	1.521	.776	OP
28	90	10	193.0	1.473	.822	OP
29	100	30	214.4	1.362	.690	OP
30	100	6.5	199.9	1.672	.784	OP
31	100	7	202.1	1.668	.795	BE (p. 302)
32	100	12	211.3	1.547	.784	BE (p. 304)
33	100	30	214.3	1.363	.698	BE (p. 306)

** - OP - Overall Performance Reading
BE - Blade Element Performance Reading

Table III. Summary of Blade Element Data Reduction Constants (Continued).

(d) Rotor - Task II

Parameter	% Immersion	Plane 0.95	Edge 1	Edge 2	Plane 1.51
No K_{bl} included	5	78.50			62.89
	10	119.70			99.21
	30	177.58			148.69
	50	157.38			133.36
	70	145.51			111.59
	90	86.66			74.96
A_j	95	49.60			36.54
	0	18.323	18.173	17.890	17.838
	5	17.835	17.706	17.525	17.462
	10	17.420	17.350	17.138	17.081
	30	15.604	15.610	15.567	15.568
	50	13.797	13.900	14.008	14.056
r_j	70	11.972	12.150	12.425	12.543
	90	9.910	10.212	10.904	11.030
	95	9.285	9.625	10.500	10.652
	100	8.737	9.125	10.141	10.287
	0	-2.68	-8.77	-5.89	-0.28
	5	-2.37	-6.58	-5.30	-0.70
e_j°	10	-1.92	-4.95	-4.47	-0.83
	30	1.05	0.28	-0.97	0.50
	50	4.85	4.53	2.81	3.14
	70	9.40	9.41	7.20	6.80
	90	15.60	16.20	12.31	11.17
	95	17.55	18.02	13.50	12.28
K_j'	100	19.59	19.46	14.86	13.42
	0		63.30	57.27	
	5		61.28	57.52	
	10		60.25	57.18	
	30		57.07	52.85	
	50		53.90	46.10	
	70		50.80	34.70	
	90		48.58	16.84	
	95		48.02	10.70	
	100		47.50	4.56	

Parameter	% Immersion	
$(W_j/W^*)_l$ $(W_j/W^*)_u$	5	1.0589
	10	1.0602
	30	1.0555
	50	1.0537
	70	1.0544
	90	1.0479
$(W_j/W^*)_2$ $(W_j/W^*)_d$	95	1.0378
	5	1.0460
	10	1.0307
	30	1.0214
	50	1.0200
	70	1.0013
\bar{r}_j (Used for Diffusion Factor)	90	0.9897
	95	0.9908
	5	17.616
	10	17.244
	30	15.589
	50	13.954
σ_j (Used for Diffusion Factor)	70	12.288
	90	10.558
	95	10.063
	5	1.431
	10	1.461
	30	1.612
	50	1.773
	70	1.964
	90	2.248
	95	2.347

Radii are in inches
Areas are in square inches

Table III. Summary of Blade Element Data Reduction Constants (Concluded).

(e) Stator - Task II

Parameter	% Immersion	Plane 1.51	Edge 1	Edge 2	Plane 2.20
No K_{bl} included	5	62.89			58.73
	10	99.21			91.59
	30	148.69			134.20
	50	133.36			121.11
	70	111.59			108.78
	90	74.96			64.09
A_j	95	36.54			29.08
	0	17.838	17.836	17.836	17.836
	5	17.462	17.450	17.463	17.478
	10	17.081	17.075	17.125	17.130
	30	15.568	15.610	15.700	15.750
	50	14.056	14.175	14.363	14.420
r_j	70	12.543	12.725	12.980	13.075
	90	11.030	11.300	11.720	11.775
	95	10.652	10.950	11.388	11.475
	100	10.287	10.625	11.100	11.168
	0	-0.28	0	0	0
	5	-0.70	0.24	0.22	0.12
ϵ_j°	10	-0.83	0.50	0.42	0.24
	30	0.50	1.70	1.28	0.71
	50	3.14	3.52	2.18	1.13
	70	6.80	6.04	3.25	1.38
	90	11.17	9.40	4.39	1.14
	95	12.28	10.31	4.80	0.92
K_j° (At nominal stator setting)	100	13.42	11.38	4.70	0.65
	0		40.09	-13.08	
	5		39.47	-11.13	
	10		39.11	-10.10	
	30		39.01	-8.87	
	50		39.80	-8.75	
	70		40.86	-9.10	
	90		42.22	-10.58	
	95		42.76	-12.36	
	100		43.32	-12.88	

Parameter	% Immersion	
$\frac{(W_j/W^*)_l}{(W_j/W^*)_u}$	5	0.9992
	10	1.0043
	30	1.0229
	50	1.0327
	70	1.0385
	90	1.0378
$\frac{(W_j/W^*)_2}{(W_j/W^*)_d}$	95	1.0334
	5	0.9880
	10	0.9873
	30	0.9904
	50	0.9932
	70	0.9987
\bar{r}_j (Used for Diffusion Factor)	90	1.0158
	95	1.0254
	5	17.457
	10	17.100
	30	15.655
	50	14.269
σ_j (Used for Diffusion Factor)	70	12.853
	90	11.510
	95	11.169
	5	1.523
	10	1.544
	30	1.631
	50	1.742
	70	1.880
	90	2.051
	95	2.098

Radii are in inches
Areas are in square inches

Table IV. Summary of Task I Stage Undistorted Inlet Test Data.

a. Honeycomb #1 Casing Treatment.

Reading Number	Percent Design Speed	Discharge Valve Setting	Inlet Corrected Weight Flow, Lbs/Sec	Stage Total-Pressure Ratio	Stage Adiabatic Efficiency	Type Point**
1	70	30	168.6	1.182	.812	OP
2	70	15	159.1	1.228	.862	OP
3	70	9	148.1	1.262	.861	OP
4	70	6	139.5	1.276	.827	OP
5	70	6	138.3	1.275	.824	OP
6	70	2	123.3	1.283	.759	OP
7	70	25*	113.9	1.285	.713	OP
8	90	50*	187.8	1.509	.843	OP
9	90	35*	173.6	1.532	.801	OP
10	90	80*	196.1	1.471	.858	OP
11	90	50	205.0	1.272	.697	OP
12	90	4.5	171.8	1.531	.788	OP
13	100	30	220.7	1.347	.691	OP
14	100	4.5	186.7	1.691	.755	OP
15	100	5	190.8	1.697	.775	BE (p. 235)
16	100	9	214.5	1.629	.835	BE (p. 237)
17	100	15	219.1	1.472	.798	BE (p. 239)
18	90	15	203.7	1.389	.823	OP
19	90	6	182.7	1.528	.822	OP
20	70	15	160.7	1.231	.865	OP
21	70	0.35	114.3	1.284	.702	OP
<p>* - Indicates discharge valve position with inner annulus discharge pipe closed. ** - OP - Overall Performance Reading BE - Blade Element Performance Reading</p>						

Table IV. Summary of Task I Stage Undistorted Inlet Test Data (Continued).

b. Honeycomb Insert #2 Casing Treatment.

Reading Number	Percent Design Speed	Discharge Valve Setting	Inlet Corrected Weight Flow, Lbs/Sec	Stage Total-Pressure Ratio	Stage Adiabatic Efficiency	Type Point**
34	70	30	166.5	1.181	.807	OP
35	70	1.5	117.3	1.279	.735	OP
36	90	30	205.9	1.292	.741	OP
37	90	4.5	172.2	1.523	.801	OP
38	100	30	220.4	1.355	.693	OP
39	100	4.5	184.3	1.686	.758	BE (p. 241)
40	100	9	213.7	1.630	.844	BE (p. 243)
41	100	15	221.1	1.484	.816	BE (p. 245)
42	90	6	180.9	1.529	.840	OP
43	90	15	202.8	1.394	.826	OP
44	70	11	152.3	1.254	.865	OP
45	70	8	144.6	1.268	.847	OP
46	70	4.5	133.0	1.281	.814	OP
47	100	6.2	201.5	1.699	.820	OP
49	100	7.8	210.3	1.659	.841	OP
60	90	10	195.6	1.470	.868	OP
61	90	8	190.2	1.503	.856	OP
62	70	15.8	159.4	1.225	.870	OP
63	70	13.5	157.1	1.236	.872	OP
64	70	11	152.0	1.250	.869	OP

* - Indicates discharge valve position with inner annulus discharge pipe closed.

** - OP - Overall Performance Reading

BE - Blade Element Performance Reading

Table IV. Summary of Task I Stage Undistorted Inlet Test Data (Continued).

c. Circumferential Grooved Insert #1 Casing Treatment.

Reading Number	Percent Design Speed	Discharge Valve Setting	Inlet Corrected Weight Flow, Lbs/Sec	Stage Total-Pressure Ratio	Stage Adiabatic Efficiency	Type Point**
65	70	30	167.3	1.181	.820	OP
66	70	13	156.6	1.236	.872	OP
67	70	8	144.5	1.263	.851	OP
68	70	2	121.6	1.280	.769	OP
69	70	4.5	132.7	1.277	.822	OP
70	90	30	203.4	1.286	.740	OP
71	90	15	201.2	1.385	.834	OP
72	90	10	196.4	1.466	.872	OP
73	90	6	181.4	1.522	.841	OP
74	90	4.5	169.3	1.522	.800	OP
75	100	30	216.7	1.341	.701	OP
76	100	30	216.9	1.342	.709	BE (p. 247)
77	100	9	212.5	1.619	.850	BE (p. 249)
78	100	6.5	202.6	1.687	.837	OP
79	100	6	199.2	1.693	.829	BE (p. 251)
80	100	5.9	198.6	1.692	.824	OP
81	70	16	160.3	1.226	.876	OP
<p>* - Indicates discharge valve position with inner annulus discharge pipe closed.</p> <p>** - OP - Overall Performance Reading</p> <p>BE - Blade Element Performance Reading</p>						

d. Circumferential Grooved Insert #2 Casing Treatment.

Reading Number	Percent Design Speed	Discharge Valve Setting	Inlet Corrected Weight Flow, Lbs/Sec	Stage Total-Pressure Ratio	Stage Adiabatic Efficiency	Type Point**
132	70	30	167.1	1.180	.797	OP
133	70	2	122.0	1.282	.758	OP
134	70	4.5	133.9	1.279	.812	OP
135	70	8	144.8	1.267	.850	OP
136	70	13.5	157.4	1.236	.872	OP
137	90	30	203.6	1.286	.742	OP
138	90	4.5	169.3	1.525	.797	OP
139	90	6	181.8	1.527	.843	OP
140	90	8	190.7	1.505	.869	OP
141	90	10	196.2	1.470	.877	OP
142	100	5	190.4	1.692	.789	BE (p. 253)
143	100	9	213.2	1.626	.857	BE (p. 255)
144	100	30	217.3	1.347	.710	BE (p. 257)
145	100	11	216.4	1.559	.847	OP
146	100	7	206.3	1.683	.848	OP

* - Indicates discharge valve position with inner annulus discharge pipe closed.
 ** - OP - Overall Performance Reading
 BE - Blade Element Performance Reading

Table IV. Summary of Task I Stage Undistorted Inlet Test Data (Continued).

e. Circumferential Grooved Insert #3 Casing Treatment.

Reading Number	Percent Design Speed	Discharge Valve Setting	Inlet Corrected Weight Flow, Lbs/Sec	Stage Total-Pressure Ratio	Stage Adiabatic Efficiency	Type Point**
194	70	30	165.0	1.182	.818	OP
195	70	13.5	155.5	1.234	.874	OP
196	70	10	149.3	1.252	.871	OP
197	70	8	143.6	1.264	.860	OP
198	70	5	133.9	1.275	.820	OP
199	70	2.5	123.1	1.280	.786	OP
200	90	30	202.8	1.288	.743	OP
201	90	15	200.7	1.284	.839	OP
202	90	10	195.6	1.466	.878	OP
203	90	8	189.6	1.498	.869	OP
204	90	6	179.6	1.517	.844	OP
205	90	4	165.6	1.518	.789	OP
206	100	30	217.9	1.345	.699	OP
207	100	4.7	186.8	1.679	.781	BE (p. 259)
208	100	9	212.4	1.621	.854	BE (p. 261)
209	100	30	216.0	1.341	.705	BE (p. 263)
210	100	11	216.9	1.564	.853	OP
211	100	7	205.2	1.676	.854	OP
212	70	10	151.1	1.255	.863	OP
213	70	1.8	121.0	1.281	.761	OP
<p>* - Indicates discharge valve position with inner annulus discharge pipe closed. ** - OP - Overall Performance Reading BE - Blade Element Performance Reading</p>						

Table IV. Summary of Task I Stage Undistorted Inlet Test Data (Continued).

f. Skewed Slotted Insert #1 Casing Treatment.

Reading Number	Percent Design Speed	Discharge Valve Setting	Inlet Corrected Weight Flow, Lbs/Sec	Stage Total-Pressure Ratio	Stage Adiabatic Efficiency	Type Point**
116	70	24*	110.9	1.287	.692	OP
117	100	4.8	187.8	1.695	.763	BE (p. 265)
118	100	9	214.0	1.630	.832	BE (p. 267)
119	100	30	219.6	1.354	.694	BE (p. 269)
120	100	11	218.1	1.567	.828	OP
121	100	7	206.1	1.692	.825	OP
122	90	4	166.5	1.535	.769	OP
123	90	6	181.7	1.538	.824	OP
124	90	8	190.4	1.512	.850	OP
125	90	10	196.9	1.477	.856	OP
126	90	15	201.9	1.394	.824	OP
127	90	30	205.3	1.292	.727	OP
128	70	30	168.6	1.184	.806	OP
129	70	13.5	157.5	1.237	.853	OP
130	70	8	145.1	1.268	.836	OP
131	70	2.5	125.5	1.285	.765	OP

* - Indicates discharge valve position with inner annulus discharge pipe closed.
 ** - OP - Overall Performance Reading
 BE - Blade Element Performance Reading

Table IV. Summary of Task I Stage Undistorted Inlet Test Data (Continued).

g. Skewed Insert #2 Casing Treatment.

Reading Number	Percent Design Speed	Discharge Valve Setting	Inlet Corrected Weight Flow, Lbs/Sec	Stage Total-Pressure Ratio	Stage Adiabatic Efficiency	Type Point**
163	90	30	202.3	1.285	.740	OP
164	90	5	172.5	1.532	.806	OP
165	90	6	181.1	1.532	.834	OP
166	90	8	190.8	1.509	.857	OP
167	90	10	196.4	1.472	.864	OP
168	90	15	200.5	1.386	.828	OP
169	100	4.5	185.2	1.687	.759	BE (p. 271)
170	100	9	212.3	1.619	.840	BE (p. 273)
171	100	30	216.3	1.344	.697	BE (p. 275)
172	100	11	214.8	1.551	.830	OP
173	100	7	207.5	1.676	.831	OP
174	70	30	167.6	1.187	.836	OP
175	70	13.5	156.0	1.237	.878	OP
176	70	8	144.5	1.266	.852	OP
177	70	2.5	124.9	1.283	.778	OP
178	70	26*	115.4	1.285	.728	OP
179	70	20	163.2	1.205	.843	OP
<p>* - Indicates discharge valve position with inner annulus discharge pipe closed. ** - OP - Overall Performance Reading BE - Blade Element Performance Reading</p>						

Table IV. Summary of Task I Stage Undistorted Inlet Test Data (Continued).

h. Skewed Slotted Insert #3 Casing Treatment.

Reading Number	Percent Design Speed	Discharge Valve Setting	Inlet Corrected Weight Flow, Lbs/Sec	Stage Total-Pressure Ratio	Stage Adiabatic Efficiency	Type Point**
228	70	30	166.4	1.182	.829	OP
229	70	18.5	161.6	1.211	.856	OP
230	70	13.5	156.7	1.237	.875	OP
231	70	10	150.2	1.255	.873	OP
232	70	8	145.5	1.267	.846	OP
233	70	5	136.31	1.277	.814	OP
234	70	26.5	116.8	1.284	.730	OP
235	90	30	204.9	1.293	.733	OP
236	90	15	204.5	1.391	.839	OP
237	90	10	197.7	1.476	.865	OP
238	90	8	190.7	1.508	.861	OP
239	90	4.5	170.7	1.531	.792	OP
240	100	30	221.5	1.355	.694	BE (p. 277)
241	100	9	215.2	1.638	.848	BE (p. 279)
242	100	4.5	184.7	1.691	.766	BE (p. 281)
243	100	7	206.5	1.692	.831	OP
244	100	11	217.3	1.574	.833	OP

* - Indicates discharge valve position with inner annulus discharge pipe closed.
 ** - OP - Overall Performance Reading
 BE - Blade Element Performance Reading

Table IV. Summary of Task I Stage Undistorted Inlet Test Data (Continued).

i. Skewed Slotted Insert #4 Casing Treatment.

Reading Number	Percent Design Speed	Discharge Valve Setting	Inlet Corrected Weight Flow, Lbs/Sec	Stage Total-Pressure Ratio	Stage Adiabatic Efficiency	Type Point**
1	70	30	167.7	1.183	.807	OP
2	70	18.5	162.2	1.213	.857	OP
3	70	13.5	158.2	1.240	.884	OP
4	70	10	151.3	1.259	.866	OP
5	90	30	205.1	1.296	.718	OP
6	90	15	202.9	1.398	.837	OP
7	90	10	196.7	1.478	.861	OP
8	90	8	190.3	1.515	.853	OP
9	70	24.8*	113.8	1.285	.712	OP
10	70	8	145.4	1.268	.838	OP
11	70	5	134.8	1.280	.812	OP
12	90	4.4	169.1	1.536	.771	OP
13	100	30	220.1	1.355	.688	BE (p. 283)
14	100	9	213.4	1.640	.832	BE (p. 285)
15	100	4.6	184.8	1.699	.745	BE (p. 287)
16	100	11	217.6	1.580	.828	OP
17	100	7	206.5	1.697	.821	OP
18	90	5	173.7	1.544	.788	OP
<p>* - Indicates discharge valve position with inner annulus discharge pipe closed. ** - OP - Overall Performance Reading BE - Blade Element Performance Reading</p>						

Table IV. Summary of Task I Stage Undistorted Inlet Test Data (Continued).

j. Blade Angle Slotted Insert #1 Casing Treatment.

Reading Number	Percent Design Speed	Discharge Valve Setting	Inlet Corrected Weight Flow, Lbs/Sec	Stage Total-Pressure Ratio	Stage Adiabatic Efficiency	Type Point**
257	70	30	166.5	1.181	.805	OP
258	70	18.5	162.2	1.211	.858	OP
259	70	13.5	157.0	1.236	.868	OP
260	70	10	151.0	1.255	.852	OP
261	70	8	144.8	1.267	.861	OP
262	70	5	135.9	1.278	.811	OP
263	90	30	205.2	1.293	.744	OP
264	90	15	203.0	1.391	.840	OP
265	90	10	195.5	1.463	.863	OP
266	90	8	190.3	1.499	.867	OP
267	70	25	113.8	1.283	.709	OP
268	90	3.6	162.4	1.514	.756	OP
269	100	30	221.7	1.443	.838	BE (p. 287)
284	100	30	220.9	1.358	.696	BE (p. 289)
285	100	9	214.4	1.620	.845	BE (p. 291)
286	100	4	180.6	1.681	.743	BE (p. 293)
287	100	7	205.1	1.670	.832	OP
288	100	11	218.2	1.565	.832	OP
289	70	10	150.8	1.256	.867	OP
290	70	8	145.1	1.266	.853	OP

* - Indicates discharge valve position with inner annulus discharge pipe closed.
** - OP - Overall Performance Reading
BE - Blade Element Performance Reading

Range and Distortion
Stages", Design Report

Stage Experimental Eval-
or Blading, Part 1,
April 1, 1967

"Evaluation of Range
nber Transonic Fan Stages,

Distortion Tolerance for
sk II Stage Data and
Flow Testing", NASA

Range and Distortion
Fan Stages, Task II
et Flow Distortion

er Case Blowing or
essor, Part VI - Final

ions of Effect of Porous
ial-Flow Compressor Rotor",

age Experimental Eval-
or Blading, Part 2,
September 22, 1967

0.01, Vehicle Inlet	6 7-element pitot-static rakes 24 total-temperature thermocouples	6 7-element pitot-static rakes 24 total-temperature thermocouples	2 7-element total pressure distortion rakes	1 4-parameter combination probe (total temperature and pressure, static pressure, flow angle)	1 4-parameter combination probe 3 hot-wire probes	7 14-element wake rakes (total temperature and pressure) 1 4-parameter combination probe	Plane 2.20, Exit	7 14-element wake rakes (total temperature and pressure) 1 static pressure wedge probe	Plane 1.51, Stator Inlet	1 static pressure wedge probe 1 cobra probe (flow angle, total temperature and pressure) 3 hot-wire probes	1 4-element wake rakes (total temperature and pressure) 1 static pressure wedge probe
---------------------------	--	--	--	---	--	--	------------------------	--	-----------------------------------	---	---

ns and Performance.

<u>TASK I</u> <u>STAGE</u>	<u>TASK II</u> <u>STAGE</u>
-------------------------------	--------------------------------

000	1500
-----	------

9.4	226.0
-----	-------

617	1.659
-----	-------

873	0.854
-----	-------

24

0.37

0

5	36.5
---	------

0.5

5	41.62
---	-------

4	1.526
---	-------

2	0.368
---	-------

6	1.686
---	-------

5	0.883
---	-------

1.4

2.36

44

0.766

0

0.435

1.22

2.155

2.065

46

Table I. Summary of Stage Design Specifications and Performance.

	<u>TASK I</u> <u>STAGE</u>	<u>TASK II</u> <u>STAGE</u>
Rotor inlet corrected tip speed, ft/sec	1400	1500
Stage inlet corrected weight flow, lbs/sec	219.4	226.0
Stage total-pressure ratio	1.617	1.659
Stage adiabatic efficiency	0.873	0.854
Number of inlet guide vanes	0	24
Inlet guide vane total-pressure loss, percent inlet total pressure	0	0.37
Inlet guide vane exit flow angle, deg.	0	0
Rotor inlet tip diameter, in.	36.5	36.5
Rotor inlet hub: tip radius ratio	0.5	0.5
Rotor inlet corrected weight flow per unit annulus area, lbs/sec-sq ft	40.25	41.62
Rotor inlet tip relative Mach number	1.414	1.526
Rotor tip diffusion factor	0.382	0.368
Rotor total-pressure ratio	1.636	1.686
Rotor adiabatic efficiency	0.8915	0.883
Rotor tip solidity	1.3	1.4
Rotor aspect ratio	2.5	2.36
Number of rotor blades	44	44
Stator inlet hub absolute Mach number	0.684	0.766
Stator exit flow angle, deg.	0	0
Stator hub diffusion factor	0.474	0.435
Stator total-pressure loss, percent stator inlet total pressure	1.17	1.22
Stator hub solidity	2.155	2.155
Stator aspect ratio	2.065	2.065
Number of stator vanes	46	46

Table II (a). Summary of Instrumentation Used for Task I Stage Testing.

INSTRUMENTATION		
LOCATION	UNDISTORTED INLET AND RADIAL DISTORTION	CIRCUMFERENTIAL DISTORTION
Plane 0.01, Vehicle Inlet	6 7-element pitot-static rakes 24 total-temperature thermocouples	6 7-element pitot-static rakes 24 total-temperature thermocouples
Plane 0.18, Stage Inlet	2 7-element total pressure distortion rakes	2 7-element total pressure distortion rakes
Plane 0.95, Rotor Inlet	1 4-parameter combination probe (total temperature and pressure, static pressure, flow angle)	1 4-parameter combination probe (total temperature and pressure, static pressure, flow angle)
Plane 1.51, Stator Inlet	1 static pressure wedge probe 1 cobra probe (flow angle, total temperature and pressure) 3 hot-wire probes	1 4-parameter combination probe 3 hot-wire probes
Plane 2.20, Stage Exit	7 14-element wake rakes (total temperature and pressure) 1 static pressure wedge probe	7 14-element wake rakes (total temperature and pressure) 1 4-parameter combination probe

Table II (b). Summary of Instrumentation Used for Task II Stage Testing.

(For all flow conditions except as noted)

LOCATION	INSTRUMENTATION
Plane 0.01 Vehicle Inlet	6 7-element pitot-static rakes 24 total temperature thermocouples
Plane 0.18 Stage Inlet	2 7-element total pressure distortion rakes 1 4-parameter combination probe (total temperature and pressure, static pressure, flow angle)
Plane 0.95 Rotor Inlet	1 4-parameter combination probe 1 static-pressure wedge probe* 3 14-element wake rakes (total pressure)**
Plane 1.51 Stator Inlet	1 4-parameter combination probe
Plane 2.20 Stage Exit	7 14-element wake rakes (total temperature and pressure) 1 4-parameter combination probe
<p>* Used during supplementary undistorted inlet tests without inlet guide vanes and without casing treatment</p> <p>** Used during circumferential distortion tests with inlet guide vanes and with casing treatment</p>	

Table III. Summary of Blade Element Data Reduction Constants.

(a) Rotor - Task I

Parameter	% Immersion	Plane 0.95	Edge 1	Edge 2	Plane 1.51
No K_{bl}	5	78.50			62.89
Included	10	119.70			99.21
A_j	30	177.58			148.69
	50	157.38			133.36
	70	145.51			111.59
	90	86.66			74.96
	95	49.60			36.54
r_j	0	18.323	18.164	17.885	17.838
	5	17.835	17.70	17.513	17.462
	10	17.420	17.310	17.137	17.081
	30	15.604	15.622	15.595	15.568
	50	13.797	13.916	14.034	14.056
	70	11.972	12.182	12.456	12.543
	90	9.910	10.257	10.895	11.030
	95	9.285	9.675	10.513	10.652
	100	8.737	9.125	10.129	10.287
ϵ_j	0	-2.68	-9.0	-5.68	-.28
	5	-2.15	-7.1	-5.1	-.78
	10	-1.88	-4.80	-4.60	-.99
	30	1.07	0.40	-1.50	-.56
	50	4.74	4.35	1.30	.98
	70	9.49	9.55	4.75	3.68
	90	15.78	16.30	10.10	7.82
	95	17.60	18.10	12.10	10.0
	100	19.59	19.46	14.95	13.42
K_j (K_{ssj})	0		61.88 (64.34)	54.93	
	5		60.60 (63.30)	54.80	
	10		59.61 (62.64)	54.42	
	30		56.01 (60.47)	50.68	
	50		52.56 (58.40)	43.79	
	70		49.71 (56.50)	32.15	
	90		47.11 (54.77)	14.29	
	95		46.13 (54.03)	8.00	
	100		45.31 (53.33)	2.86	

Radii are in inches
Areas are in square inches

Parameter	% Immersion	
$\frac{(w_j/w^*)_1}{(w_j/w^*)_u}$	5	1.0843
	10	1.0837
	30	1.0707
	50	1.0586
	70	1.0565
	90	1.0388
	95	1.0330
$\frac{(w_j/w^*)_2}{(w_j/w^*)_d}$	5	.9983
	10	.9932
	30	.9768
	50	.9762
	70	.9729
	90	.9747
	95	.9754
\bar{r}_j (Used for Diffusion Factor)	5	17.640
	10	17.201
	30	15.613
	50	13.989
	70	12.355
	90	10.622
	95	10.065
σ_j	5	1.334
	10	1.369
	30	1.508
	50	1.684
(Used for Diffusion Factor)	70	1.906
	90	2.217
	95	2.339

Table III. Summary of Blade Element Data Reduction Constants (Continued).

(b) Stator - Task I

Parameter	% Immersion	Plane 1.51	Edge 1	Edge 2	Plane 2.20
No K_{bl}	5	62.89			58.73
	10	99.21			91.59
Included	30	148.69			134.20
	50	133.36			121.11
A_j	70	111.59			108.78
	90	74.96			64.09
	95	36.54			29.08
	0	17.838	17.836	17.836	17.836
	5	17.462	17.450	17.463	17.478
	10	17.081	17.075	17.125	17.130
	30	15.568	15.610	15.700	15.750
	50	14.056	14.175	14.363	14.420
	70	12.543	12.725	12.980	13.075
	90	11.030	11.300	11.720	11.775
	95	10.652	10.950	11.388	11.475
	100	10.287	10.625	11.100	11.168
	0	-.28	0	0	0
	5	-.78	.30	.28	.155
	10	-.99	.575	.60	.30
	30	-.56	2.18	1.65	.89
	50	.98	4.50	2.70	1.325
	70	3.68	7.40	3.75	1.60
	90	7.82	10.30	4.50	1.28
	95	10.0	11.0	4.60	1.035
	100	13.42	11.38	4.70	.650
	0		40.09	-13.08	
	5		39.47	-11.13	
	10		39.11	-10.10	
	30		39.01	- 8.87	
	50		39.80	- 8.75	
	70		40.86	- 9.10	
	90		42.22	-10.58	
	95		42.76	-12.36	
	100		43.32	-12.88	

Parameter	% Immersion	
$(w_j/w^*)_l$	5	1.0028
$(w_j/w^*)_u$	10	1.0099
	30	1.0294
	50	1.0388
	70	1.0339
	90	1.0178
	95	1.0104
	5	.9842
	10	.9856
	30	.9884
	50	.9879
	70	1.00
	90	1.028
	95	1.0356
	5	17.457
	10	17.100
	30	15.655
	50	14.269
	70	12.853
	90	11.510
	95	11.169
	5	1.523
	10	1.544
	30	1.631
	50	1.742
	70	1.880
	90	2.051
	95	2.098

Radii are in inches
Areas are in square inches

Table III. Summary of Blade Element Data Reduction Constants (Continued).

(c) IGV - Task II

Parameter	% Immersion	Plane 0.18	Edge 1	Edge 2	Plane 0.95
No K_{bl} included	5	88.40			78.50
	10	133.95			119.70
	30	198.79			177.58
	50	179.55			157.38
	70	163.26			145.51
	90	93.31			86.66
A_j	95	51.94			49.60
r_j	0	18.412	18.408	18.370	18.323
	5	17.893	17.900	17.870	17.835
	10	17.415	17.420	17.450	17.420
	30	15.388	15.39	15.580	15.604
	50	13.300	13.330	13.600	13.797
	70	11.080	11.160	11.590	11.972
	90	8.580	8.700	9.180	9.910
	95	7.781	7.820	8.380	9.285
	100	7.099	7.099	7.680	8.737
ϵ_j°	0	-0.99	-0.01	-1.34	-2.68
	5	-1.05	0.12	-0.78	-2.37
	10	-1.29	0.290	-0.35	-1.91
	30	-1.44	0.90	1.80	1.05
	50	-1.08	1.70	4.46	4.85
	70	-0.66	2.65	7.80	9.38
	90	-0.33	3.05	12.70	15.45
	95	-0.17	2.35	15.15	17.55
	100	0	1.80	17.80	19.59
K_j°	0		0	Equal to	
	5		↓	guide vane	
	10			setting	
	30			angle	
	50				
	70				
	90				
	95		↓		
	100		0		

Parameter	% Immersion	
$(W_j/W^*)_1$ $(W_j/W^*)_u$	5	0.9864
	10	0.9945
	30	1.0128
	50	1.0237
	70	1.0216
	90	1.0111
	95	1.0063
$(W_j/W^*)_2$ $(W_j/W^*)_d$	5	0.9756
	10	0.9739
	30	0.9607
	50	0.9663
	70	0.9576
	90	0.9140
	95	0.8830
\bar{r}_j (Used for Diffusion Factor)	5	17.885
	10	17.435
	30	15.485
	50	13.465
	70	11.375
	90	8.940
	95	8.10
σ_j (Used for Diffusion Factor) (Based on total chord)	5	1.309
	10	1.317
	30	1.361
	50	1.419
	70	1.502
	90	1.646
	95	1.716

Radii are in inches
Areas are in square inches

Table VIII. Summary of Task II Stage Undistorted Inlet Test Data (Continued).

b. Without Inlet Guide Vanes and with Blade Angle Slots #1 Casing Treatment.

Reading Number	Percent Design Speed	Discharge Valve Setting	Inlet Corrected Weight Flow, Lbs/Sec	Stage Total-Pressure Ratio	Stage Adiabatic Efficiency	Type Point**
536	70	30	171.9	1.199	.787	OP
537	70	24.2*	119.8	1.323	.716	OP
538	90	9	201.5	1.536	.836	OP
539	90	3.6	173.2	1.601	.753	OP
540	90	7	195.8	1.577	.834	OP
541	90	15	208.8	1.428	.803	OP
542	90	30	208.5	1.314	.692	OP
543	100	30	226.2	1.383	.668	BE (p. 393)
544	70	15	165.7	1.251	.827	OP
545	70	11	160.1	1.279	.861	OP
546	70	6	145.8	1.305	.807	OP
547	100	15	224.9	1.507	.774	OP
548	100	9	221.4	1.676	.822	BE (p. 395)
549	90	9	201.0	1.539	.841	BE (p. 397)
550	90	5	187.6	1.642	.836	OP
551	70	2.5	131.5	1.313	.756	OP
552	100	7	218.5	1.755	.826	OP
553	100	3.7	190.9	1.806	.737	OP
554	100	4	195.2	1.814	.753	BE (p. 399)
<p>* - Indicates discharge valve position with inner annulus discharge pipe closed. ** - OP - Overall Performance Reading BE - Blade Element Performance Reading</p>						

Table VIII. Summary of Task II Stage Undistorted Inlet Test Data (Continued).

c. Without Inlet Guide Vanes and Without Blade Angle Slots #1 Casing Treatment.

Reading Number	Percent Design Speed	Discharge Valve Setting	Inlet Corrected Weight Flow, Lbs/Sec	Stage Total-Pressure Ratio	Stage Adiabatic Efficiency	Type Point**
586	70	30	173.6	1.199	.804	OP
587	70	10	157.7	1.281	.861	OP
588	70	2	129.8	1.318	.768	OP
589	90	30	209.7	1.319	.712	OP
590	90	5.2	184.6	1.603	.823	OP
591	90	8.5	200.1	1.549	.851	OP
592	90	12	206.5	1.475	.839	OP
593	100	30	224.6	1.374	.681	BE (p. 401)
594	100	6	212.6	1.788	.825	BE (p. 403)
595	100	8	221.2	1.722	.845	BE (p. 405)
596	100	15	224.3	1.513	.798	OP
597	100	10	222.9	1.644	.839	OP
598	100	9	223.0	1.680	.843	OP
599	100	6.6	226.3	1.859	.911	OP
600	90	9.8	203.2	1.516	.848	OP
601	90	6.6	193.3	1.577	.838	OP
602	70	15	165.3	1.248	.851	OP
603	70	8	152.9	1.293	.844	OP
604	70	4	138.1	1.312	.804	OP
605	70	11.4	160.0	1.270	.861	OP
(continued)						

** - OP - Overall Performance Reading
BE - Blade Element Performance Reading

Table VIII. Summary of Task II Stage Undistorted Inlet Test Data (Concluded).

c. Without Inlet Guide Vanes and Without Blade Angle Slots #1 Casing Treatment (Concluded).

Reading Number	Percent Design Speed	Discharge Valve Setting	Inlet Corrected Weight Flow, Lbs/Sec	Stage Total-Pressure Ratio	Stage Adiabatic Efficiency	Type Point**
642	100	6	210.5	1.778	.820	BE (p. 407)
643	100	8	218.3	1.716	.840	BE (p. 409)
644	100	6.6	213.1	1.759	.828	OP
645	100	9	220.6	1.680	.843	BE (p. 411)
646	100	10	221.8	1.645	.837	BE (p. 413)
647	100	12	223.0	1.585	.825	OP
** - OP - Overall Performance Reading BE - Blade Element Performance Reading						

Table IX. Summary of Task II Stage Radial Distortion Test Data.

a. With Inlet Guide Vanes and Blade Angle Slots #1 Casing Treatment.

Reading Number	Percent Design Speed	Discharge Valve Setting	Inlet Corrected Weight Flow, Lbs/Sec	Stage Total-Pressure Ratio	Stage Adiabatic Efficiency	Type Point**
433	70	30	168.9	1.214	.775	OP
434	70	4	134.2	1.309	.764	OP
435	70	14	159.6	1.265	.812	OP
436	90	30	203.3	1.328	.698	OP
437	90	5.1	179.0	1.574	.758	OP
438	90	10.8	197.2	1.491	.788	OP
439	100	30	215.5	1.380	.660	BE (p. 416)
440	100	6	204.0	1.732	.755	BE (p. 419)
441	100	10	212.3	1.618	.763	BE (p. 422)
442	100	12	213.5	1.571	.752	OP
443	90	8	192.2	1.541	.801	OP
444	70	11	155.0	1.282	.815	OP

** - OP - Overall Performance Reading
BE - Blade Element Performance Reading

Table IX. Summary of Task II Stage Radial Distortion Test Data (Continued).

b. Without Inlet Guide Vanes and with Blade Angle Slots #1 Casing Treatment.

Reading Number	Percent Design Speed	Discharge Valve Setting	Inlet Corrected Weight Flow, Lbs/Sec	Stage Total-Pressure Ratio	Stage Adiabatic Efficiency	Type Point**
555	70	30	169.8	1.217	.779	OP
556	70	14	161.9	1.269	.824	OP
557	70	5.2	140.3	1.313	.792	OP
558	90	30	203.8	1.329	.697	OP
559	90	10.3	198.4	1.505	.797	OP
560	90	6.3	186.5	1.569	.781	OP
561	100	30	216.3	1.384	.658	BE (p. 425)
562	100	10.5	213.6	1.612	.758	BE (p. 427)
563	100	6.5	206.8	1.728	.757	BE (p. 429)
564	100	8	210.0	1.685	.768	OP
565	100	11.2	214.1	1.592	.756	OP
566	90	9.2	194.9	1.527	.797	OP
568	70	11	156.6	1.286	.813	OP
569	70	8	150.2	1.304	.809	OP
<p>** - OP - Overall Performance Reading BE - Blade Element Performance Reading</p>						

Table IX. Summary of Task II Stage Radial Distortion Test Data (Concluded).

c. Without Inlet Guide Vanes and Without Blade Angle Slots #1 Casing Treatment.

Reading Number	Percent Design Speed	Discharge Valve Setting	Inlet Corrected Weight Flow, Lbs/Sec	Stage Total-Pressure Ratio	Stage Adiabatic Efficiency	Type Point**
571	70	14	161.6	1.269	.816	OP
572	70	30	171.1	1.216	.784	OP
573	70	9.3	152.4	1.293	.817	OP
574	90	30	203.8	1.327	.695	OP
575	90	10.5	198.5	1.494	.795	OP
576	100	30	218.8	1.388	.676	BE (p. 431)
577	100	10.5	214.4	1.613	.772	BE (p. 433)
578	100	12.3	216.8	1.575	.773	BE (p. 435)
579	100	14	217.5	1.541	.761	OP
580	100	11.1	214.1	1.601	.770	OP
581	90	15	202.4	1.432	.769	OP
582	90	13.3	201.3	1.454	.783	OP
583	90	12	199.3	1.470	.788	OP
584	70	15	162.8	1.264	.807	OP
585	70	11	156.1	1.283	.821	OP

** - OP - Overall Performance Reading
BE - Blade Element Performance Reading

Table X. Summary of Task II Stage Circumferential Distortion Test Data.

a. With Inlet Guide Vanes and with Blade Angle Slots #1 Casing Treatment.

Reading Number	Percent Design Speed	Discharge Valve Setting	Inlet Corrected Weight Flow, Lbs/Sec	Stage Total-Pressure Ratio	Stage Adiabatic Efficiency	Type Point*	Distortion Screen Pos. From TDC
406	70	30	167.8	1.220	.774	OP	195
407	90	30	207.0	1.357	.732	OP	195
408	90	4.5	172.1	1.579	.759	OP	195
409	90	11	198.9	1.505	.818	OP	195
410	90	13	201.8	1.476	.806	OP	195
411	100	30	222.0	1.422	.714	OP	195
412	100	6.3	199.3	1.709	.776	OP	195
413	100	10	213.9	1.642	.808	OP	195
414	100	12	217.7	1.600	.802	OP	195
415	70	11	155.1	1.286	.818	OP	195
416	70	25.7*	116.6	1.311	.689	OP	195
417	70	13	158.0	1.274	.812	OP	195
457	100	7.3	205.2	1.699	.802	OP	195
471	70	11	153.7	1.283	.810	OP	195
445-456	100	30	220.3	1.411	.716	SRT	195-165 (p. 450)
457-468	100	7.3	205.2	1.685	.774	SRT	195-165 (p. 435)
471-483	70	11	153.7	1.274	.843	SRT	195-165 (p. 462)
<p>* - Indicates discharge valve position with inner annulus discharge pipe closed.</p> <p>** - OP - Overall Performance Reading</p> <p>SRT- Screen Rotating Test (12 Circumferential Distortion Screen Positions in 30° Intervals from 195° TDC)</p>							

Table X. Summary of Task II Stage Circumferential Distortion Test Data (Continued).

b. Without Inlet Guide Vanes and with Blade Angle Slots #1 Casing Treatment.

Reading Number	Percent Design Speed	Discharge Valve Setting	Inlet Corrected Weight Flow, Lbs/Sec	Stage Total-Pressure Ratio	Stage Adiabatic Efficiency	Type Point*	Distortion Screen Pos. From TDC
484	70	30	168.1	1.213	.760	OP	195
485	70	20	165.7	1.232	.785	OP	195
486	70	13	157.8	1.266	.800	OP	195
487	70	11	155.1	1.277	.802	OP	195
500	70	1.0	120.7	1.314	.693	OP	195
501	90	30	209.2	1.367	.750	OP	195
502	90	20	208.0	1.403	.778	OP	195
503	90	13	202.0	1.472	.810	OP	195
504	90	11	198.1	1.499	.819	OP	195
505	90	7	185.9	1.551	.806	OP	195
506	90	9	193.3	1.526	.815	OP	195
507	100	30	225.2	1.435	.736	OP	195
519	100	12.5	219.5	1.591	.806	OP	195
520	100	10	214.8	1.642	.819	OP	195
521	100	11	217.4	1.616	.808	OP	195
523	70	8	148.2	1.297	.808	OP	195
524	70	5	138.5	1.311	.778	OP	195
648	100	7	200.9	1.693	.776	OP	195
649	100	8.5	207.6	1.665	.796	OP	195
650	100	11	213.6	1.610	.808	OP	195
651	90	5.2	174.8	1.561	.764	OP	195
652	90	11	196.5	1.493	.818	OP	195
653	90	13	199.0	1.464	.807	OP	195
488-499	70	11	154.8	1.274	.829	SRT	195-165 (p. 492)
507-518	100	30	225.3	1.438	.719	SRT	195-165 (p. 483)
521-534	100	11	217.4	1.617	.789	SRT	195-165 (p. 474)

* - OP - Overall Performance Reading

SRT- Screen Rotating Test (12 Circumferential Distortion Screen Positions in 30° Intervals from 195° TDC)

Table X. Summary of Task II Stage Circumferential Distortion Test Data (Concluded).

c. Without Inlet Guide Vanes and Without Blade Angle Slots #1 Casing Treatment.

Reading Number	Percent Design Speed	Discharge Valve Setting	Inlet Corrected Weight Flow, Lbs/Sec	Stage Total-Pressure Ratio	Stage Adiabatic Efficiency	Type Point*	Distortion Screen Pos. From TDC
606	70	30	168.1	1.210	.773	OP	195
607	70	11	154.3	1.275	.813	OP	195
608	70	4.3	135.4	1.310	.771	OP	195
609	70	13	157.4	1.266	.806	OP	195
610	90	30	206.7	1.370	.752	OP	195
611	90	11	197.7	1.495	.831	OP	195
612	90	7.2	185.5	1.543	.811	OP	195
613	100	30	221.7	1.420	.742	OP	195
614	100	12	217.0	1.598	.823	OP	195
615	100	9.5	212.9	1.645	.817	OP	195
627	100	9	209.4	1.652	.805	OP	195
628	100	30	222.5	1.426	.753	OP	195
640	100	10	211.7	1.631	.807	OP	195
641	90	13	199.6	1.463	.810	OP	195
615-626	100	9.5	212.9	1.647	.804	SRT	195-165 (p. 501)
628-639	100	30	222.6	1.430	.733	SRT	195-165 (p. 510)
<p>* - OP - Overall Performance Reading SRT- Screen Rotating Test (12 Circumferential Distortion Screen Positions in 30° Intervals from 195° TDC)</p>							

Table XI(a). Summary of Task II Stage Undistorted Inlet Performance.

Test Vehicle Configuration	70% Design Speed		90% Design Speed		100% Design Speed	
	Stall Margin	Peak η_{ad}	Stall Margin	Peak η_{ad}	Stall Margin	Peak η_{ad}
With IGV*; With Solid Casing	.246	.855	.133	.845	.129	.837
With IGV; With C.T.**	.390	.835	.308	.840	.320	.827
Without IGV; With C.T.	.384	.860	.305	.835	.360	.826
With IGV; With Solid Casing	.271	.861	.156	.851	.182	.845

* Inlet Guide Vanes; ** Blade Angle Slots #1 Casing Treatment

Table XI(b). Summary of Task II Stage Radial Distortion Performance.

Test Vehicle Configuration	70% Design Speed		90% Design Speed		100% Design Speed	
	Stall Margin	Peak η_{ad}	Stall Margin	Peak η_{ad}	Stall Margin	Peak η_{ad}
With IGV*; With Solid Casing	.067	.830	.021	.797	.036	.780
With IGV; With C.T.**	.200	.820	.168	.807	.160	.770
Without IGV; With C.T.	.189	.824	.145	.798	.146	.768
Without IGV; With Solid Casing	.046	.821	-.010	.796	.017	.774
* Inlet Guide Vanes; ** Blade Angle Slots #1 Casing Treatment						

Table XI(c). Summary of Task II Stage Circumferential Distortion Performance.

Test Vehicle Configuration	70% Design Speed		90% Design Speed		100% Design Speed	
	Stall Margin	Peak η_{ad}	Stall Margin	Peak η_{ad}	Stall Margin	Peak η_{ad}
With IGV*; With Solid Casing	.239	.838	.069	.817	.077	.800
With IGV; With C.T.**	.391	.818	.224	.819	.154	.809
Without IGV; With C.T.	.357	.808	.210	.819	.185	.810
Without IGV; With Solid Casing	.195	.814	.117	.831	.081	.824

* Inlet Guide Vanes; ** Blade Angle Slots #1 Casing Treatment

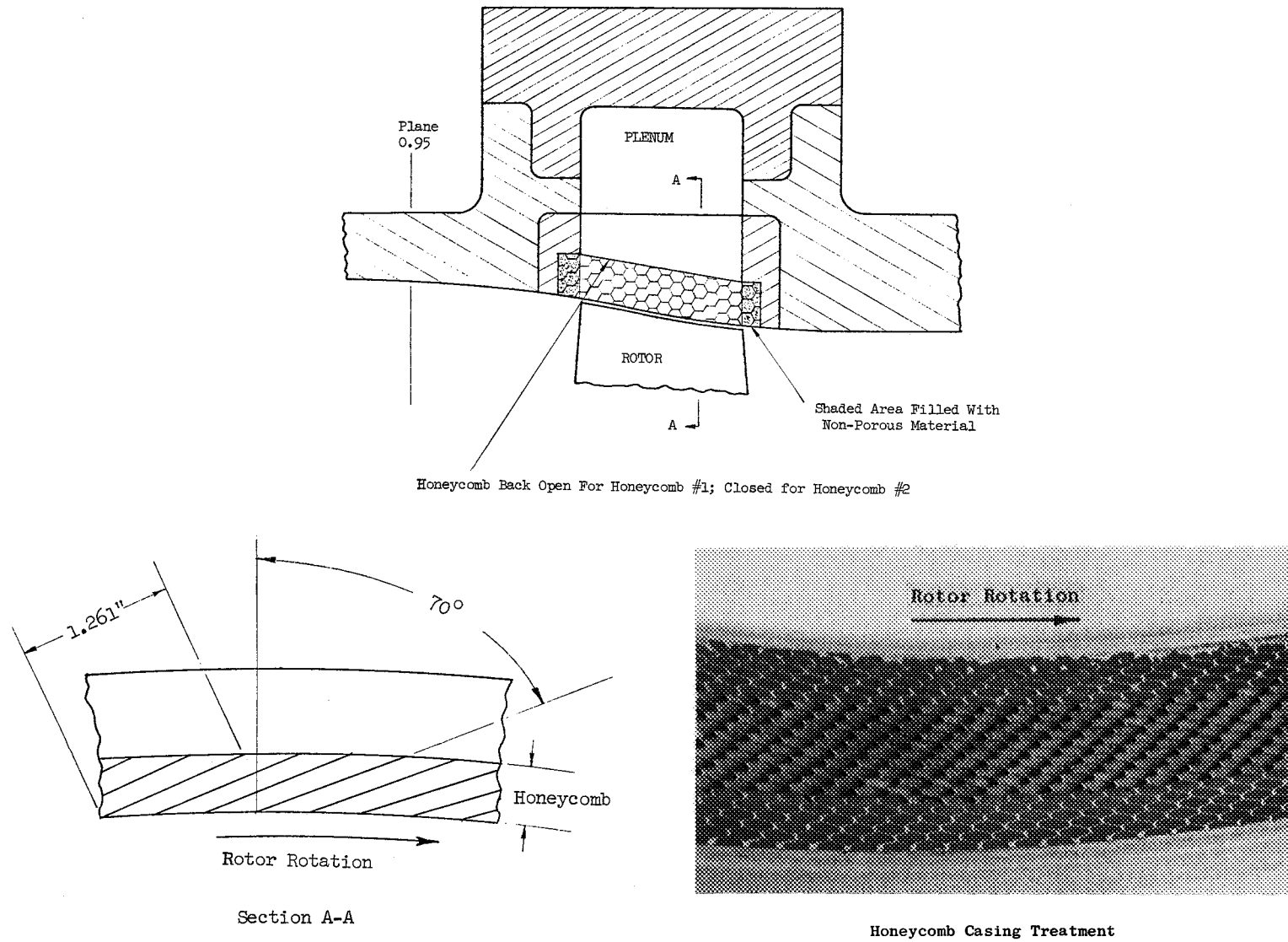
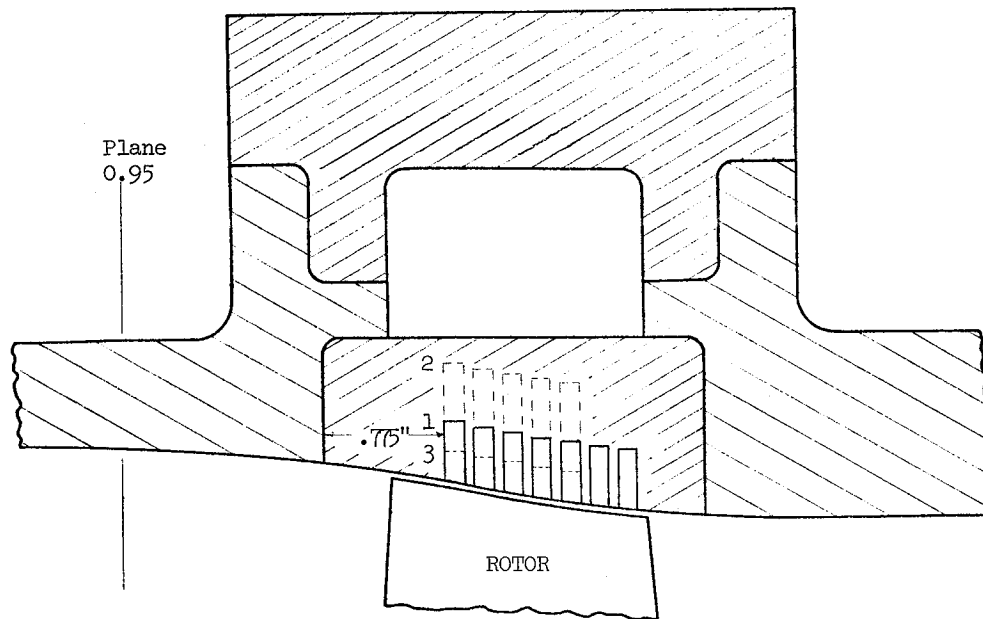
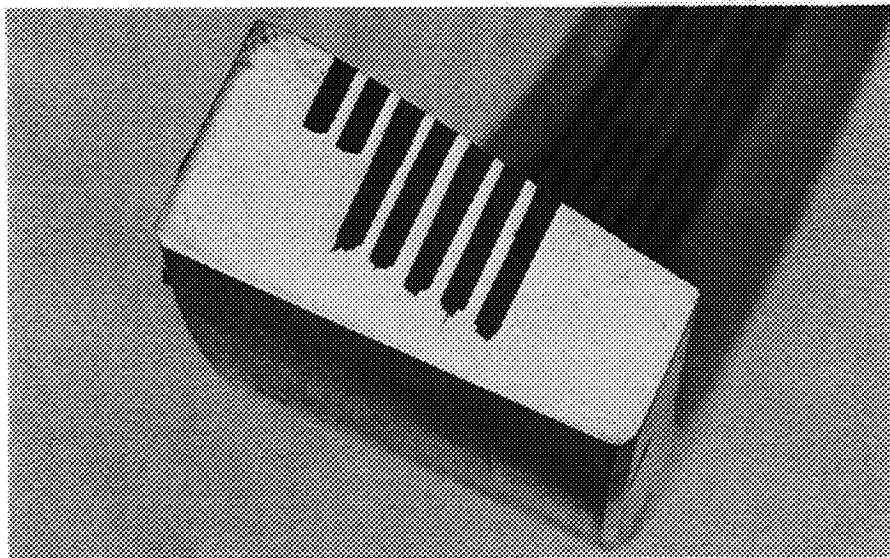


Figure 1 (a). Honeycomb Casing Treatment Configurations Used In The Task IV Program.

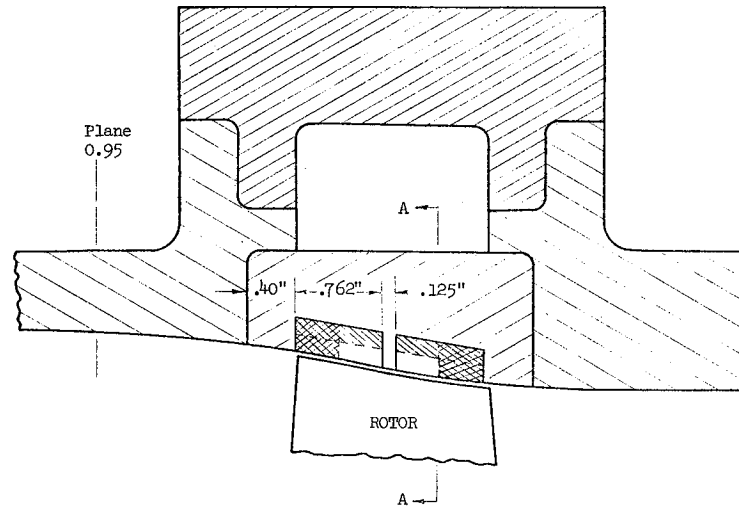


1. Circumferential Grooves #1; 7 Grooves; $1/8'' \times 3/8''$
2. Circumferential Grooves #2; 5 Grooves; $1/8'' \times 3/4''$
3. Circumferential Grooves #3; 5 Grooves; $1/8'' \times 3/16''$




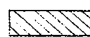
Circumferential Grooves #3 Casing Treatment

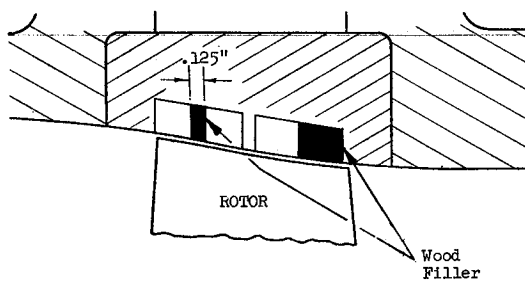
Figure 1 (b). Circumferential Grooved Casing Treatment Configurations Used In The Task IV Program.



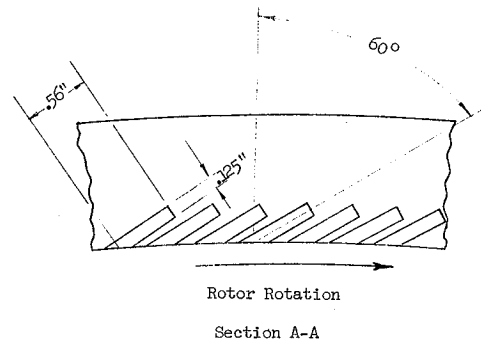
- Solid Lines Indicate Skewed Slot #1 Configuration

 - Indicates Area Filled To Yield Skewed Slots #2 Configuration

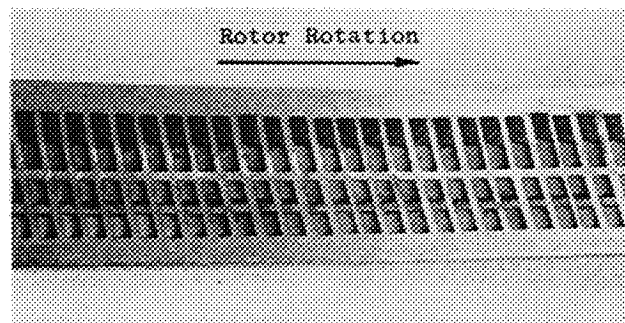
 - Indicates Area Filled in Addition To Skewed Slots #2 To Yield Skewed Slots #3 Configuration



- Solid Lines Indicate Skewed Slots #4 Configuration



Skewed Slots #1 Configuration



Skewed Slots #4 Casing Treatment

Figure 1 (c). Skewed Slot Casing Treatment Configurations Used In The Task IV Program.

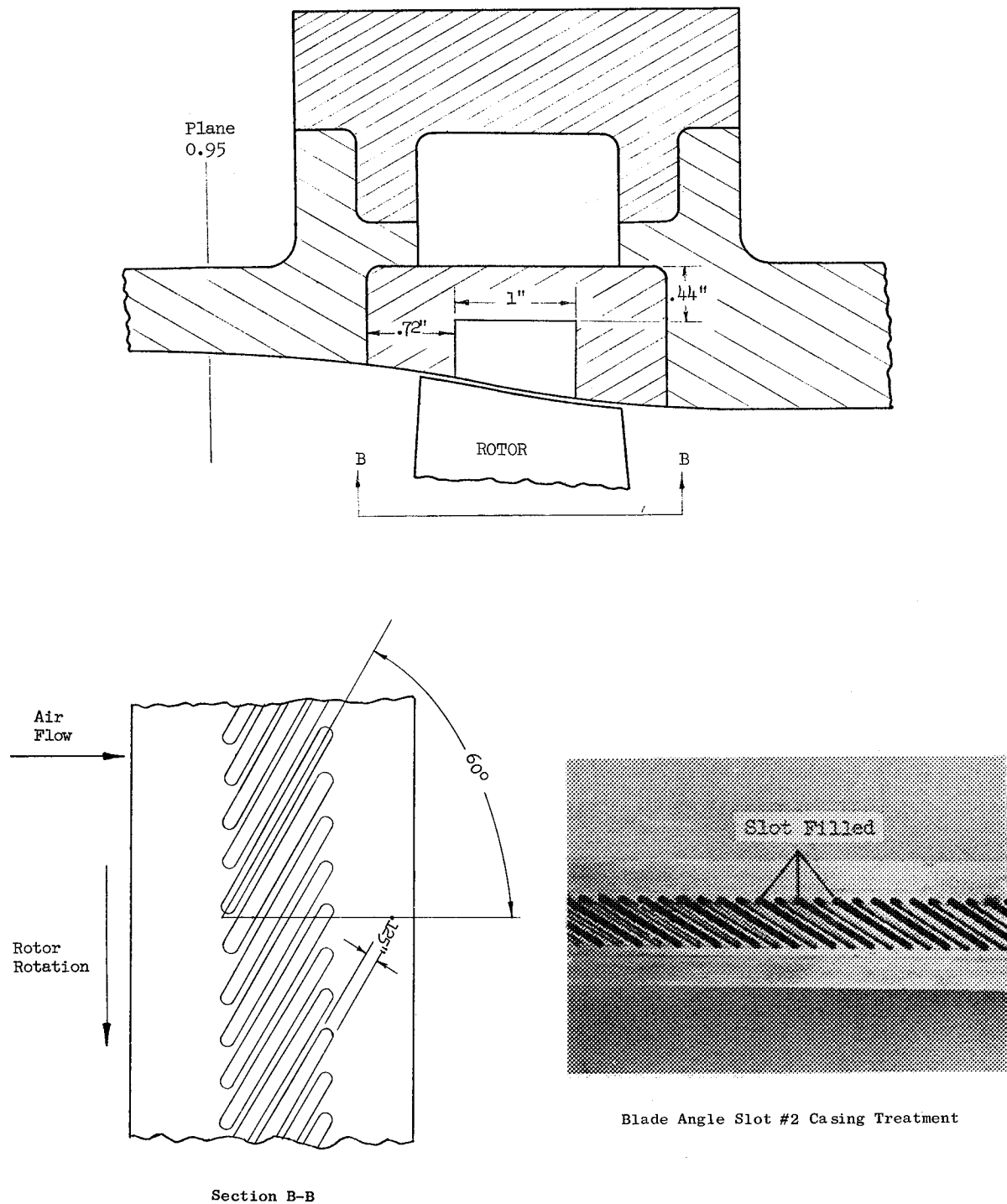


Figure 1 (d). Blade Angle Slot Casing Treatment Configurations Used In The Task IV Program.

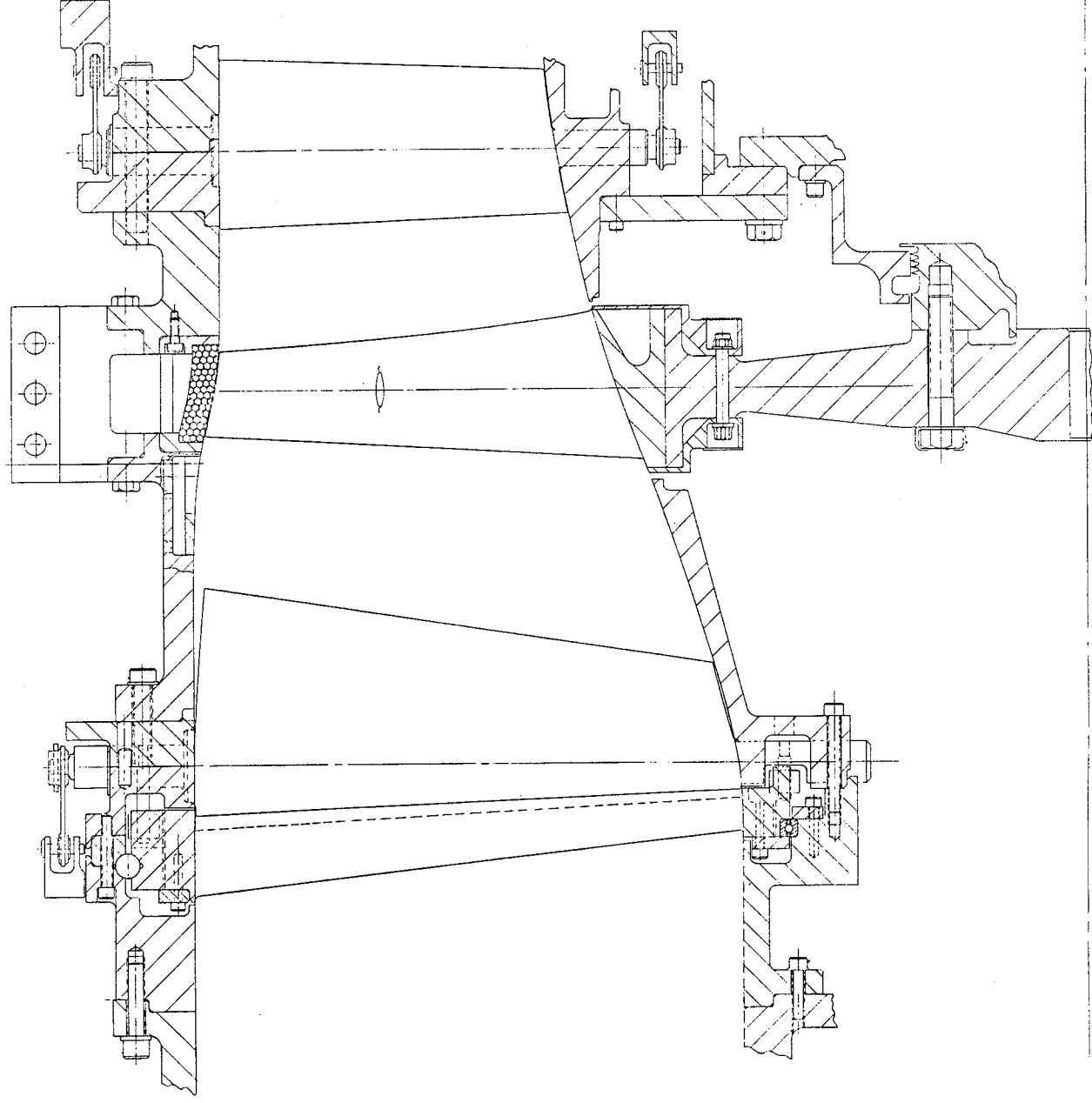


Figure 2. Meridional Sectional View of Task II Stage Test Vehicle.

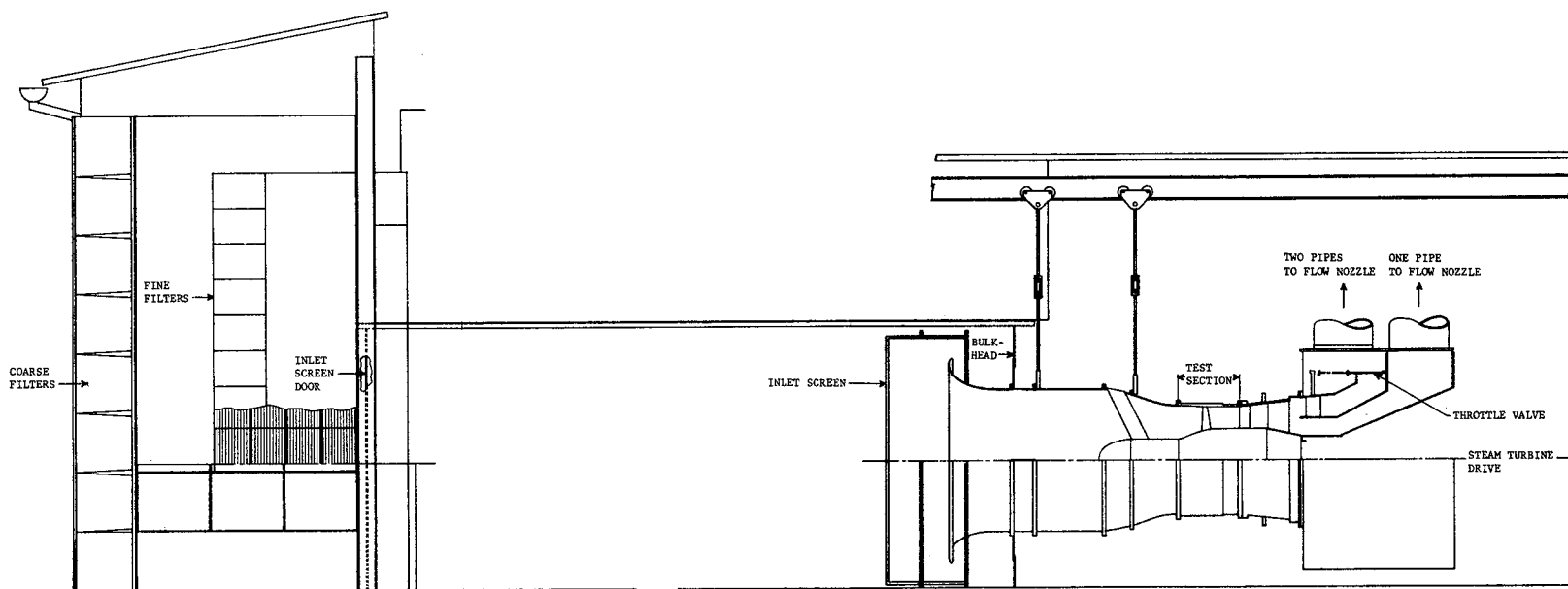


Figure 3. Schematic Diagram of House Compressor Test Facility.

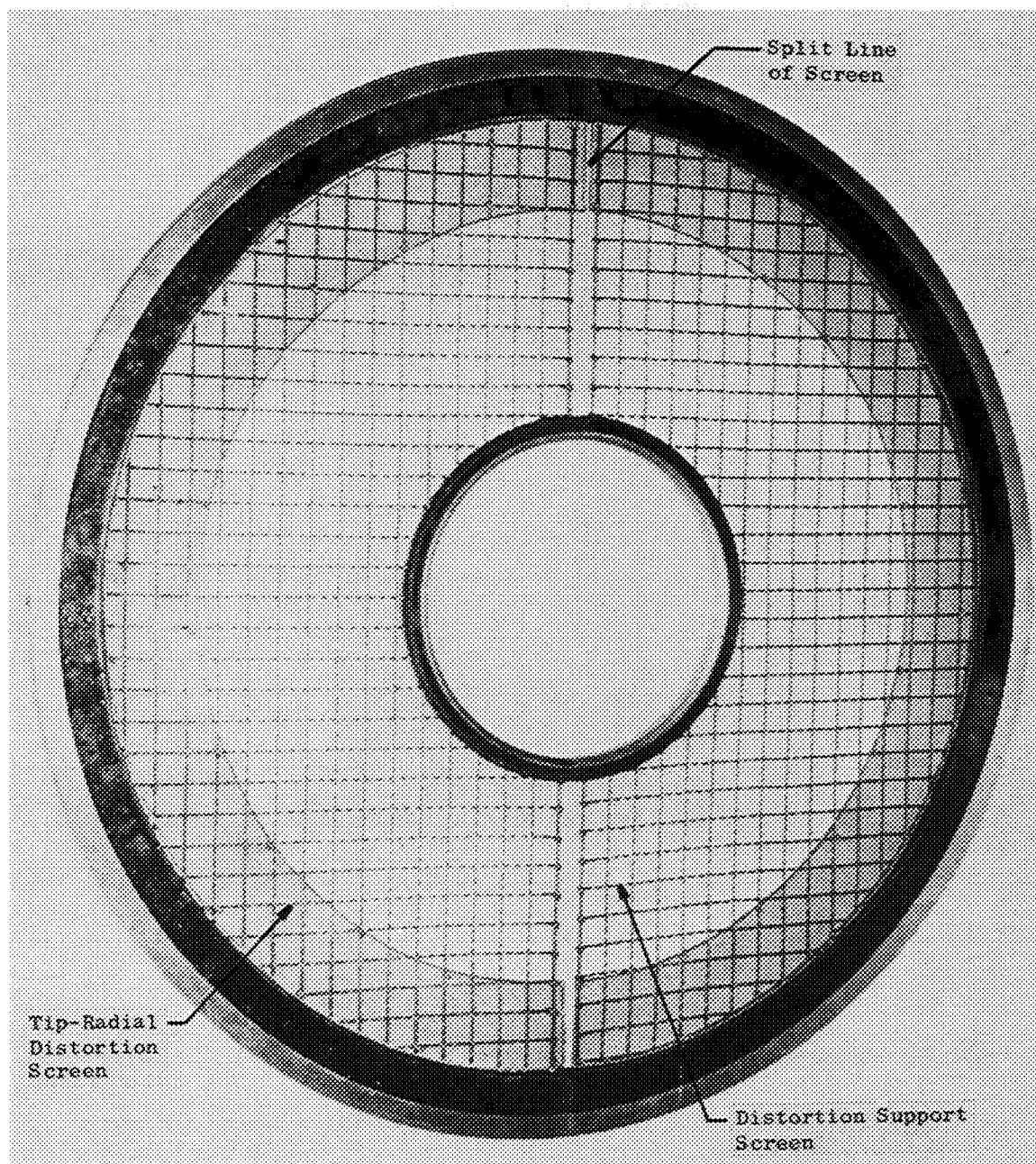


Figure 4 (a). Tip-Radial Distortion Screen.

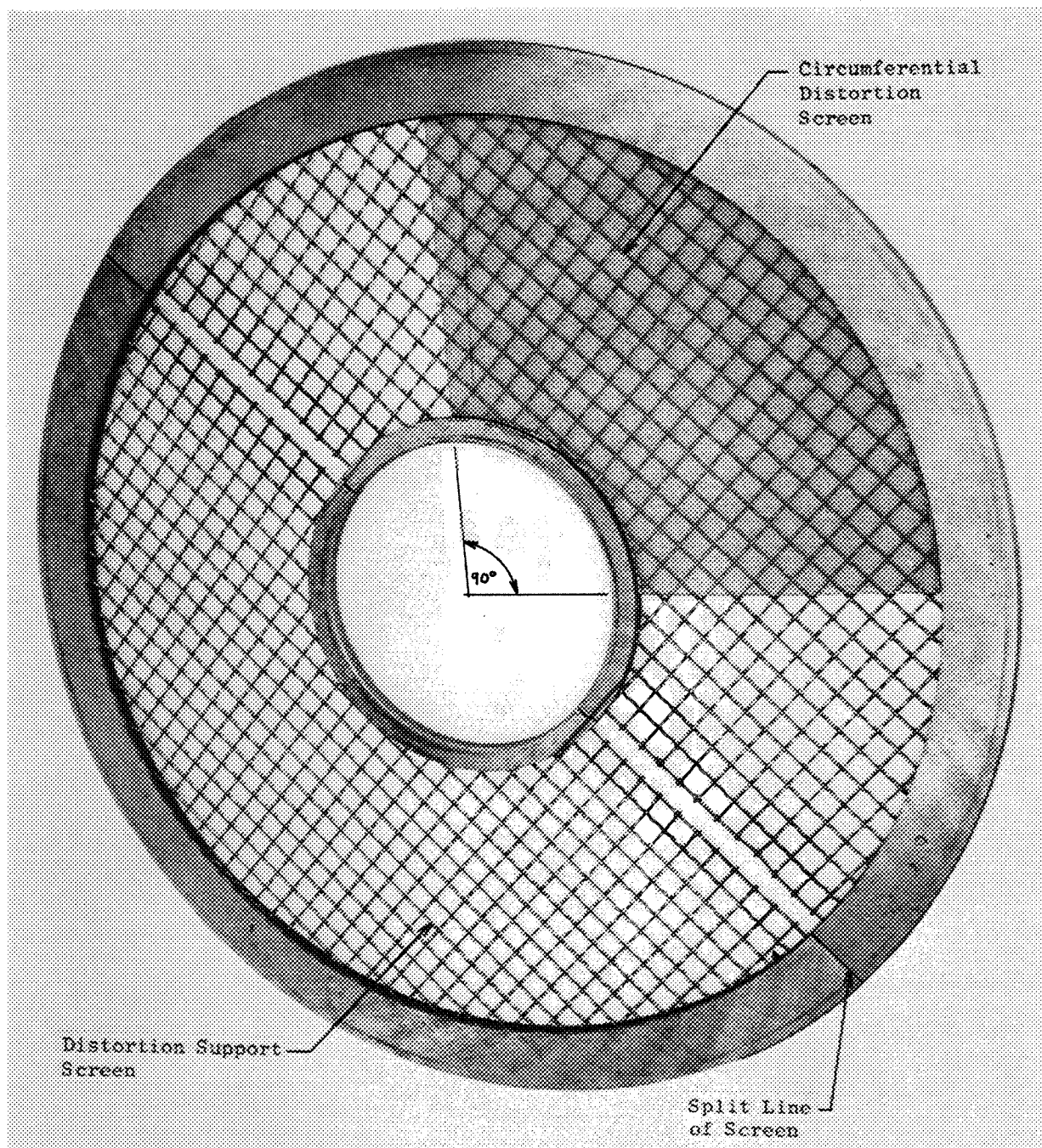


Figure 4 (b). Circumferential Distortion Screen.

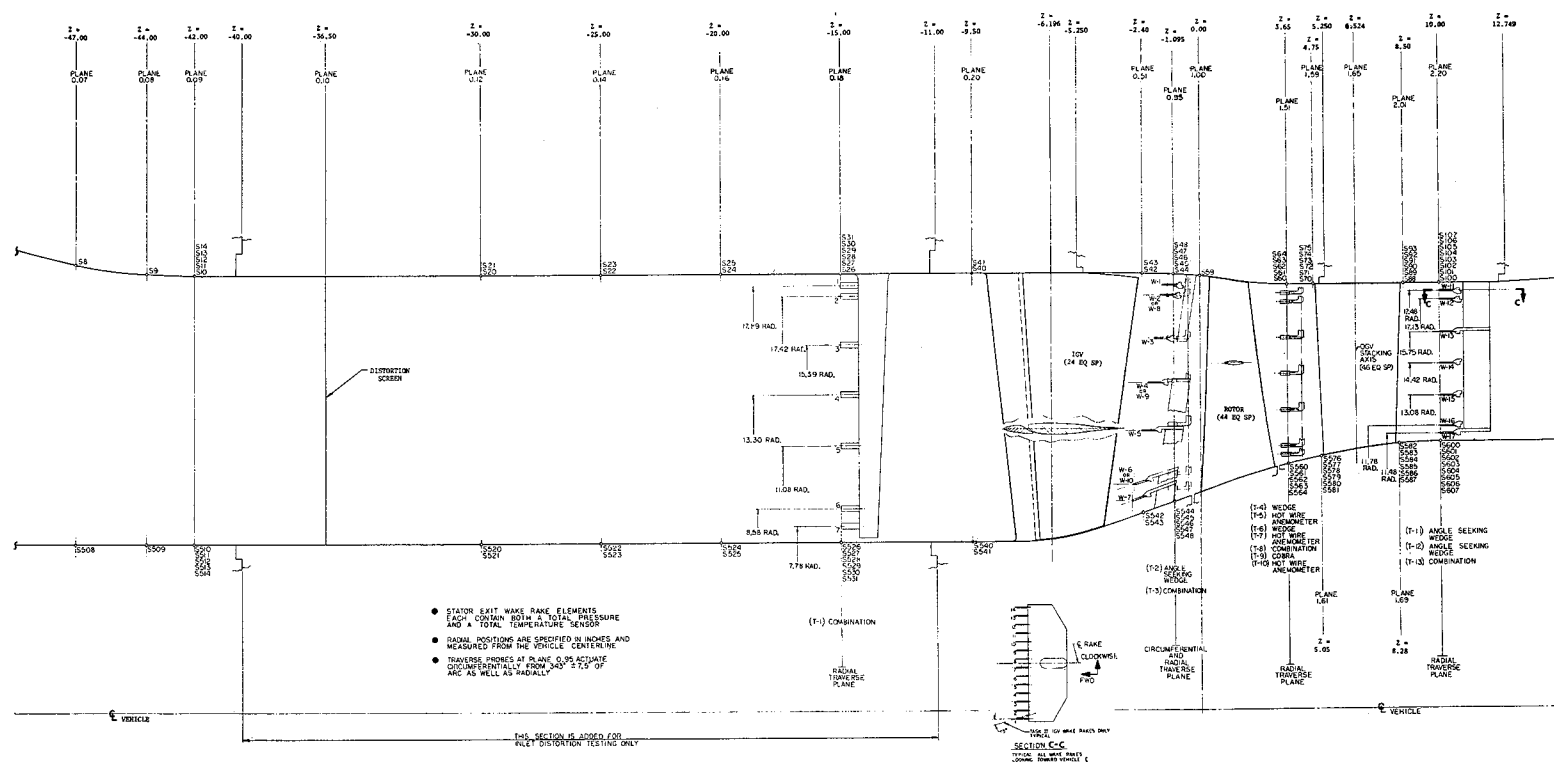


Figure 5 (a). Meridional View Showing Instrumentation Locations.

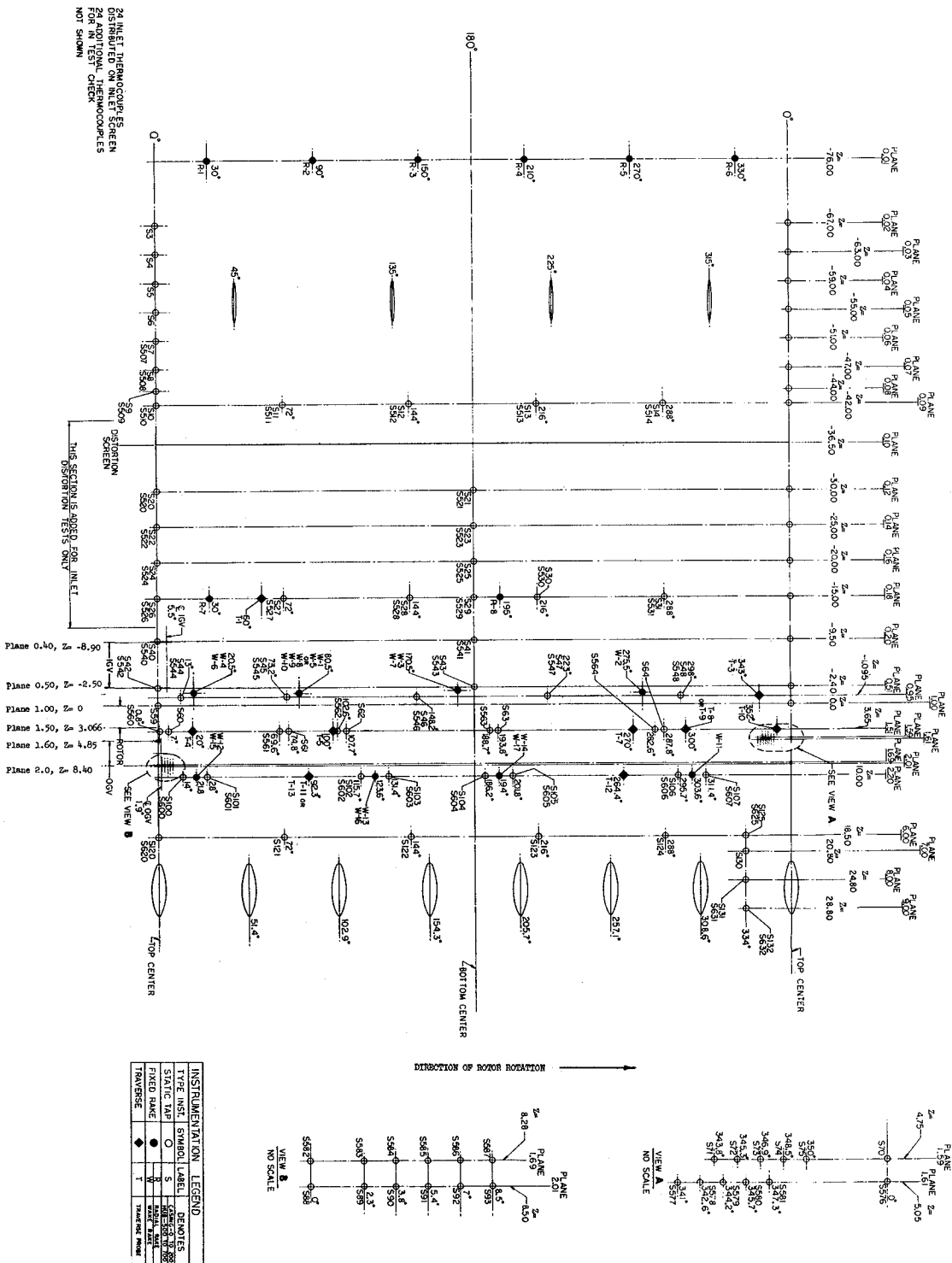
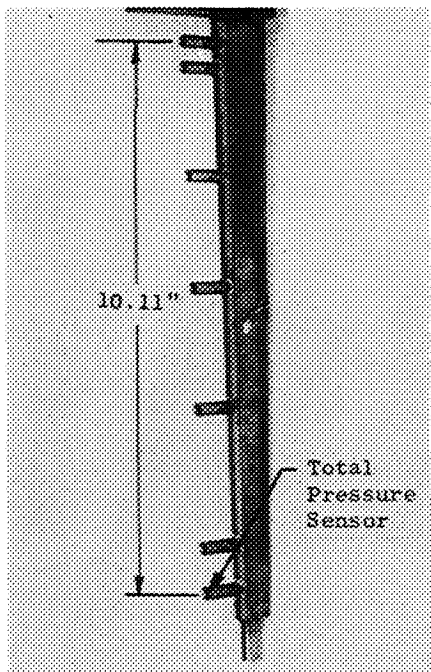
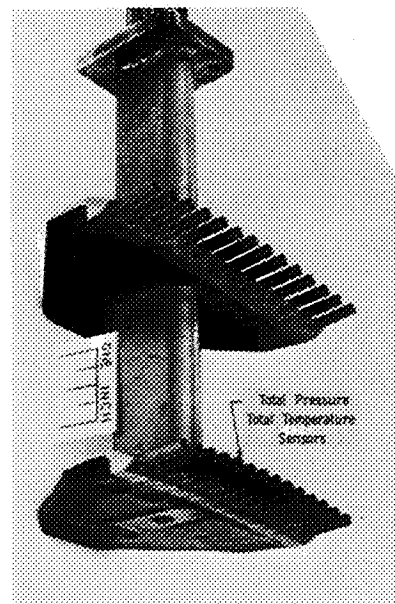


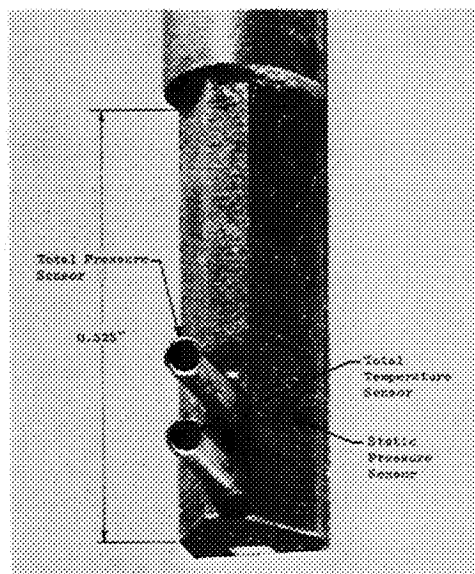
Figure 5 (b). Circumferential Development Showing Instrumentation Locations.



(a) Fixed Inlet Distortion
Total Pressure Rake at
Plane 0.18

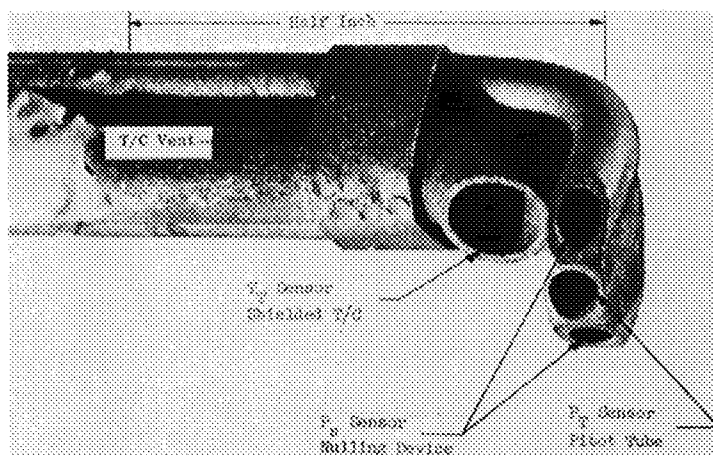


(b) Fixed Discharge Total Pressure - Total Temperature Wake
Rake Located at Plane 2.20



(c) Sensing Element of Four-Parameter
Combination Traverse Probe

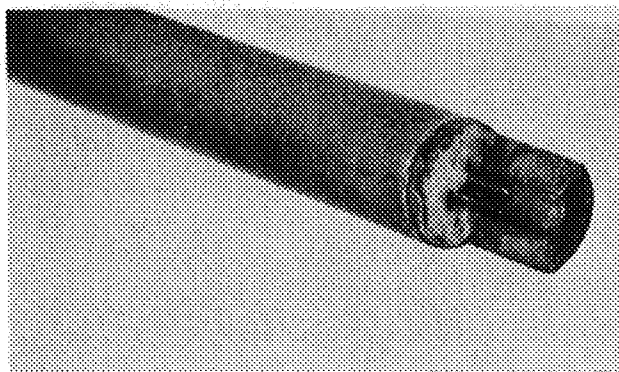
Figure 6. Fixed and Traverse Instrumentation Used In The Task IV Program.



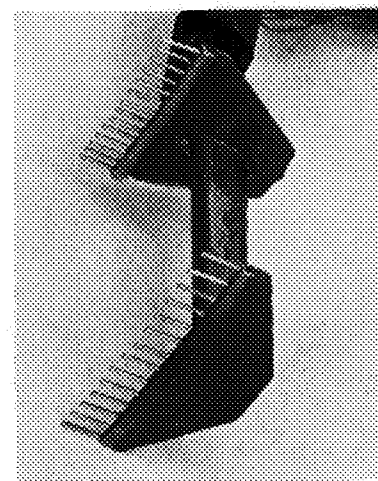
(d) Sensing Element of Cobra Traverse Probe



(e) Sensing Element of Static Pressure Wedge Traverse Probe



(f) Sensing Element of Shielded Hot-Wire Anemometer Traverse Probe



(g) Fixed IGV Discharge Total Pressure Wake Rake Located at Plane 0.95

Figure 6. Fixed and Traverse Instrumentation Used In The Task IV Program (Concluded).

(Dashed lines with arrows and inset formulas indicate calculation sequence for sample case.)

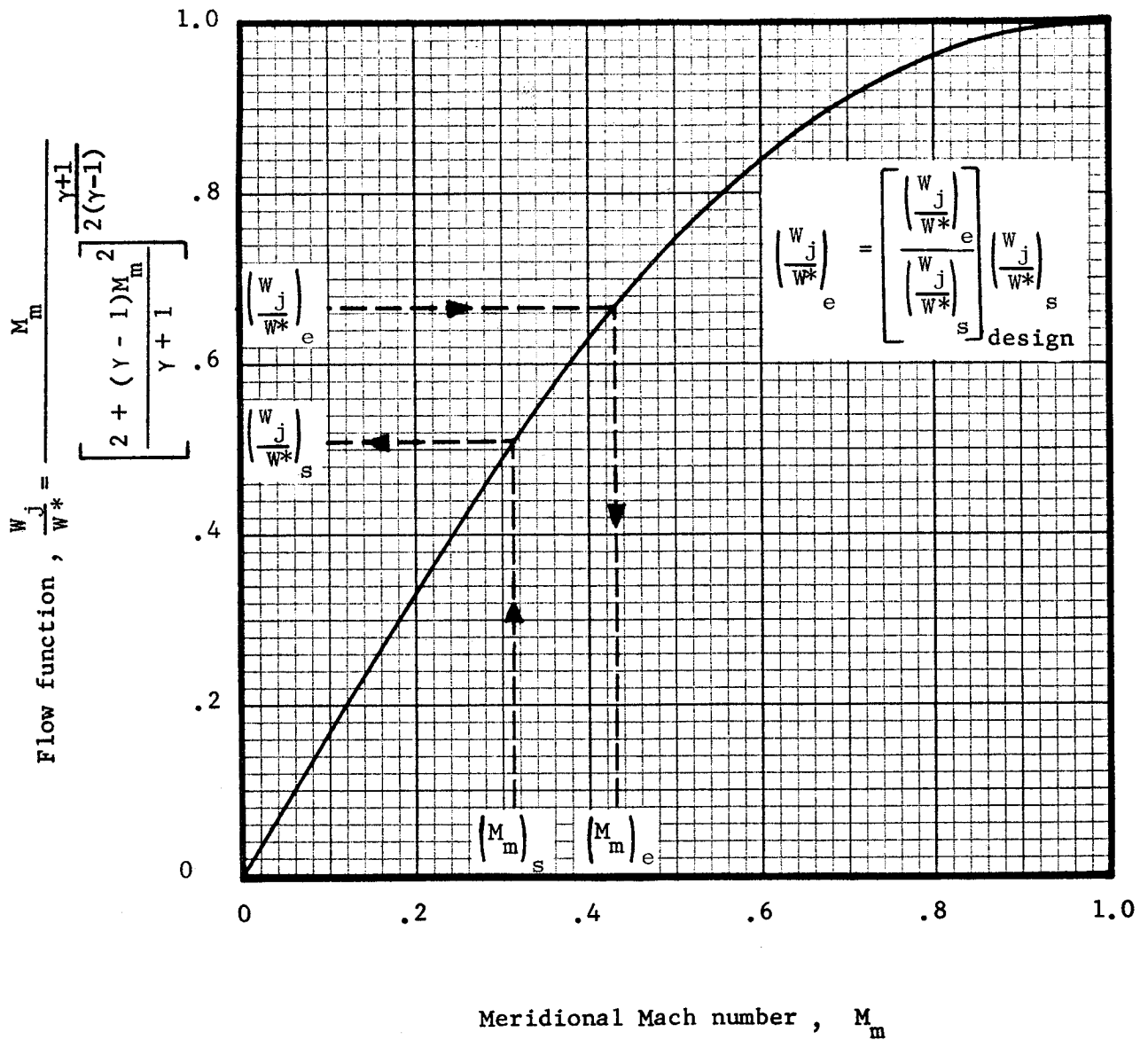


Figure 7. Relationship Between Flow Function and Meridional Mach No. Used for Transferring Traverse Measurements to Blade Edges.

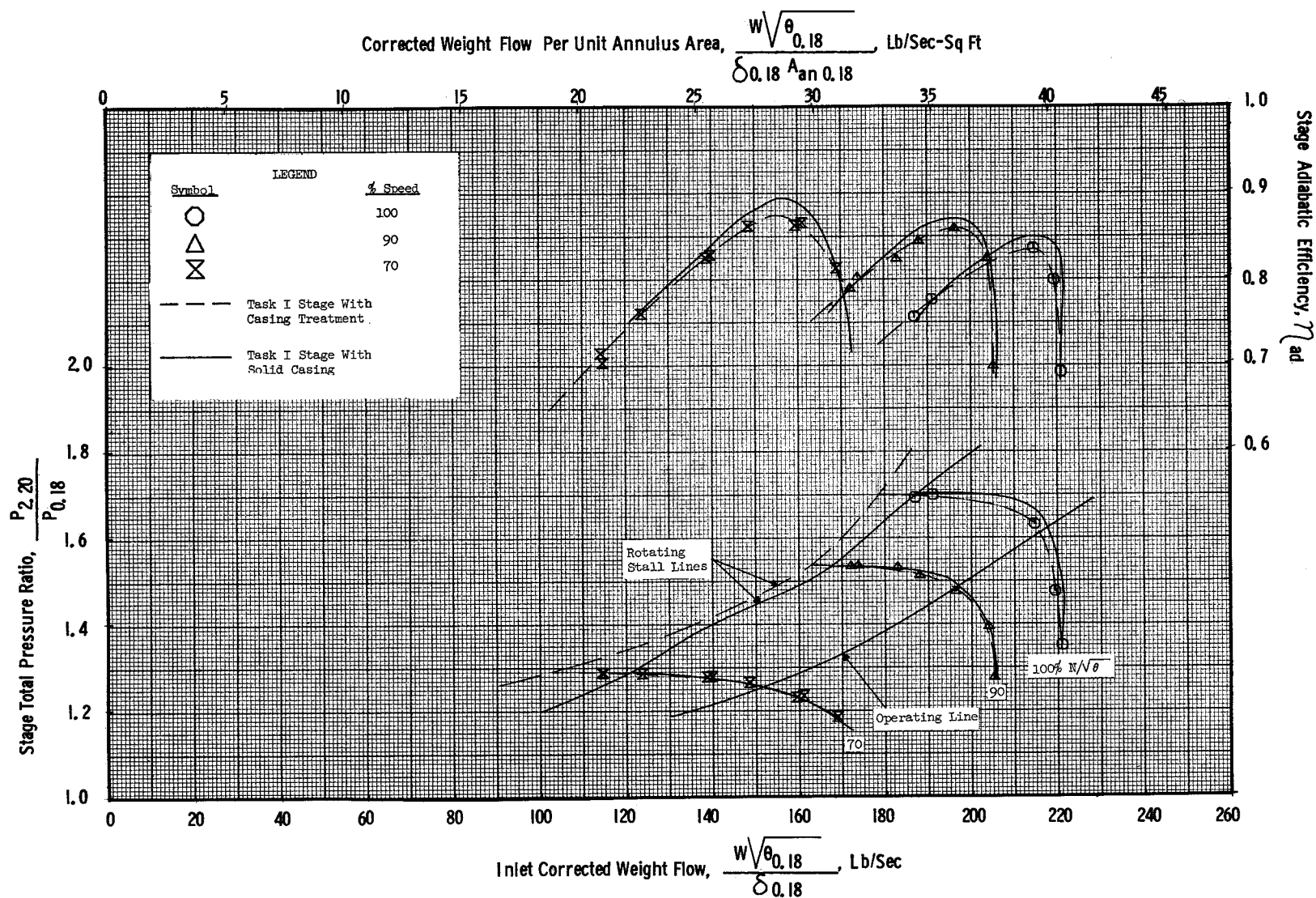


Figure 8 (a). Task I Stage Undistorted Inlet Performance Map; Honeycomb #1 Casing Treatment.

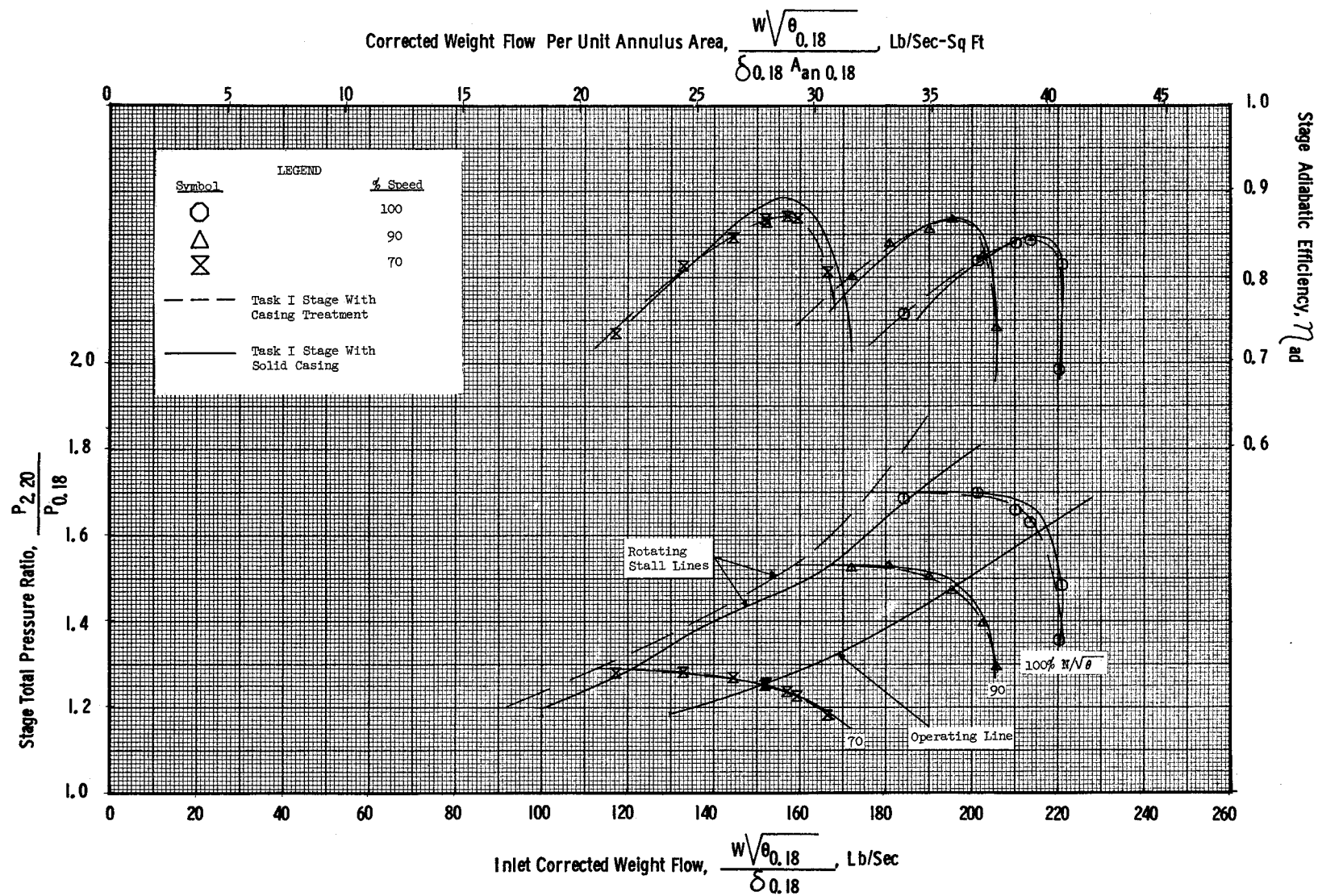


Figure 8 (b). Task I Stage Undistorted Inlet Performance Map; Honeycomb #2 Casing Treatment.

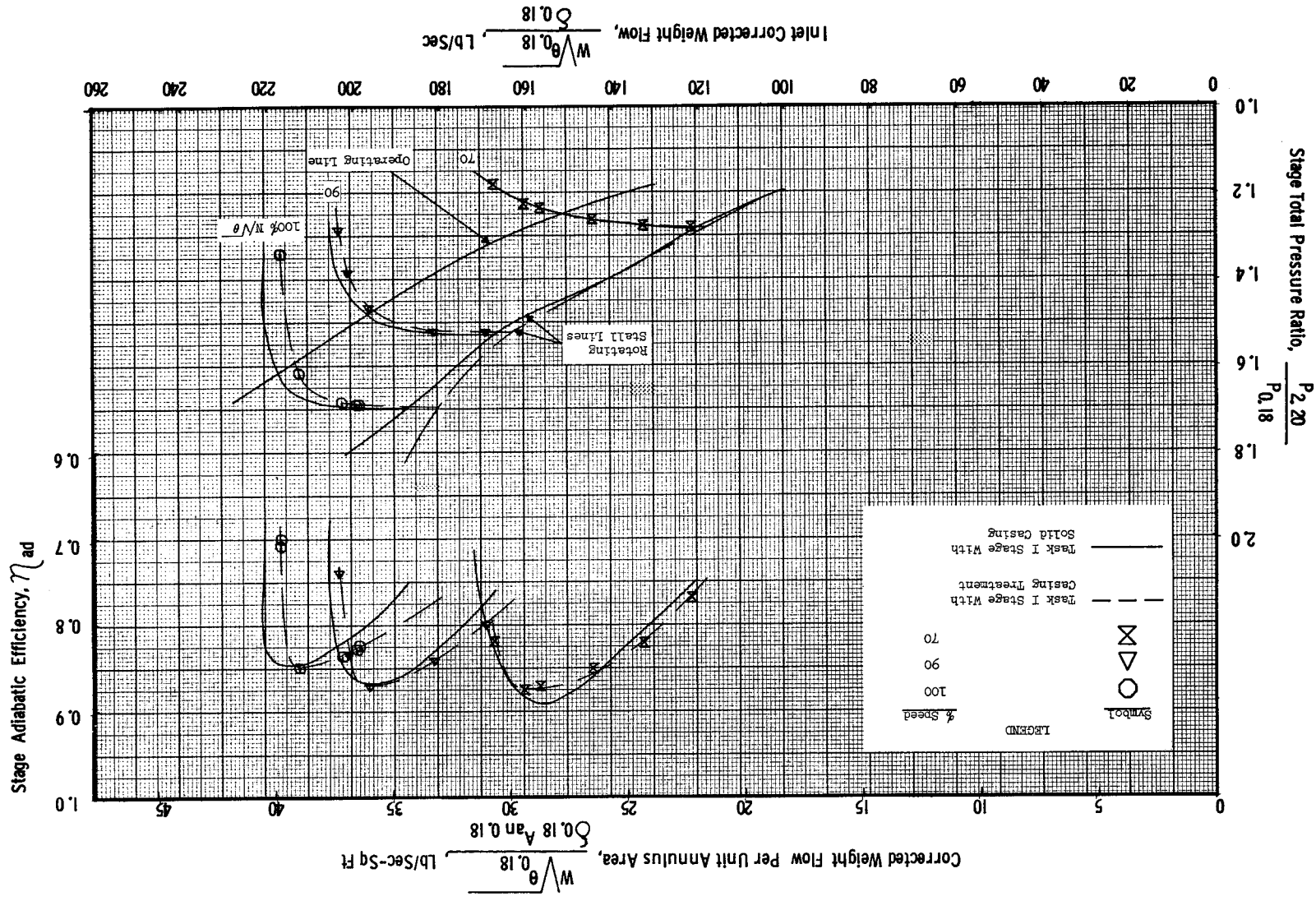


Figure 8 (c). Task I Stage Undistorted Inlet Performance Map; Circumferential Grooves #1 Casing Treatment.

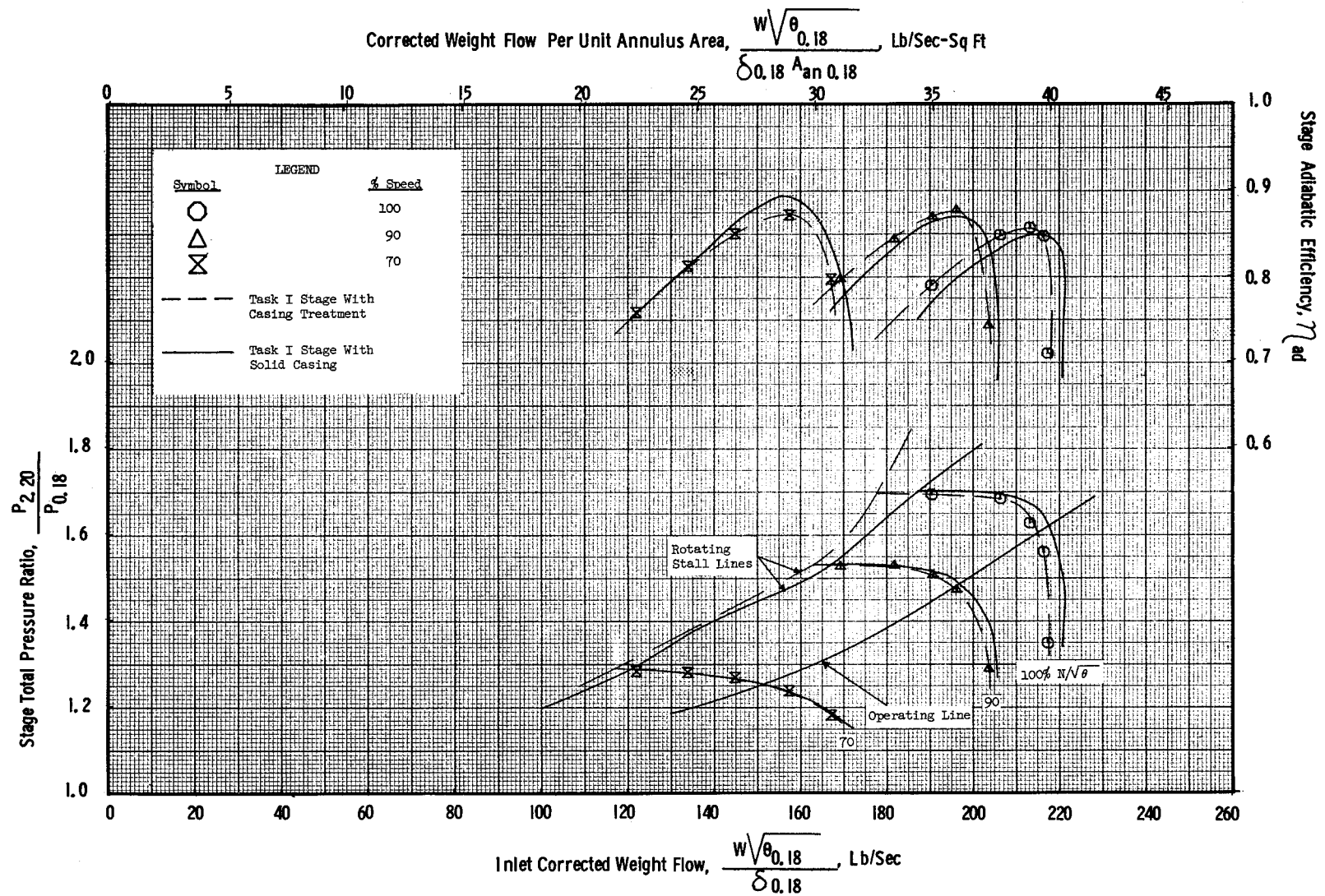


Figure 8 (d). Task I Stage Undistorted Inlet Performance Map; Circumferential Grooves #2 Casing Treatment.

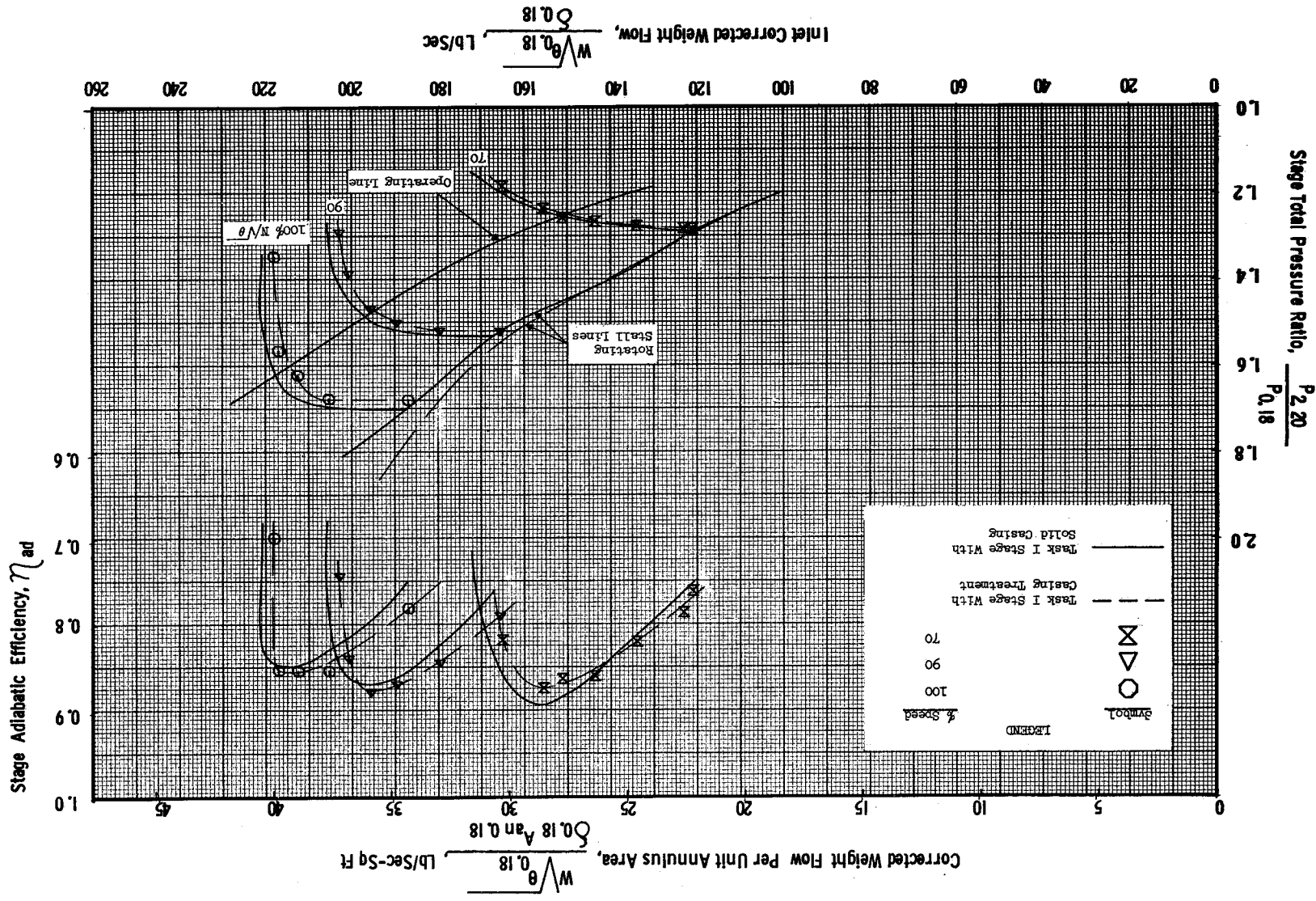


Figure 8 (e). Task I Stage Undistorted Inlet Performance Map; Circumferential Grooves #3
Casing Treatment.

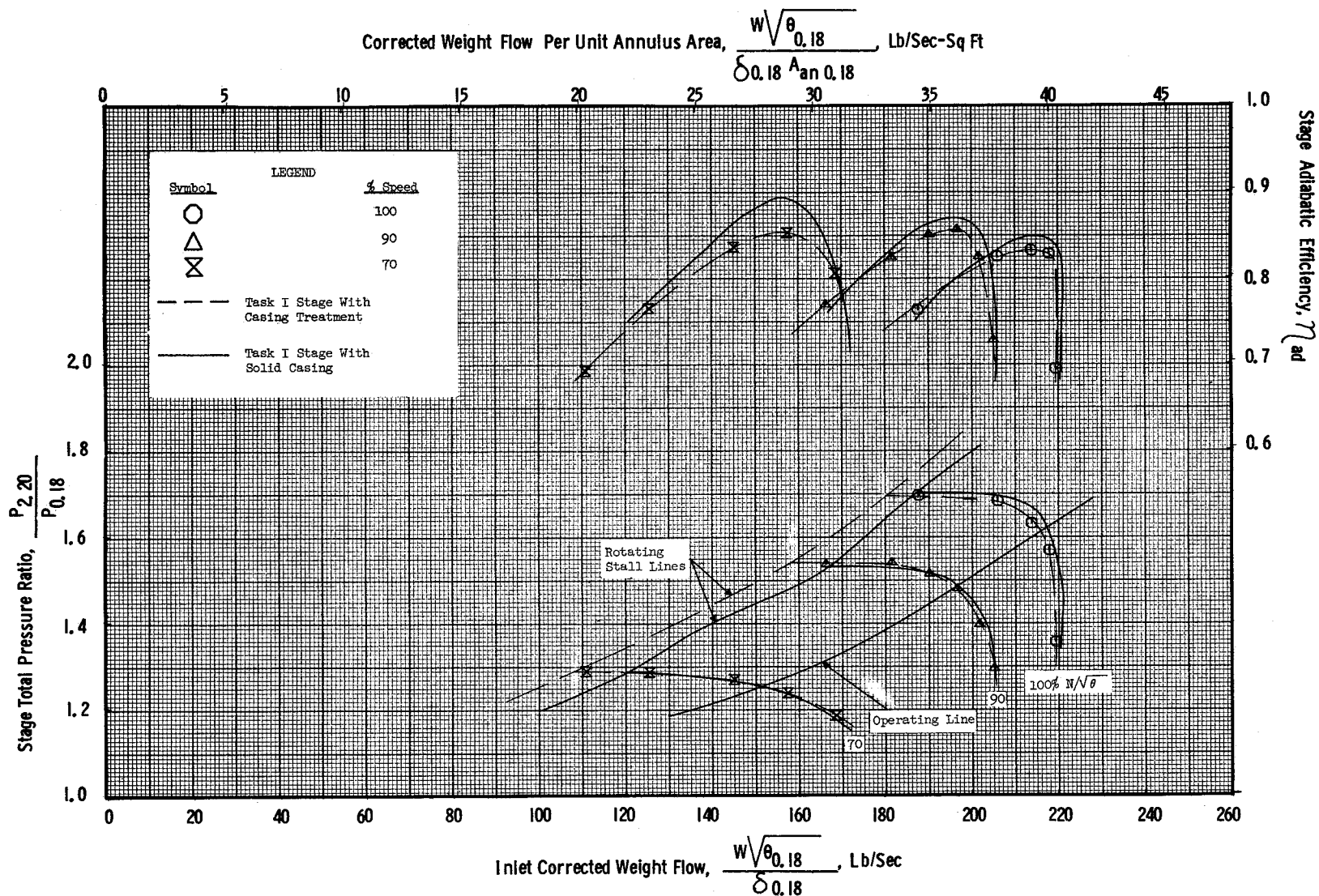


Figure 8 (f). Task I Stage Undistorted Inlet Performance Map; Skewed Slots #1 Casing Treatment.

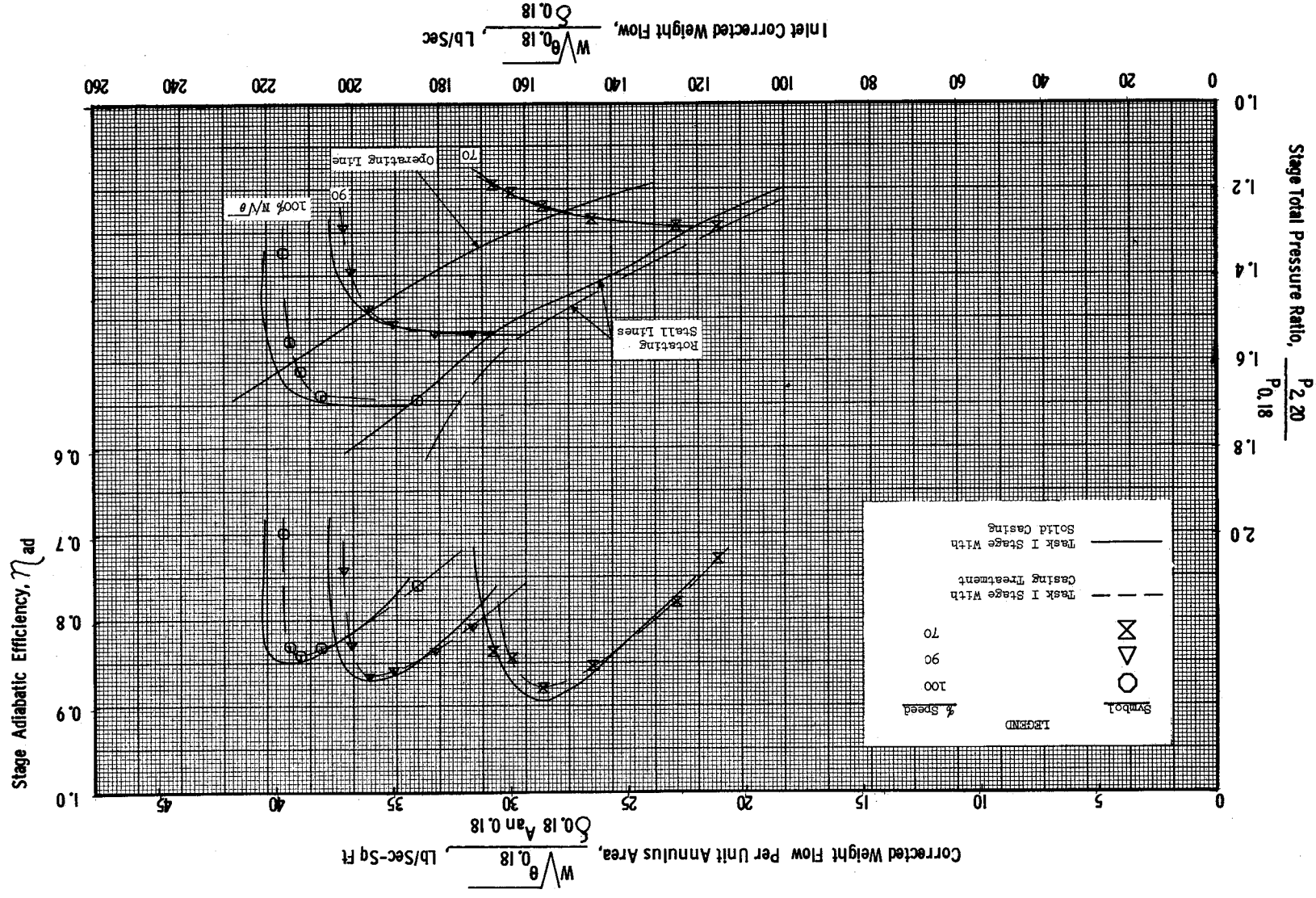


Figure 8 (g). Task I Stage Undistorted Inlet Performance Map; Skewed Slots #2 Casing Treatment.

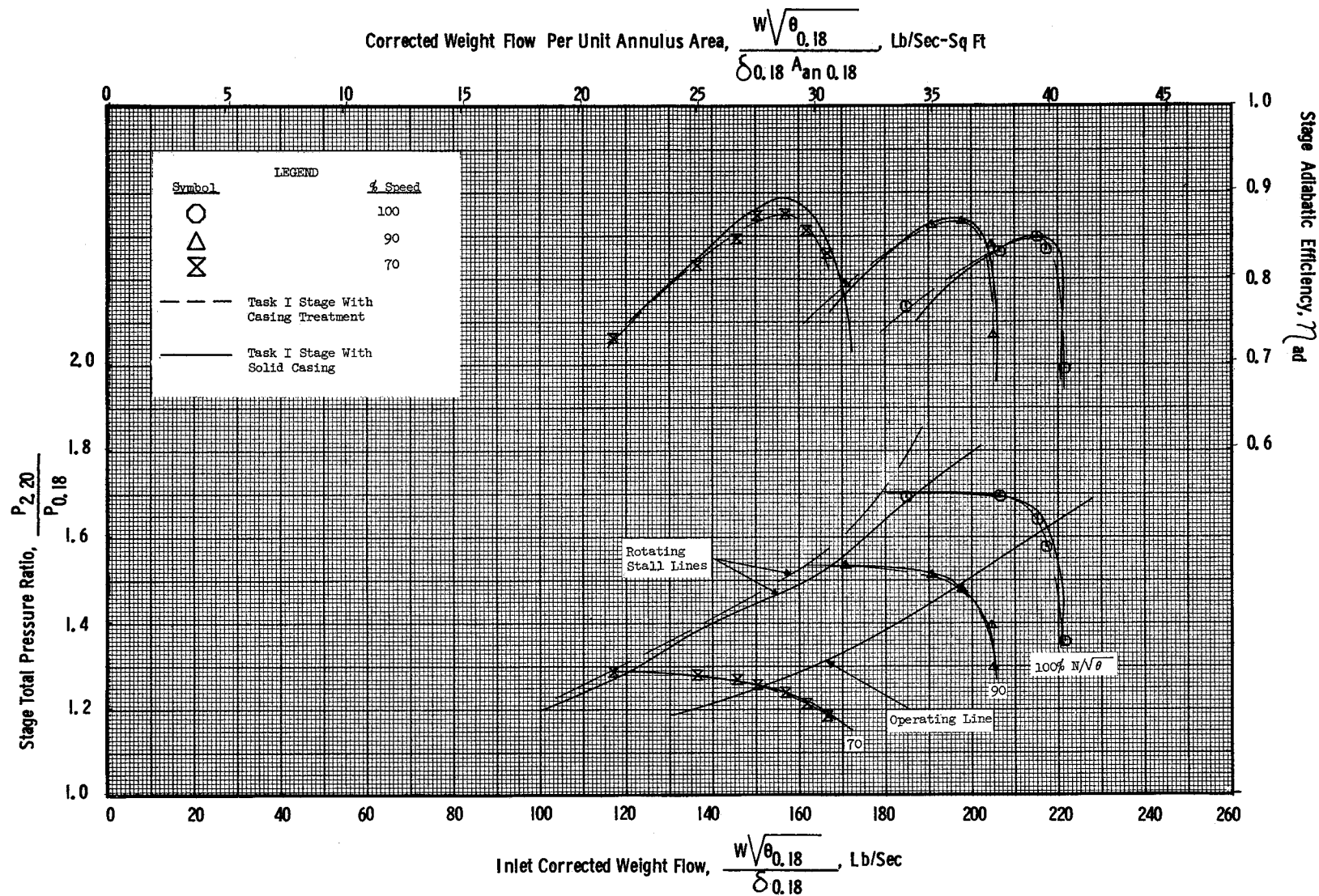


Figure 8 (h). Task I Stage Undistorted Inlet Performance Map; Skewed Slots #3 Casing Treatment.

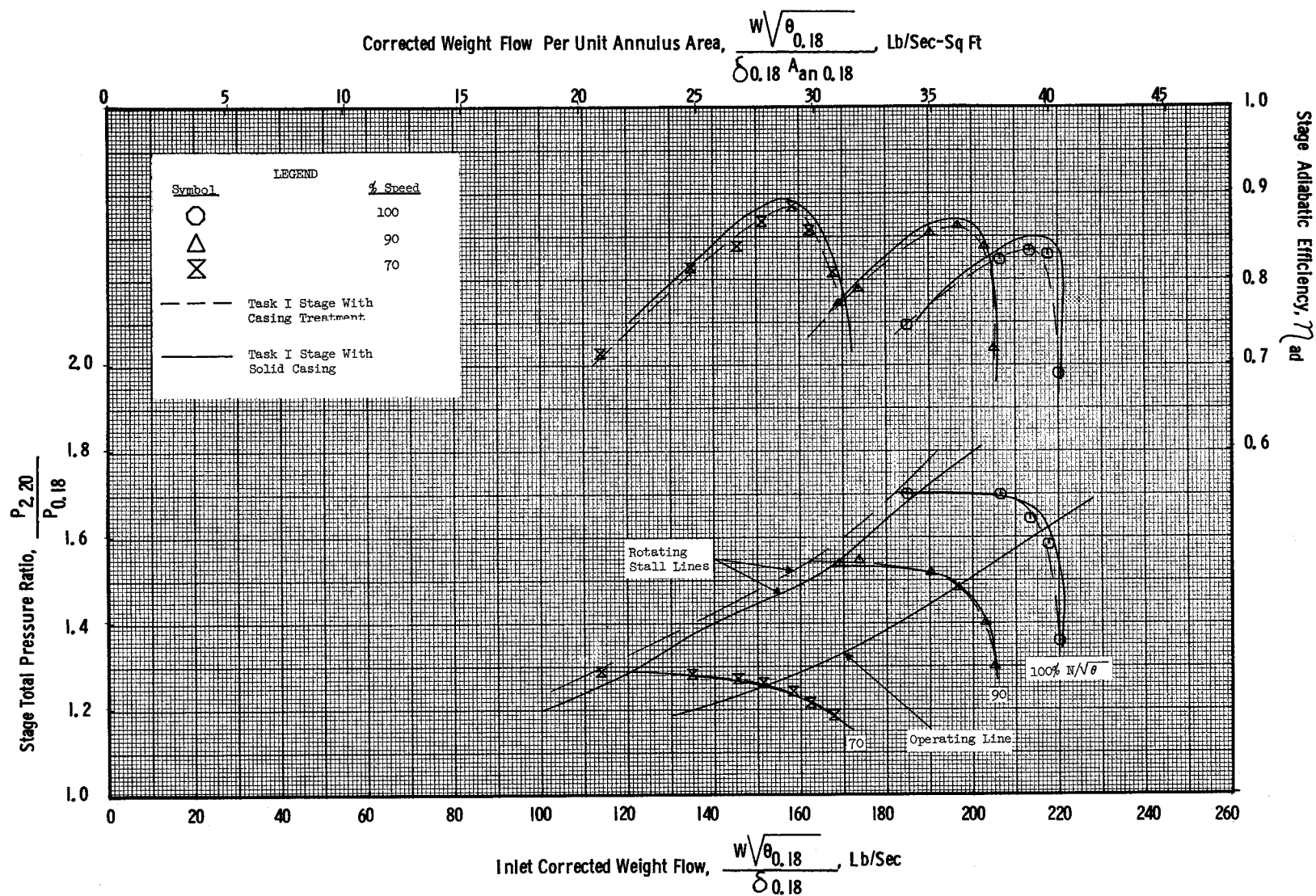


Figure 8 (i). Task I Stage Undistorted Inlet Performance Map; Skewed Slots #4 Casing Treatment.

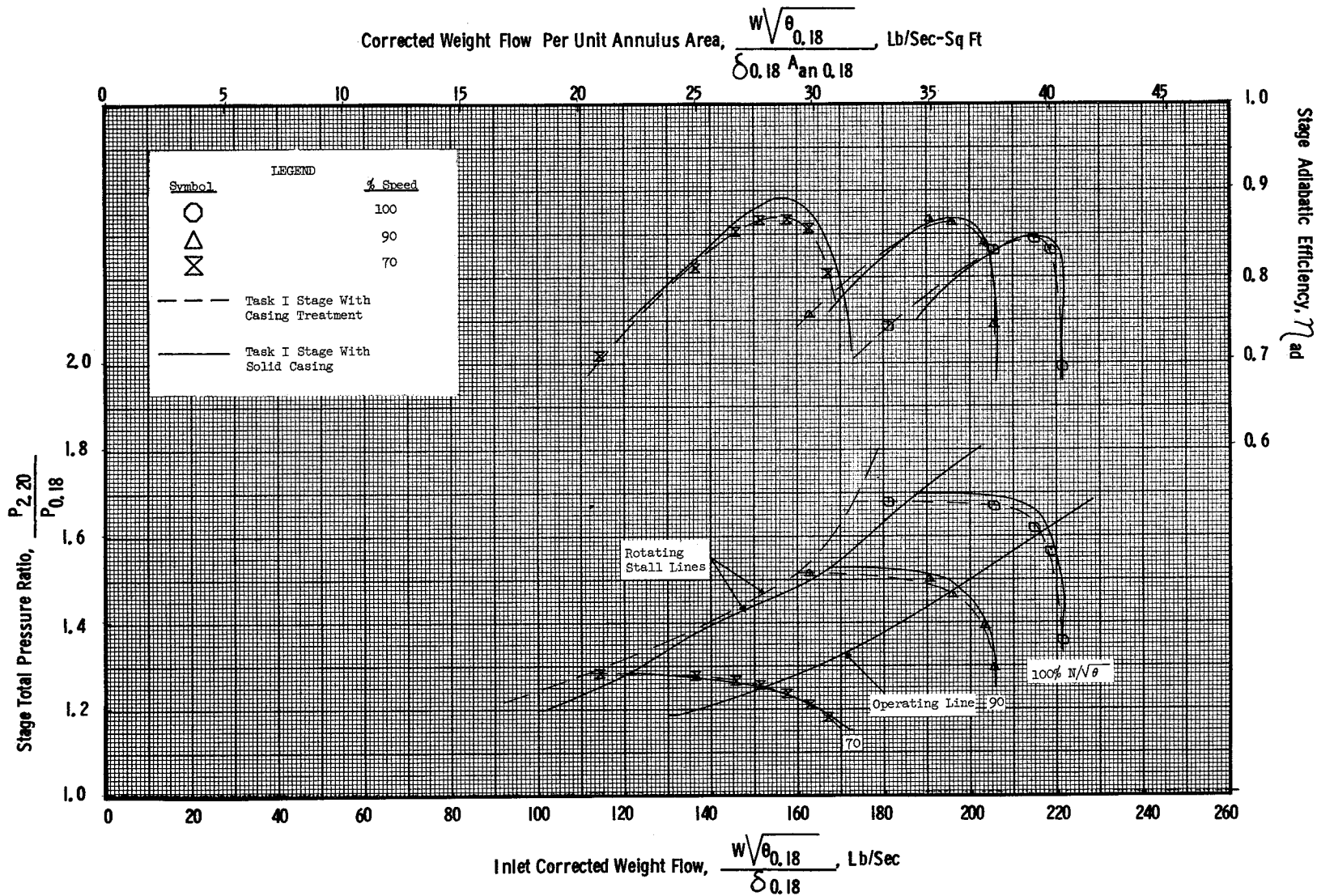


Figure 8 (j). Task I Stage Undistorted Inlet Performance Map; Blade Angle Slots #1 Casing Treatment.

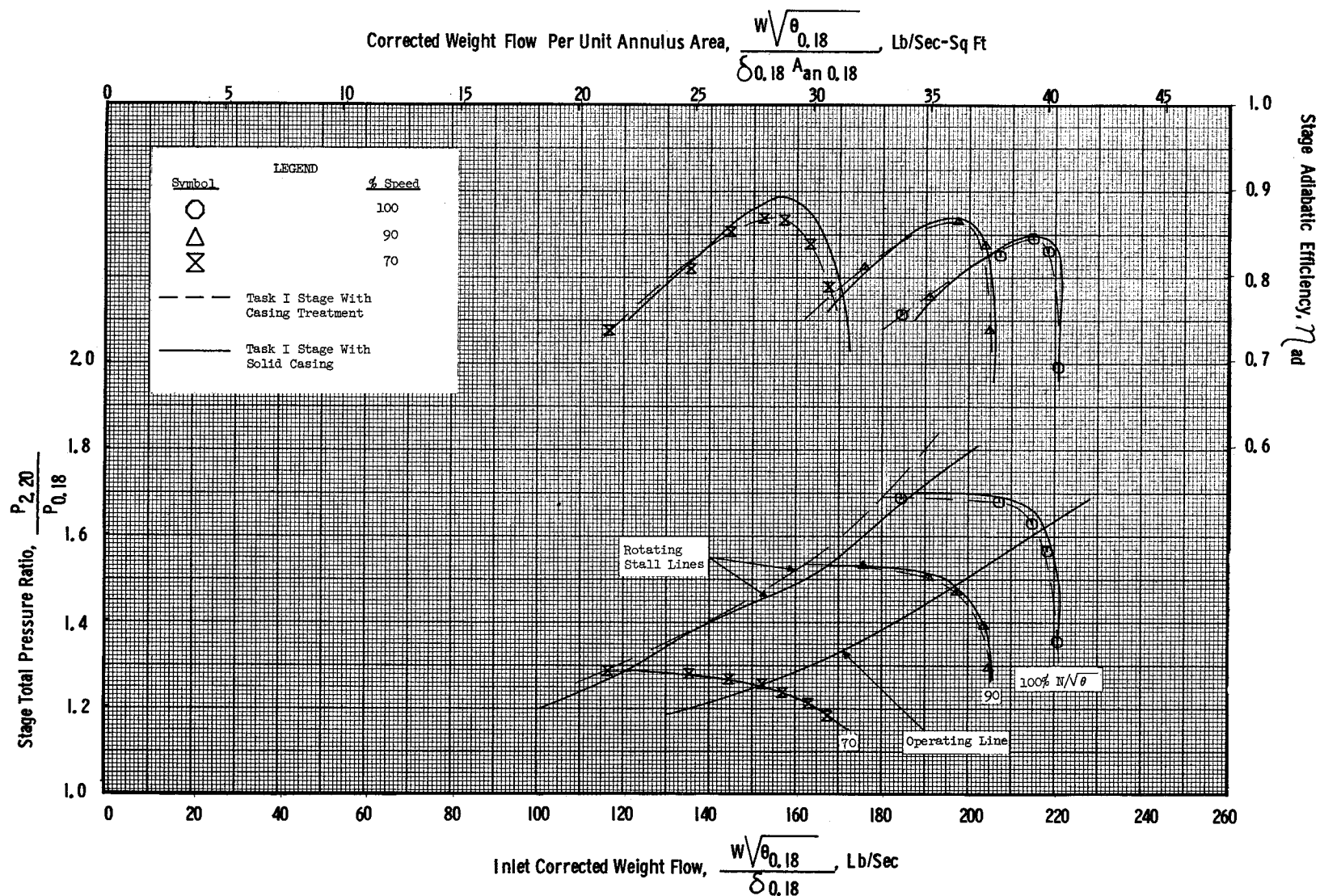


Figure 8 (k). Task I Stage Undistorted Inlet Performance Map; Blade Angle Slots #2 Casing Treatment.

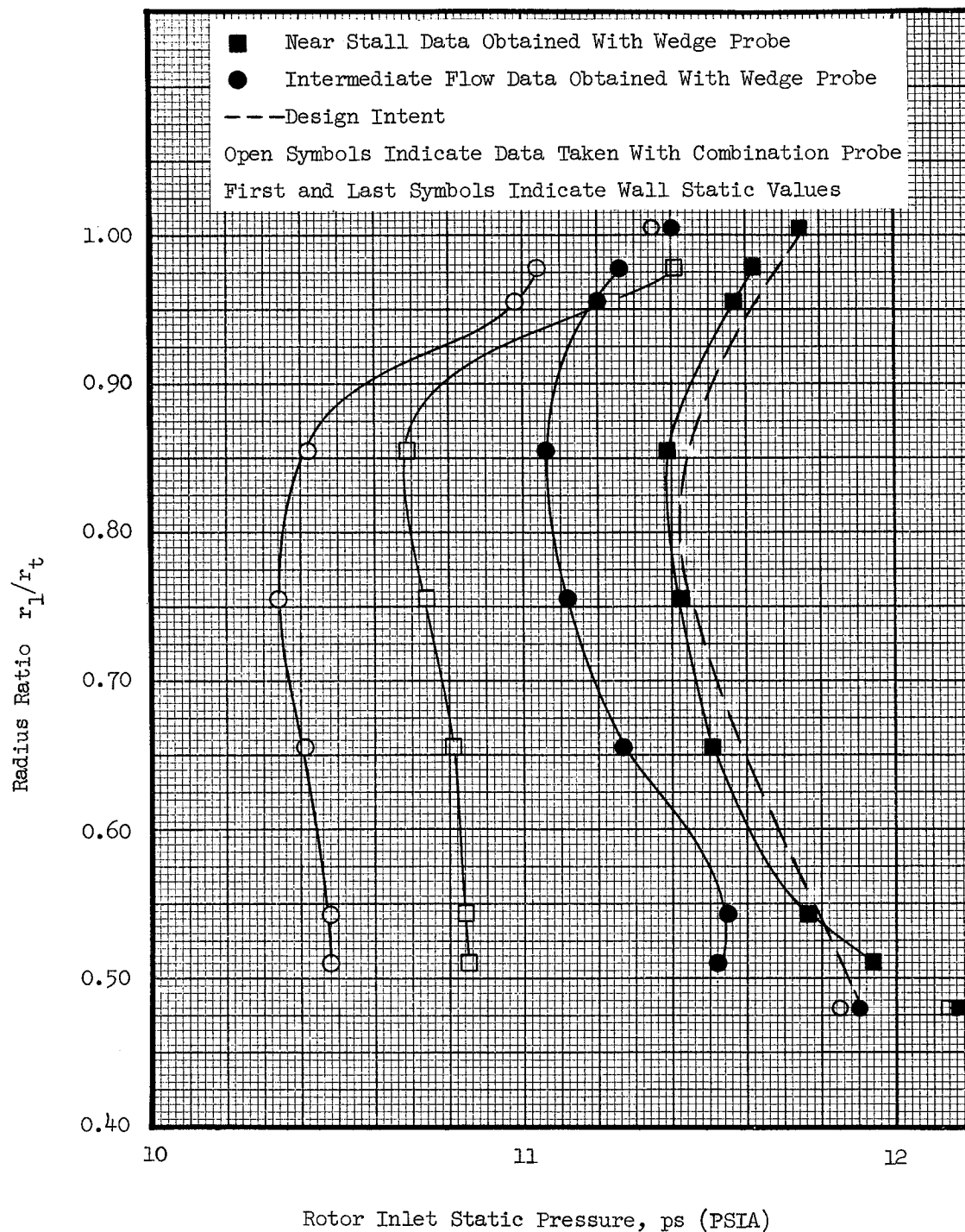


Figure 9. Task II Rotor Inlet Static-Pressure As Measured By a 4-Parameter Combination Probe and a Static-Pressure Wedge Probe.

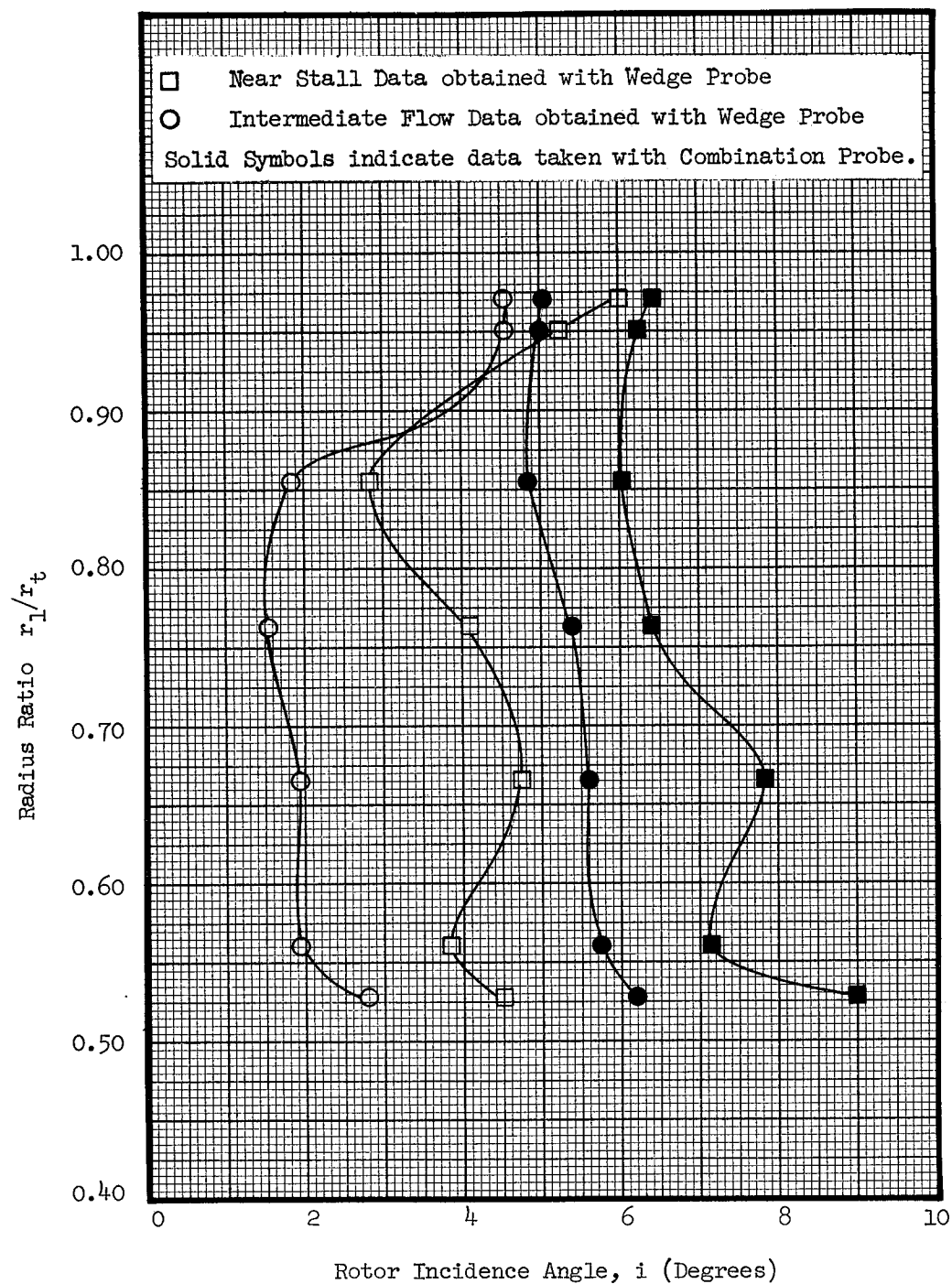


Figure 10. Task II Rotor Incidence Angle as Calculated From Measurements by a 4-Parameter Combination Probe and a Static-Pressure Wedge Probe.

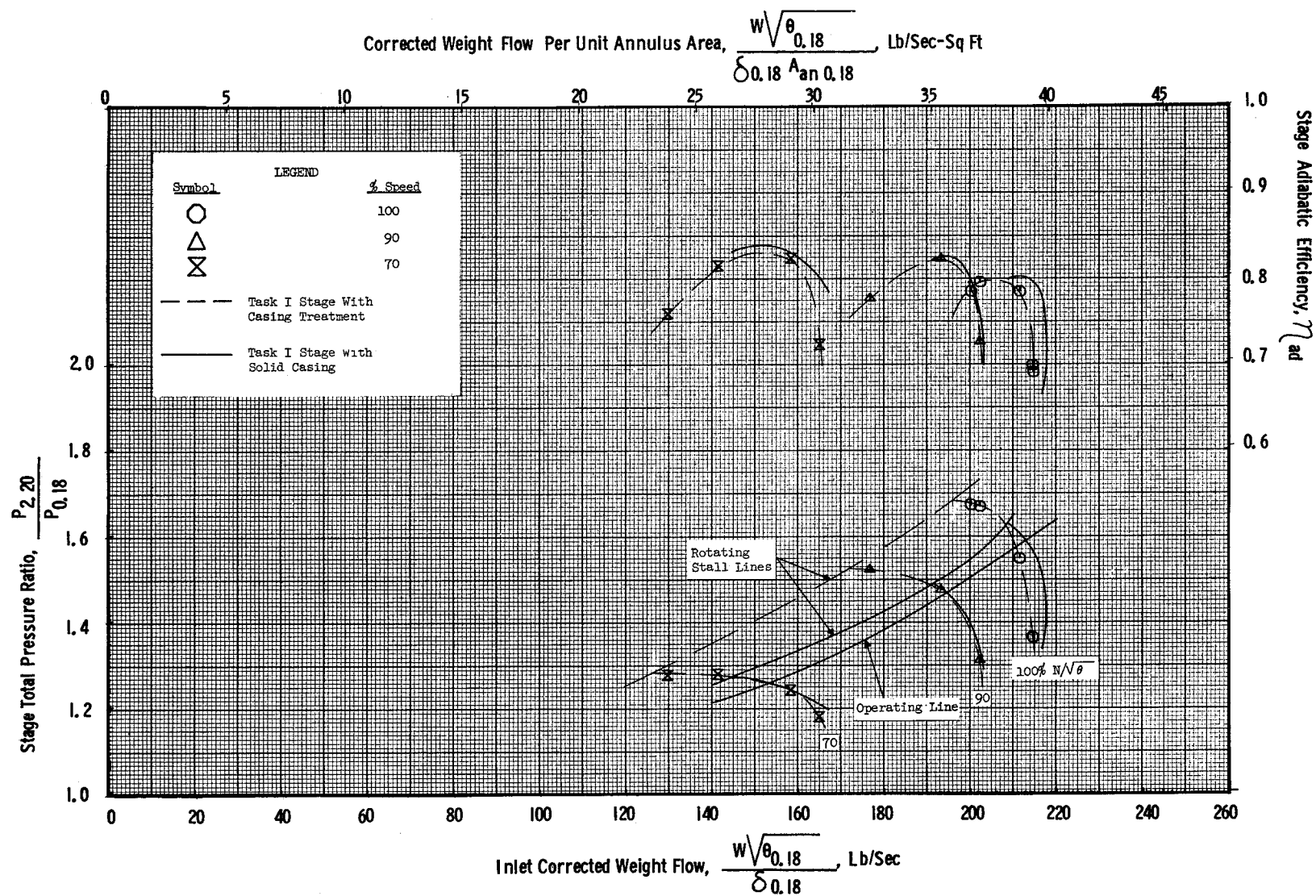


Figure 11 (a). Task I Stage Radial Distortion Performance Map; Honeycomb #1 Casing Treatment.

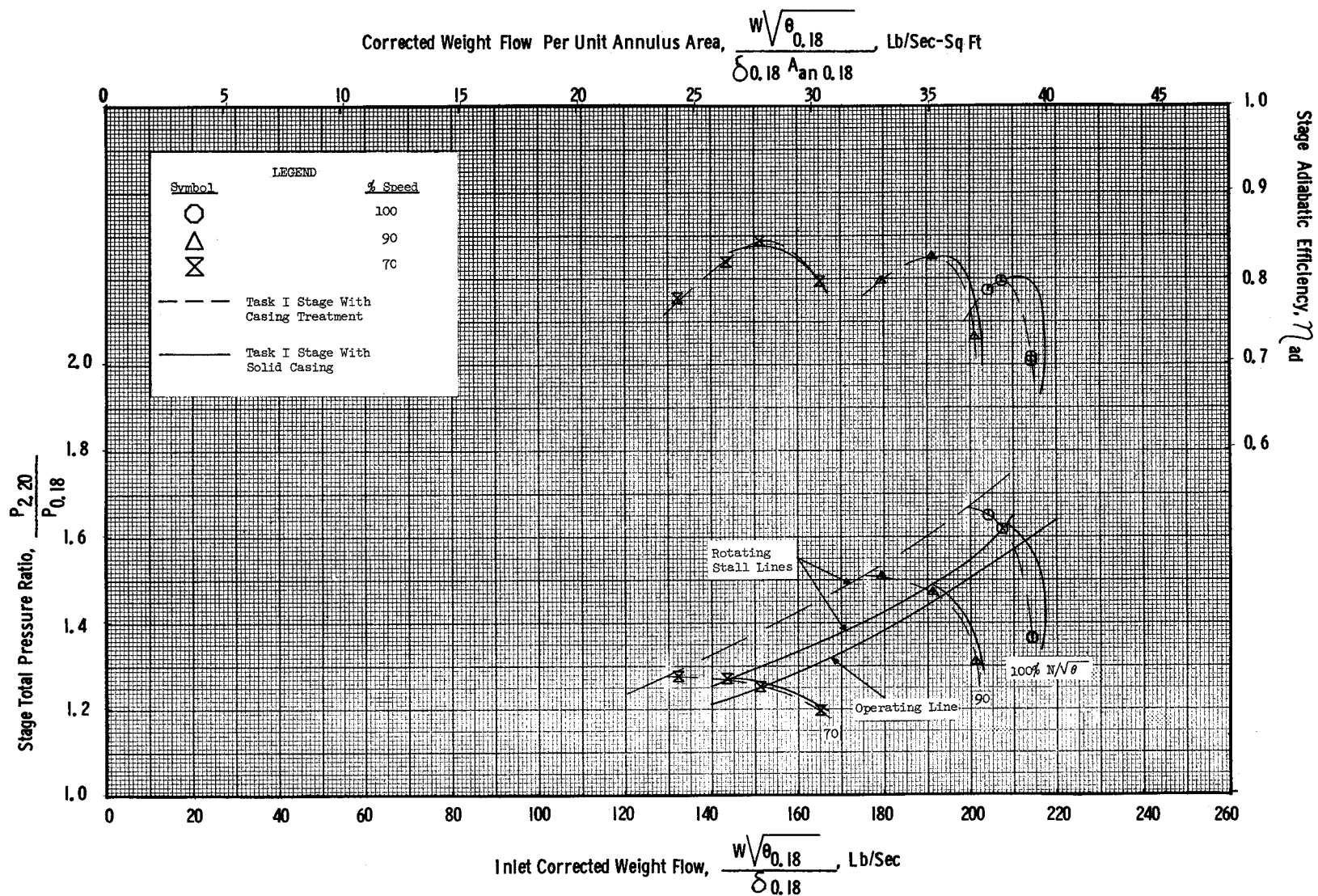


Figure 11 (b). Task I Stage Radial Distortion Performance Map; Honeycomb #2 Casing Treatment.

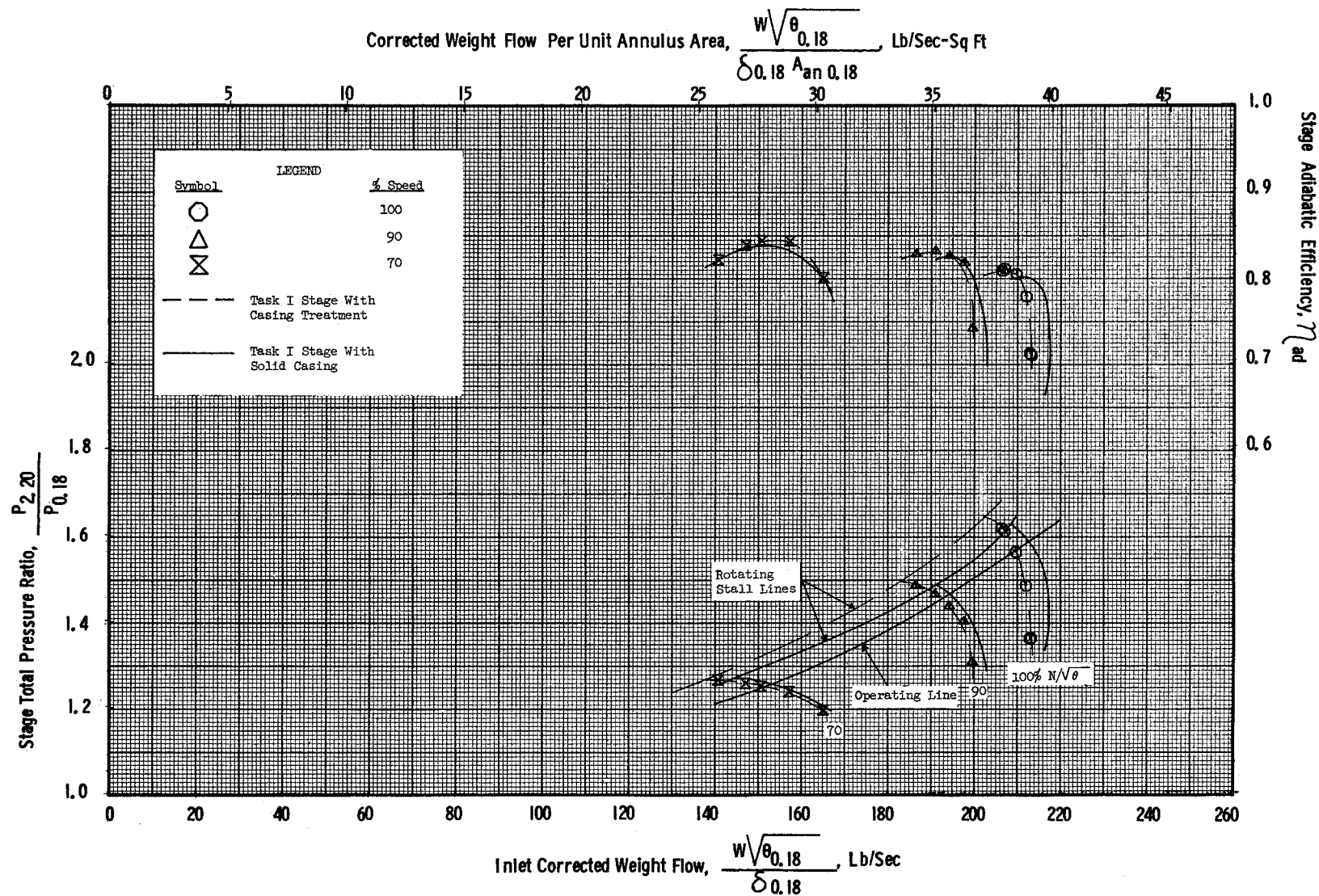


Figure 11 (c). Task I Stage Radial Distortion Performance Map; Circumferential Grooves #1 Casing Treatment.

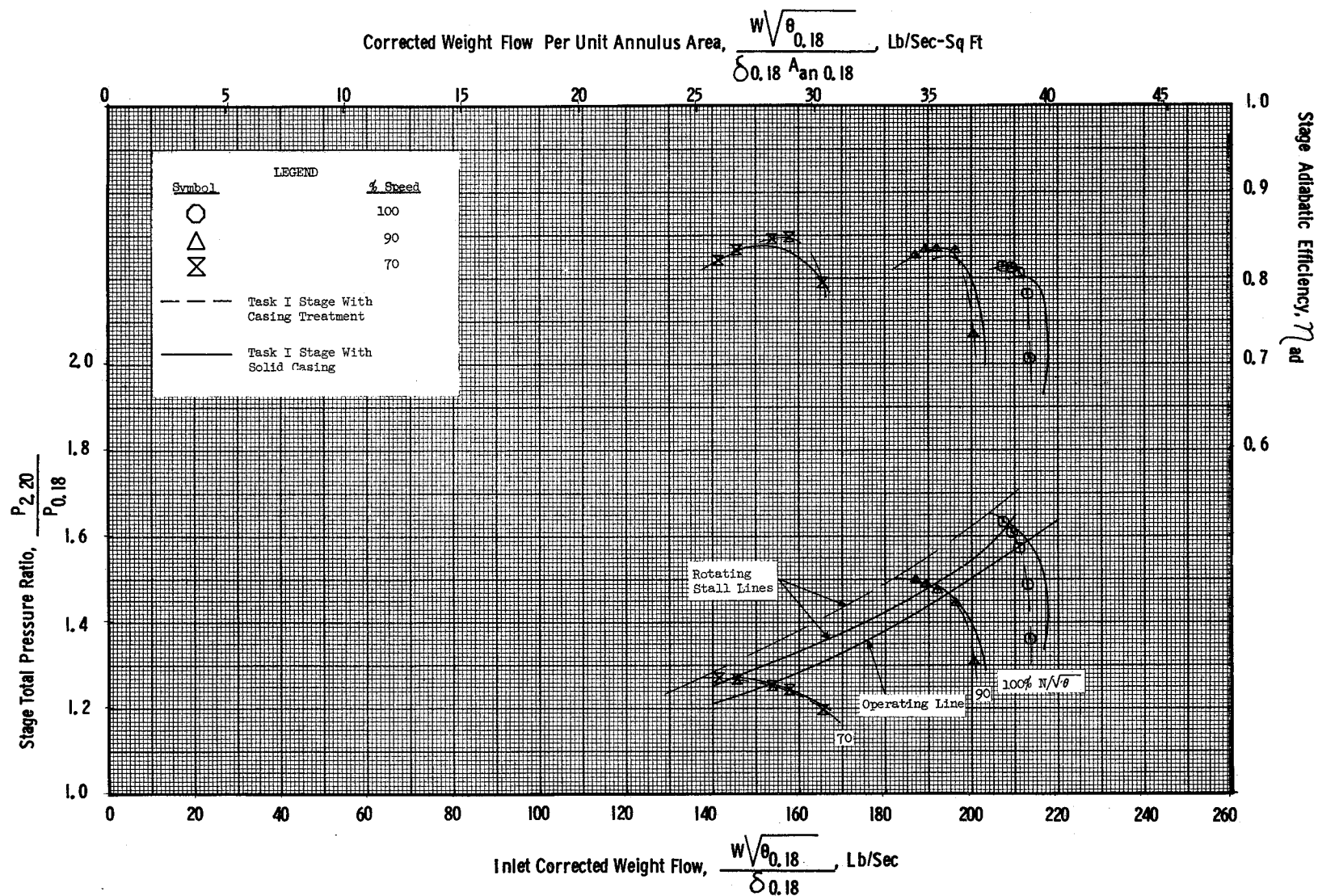


Figure 11 (d). Task I Stage Radial Distortion Performance Map; Circumferential Grooves #2 Casing Treatment.

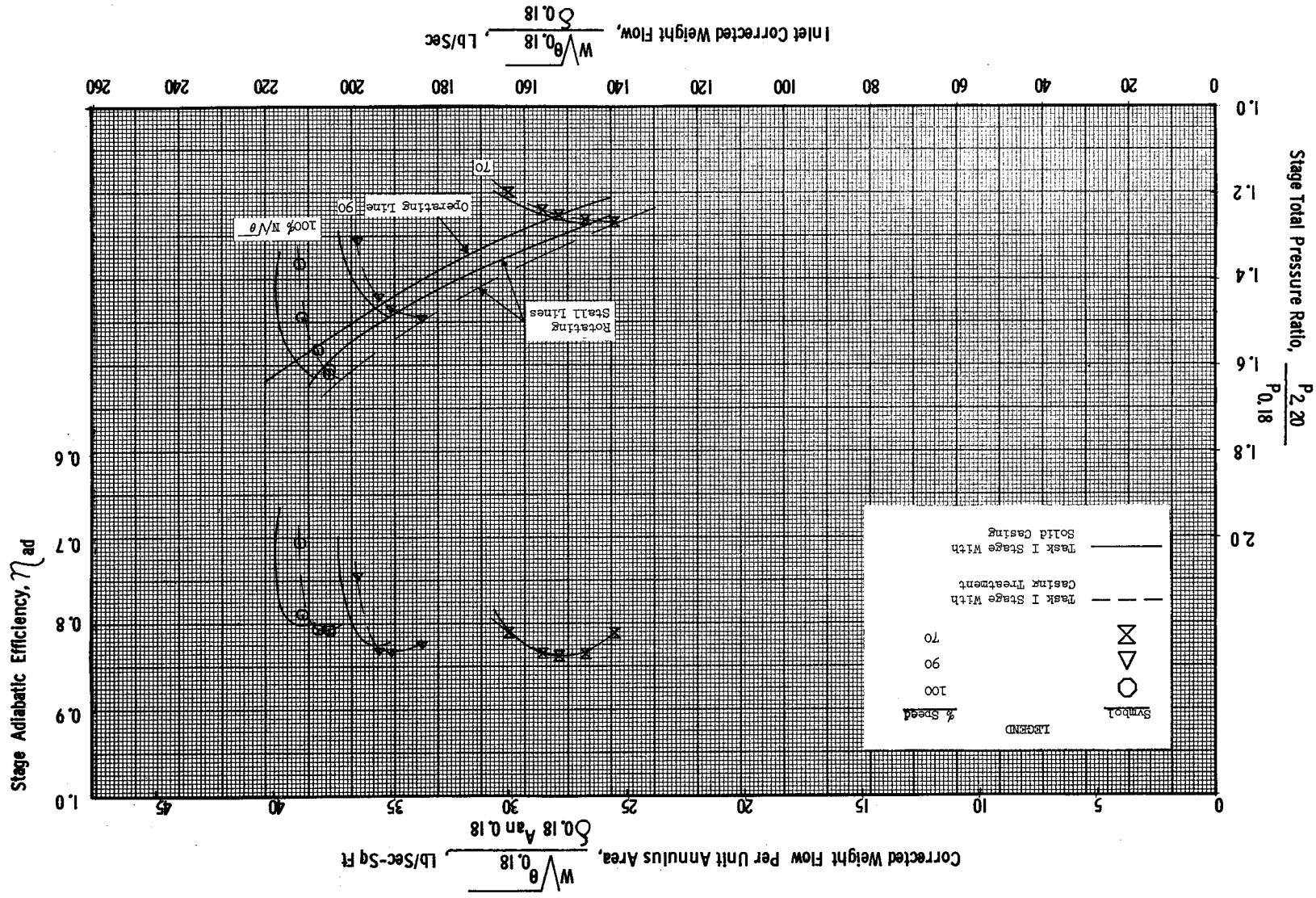


Figure 11 (e). Task I Stage Radial Distortion Performance Map; Circumferential Grooves #3 Casing Treatment.

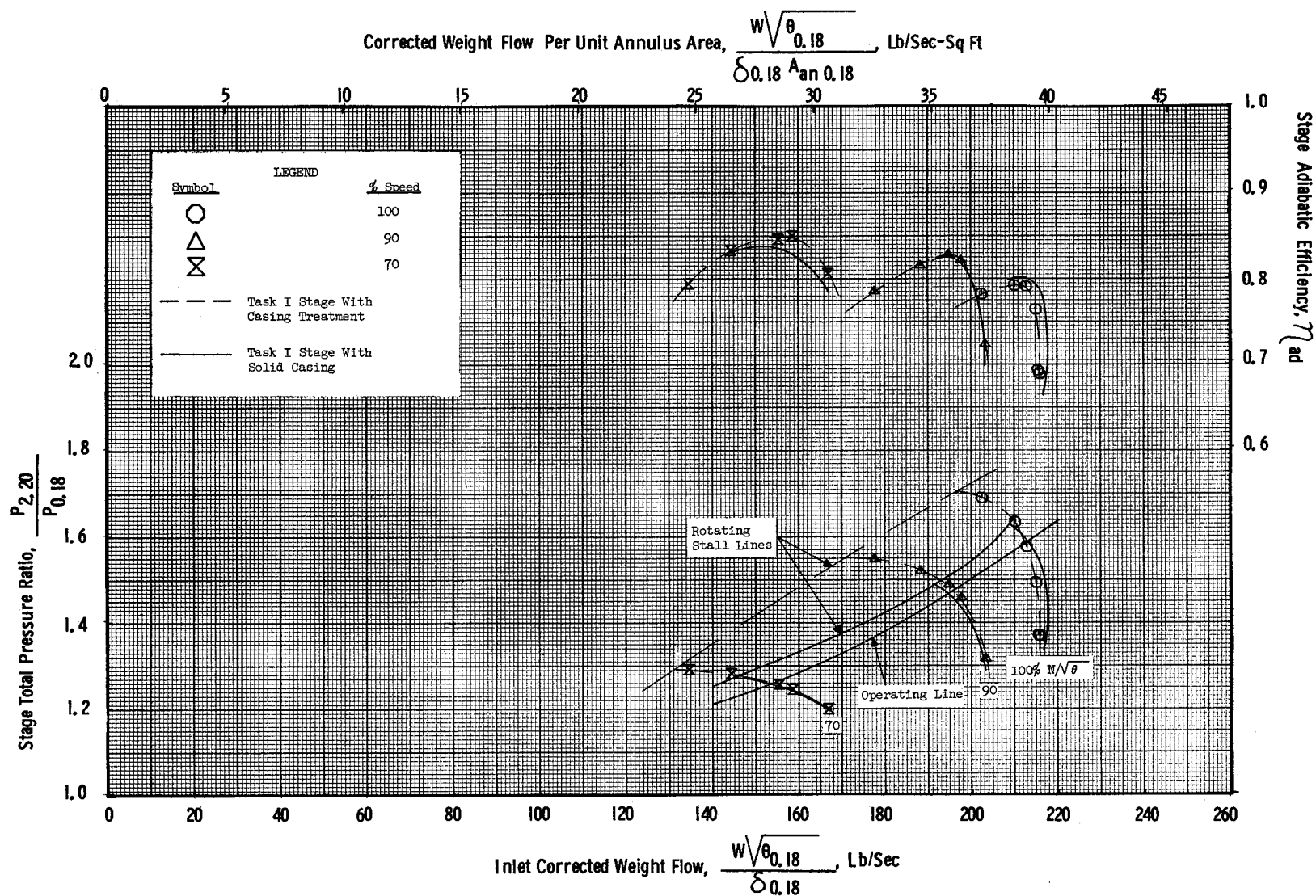


Figure 11 (f). Task I Stage Radial Distortion Performance Map; Skewed Slots #1 Casing Treatment.

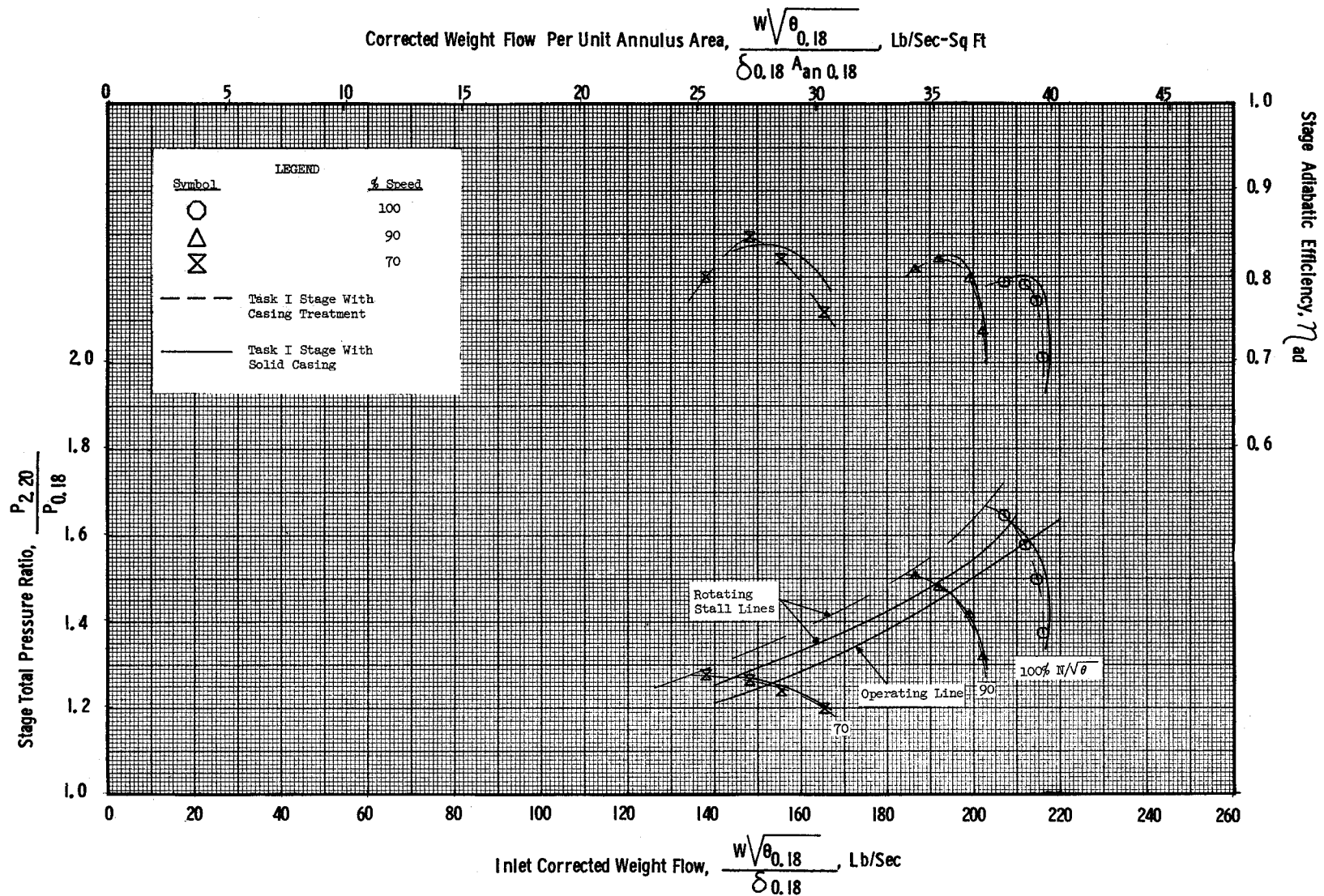


Figure 11 (g). Task I Stage Radial Distortion Performance Map; Skewed Slots #3 Casing Treatment.

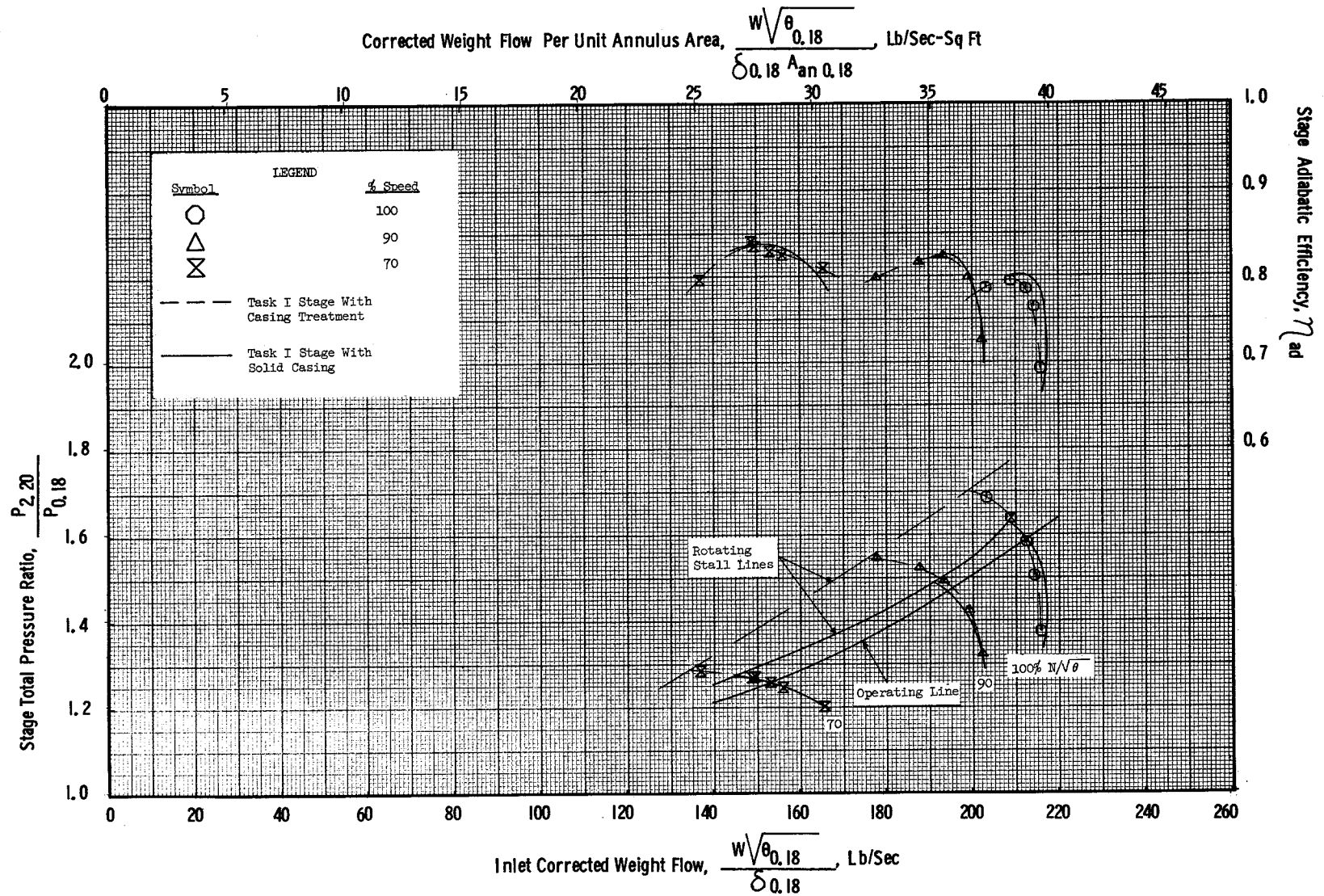


Figure 11 (h). Task I Stage Radial Distortion Performance Map; Skewed Slots #4 Casing Treatment.

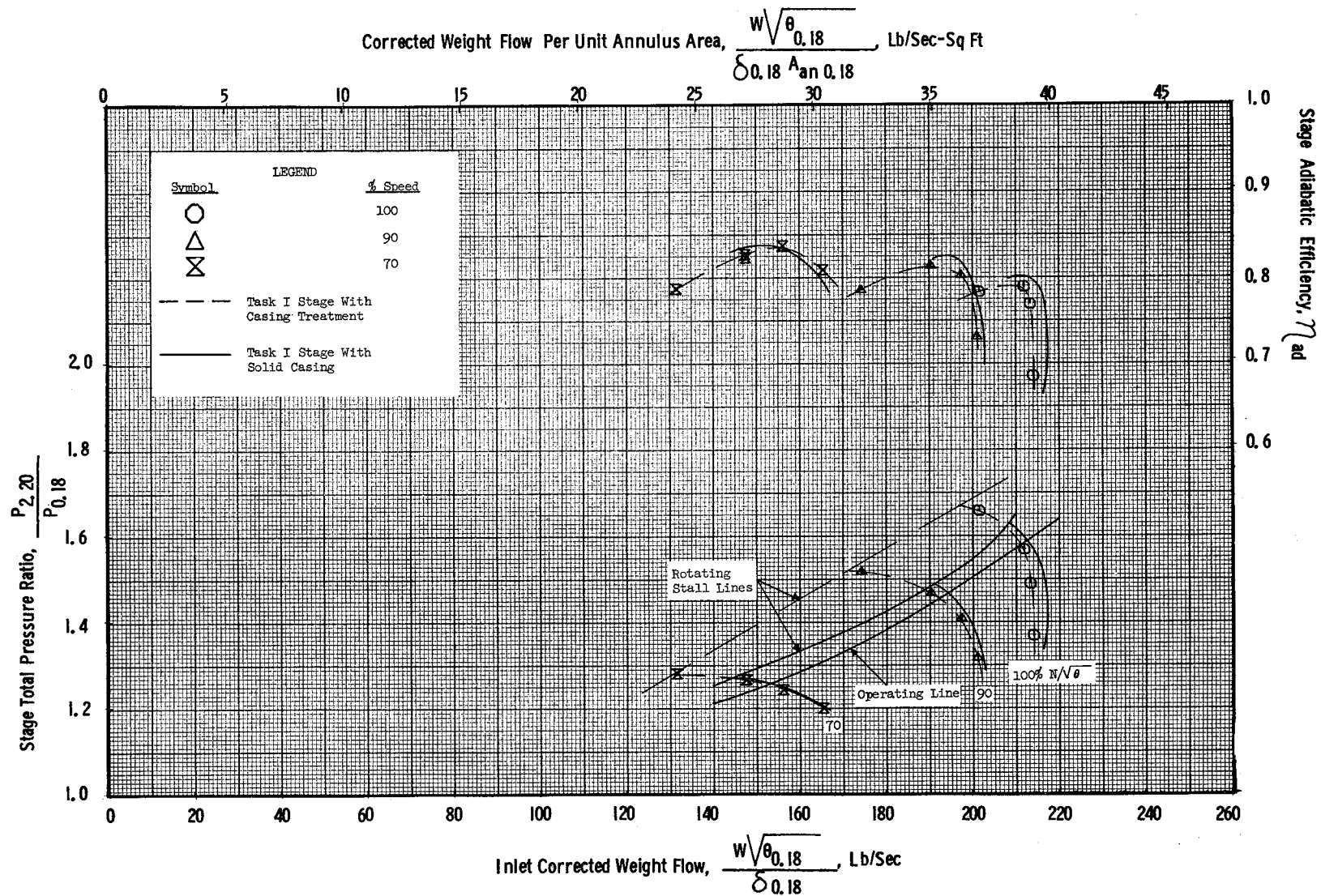


Figure 11 (i). Task I Stage Radial Distortion Performance Map; Blade Angle Slots #1 Casing Treatment.

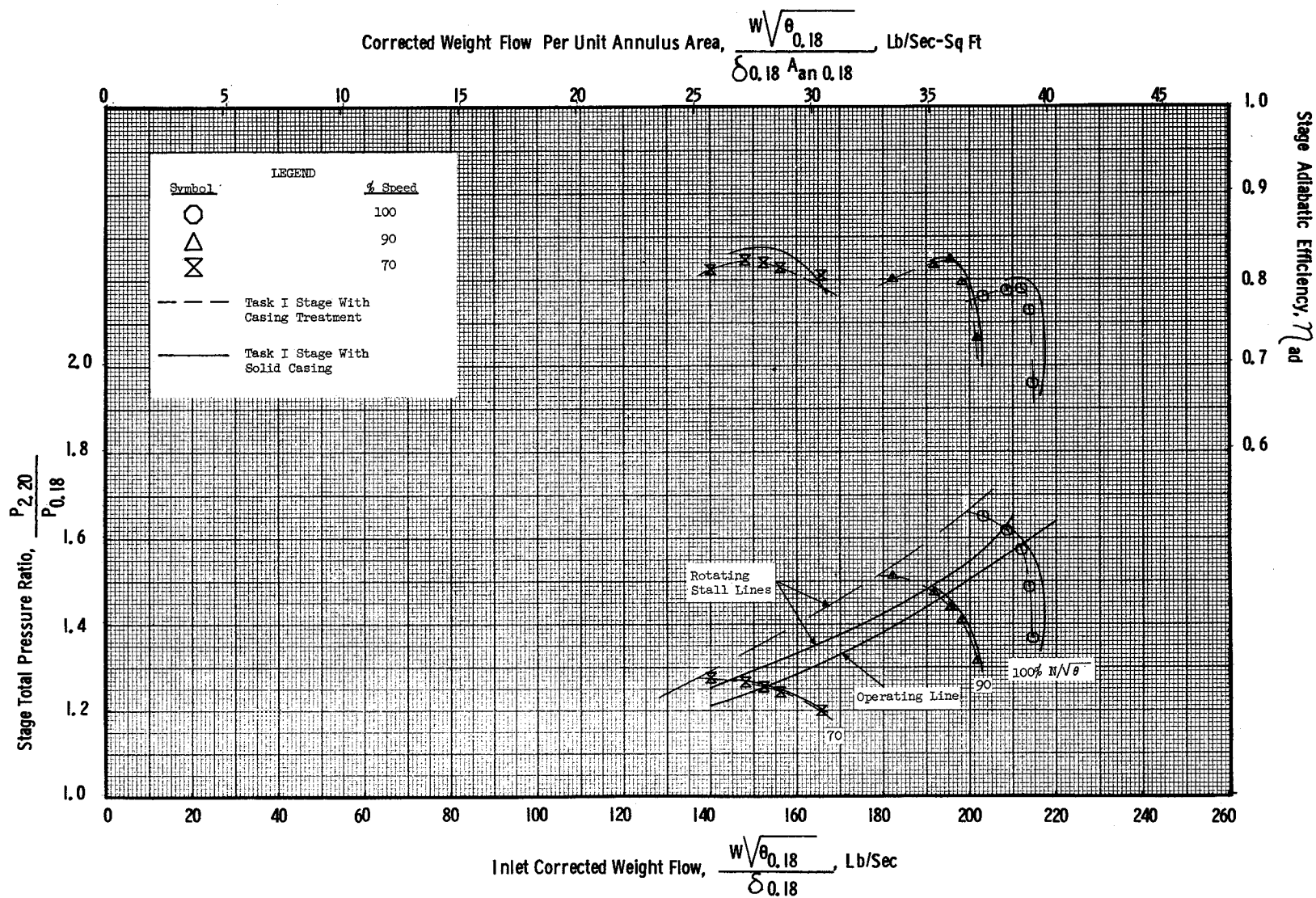


Figure 11 (j). Task I Stage Radial Distortion Performance Map; Blade Angle Slots #2 Casing Treatment.

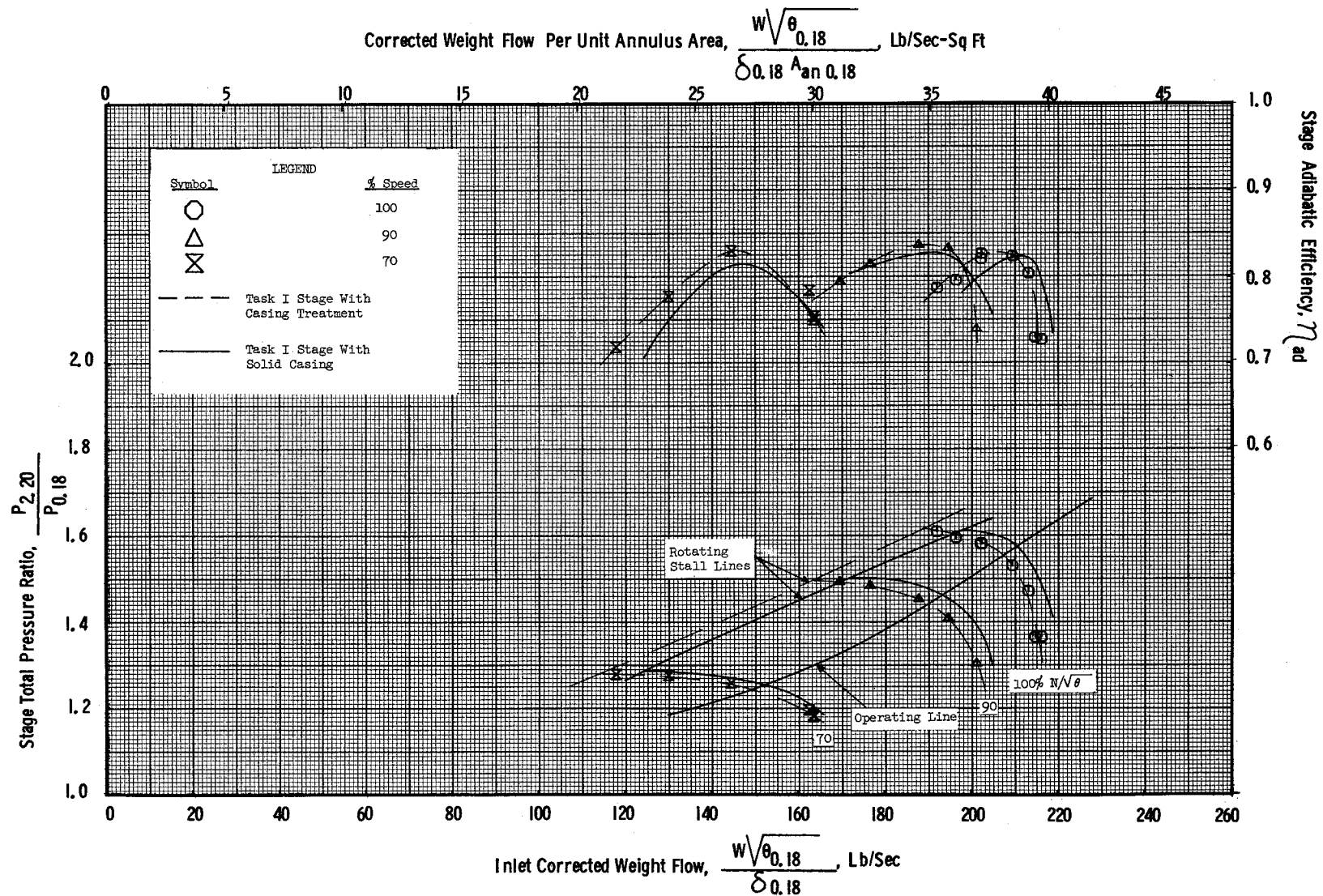


Figure 12. Task I Stage Circumferential Distortion Performance Map; Skewed Slots #2 Casing Treatment.

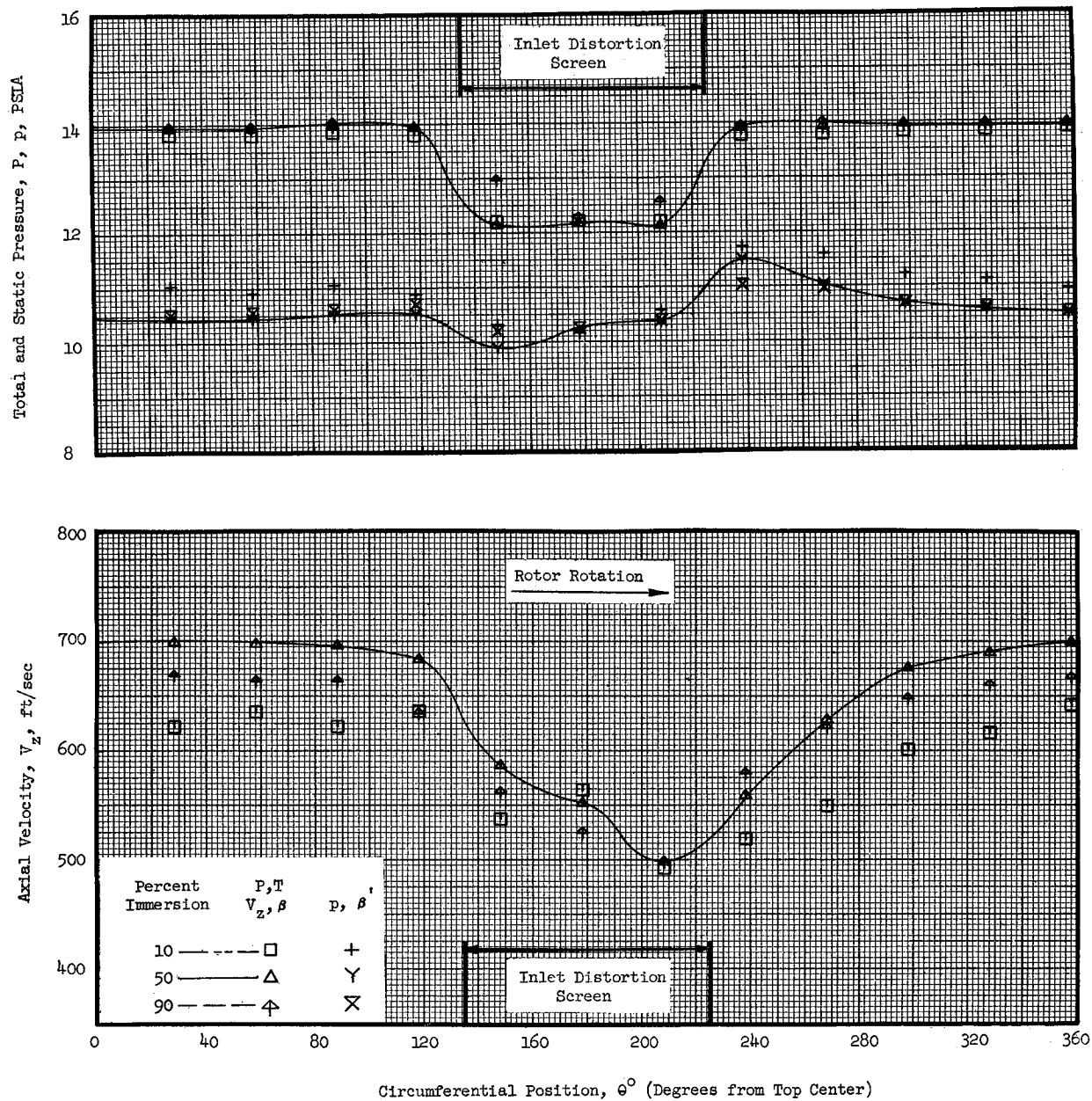


Figure 13 (a). Task I Stage Circumferential Distortion Profiles of Flow Conditions at 100% Speed Near Stall at Plane 0.95.

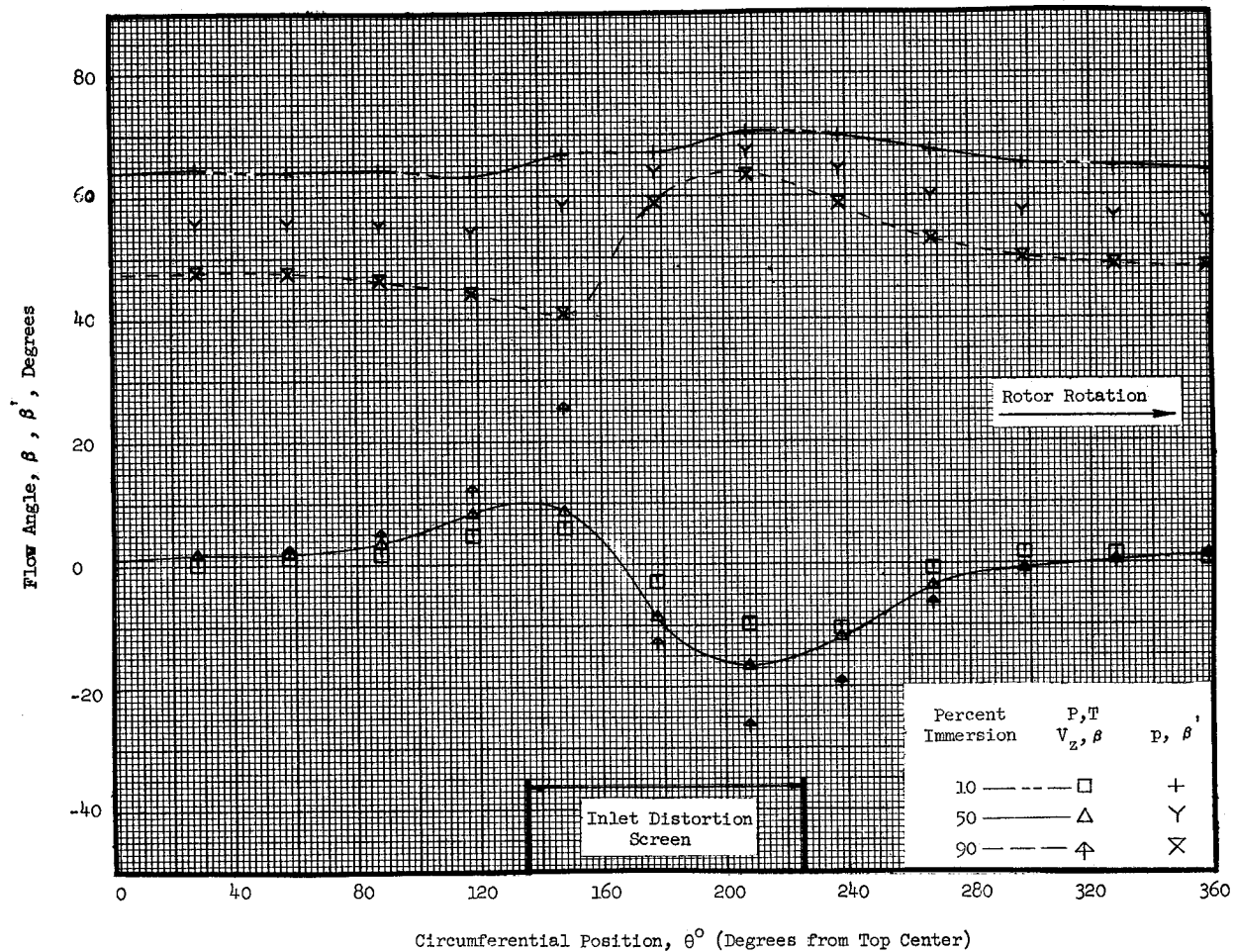


Figure 13 (a). Task I Stage Circumferential Distortion Profiles of Flow Conditions at 100% Speed Near Stall at Plane 0.95 (Concluded).

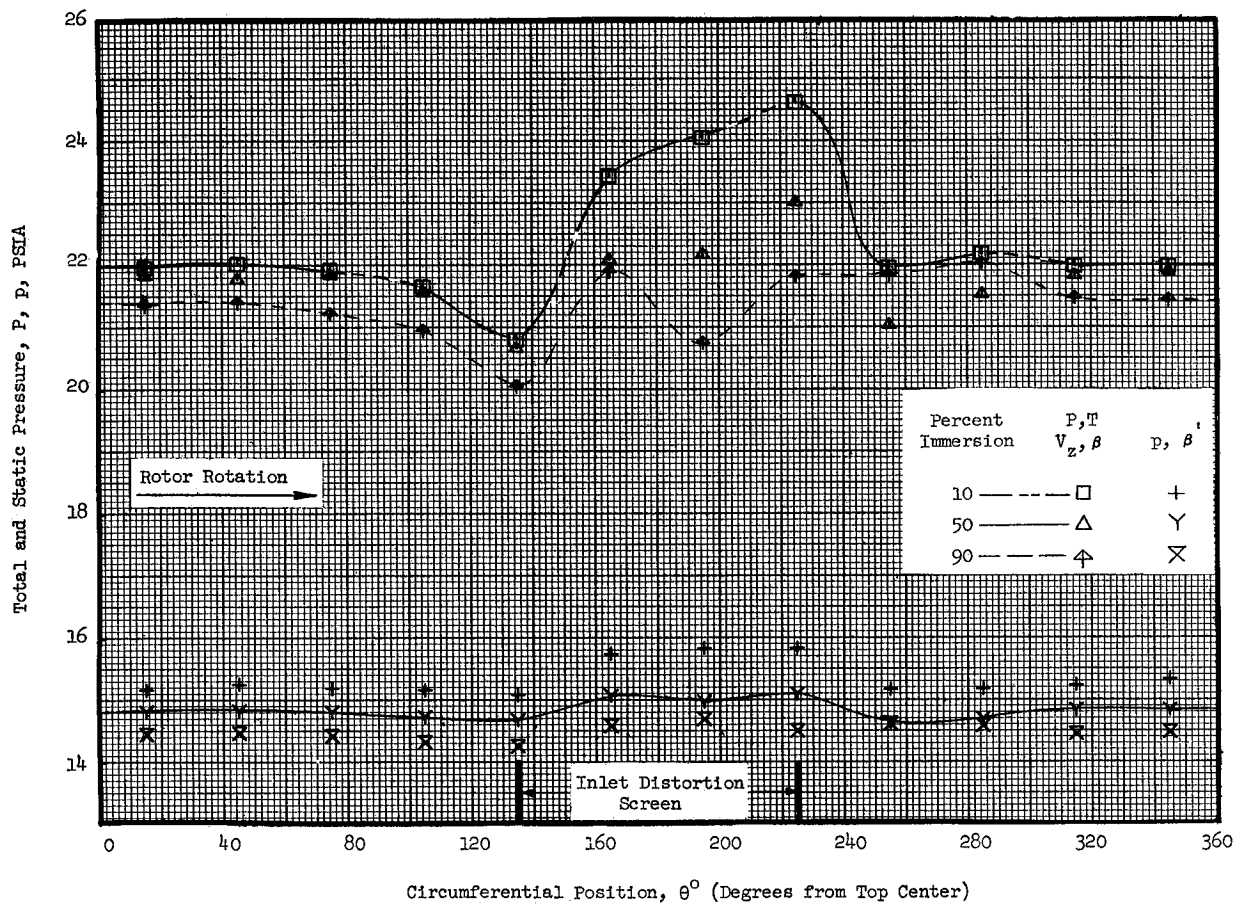


Figure 13 (b). Task I Stage Circumferential Distortion Profiles of Flow Conditions at 100% Speed Near Stall at Plane 1.51.

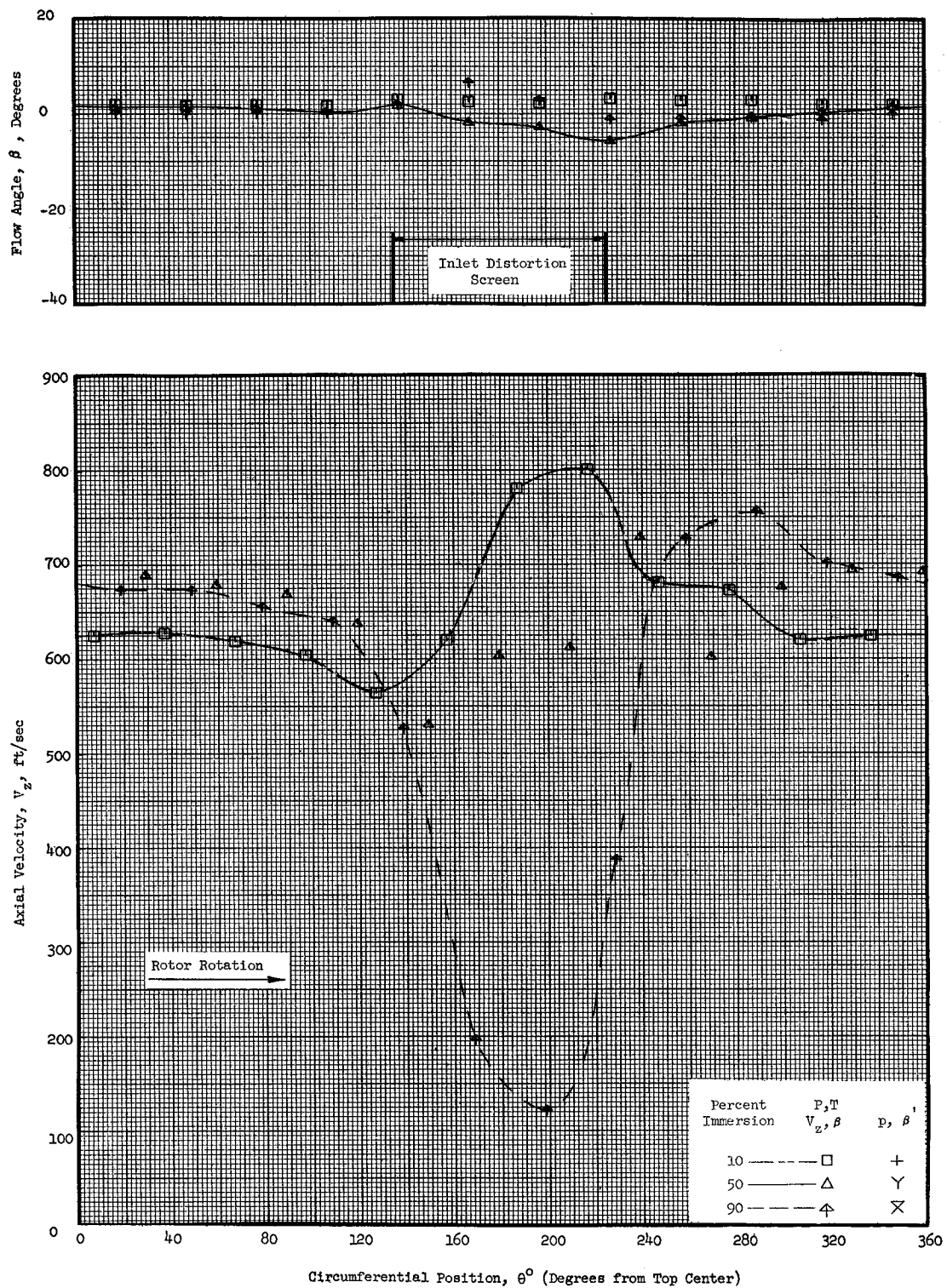


Figure 13 (b). Task I Stage Circumferential Distortion Profiles of Flow Conditions at 100% Speed Near Stall at Plane 1.51 (Concluded).

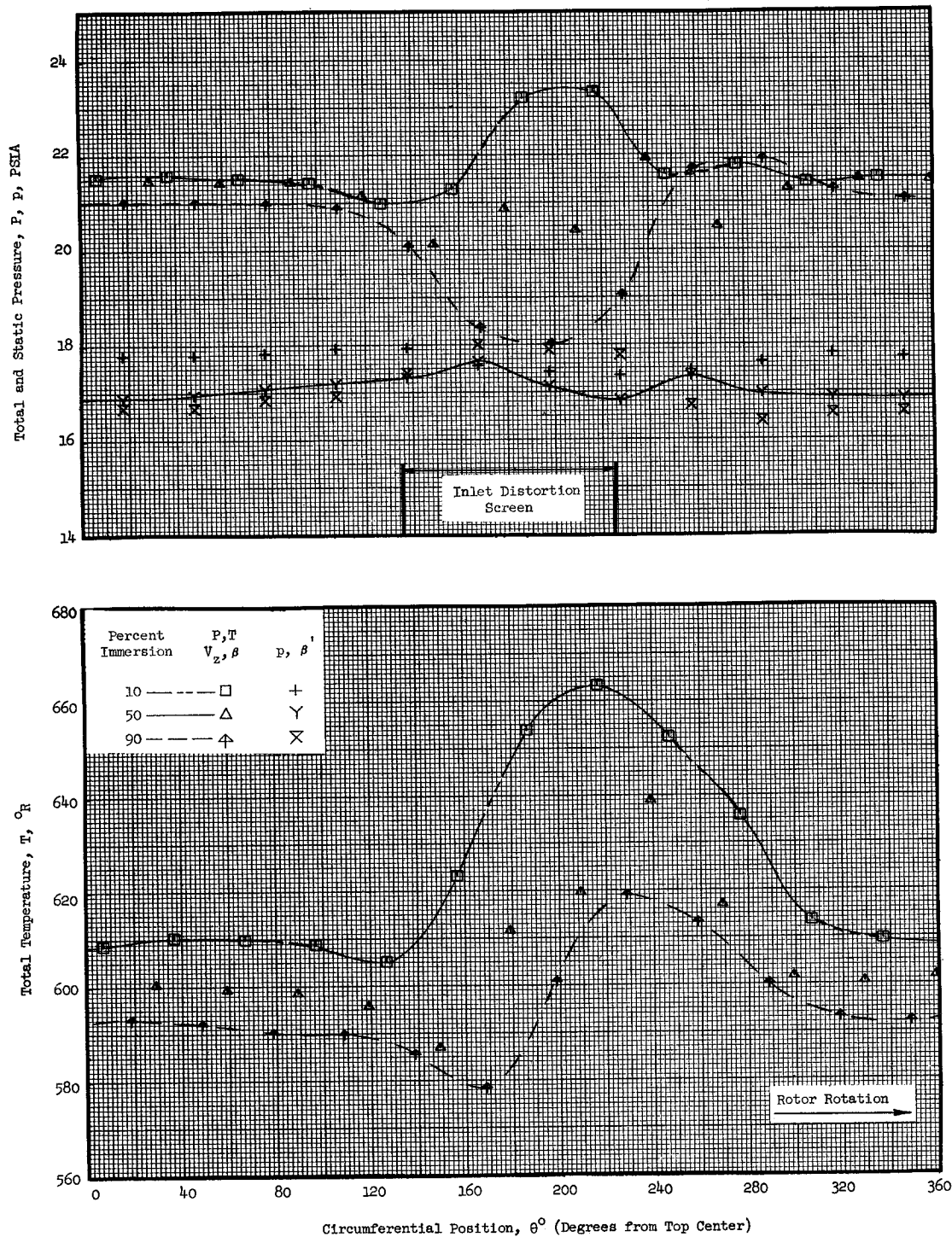


Figure 13 (c). Task I Stage Circumferential Distortion Profiles of Flow Conditions at 100% Speed Near Stall at Plane 2.20.

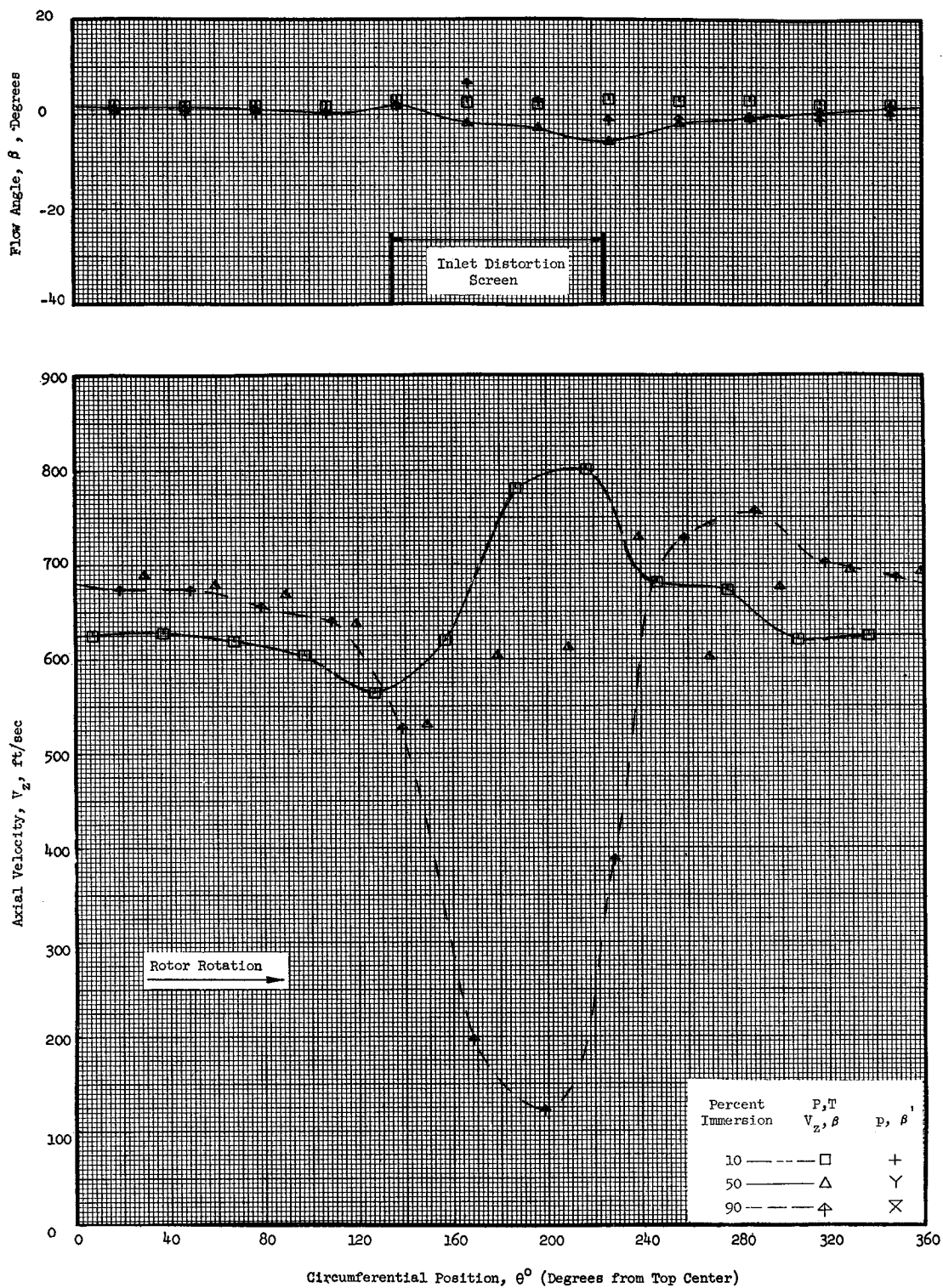


Figure 13 (c). Task I Stage Circumferential Distortion Profiles of Flow Conditions at 100% Speed Near Stall at Plane 2.20 (Concluded).

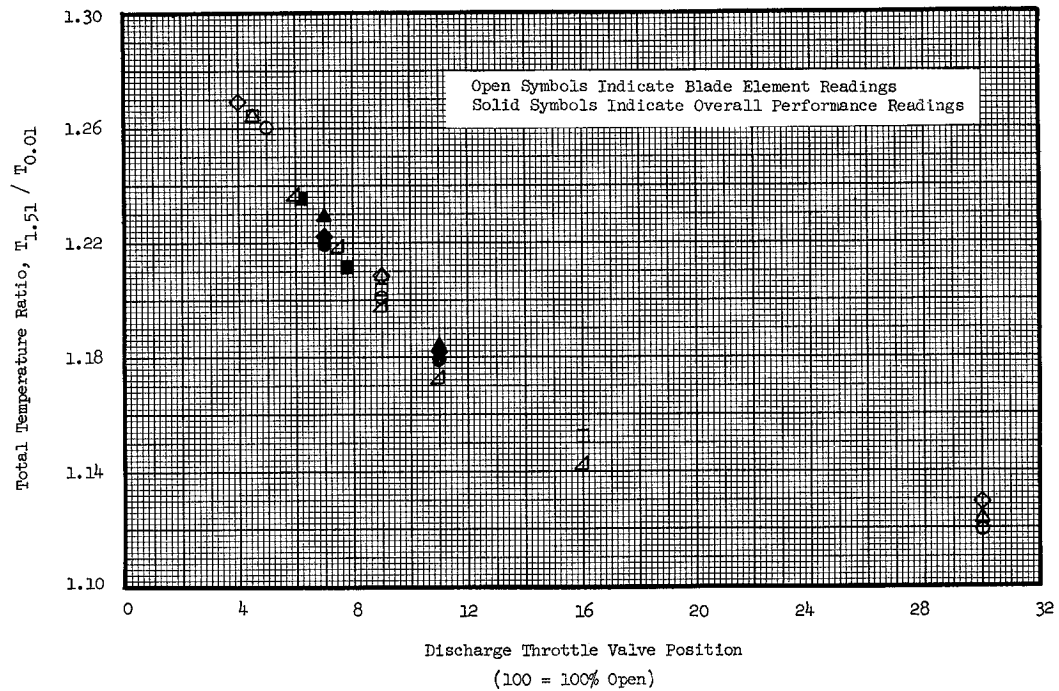
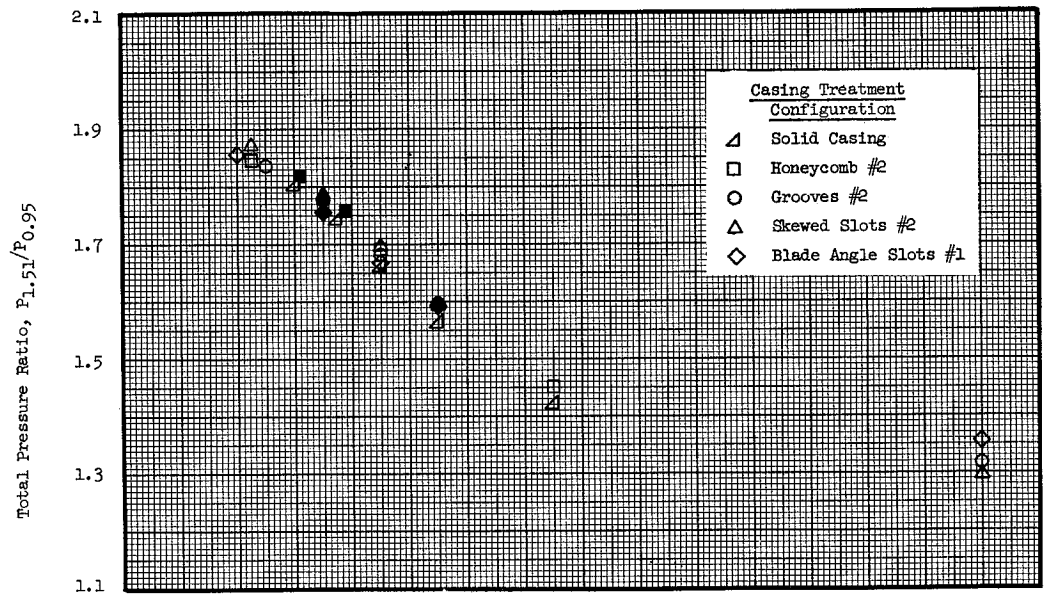


Figure 14 (a). Task I Rotor Blade Element Data, 5% Immersion, 100% Speed, Undistorted Inlet.

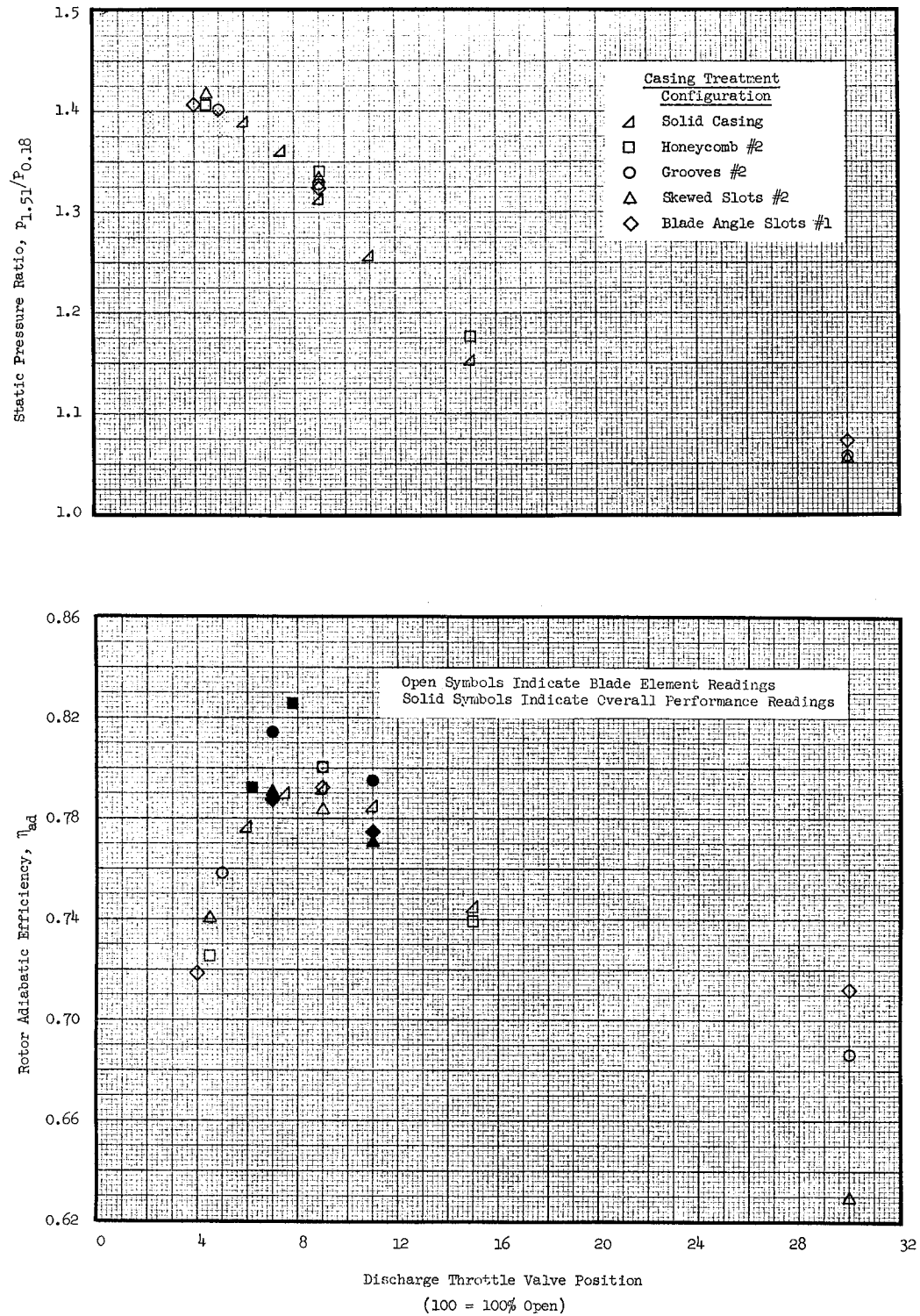


Figure 14 (a). Task I Rotor Blade Element Data, 5% Immersion, 100% Speed, Undistorted Inlet (Concluded).

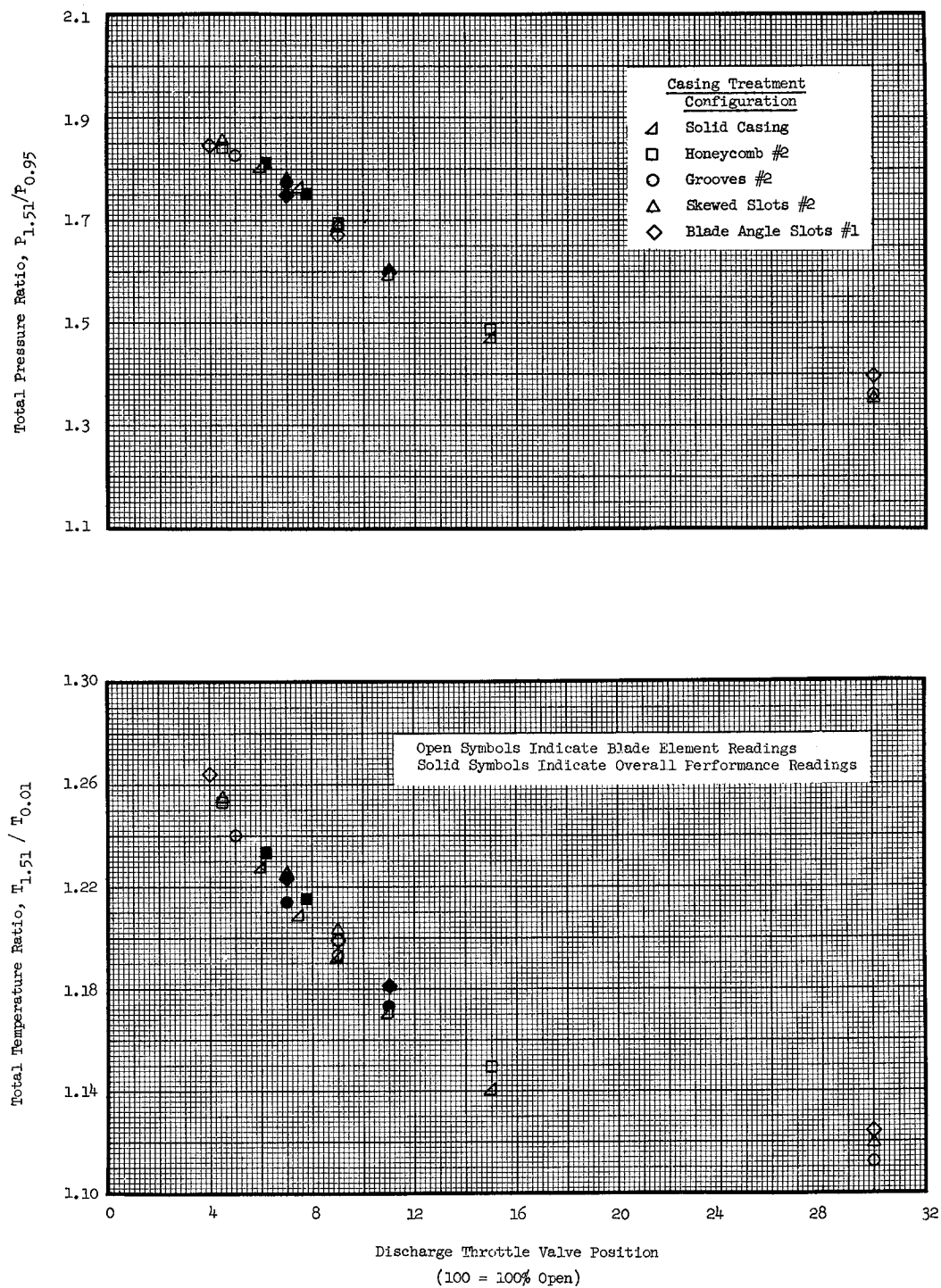


Figure 14 (b). Task I Rotor Blade Element Data, 10% Immersion, 100% Speed, Undistorted Inlet.

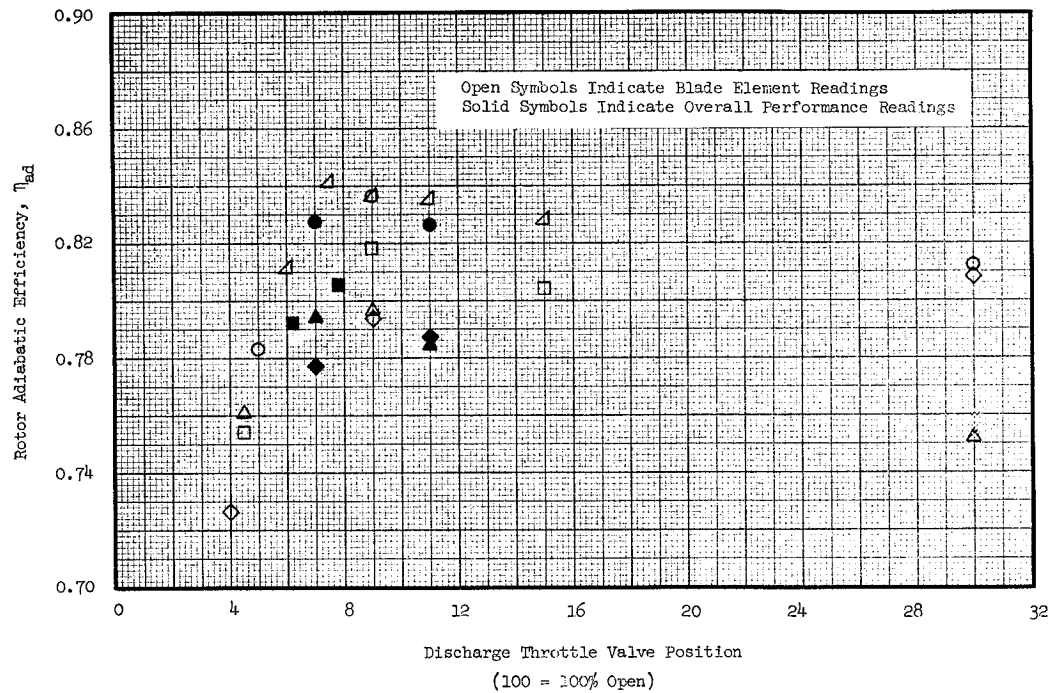
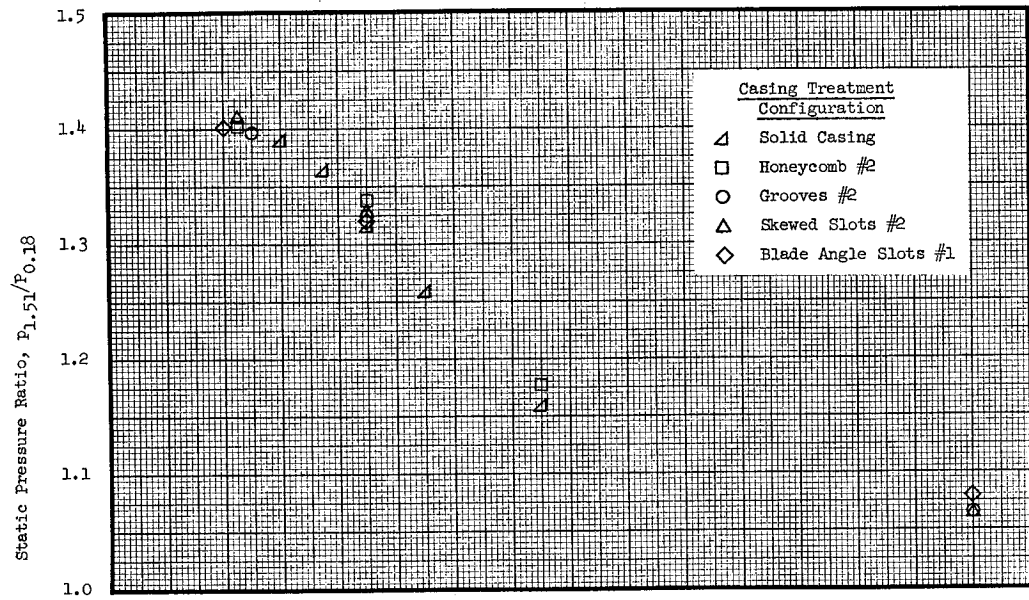


Figure 14 (b). Task I Rotor Blade Element Data, 10% Immersion, 100% Speed, Undistorted Inlet (Concluded).

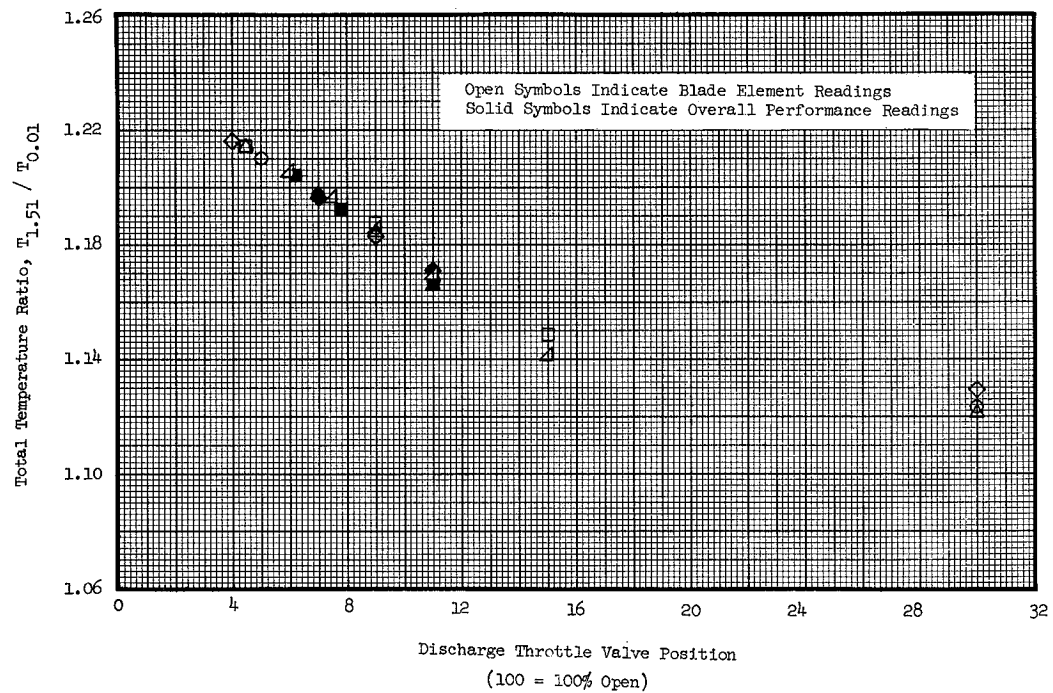
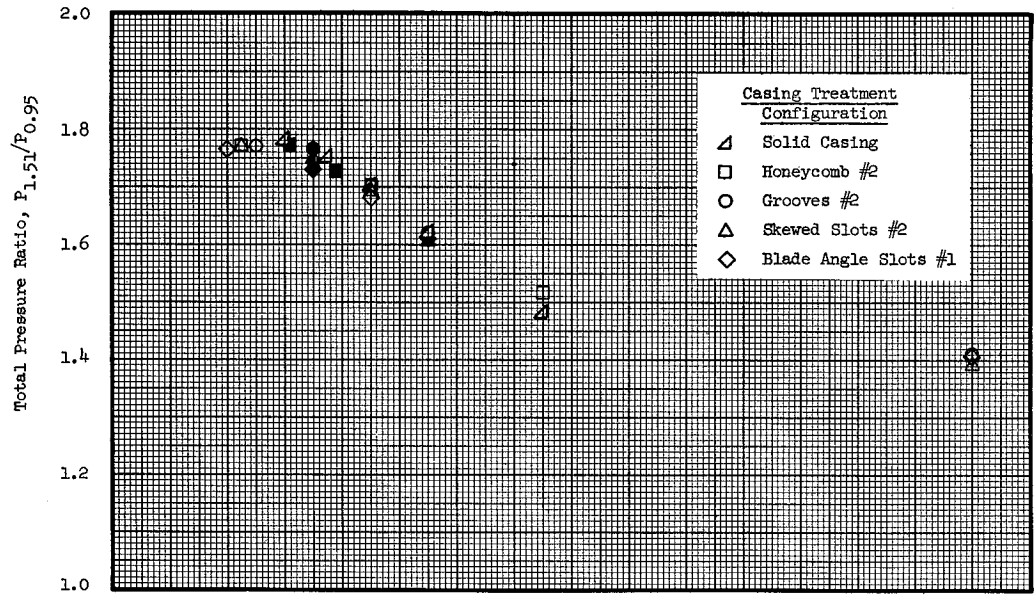


Figure 14 (c). Task I Rotor Blade Element Data, 30% Immersion, 100% Speed, Undistorted Inlet.

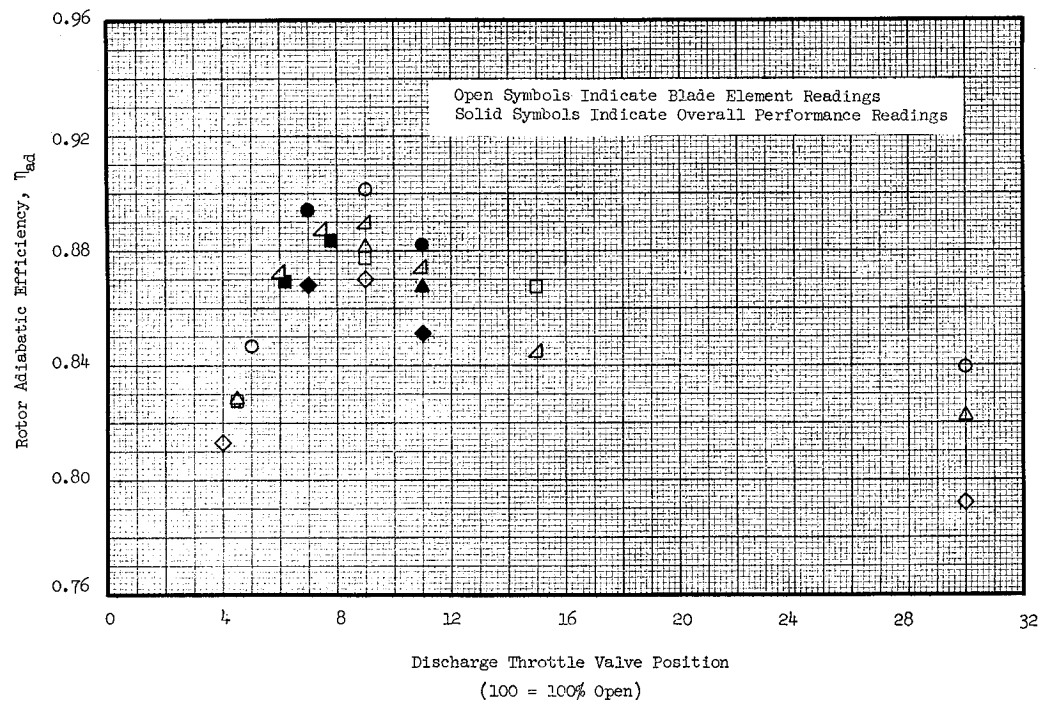
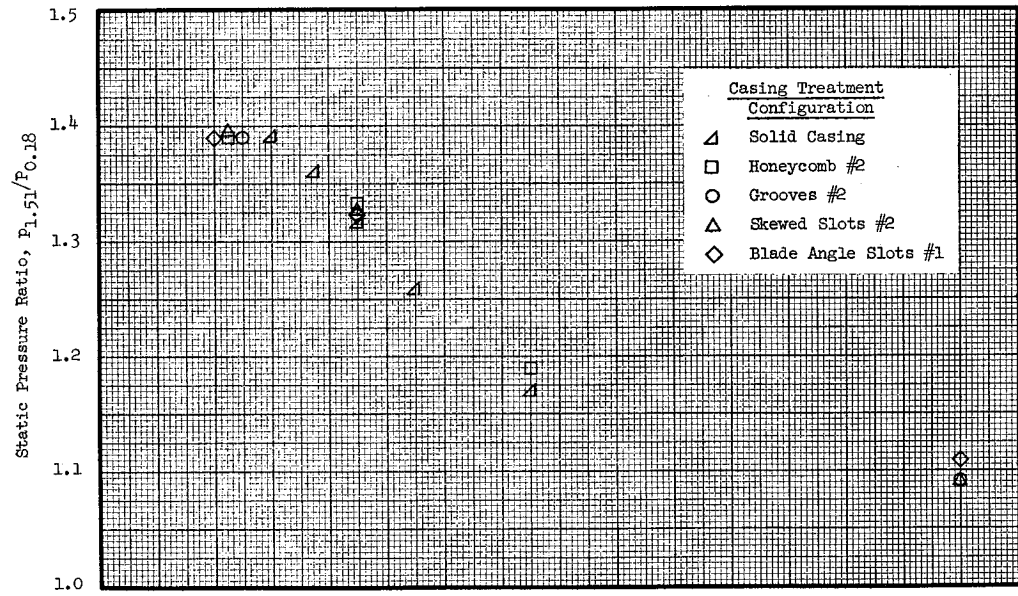


Figure 14 (c). Task I Rotor Blade Element Data, 30% Immersion, 100% Speed, Undistorted Inlet (Concluded).

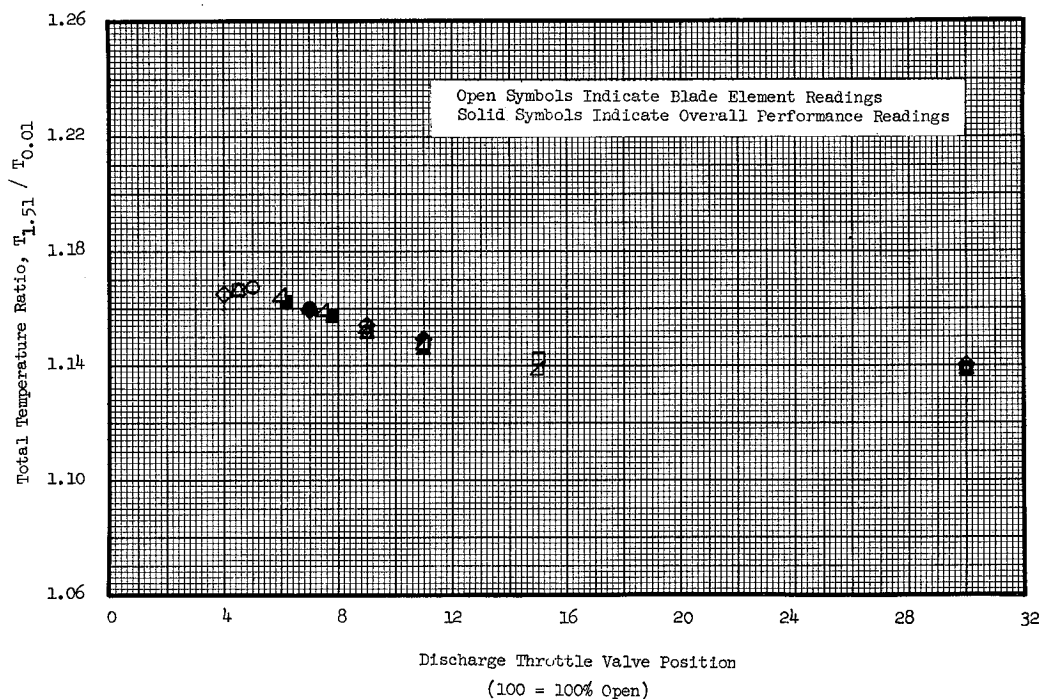
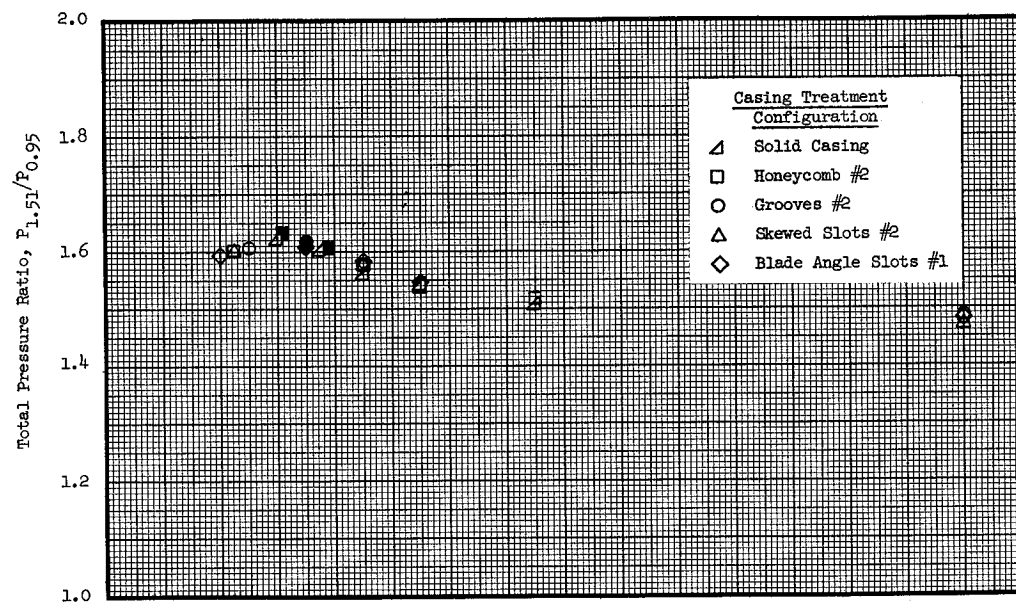


Figure 14 (d). Task I Rotor Blade Element Data, 90% Immersion, 100% Speed, Undistorted Inlet.

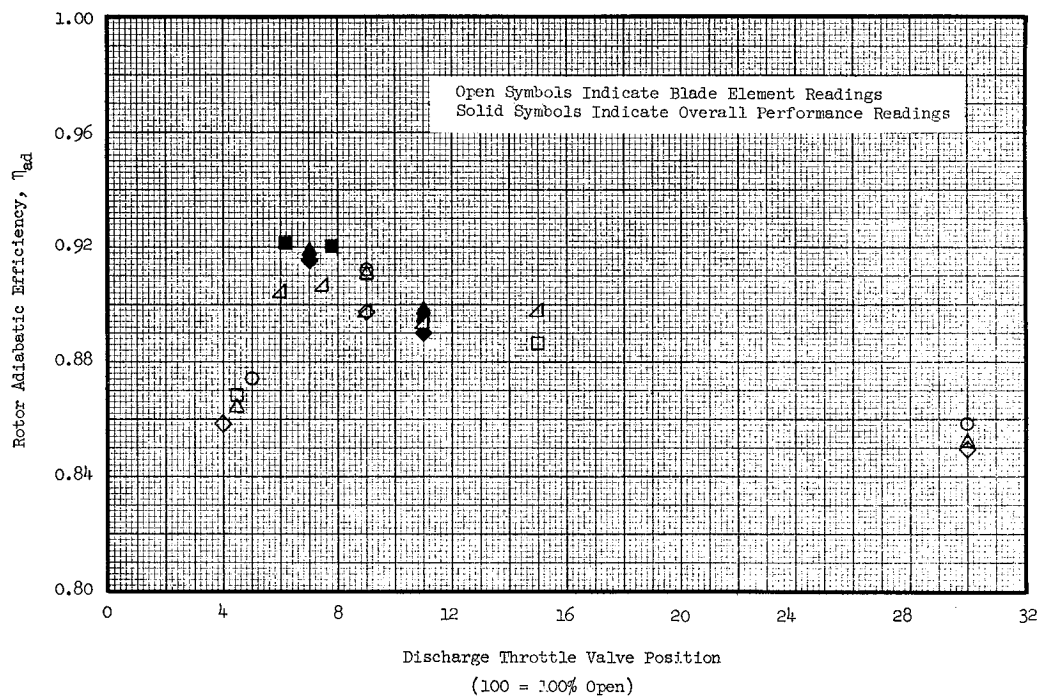
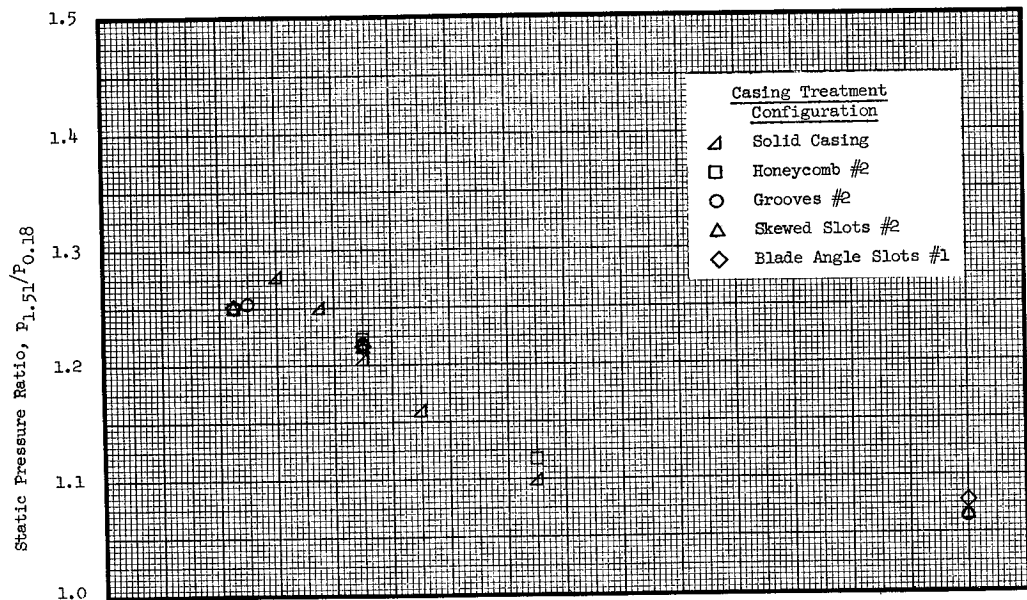


Figure 14 (d). Task I Rotor Blade Element Data, 90% Immersion, 100% Speed, Undistorted Inlet (Concluded).

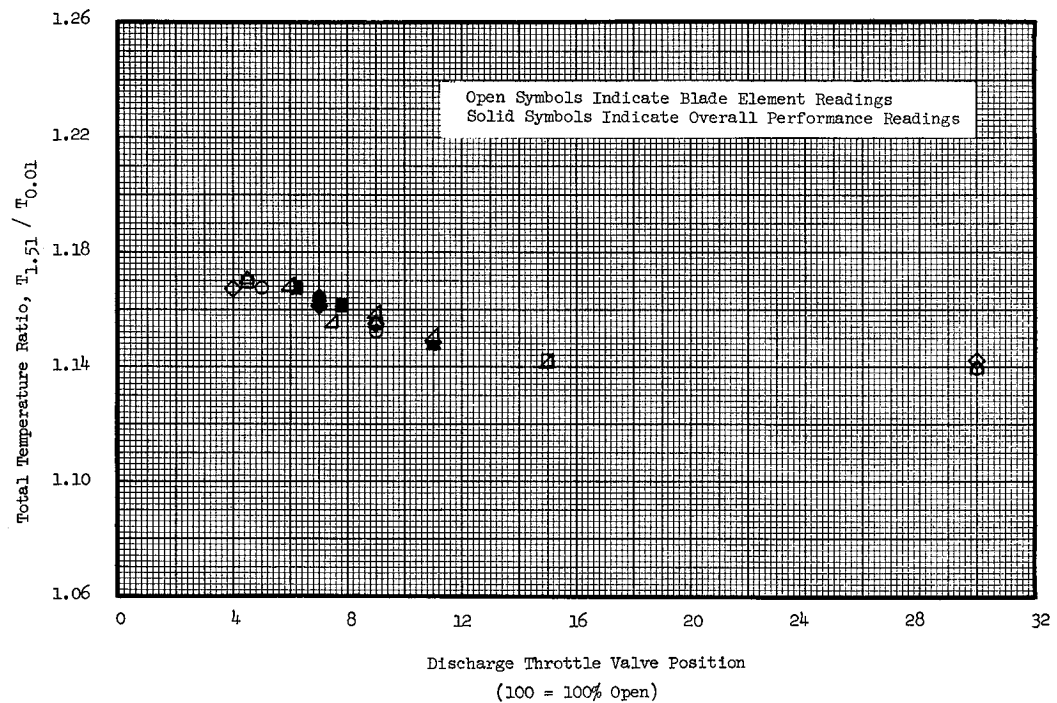
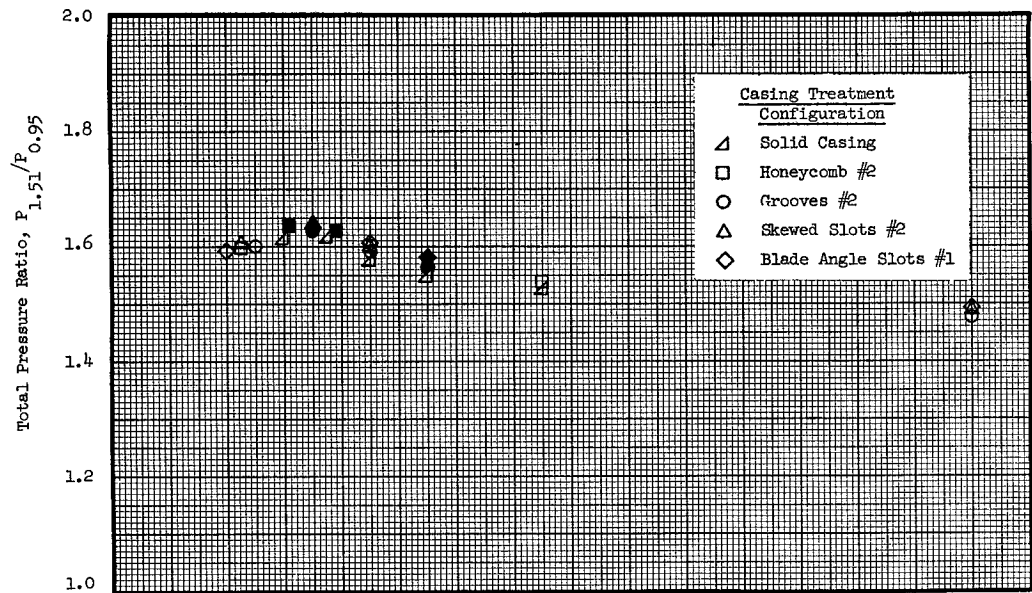


Figure 14 (e). Task I Rotor Blade Element Data, 95% Immersion, 100% Speed, Undistorted Inlet.

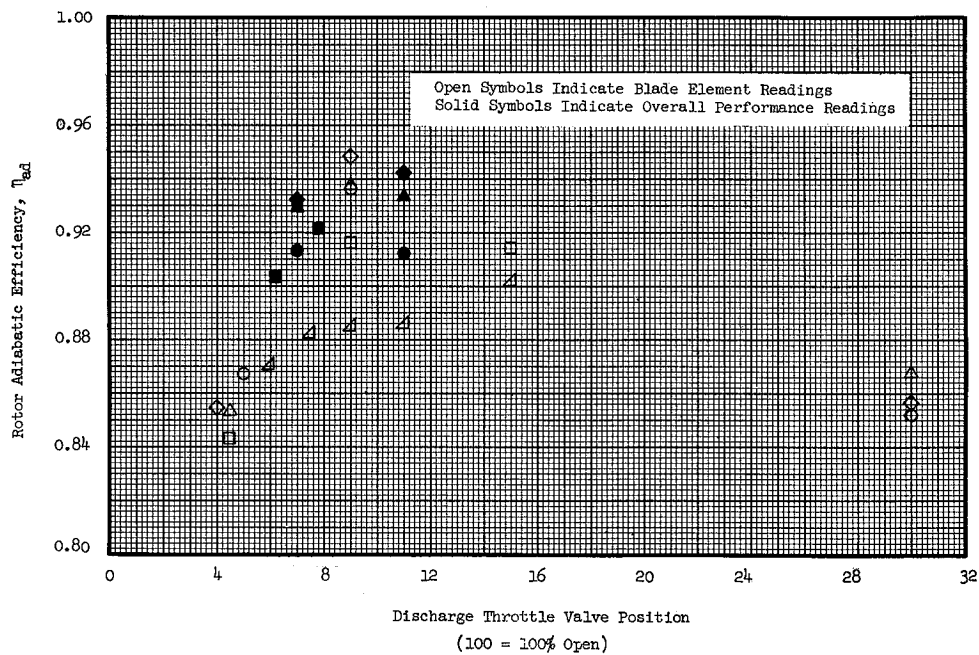
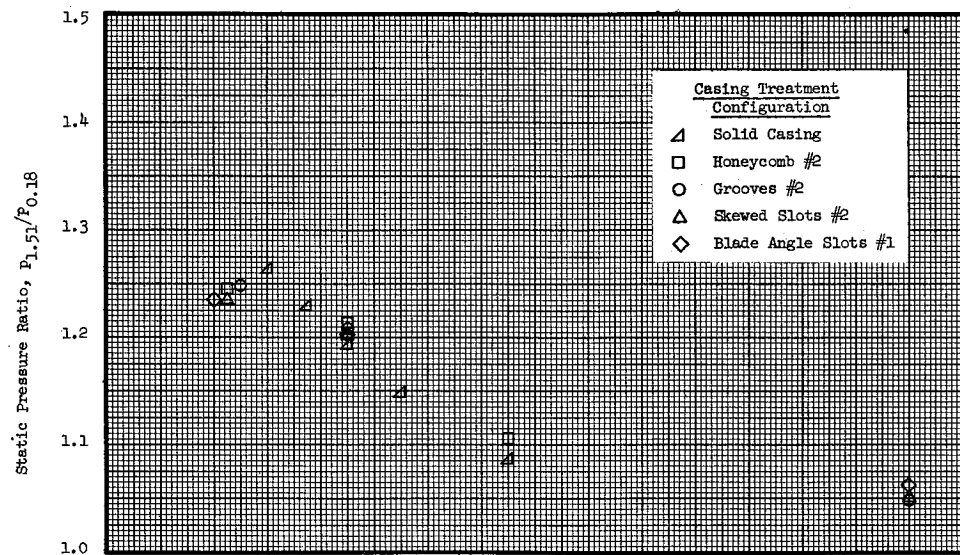


Figure 14 (e). Task I Rotor Blade Element Data, 95% Immersion, 100% Speed, Undistorted Inlet (Concluded).

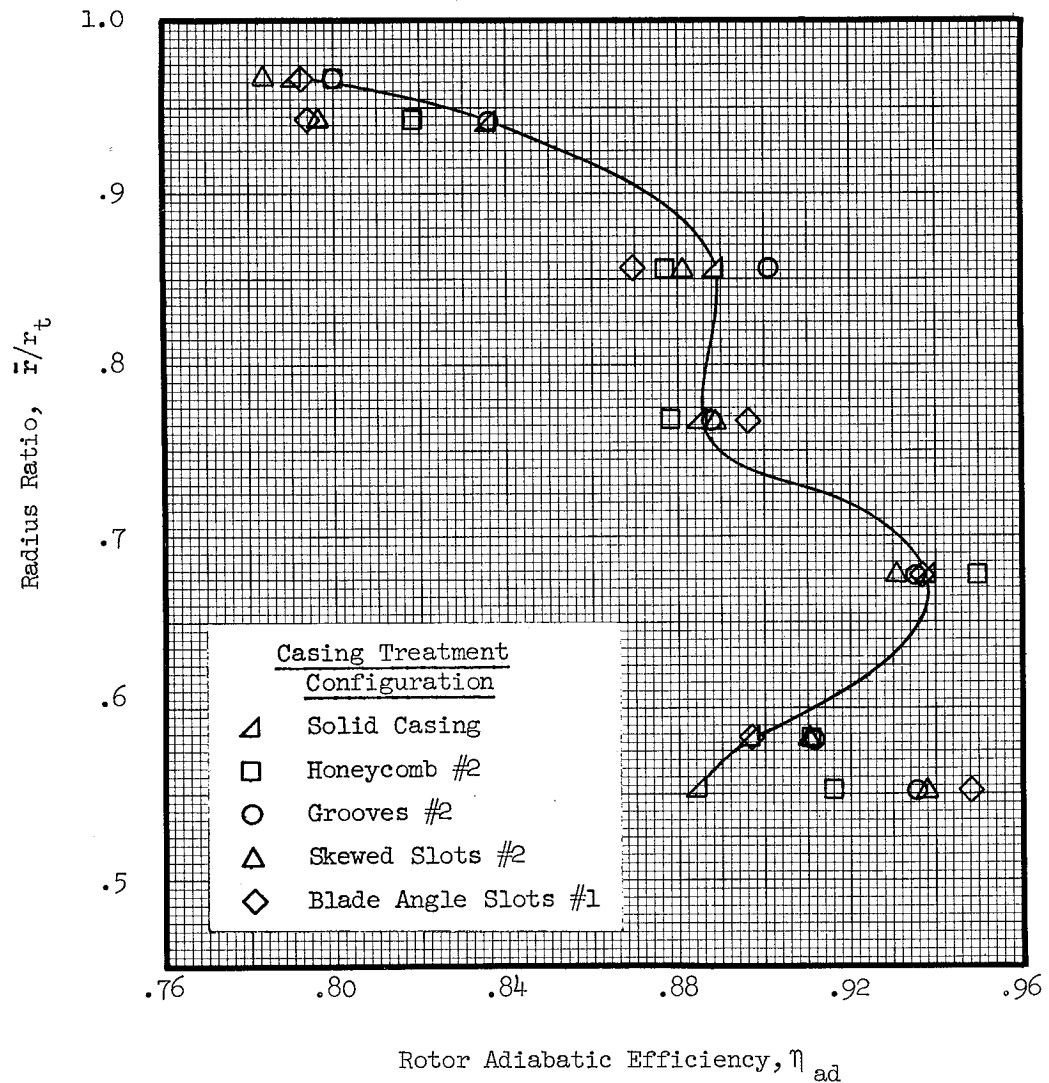


Figure 15. Radial Distribution of Task I Rotor Adiabatic Efficiency (at 100% Speed, Undistorted Inlet, Intermediate Flow) With Casing Treatments Honeycomb #2, Circumferential Grooves #2, Skewed Slots #2 and Blade Angle Slots #1.

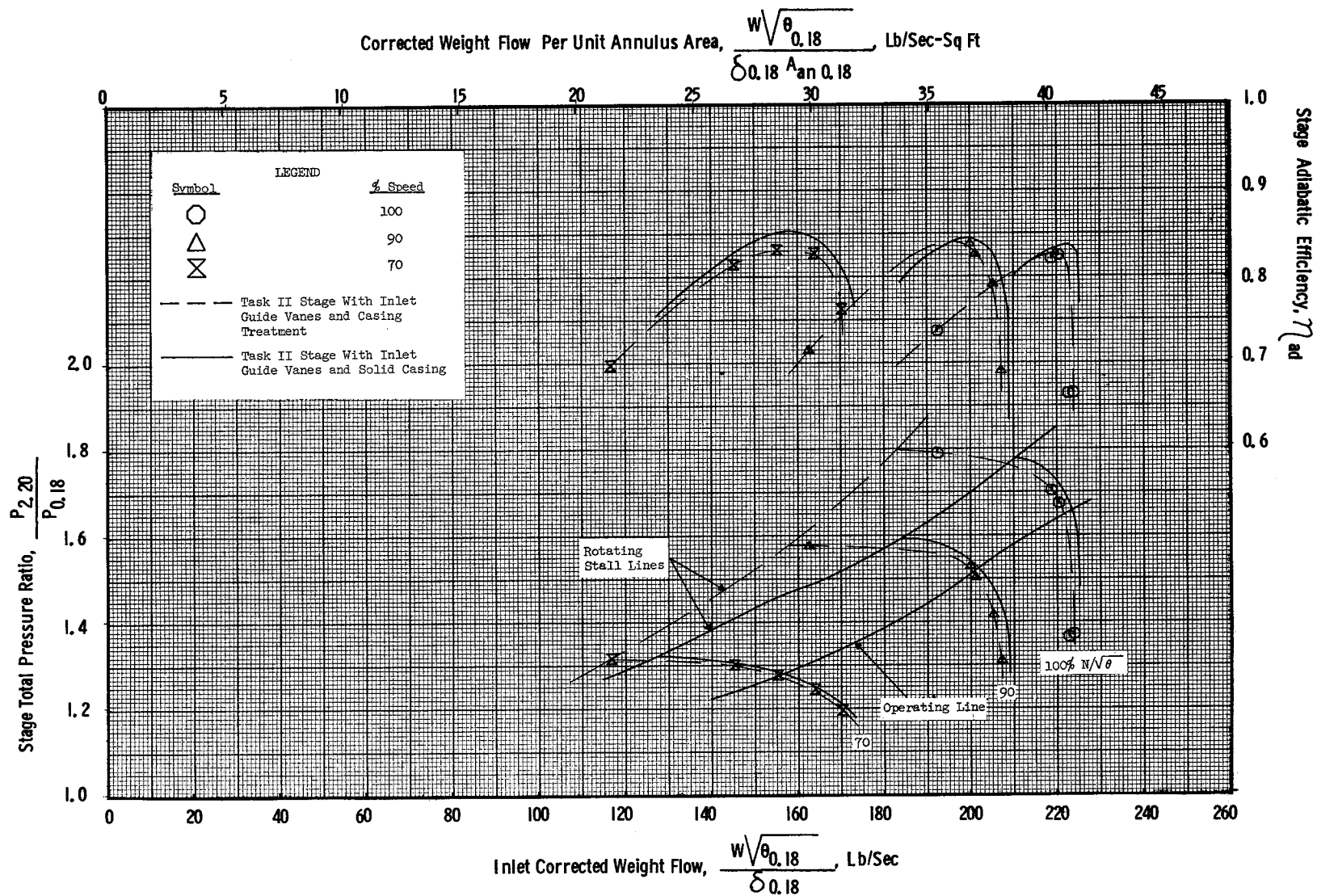


Figure 16 (a). Task II Stage Undistorted Inlet Performance Map Illustrating the Effects of Casing Treatment With Inlet Guide Vanes Installed.

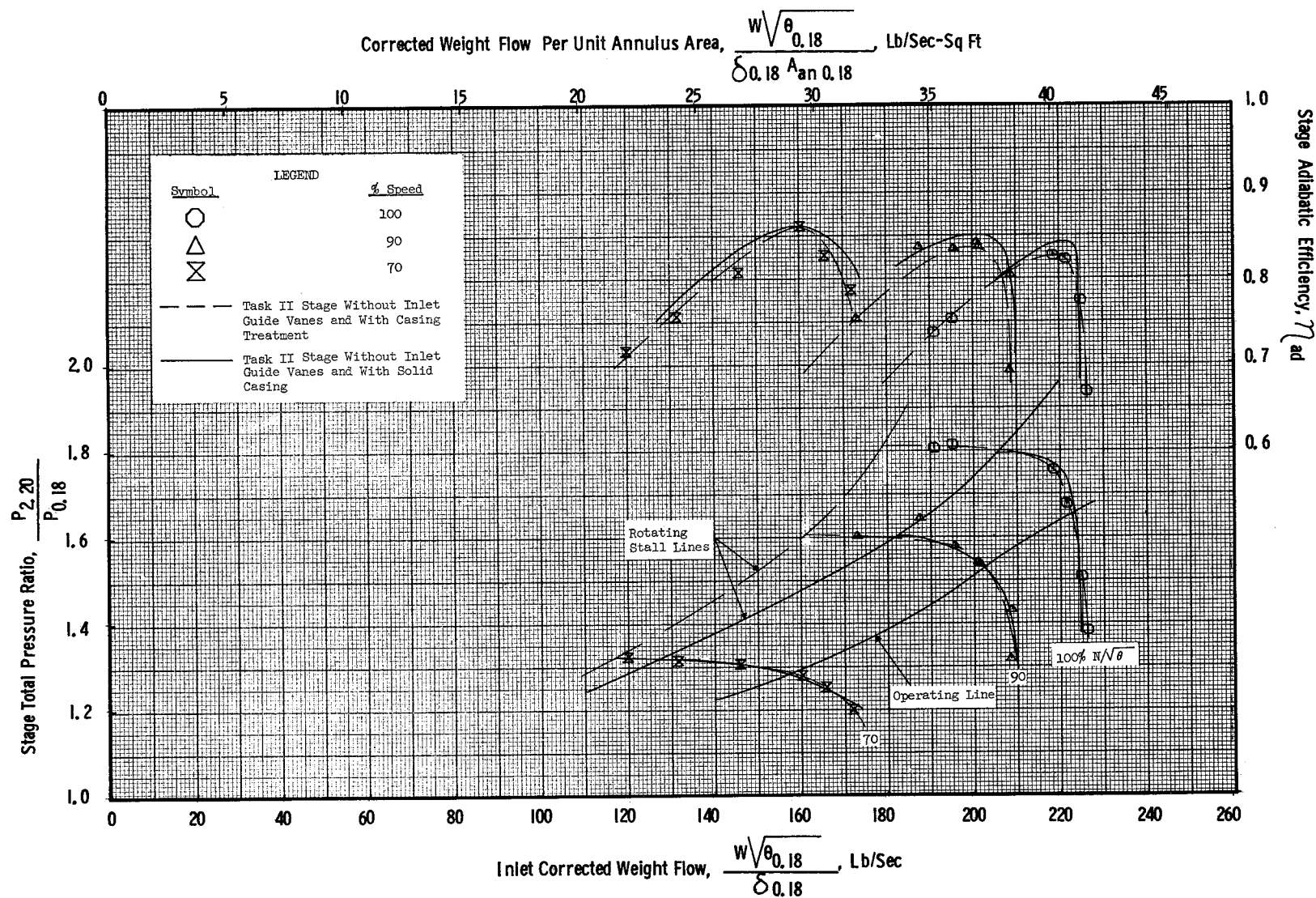


Figure 16 (b). Task II Stage Undistorted Inlet Performance Map Illustrating the Effects of Casing Treatment Without Inlet Guide Vanes Installed.

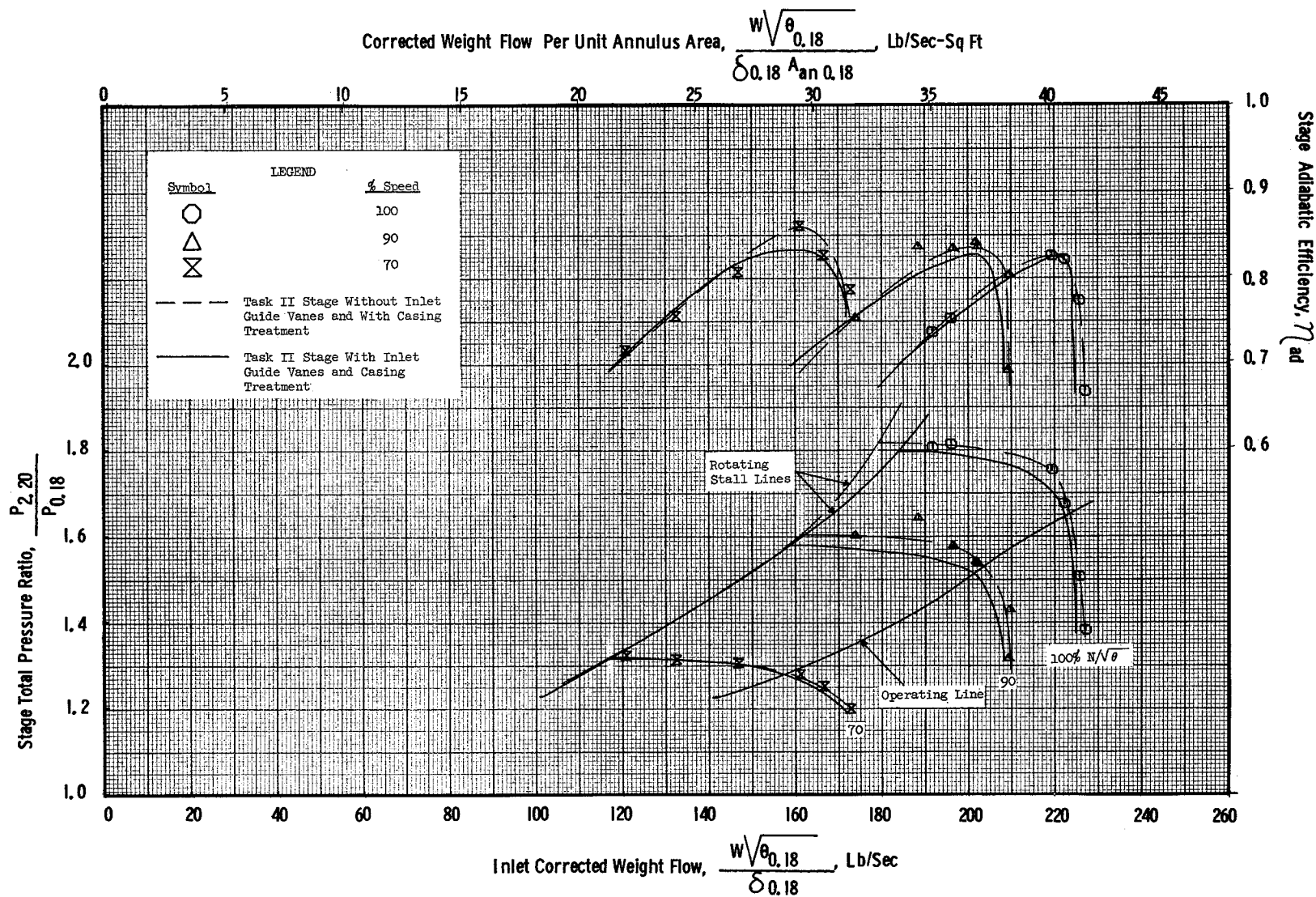


Figure 16 (c). Task II Stage Undistorted Inlet Performance Map Illustrating the Effects of Inlet Guide Vanes With Casing Treatment Installed.

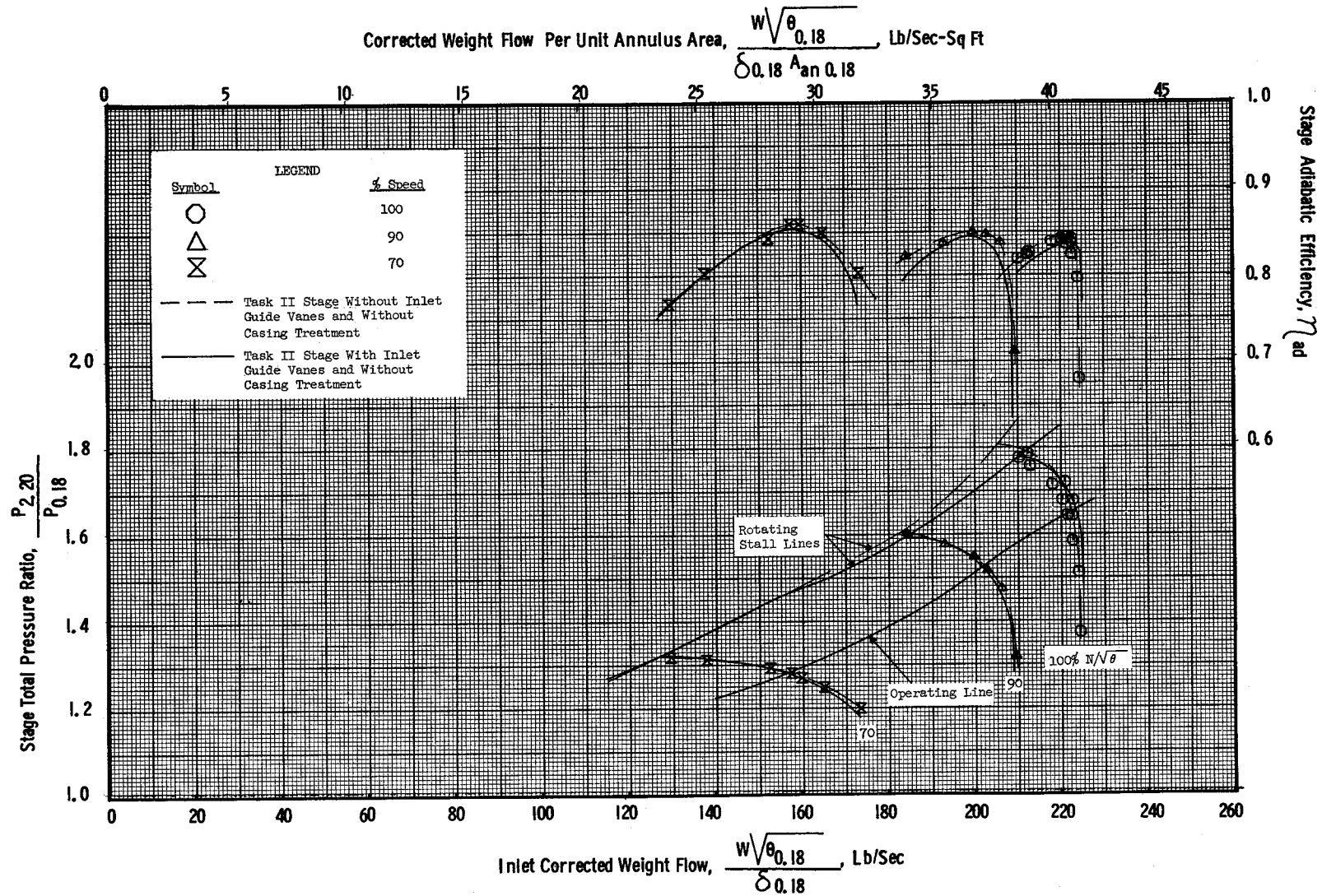


Figure 16 (d). Task II Stage Undistorted Inlet Performance Map Illustrating the Effects of Inlet Guide Vanes Without Casing Treatment Installed.

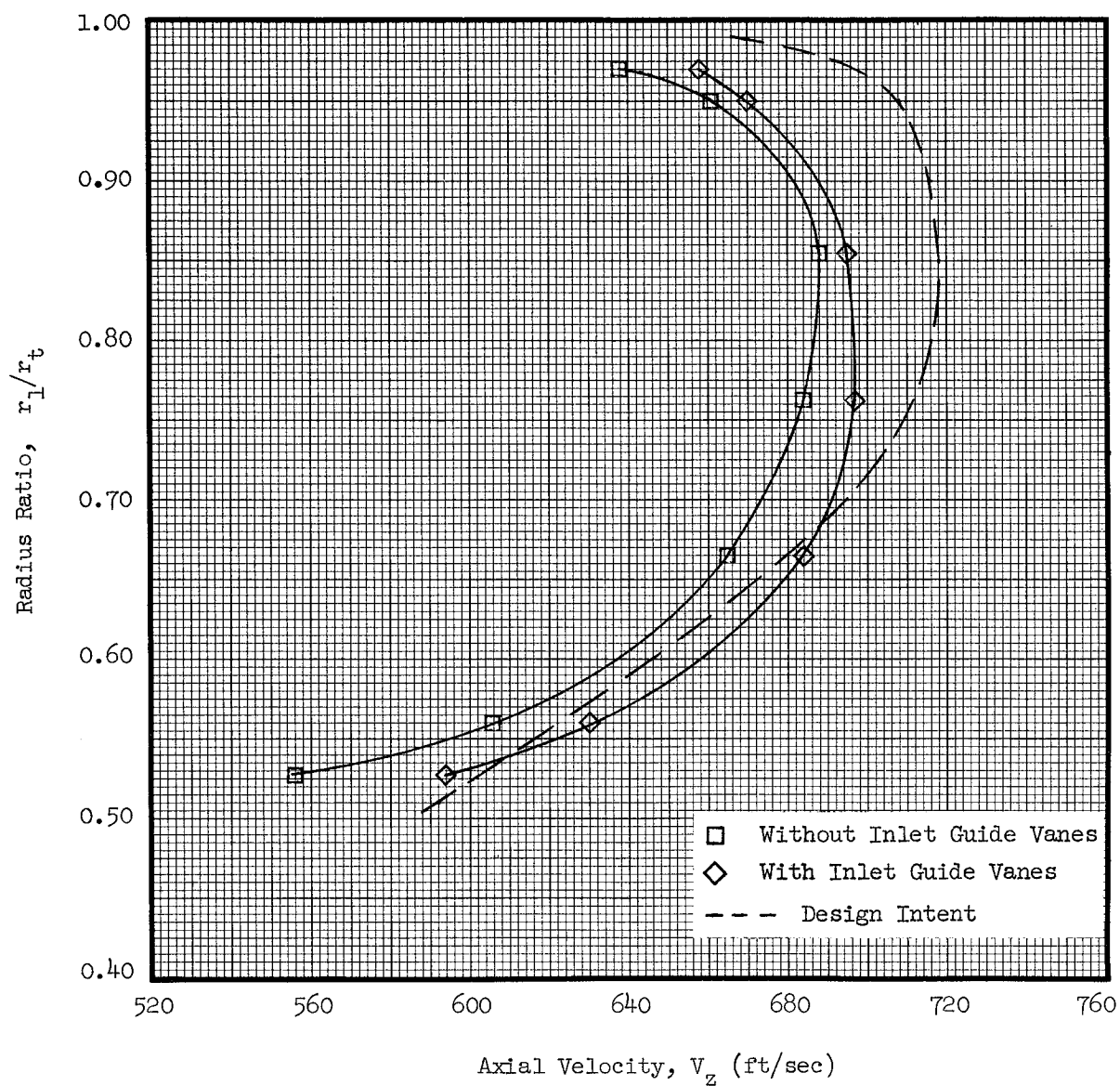


Figure 17 (a). Task II Rotor Inlet Axial Velocity With and Without Inlet Guide Vanes; 100% Speed Intermediate Flow, Undistorted Inlet (Solid Casing).

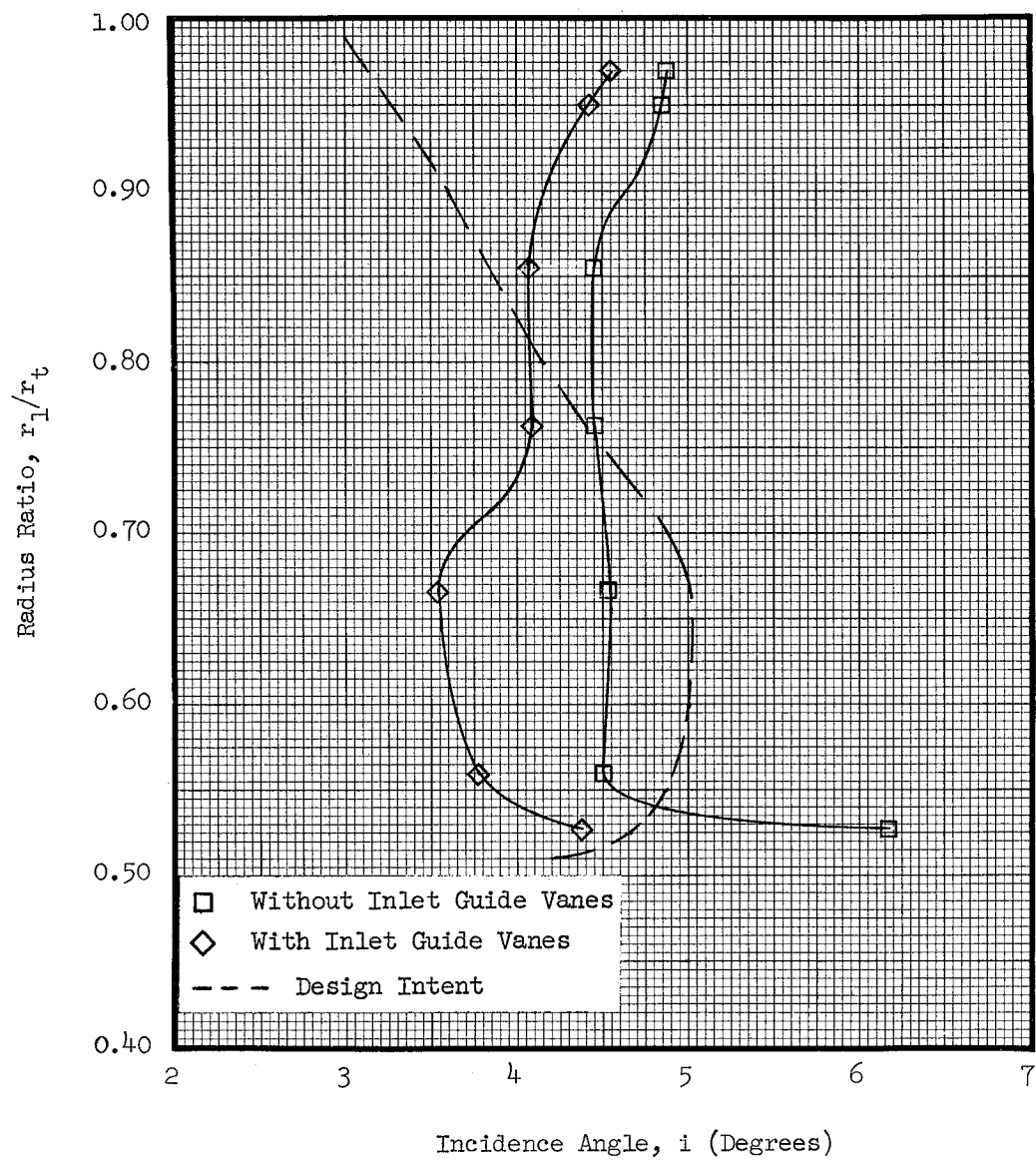


Figure 17 (b). Task II Rotor Incidence Angle With and Without Inlet Guide Vanes; 100% Speed Intermediate Flow, Undistorted Inlet (Solid Casing).

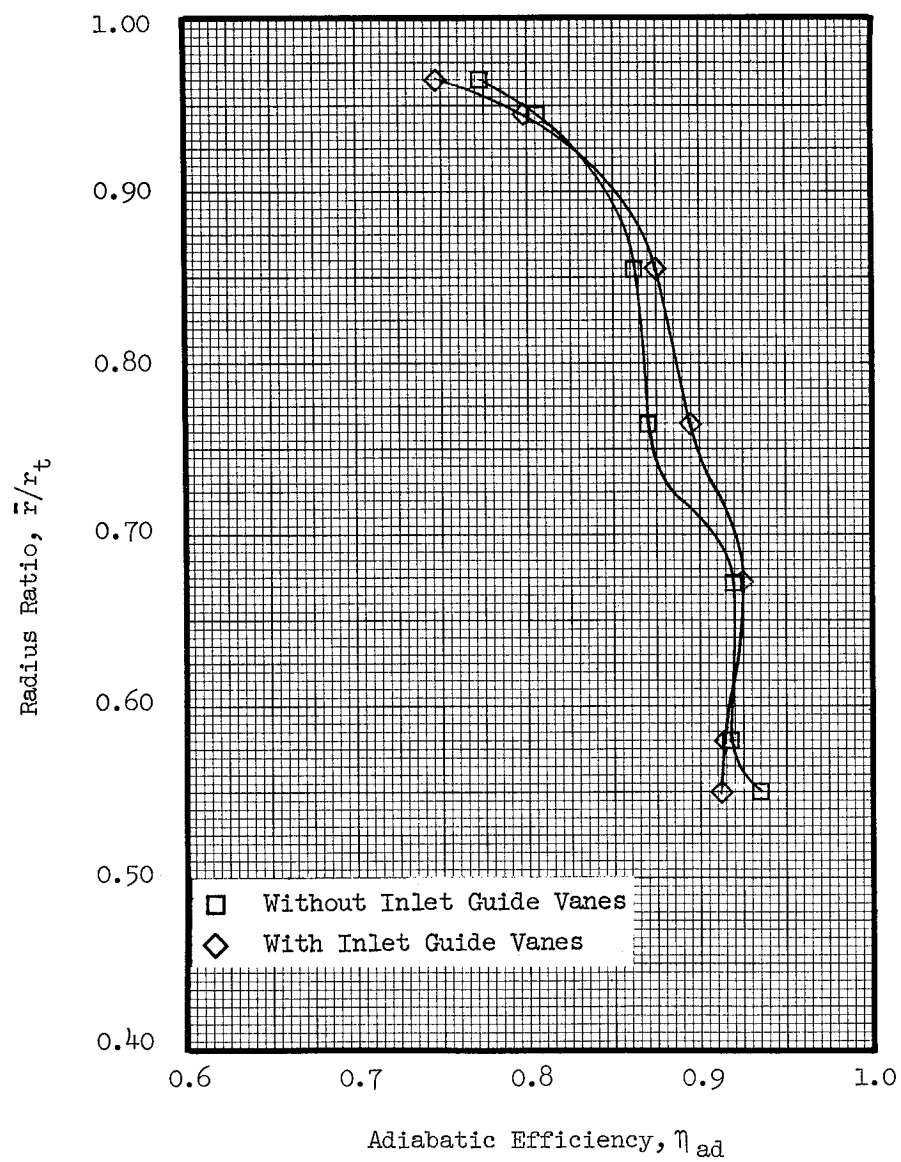
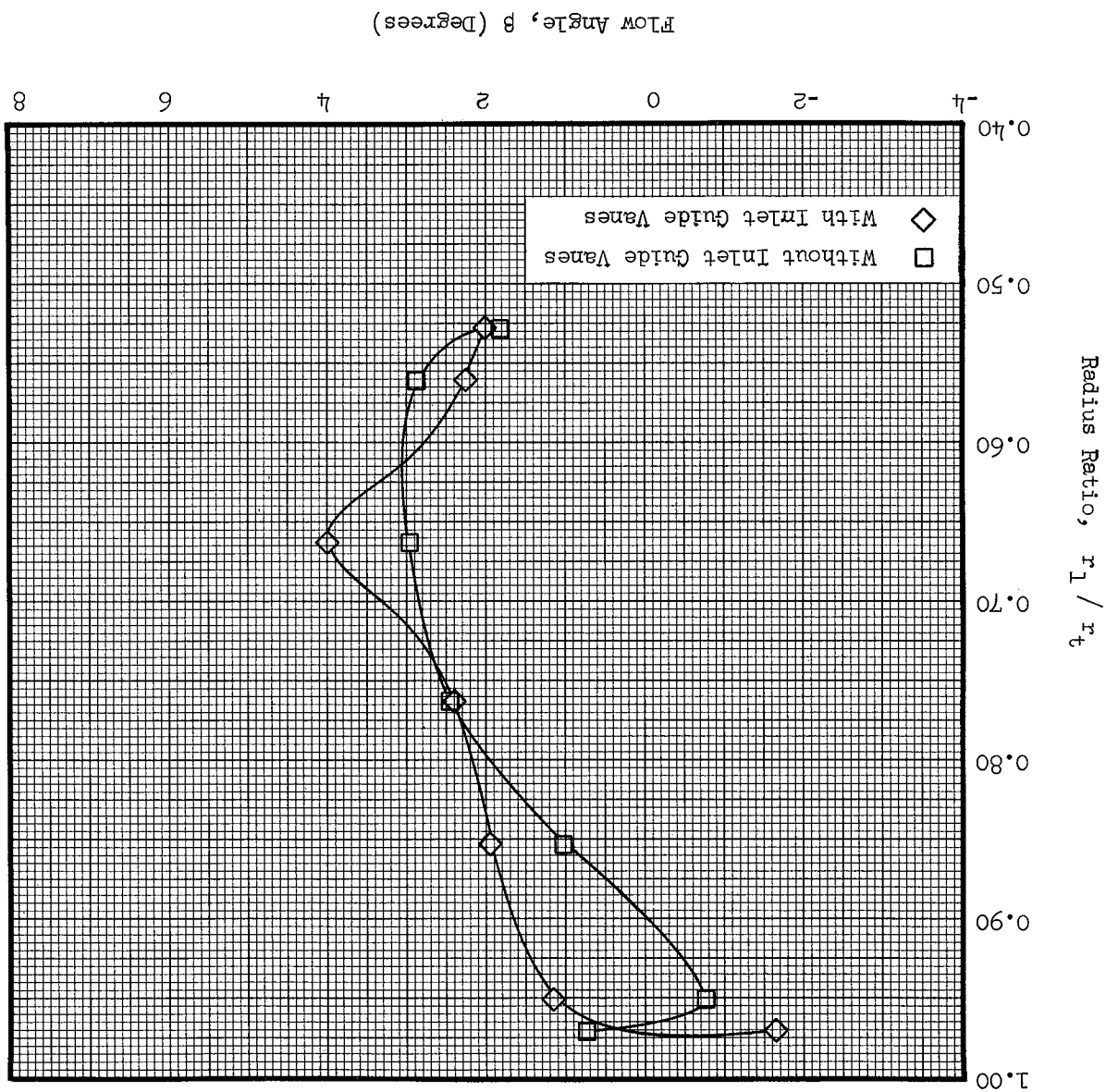


Figure 17 (c). Task II Rotor Adiabatic Efficiency With and Without Inlet Guide Vanes; 100% Speed Intermediate Flow, Undistorted Inlet (Solid Casing).

Figure 17 (d). Task II Rotor Inlet Absolute Flow Angle With and Without Inlet Guide Vanes; 100% Speed Intermediate Flow, Undistorted Inlet (Solid Casing).



Stator Adiabatic Efficiency Contribution; $\eta_{ad}(\text{rotor}) - \eta_{ad}(\text{rotor \& stator})$

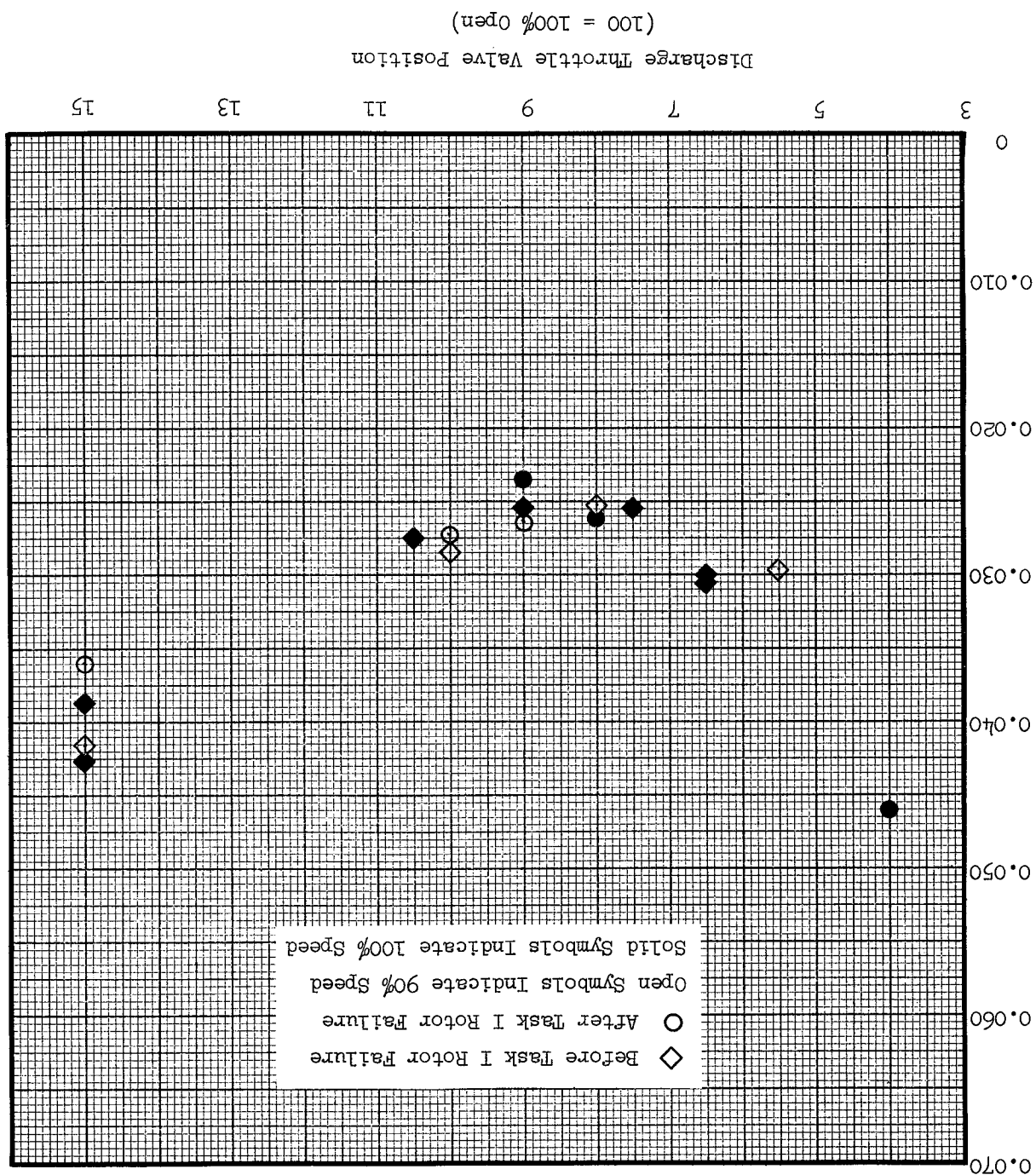


Figure 18. Stator Contribution to Task II Stage Adiabatic Efficiency Before and After Task I Rotor Failure.

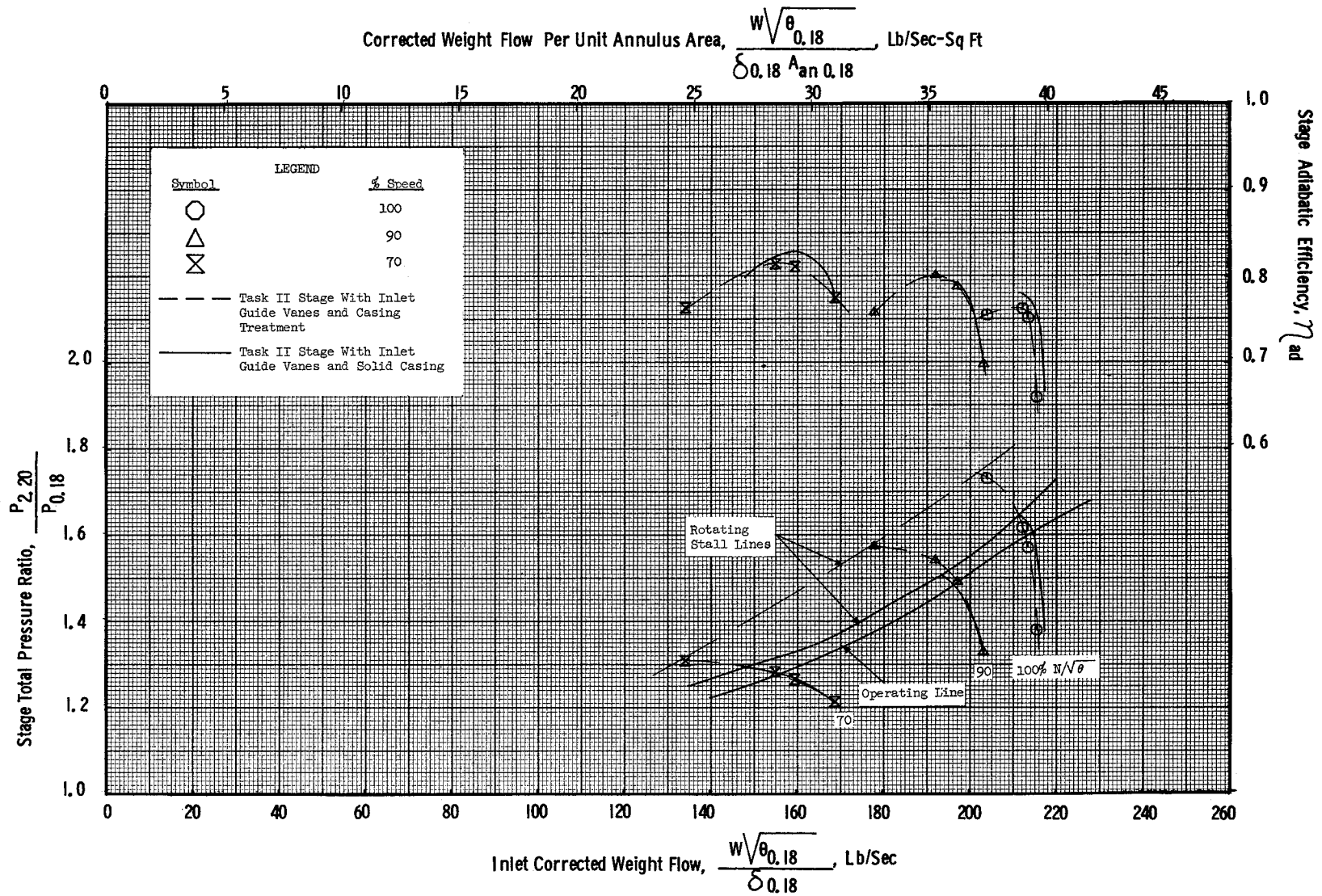


Figure 19 (a). Task II Stage Radial Distortion Performance Map Illustrating The Effects of Casing Treatment With Inlet Guide Vanes Installed.

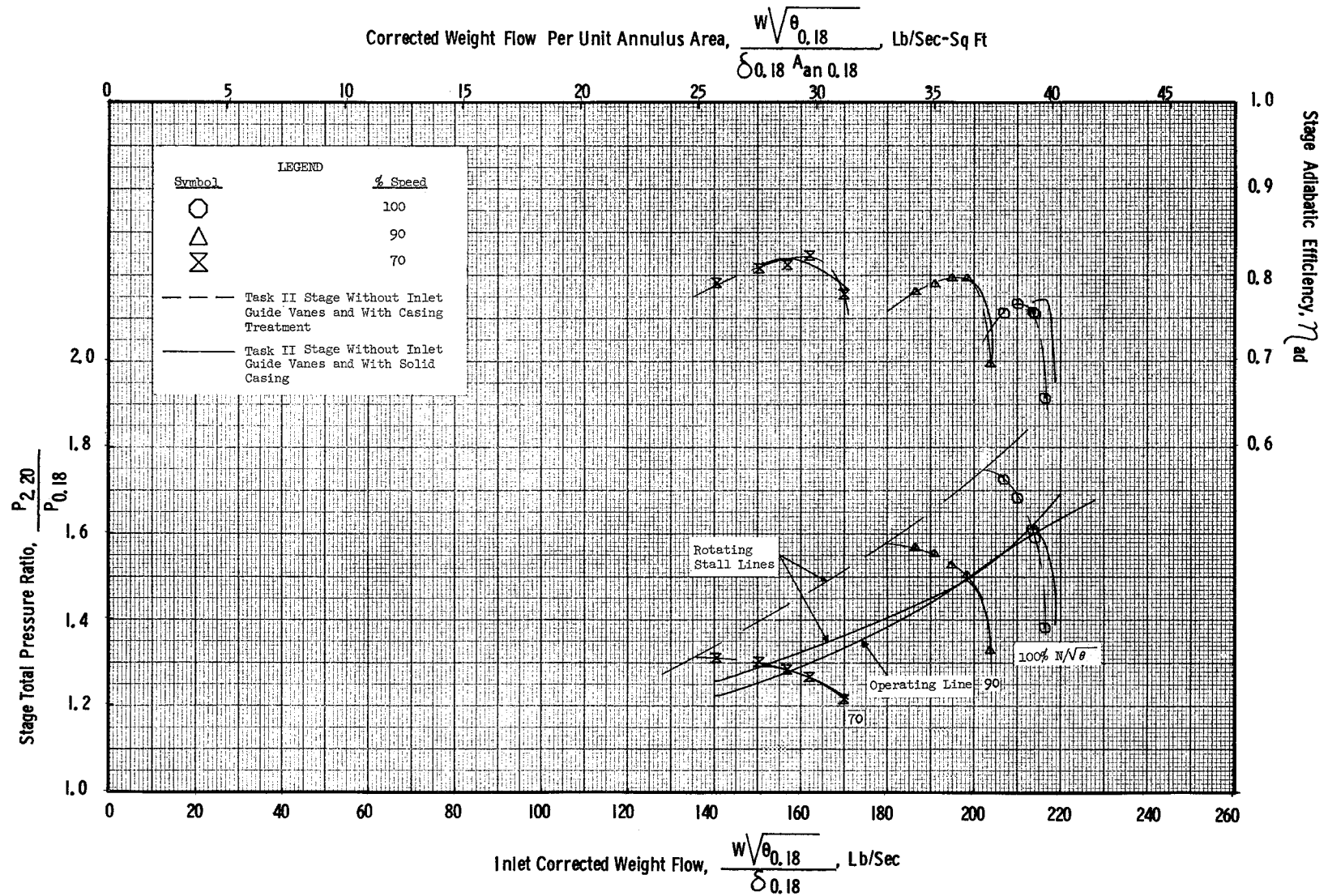


Figure 19 (b). Task II Stage Radial Distortion Performance Map Illustrating The Effects of Casing Treatment Without Inlet Guide Vanes Installed.

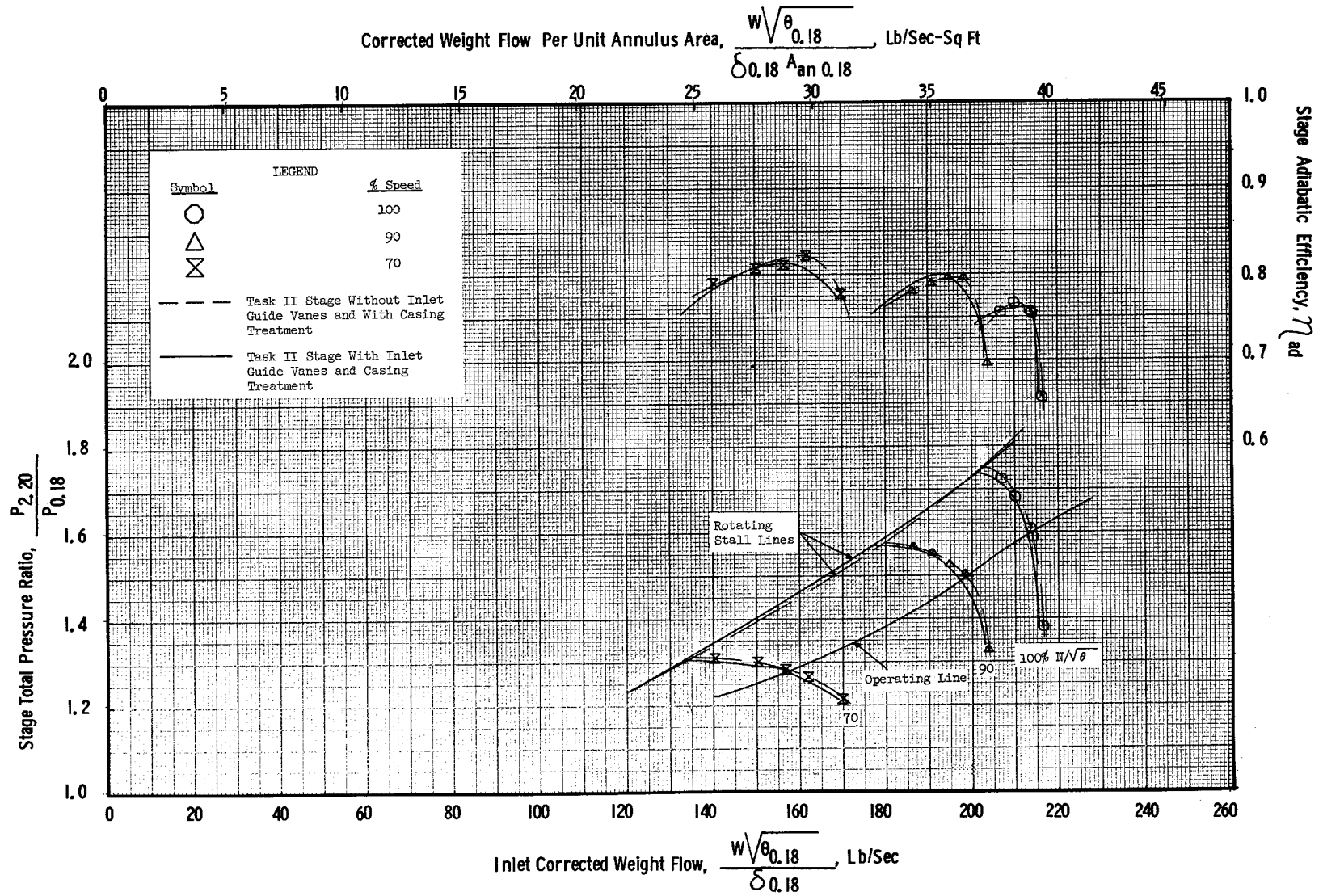


Figure 19 (c). Task II Stage Radial Distortion Performance Map Illustrating The Effects of Inlet Guide Vanes With Casing Treatment Installed.

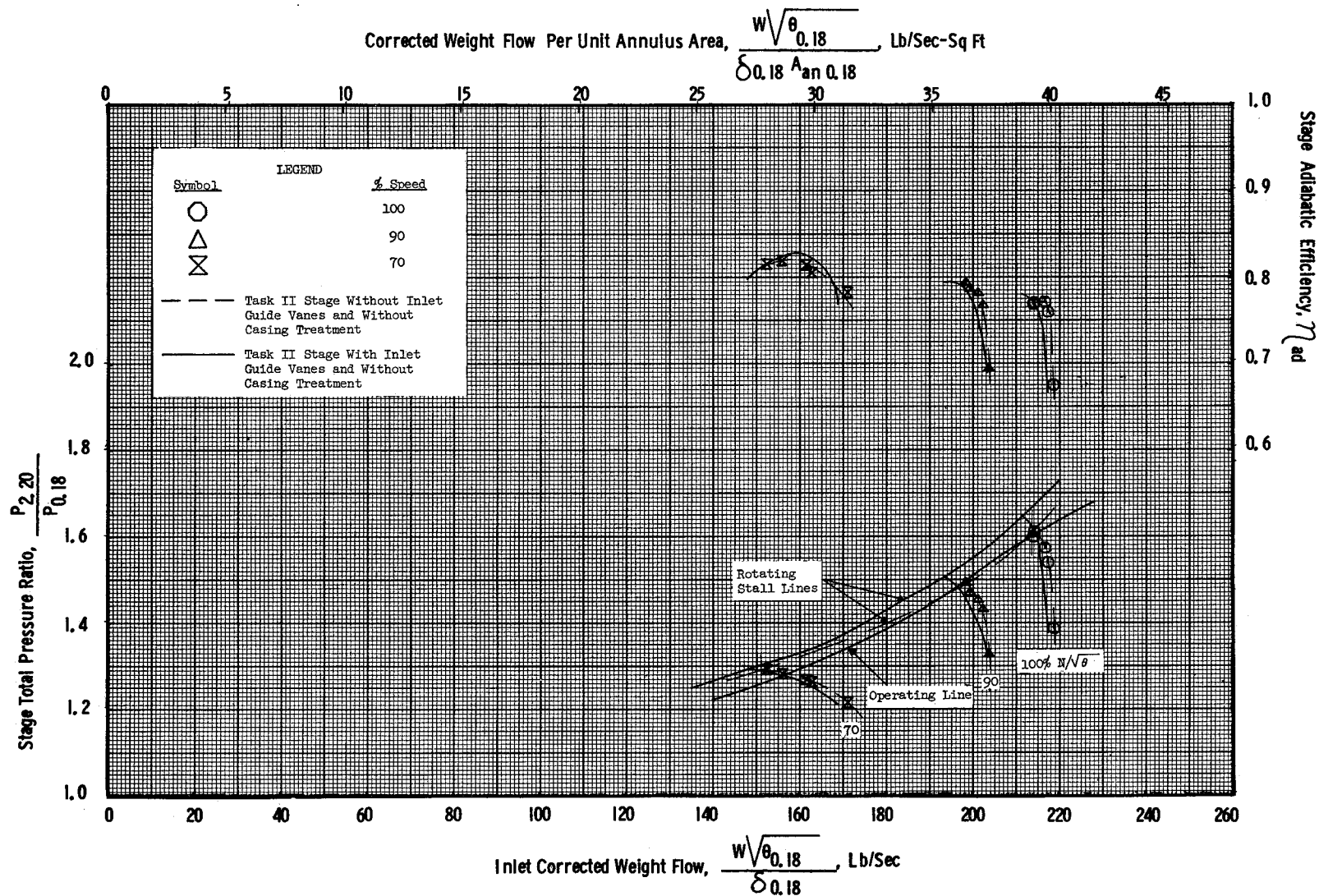


Figure 19 (d). Task II Stage Radial Distortion Performance Map Illustrating the Effects of Inlet Guide Vanes Without Casing Treatment Installed.

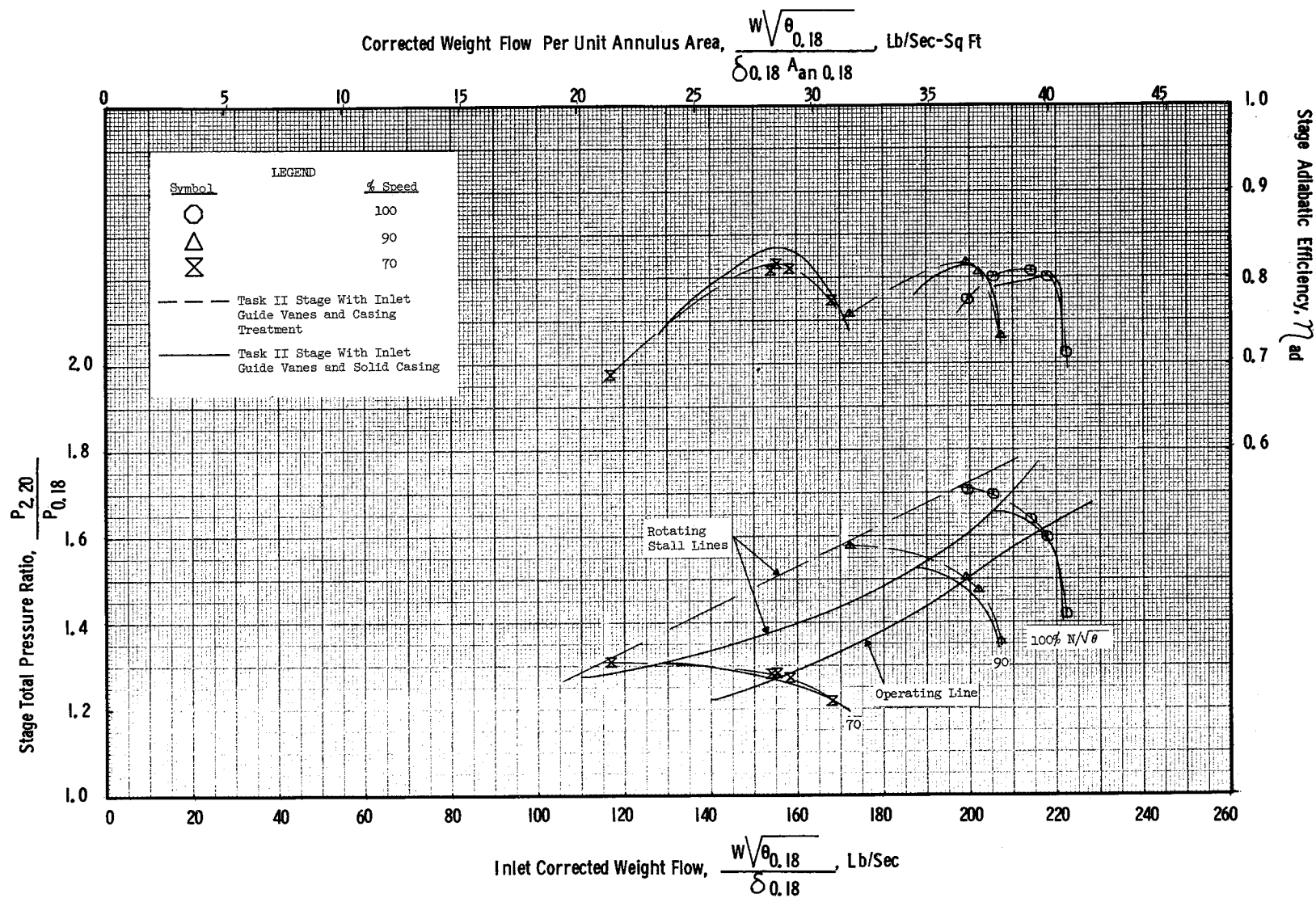


Figure 20 (a). Task II Stage Circumferential Distortion Performance Map Illustrating The Effects of Casing Treatment With Inlet Guide Vanes Installed.

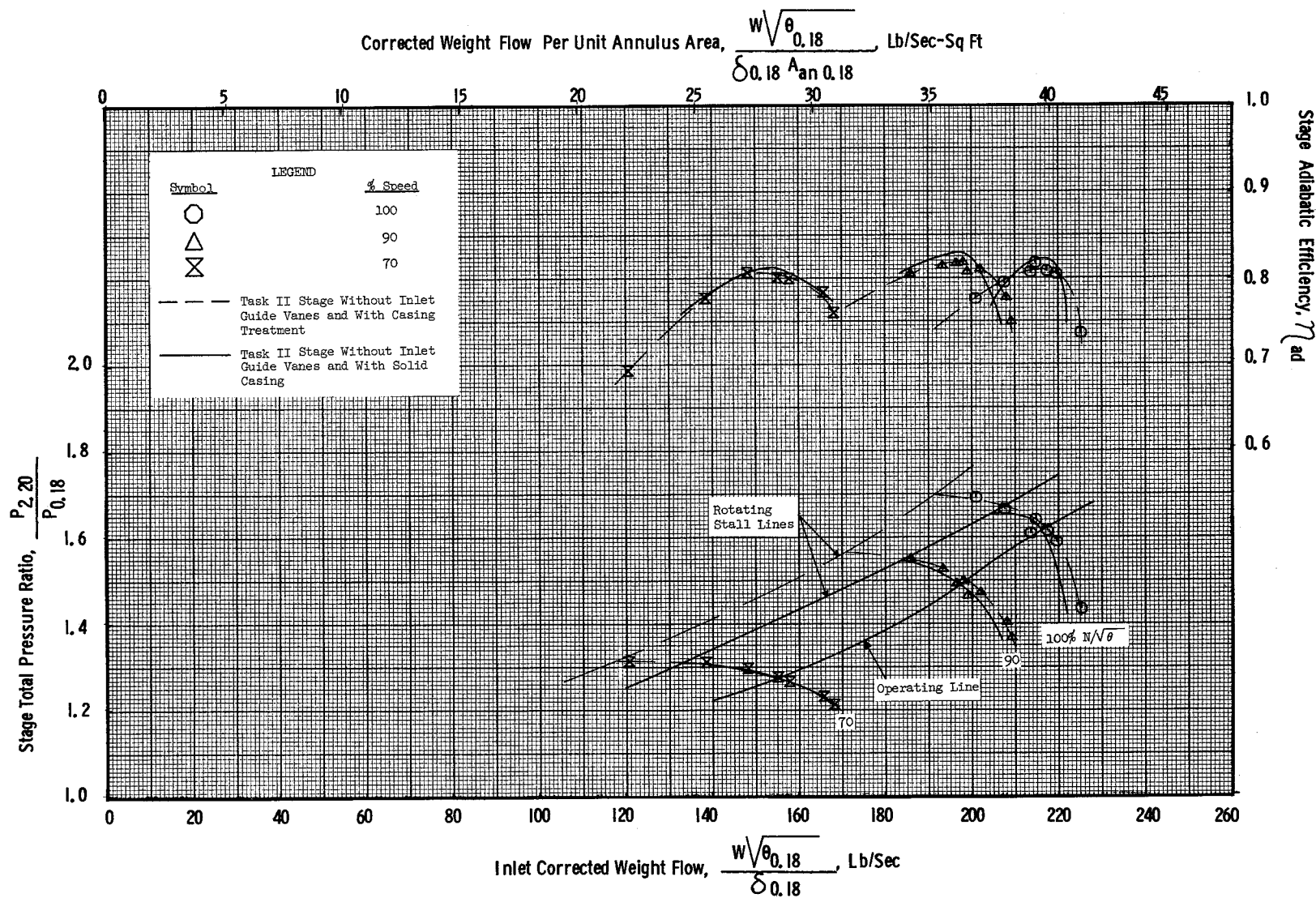


Figure 20 (b). Task II Stage Circumferential Distortion Performance Map Illustrating The Effects of Casing Treatment Without Inlet Guide Vanes Installed.

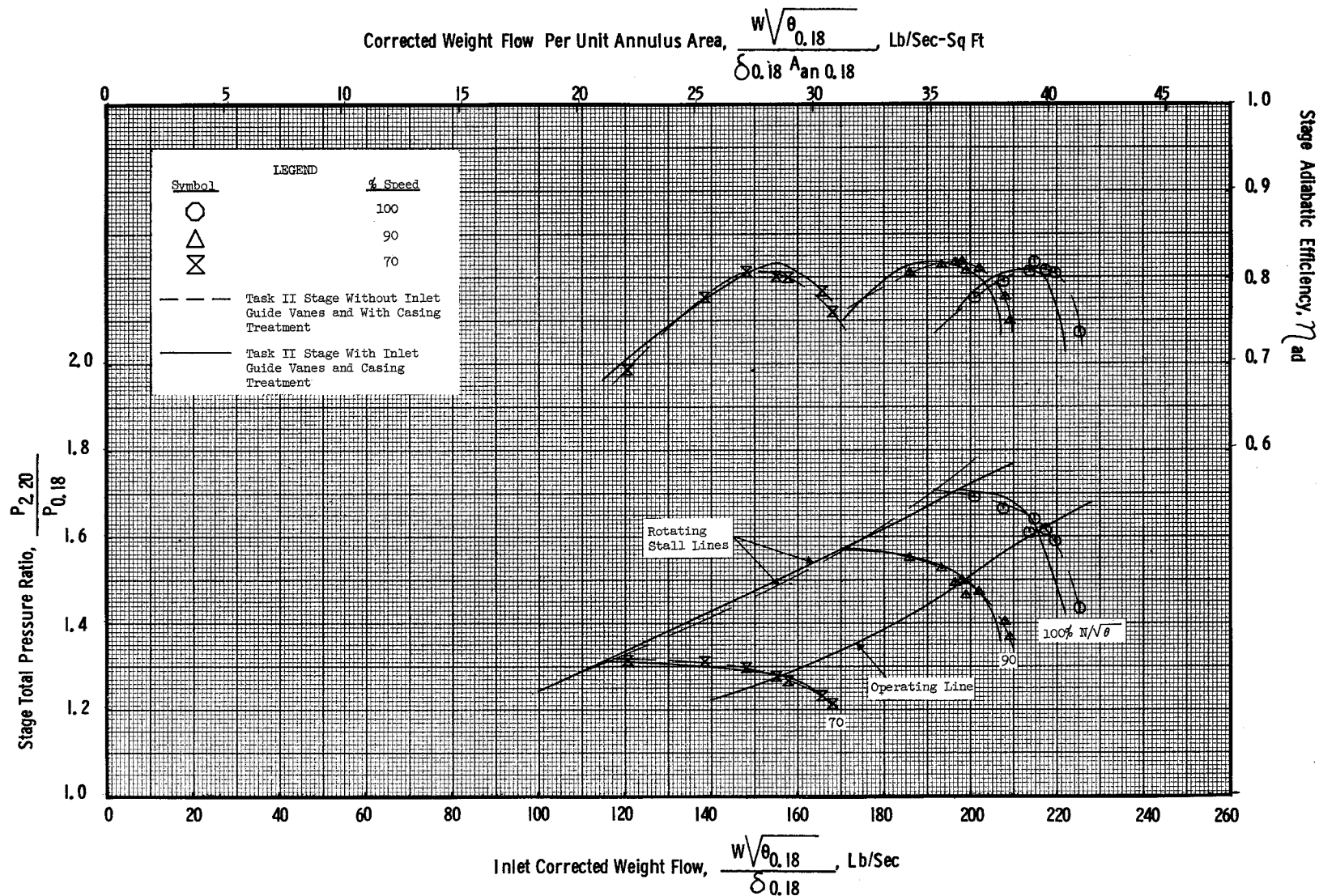


Figure 20 (c). Task II Stage Circumferential Distortion Performance Map Illustrating The Effects of Inlet Guide Vanes With Casing Treatment Installed.

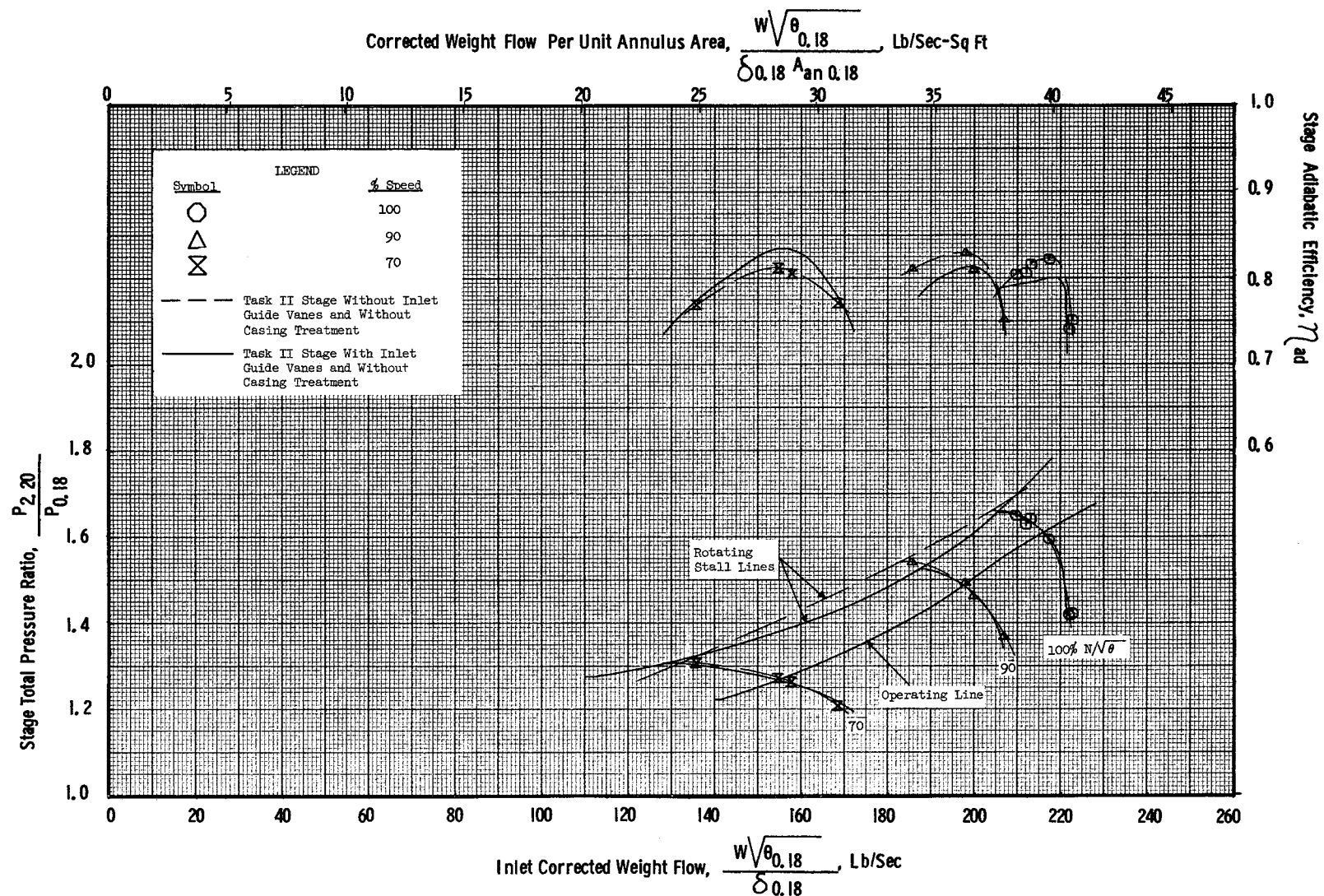


Figure 20 (d). Task II Stage Circumferential Distortion Map Illustrating the Effects of Inlet Guide Vanes Without Casing Treatment Installed.

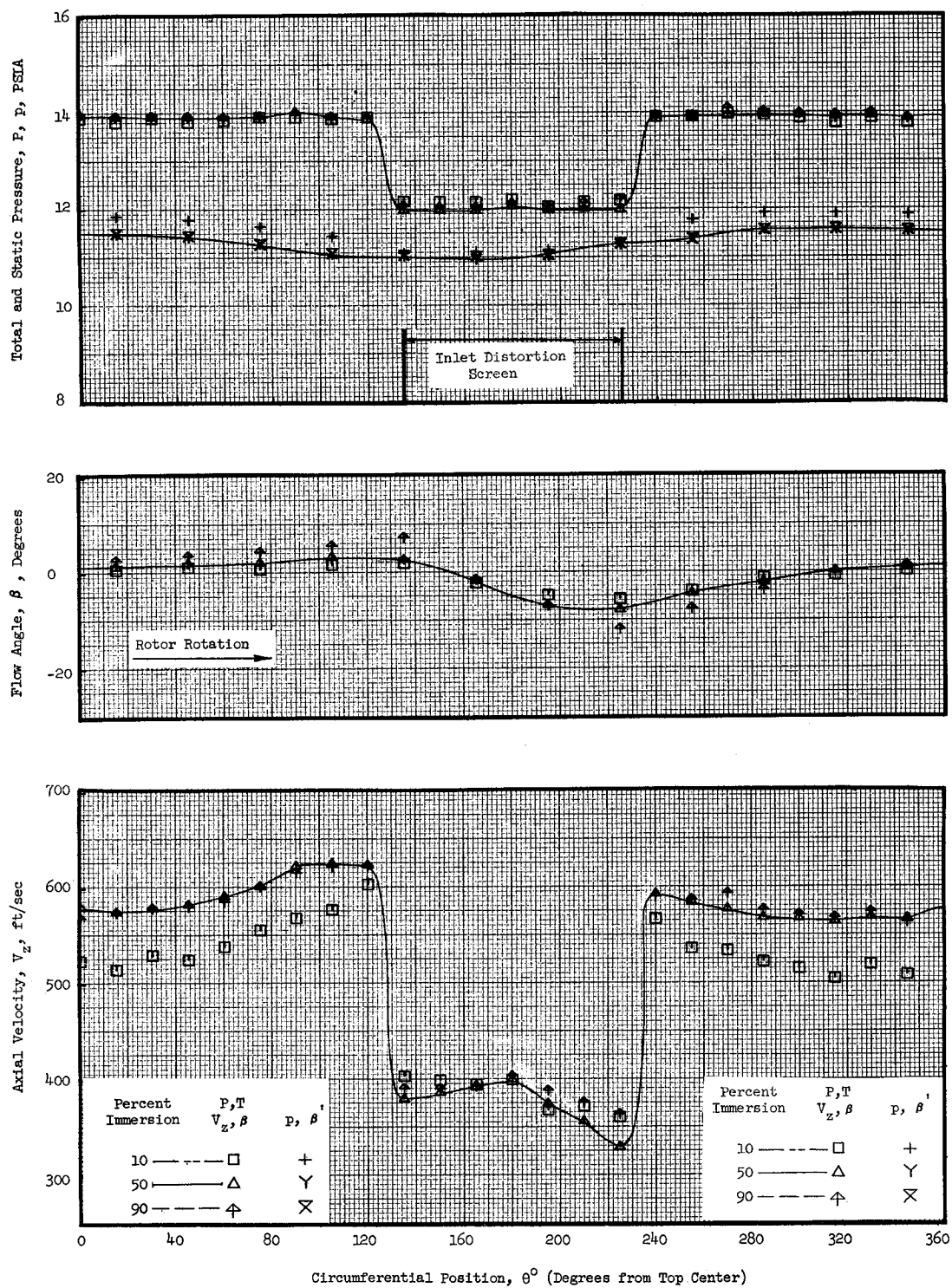


Figure 21 (a). Task II Stage Circumferential Distortion Profiles of Flow Conditions at 100% Speed Near Stall With Inlet Guide Vanes and With Casing Treatment Installed at Plane 0.18.

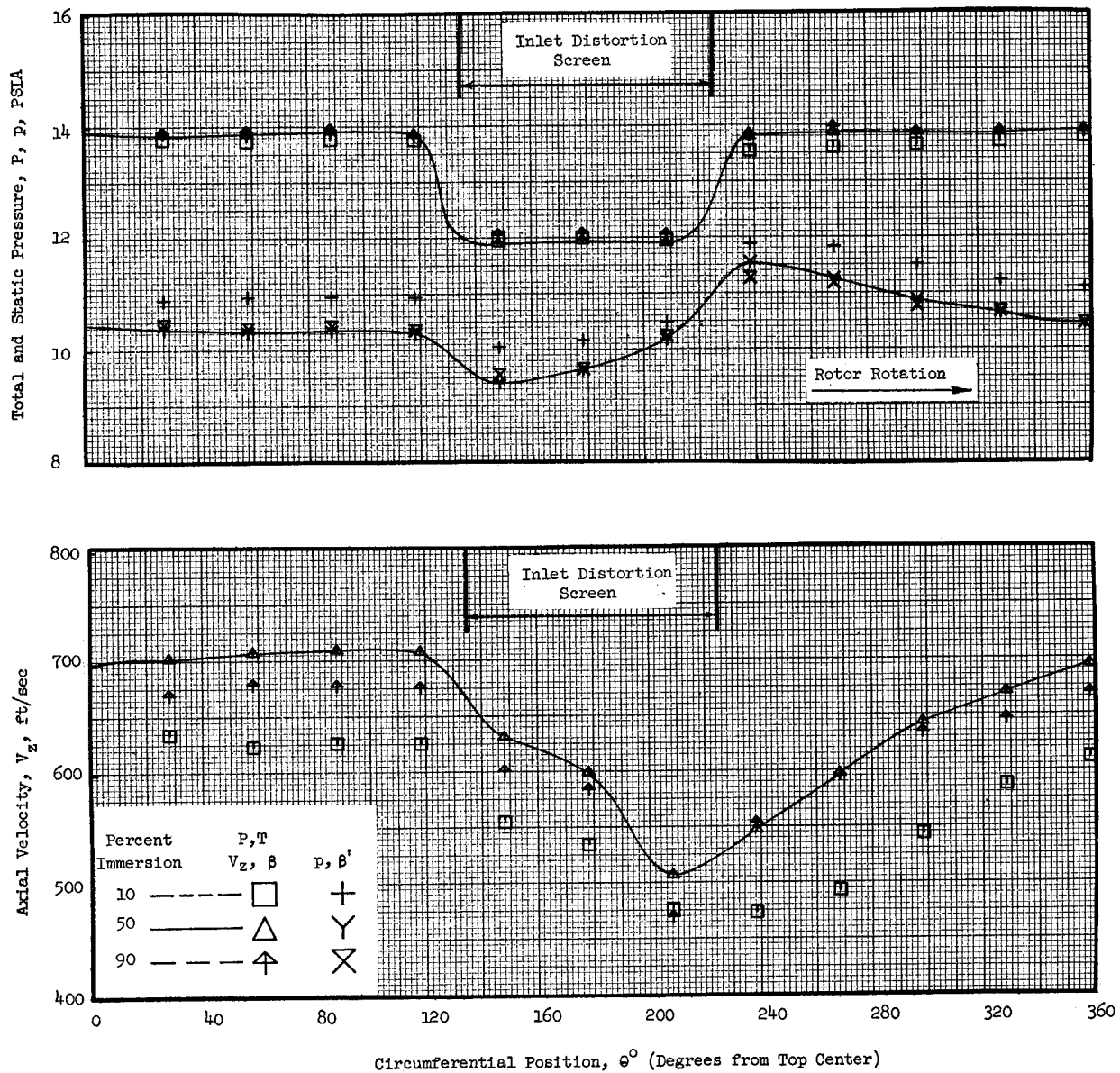


Figure 21 (b). Task II Stage Circumferential Distortion Profiles of Flow Conditions at 100% Speed Near Stall With Inlet Guide Vanes and With Casing Treatment Installed at Plane 0.95.

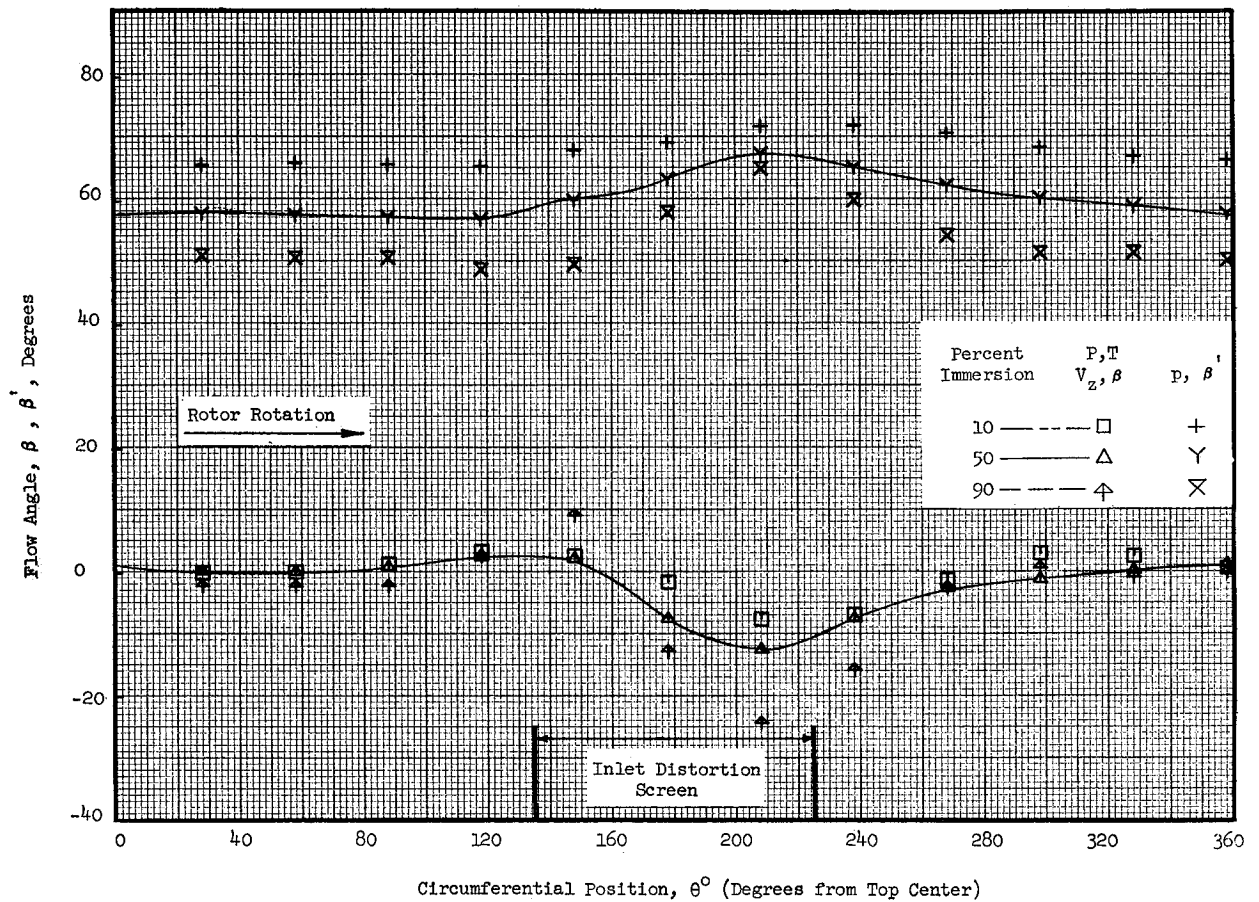


Figure 21 (b). Task II Stage Circumferential Distortion Profiles of Flow Conditions at 100% Speed Near Stall With Inlet Guide Vanes and With Casing Treatment Installed at Plane 0.95 (Concluded).

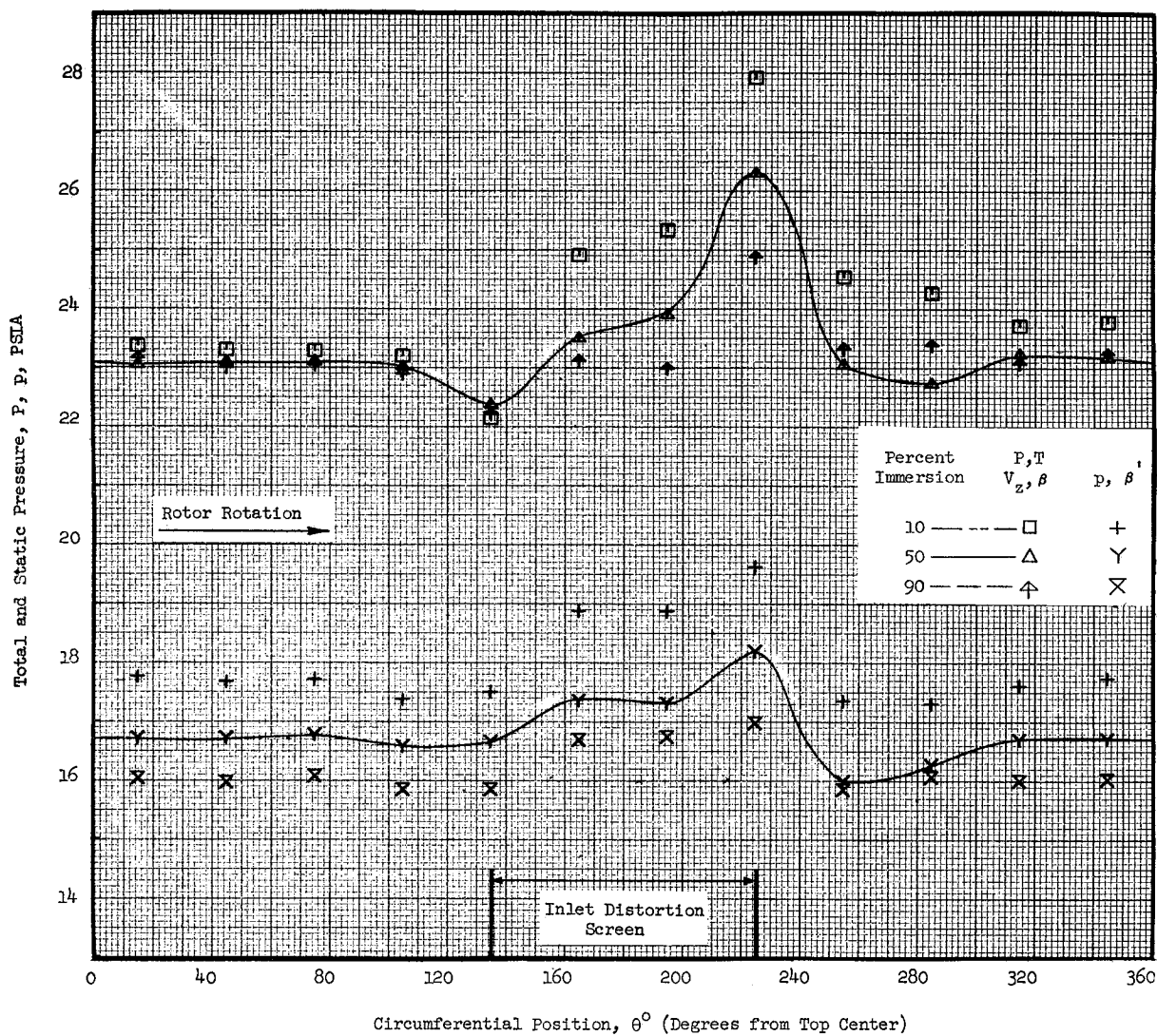


Figure 21 (c). Task II Stage Circumferential Distortion Profiles of Flow Conditions at 100% Speed Near Stall With Inlet Guide Vanes and With Casing Treatment Installed at Plane 1.51.

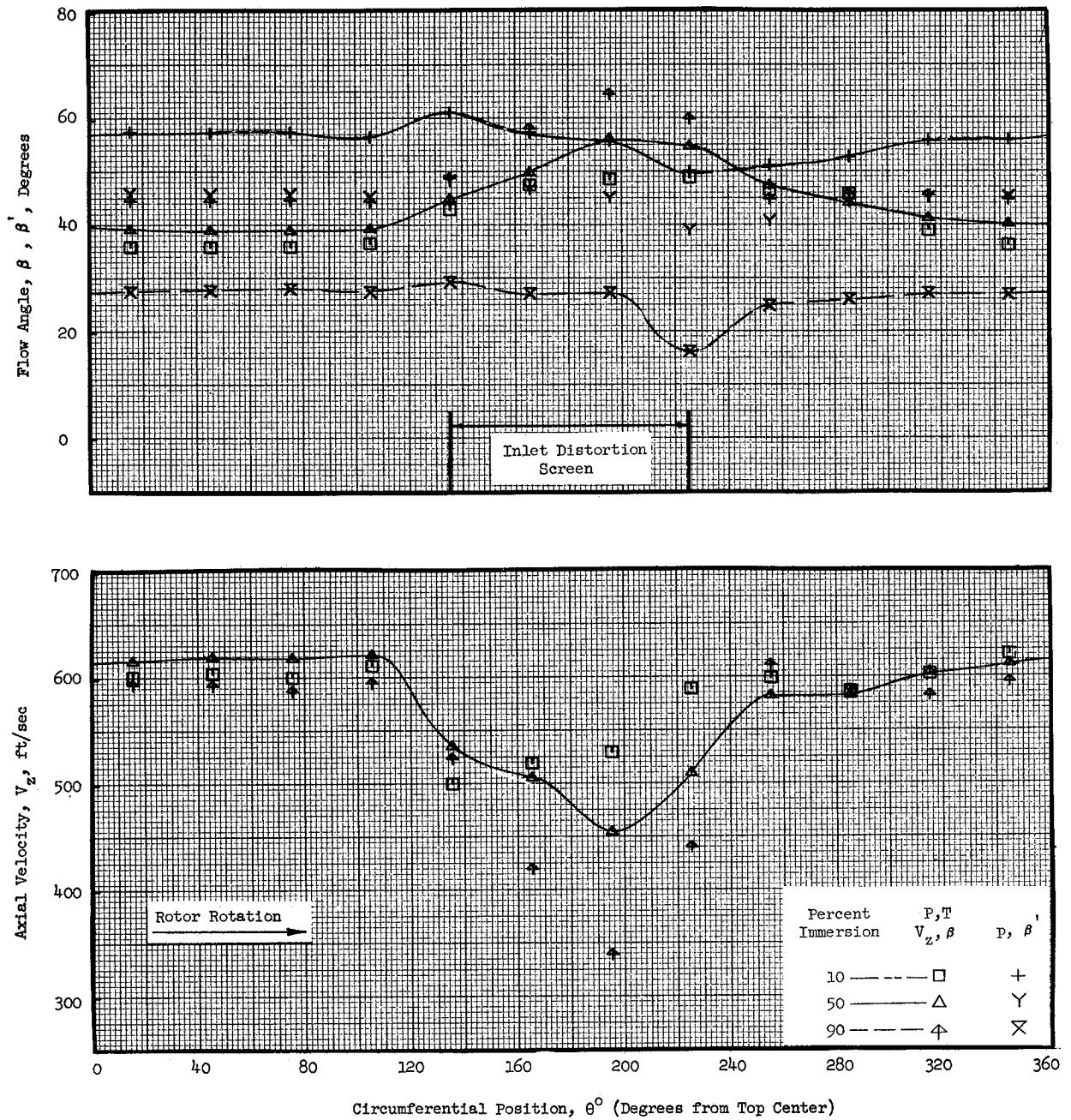


Figure 21 (c). Task II Stage Circumferential Distortion Profiles of Flow Conditions at 100% Speed Near Stall With Inlet Guide Vanes and With Casing Treatment Installed at Plane 1.51 (Concluded).

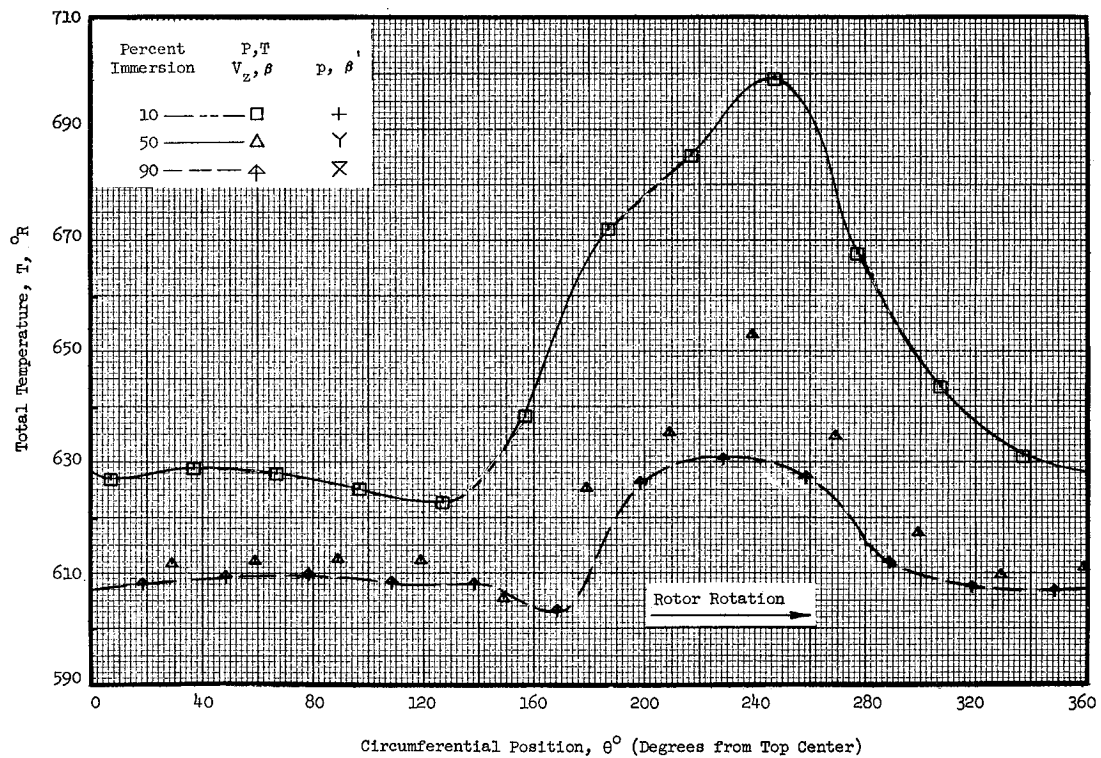
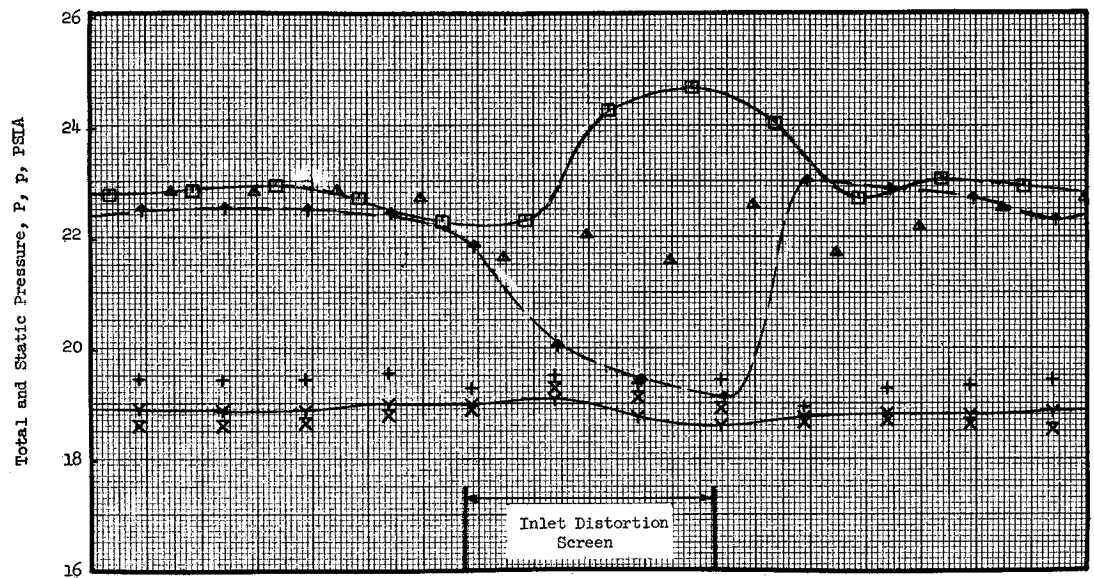


Figure 21 (d). Task II Stage Circumferential Distortion Profiles of Flow Conditions at 100% Speed Near Stall With Inlet Guide Vanes and With Casing Treatment Installed at Plane 2.20.

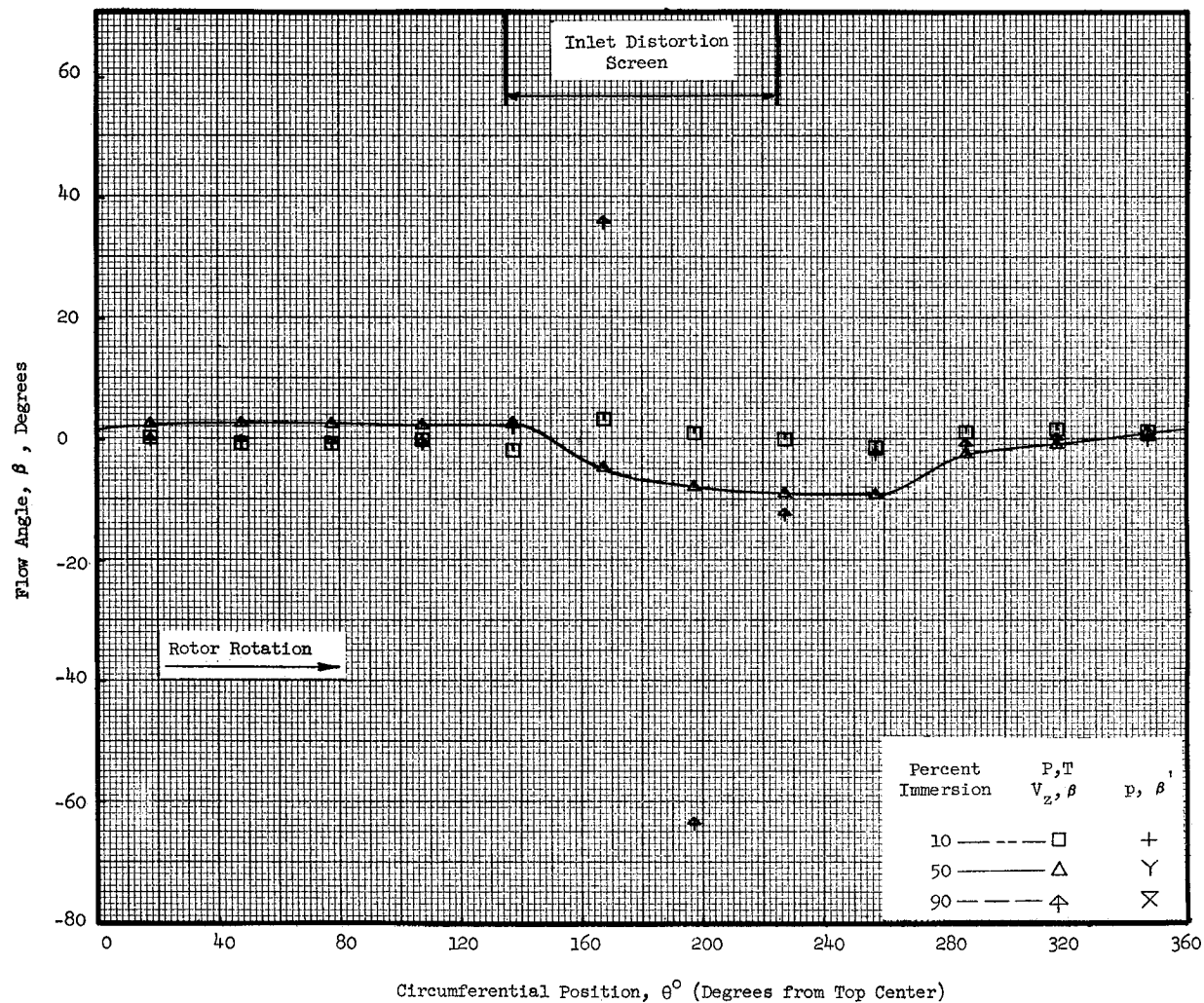


Figure 21 (d). Task II Stage Circumferential Distortion Profiles of Flow Conditions at 100% Speed Near Stall With Inlet Guide Vanes and With Casing Treatment Installed at Plane 2.20 (Continued).

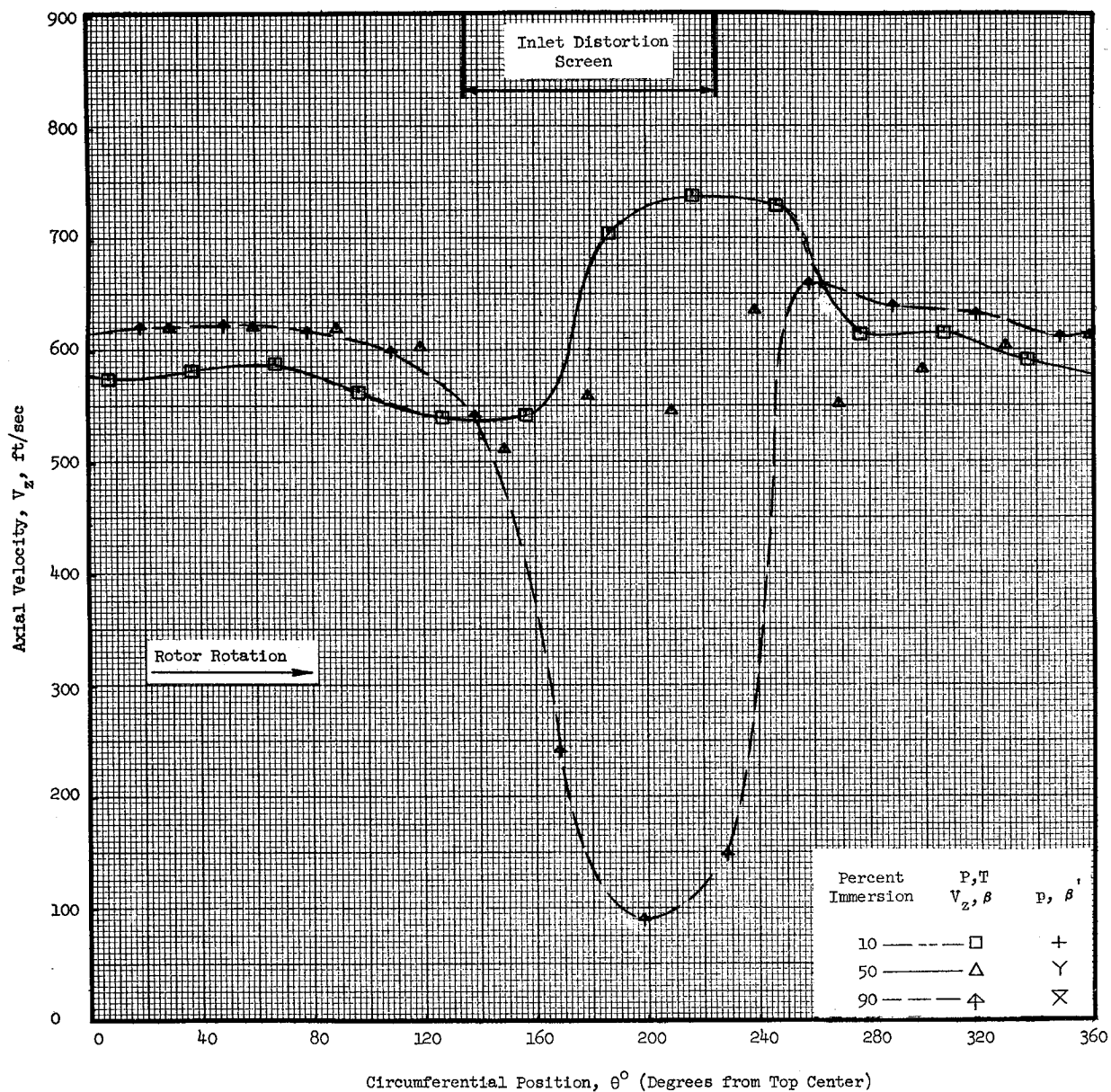


Figure 21 (d). Task II Stage Circumferential Distortion Profiles of Flow Conditions at 100% Speed Near Stall With Inlet Guide Vanes and With Casing Treatment Installed at Plane 2.20 (Concluded).

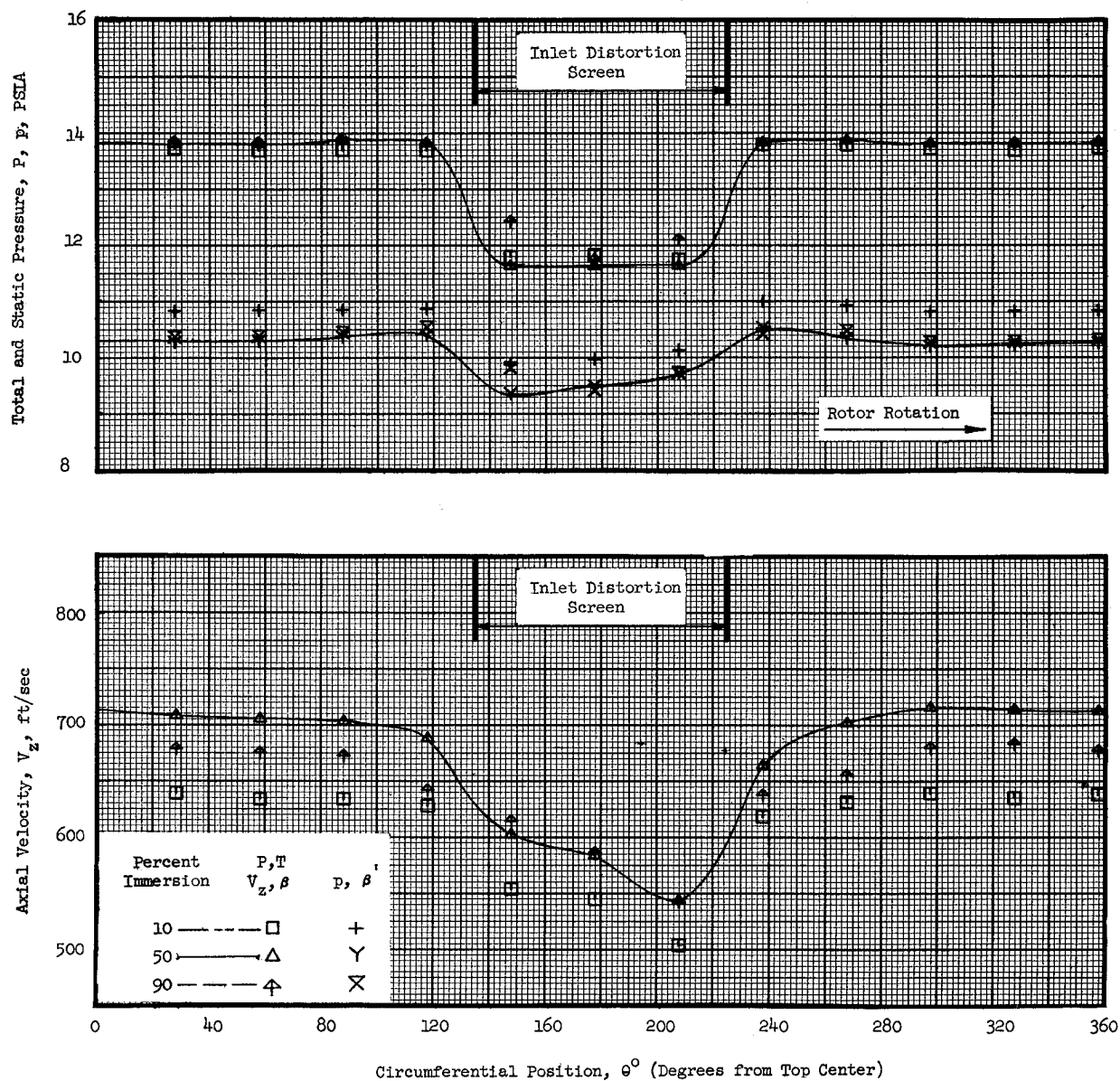


Figure 22 (a). Task II Stage Circumferential Distortion Profiles of Flow Conditions at 100% Speed Near Stall Without Inlet Guide Vanes and With Casing Treatment Installed at Plane 0.95.

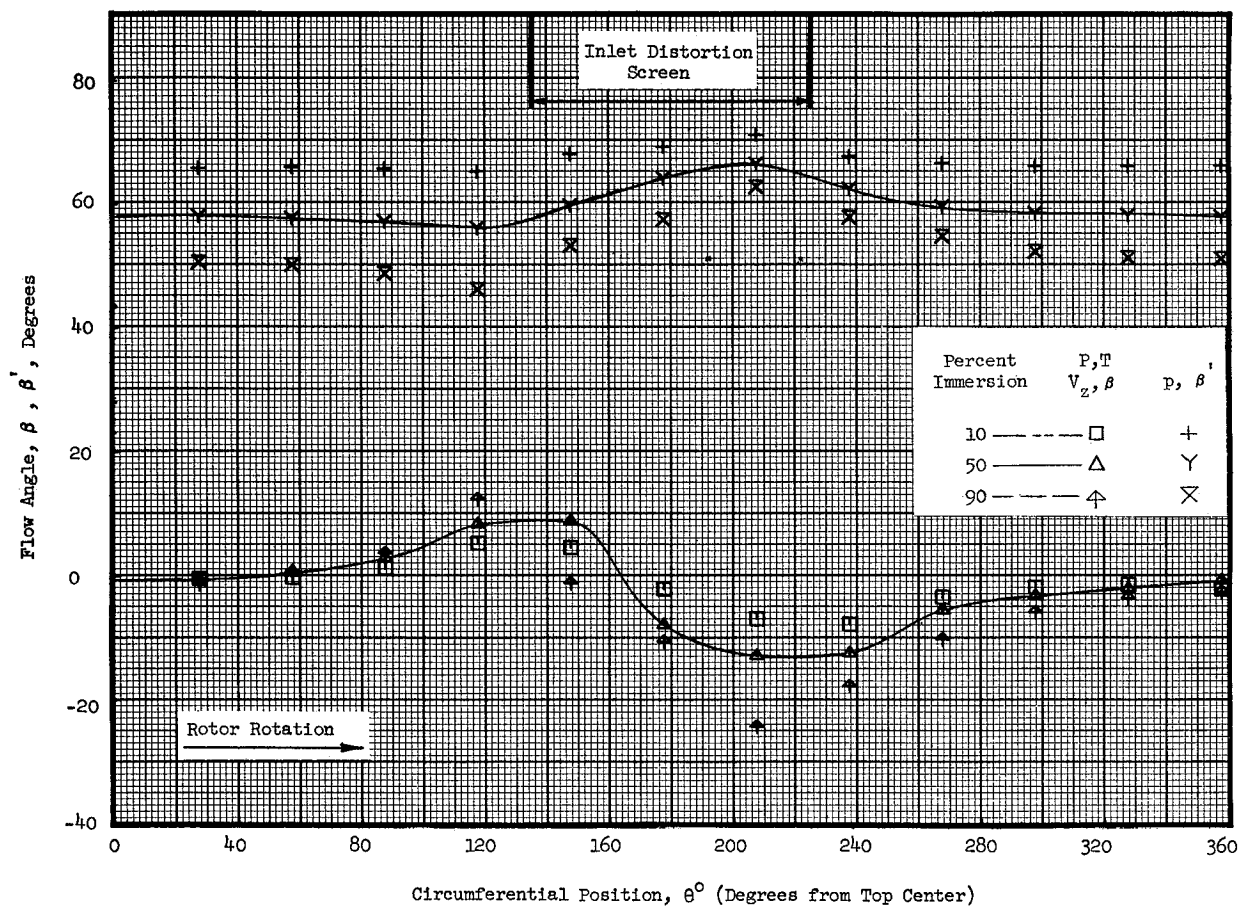


Figure 22 (a). Task II Stage Circumferential Distortion Profiles of Flow Conditions at 100% Speed Near Stall Without Inlet Guide Vanes and With Casing Treatment Installed at Plane 0.95 (Concluded).

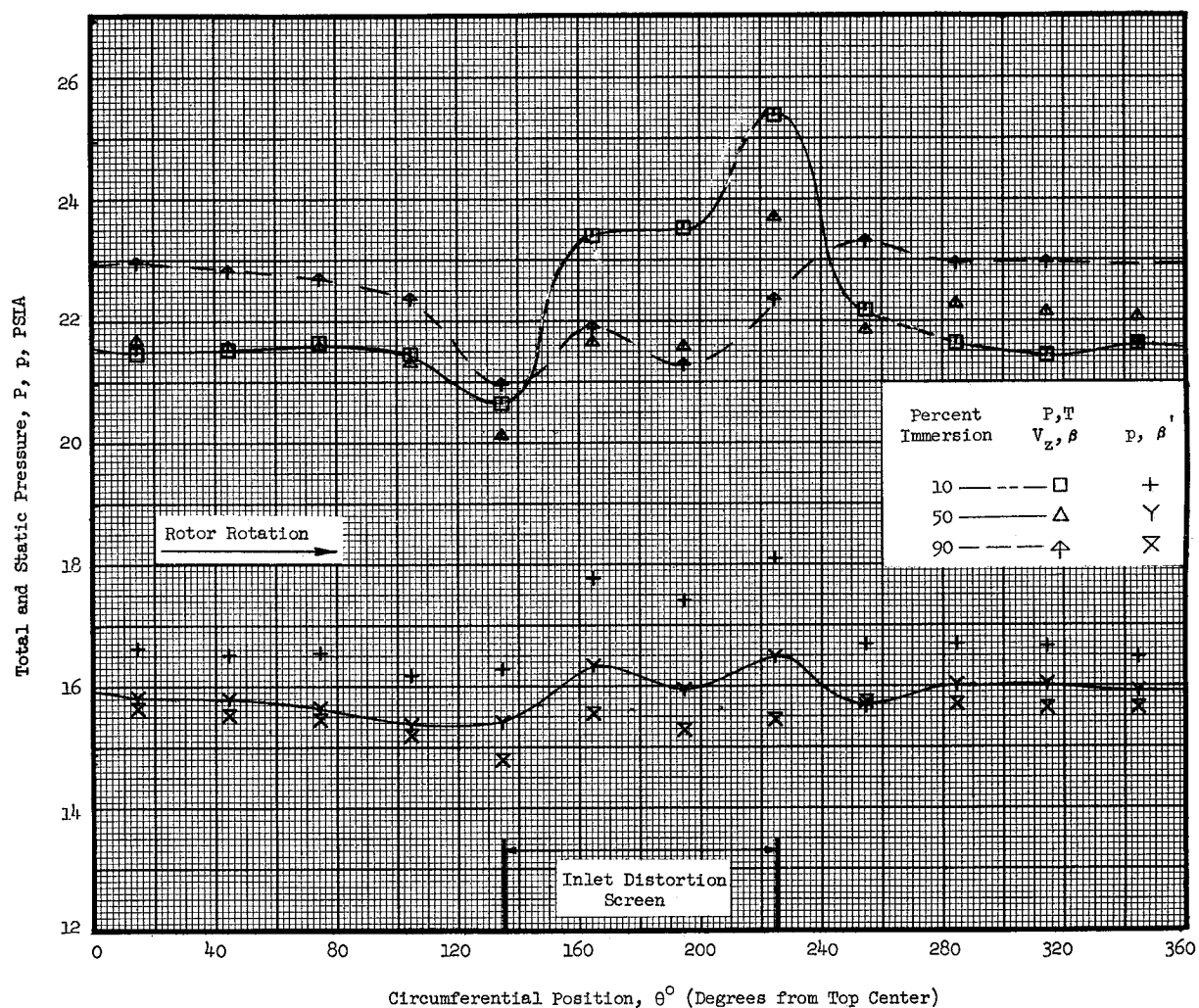


Figure 22 (b). Task II Stage Circumferential Distortion Profiles of Flow Conditions at 100% Speed Near Stall Without Inlet Guide Vanes and With Casing Treatment Installed at Plane 1.51.

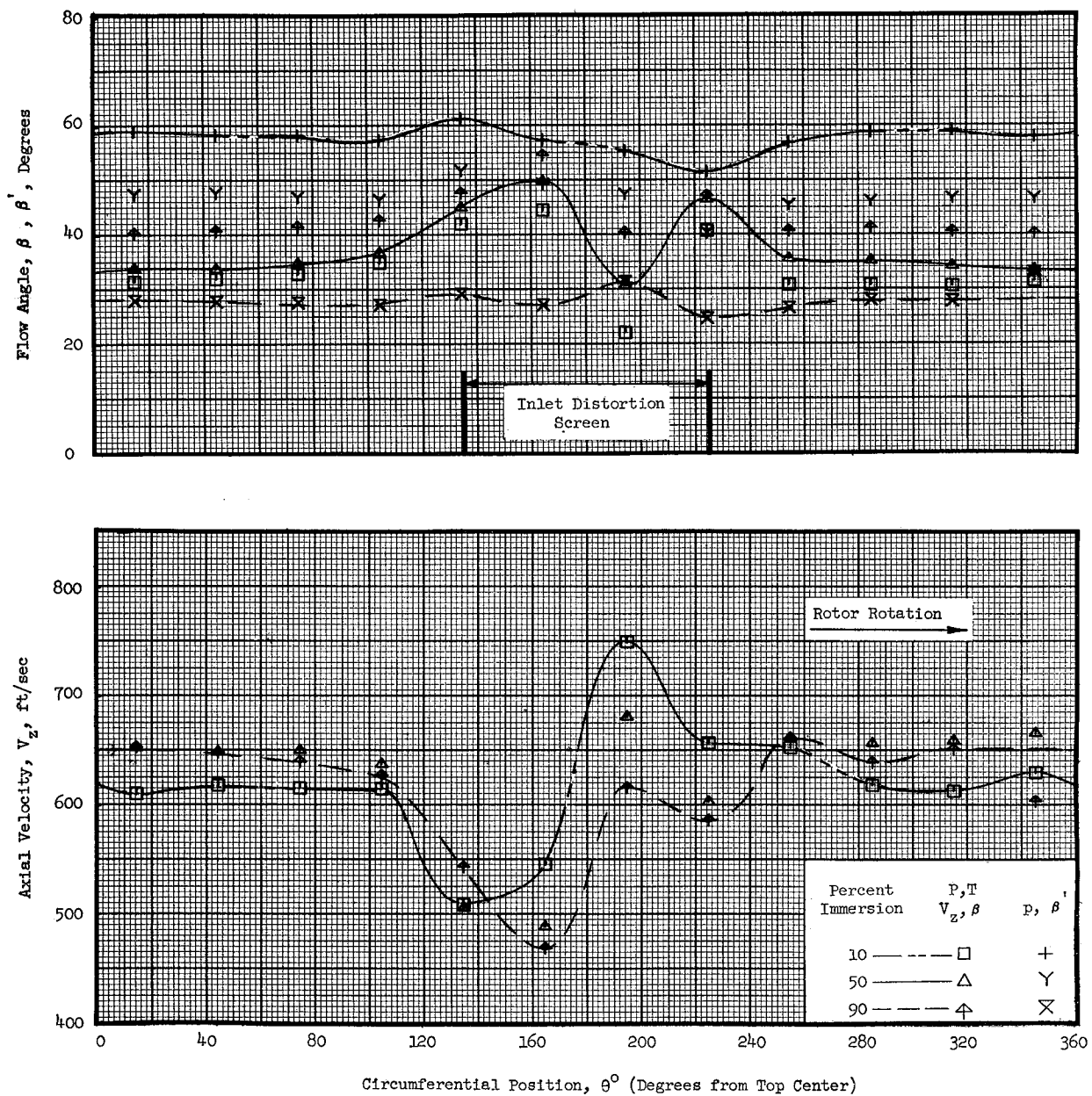


Figure 22 (b). Task II Stage Circumferential Distortion Profiles of Flow Conditions at 100% Speed Near Stall Without Inlet Guide Vanes and With Casing Treatment Installed at Plane 1.51 (Concluded).

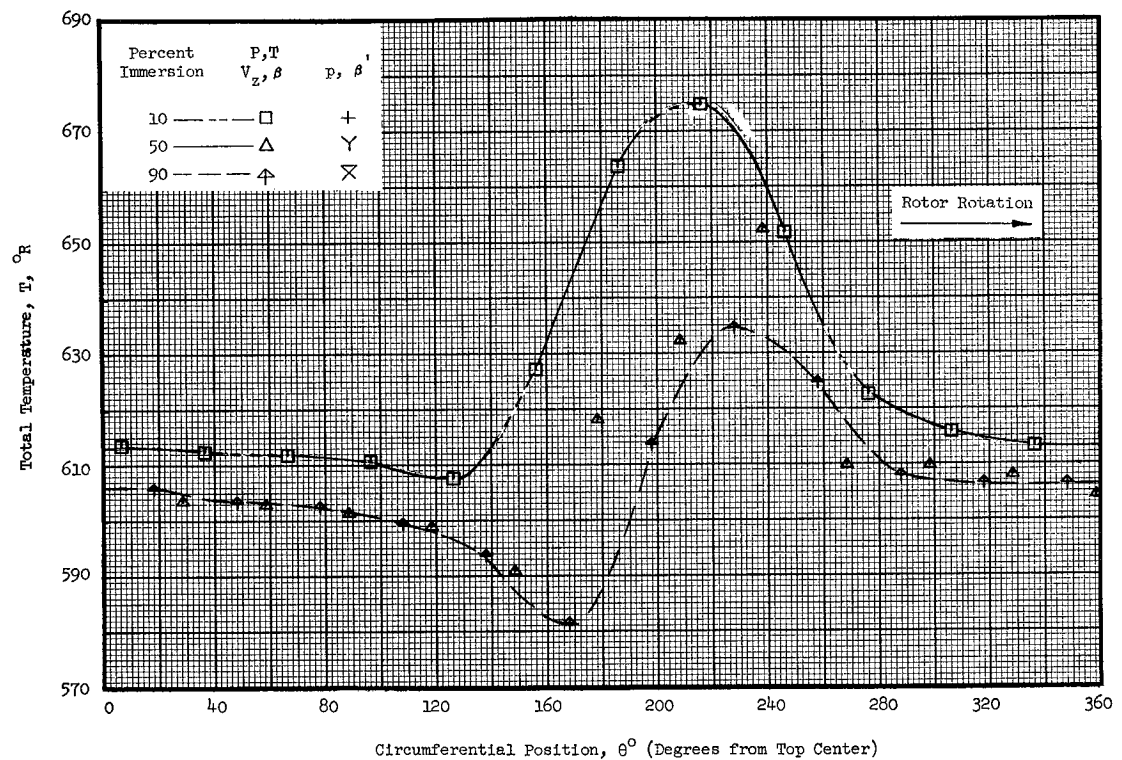
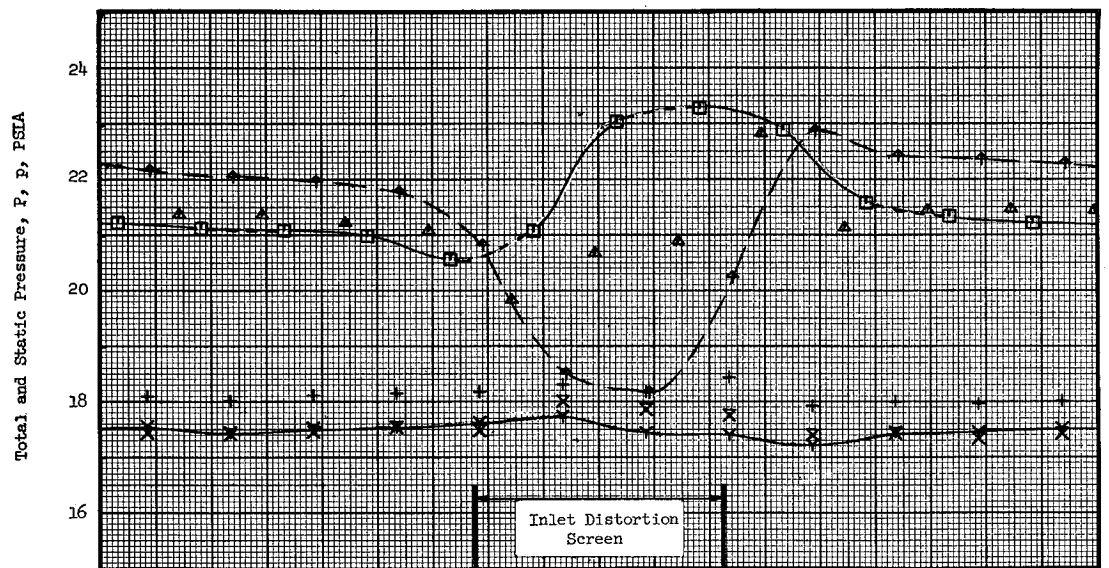


Figure 22 (c). Task II Stage Circumferential Distortion Profiles of Flow Conditions at 100% Speed Near Stall Without Inlet Guide Vanes and With Casing Treatment Installed at Plane 2.20.

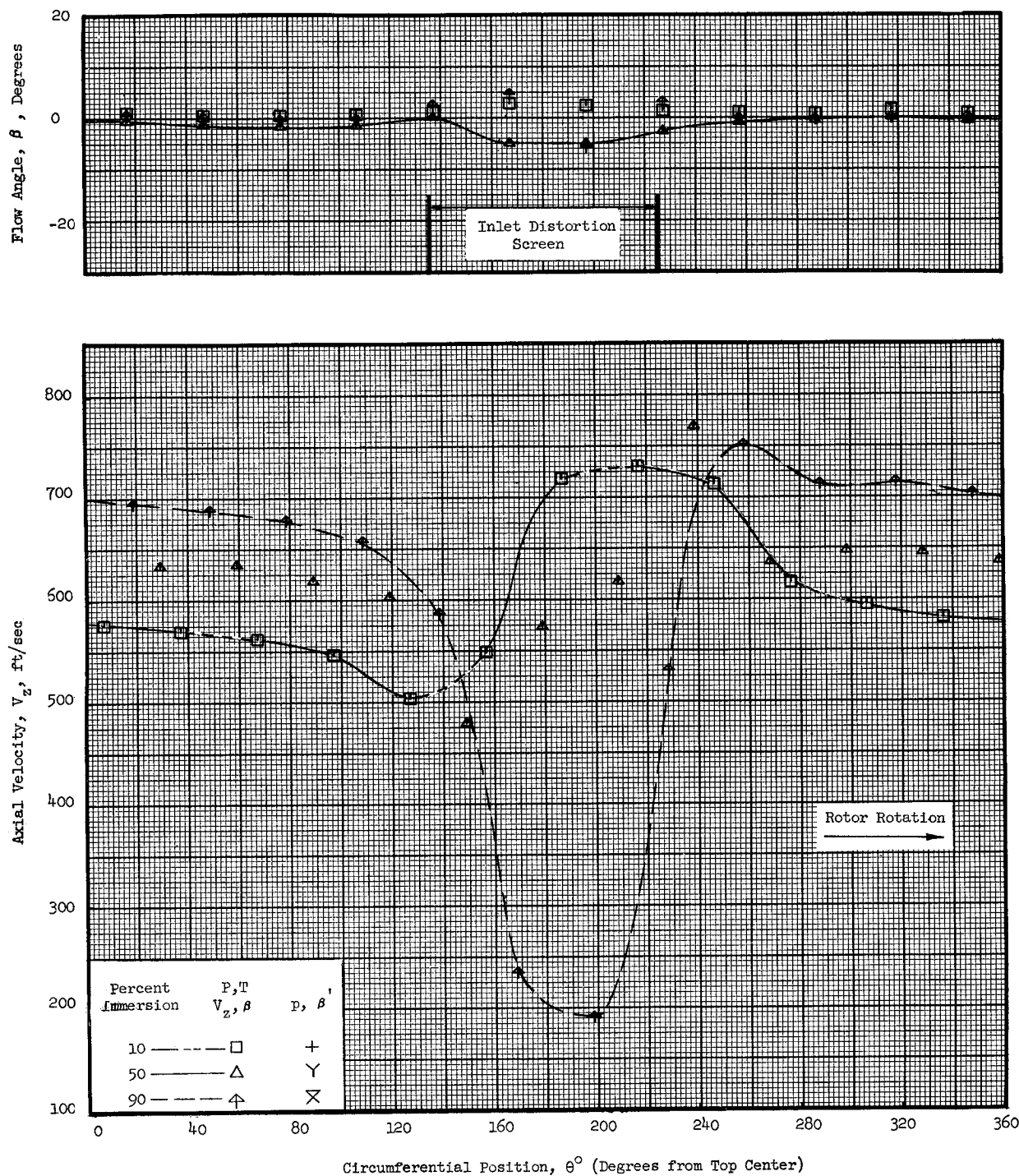


Figure 22 (c). Task II Stage Circumferential Distortion Profiles of Flow Conditions at 100% Speed Near Stall Without Inlet Guide Vanes and With Casing Treatment Installed at Plane 2.20 (Concluded).

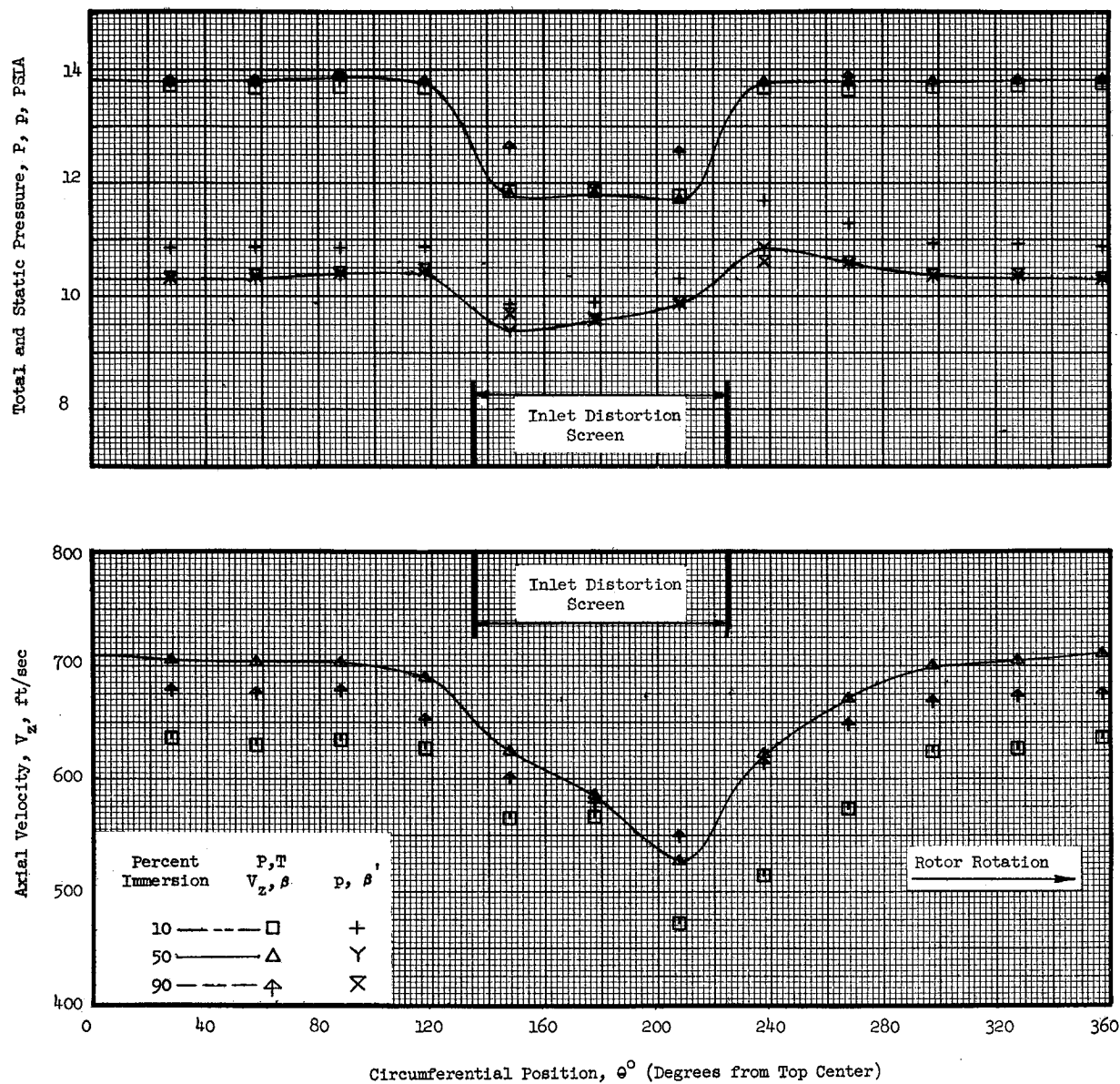


Figure 23 (a). Task II Stage Circumferential Distortion Profiles of Flow Conditions at 100% Speed Near Stall Without Inlet Guide Vanes and Without Casing Treatment Installed at Plane 0.95.

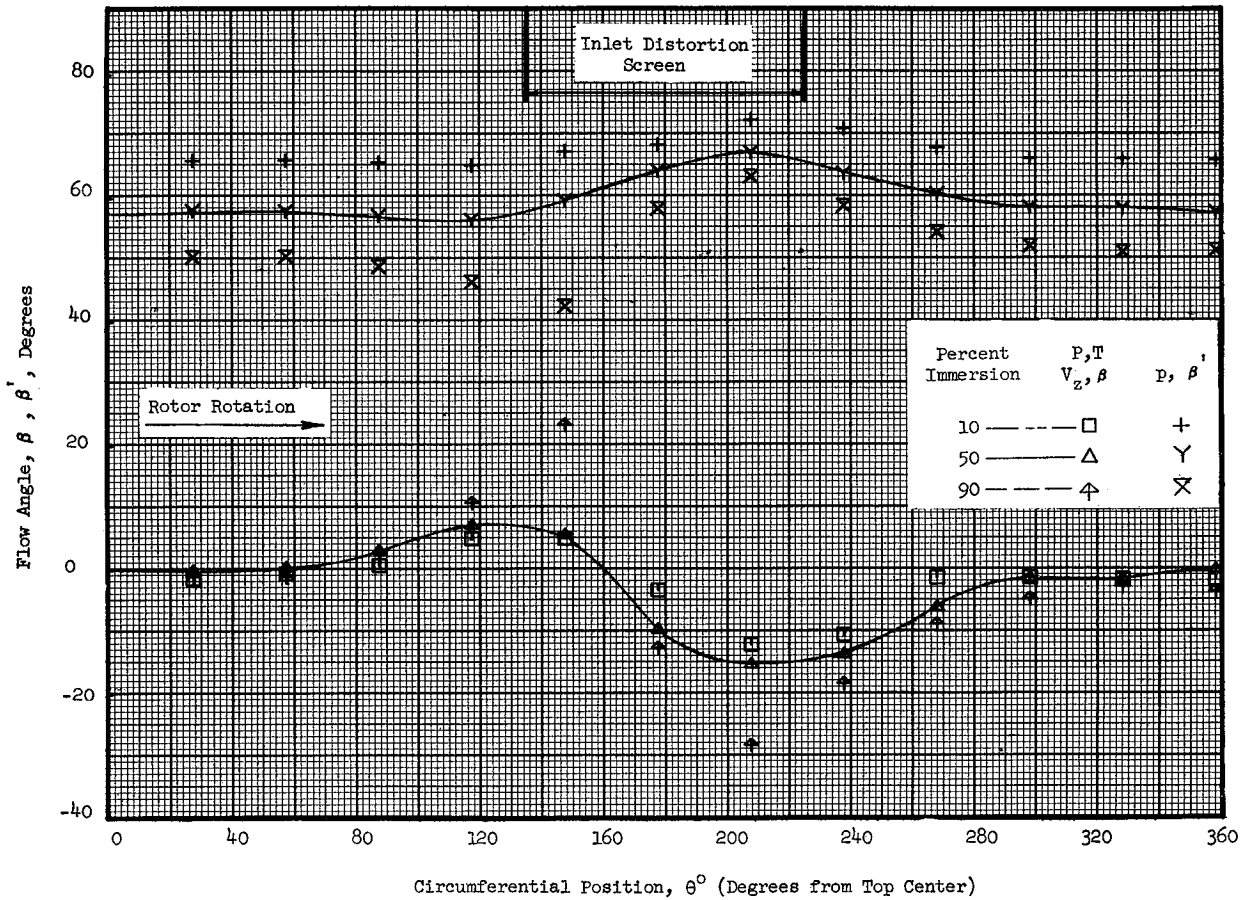


Figure 23 (a). Task II Stage Circumferential Distortion Profiles of Flow Conditions at 100% Speed Near Stall Without Inlet Guide Vanes and Without Casing Treatment Installed at Plane 0.95 (Concluded).

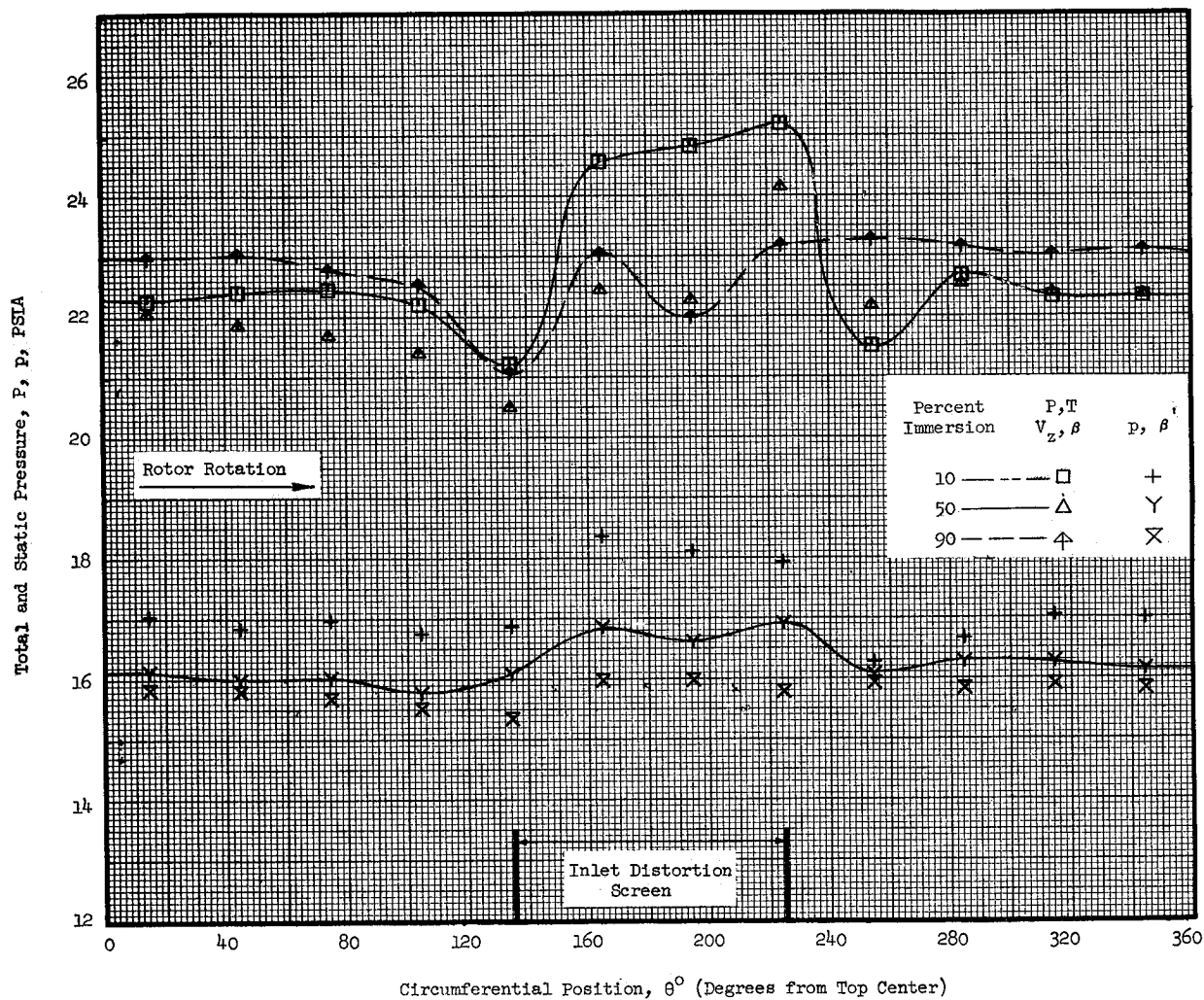


Figure 23 (b). Task II Stage Circumferential Distortion Profiles of Flow Conditions at 100% Speed Near Stall Without Inlet Guide Vanes and Without Casing Treatment Installed at Plane 1.51.

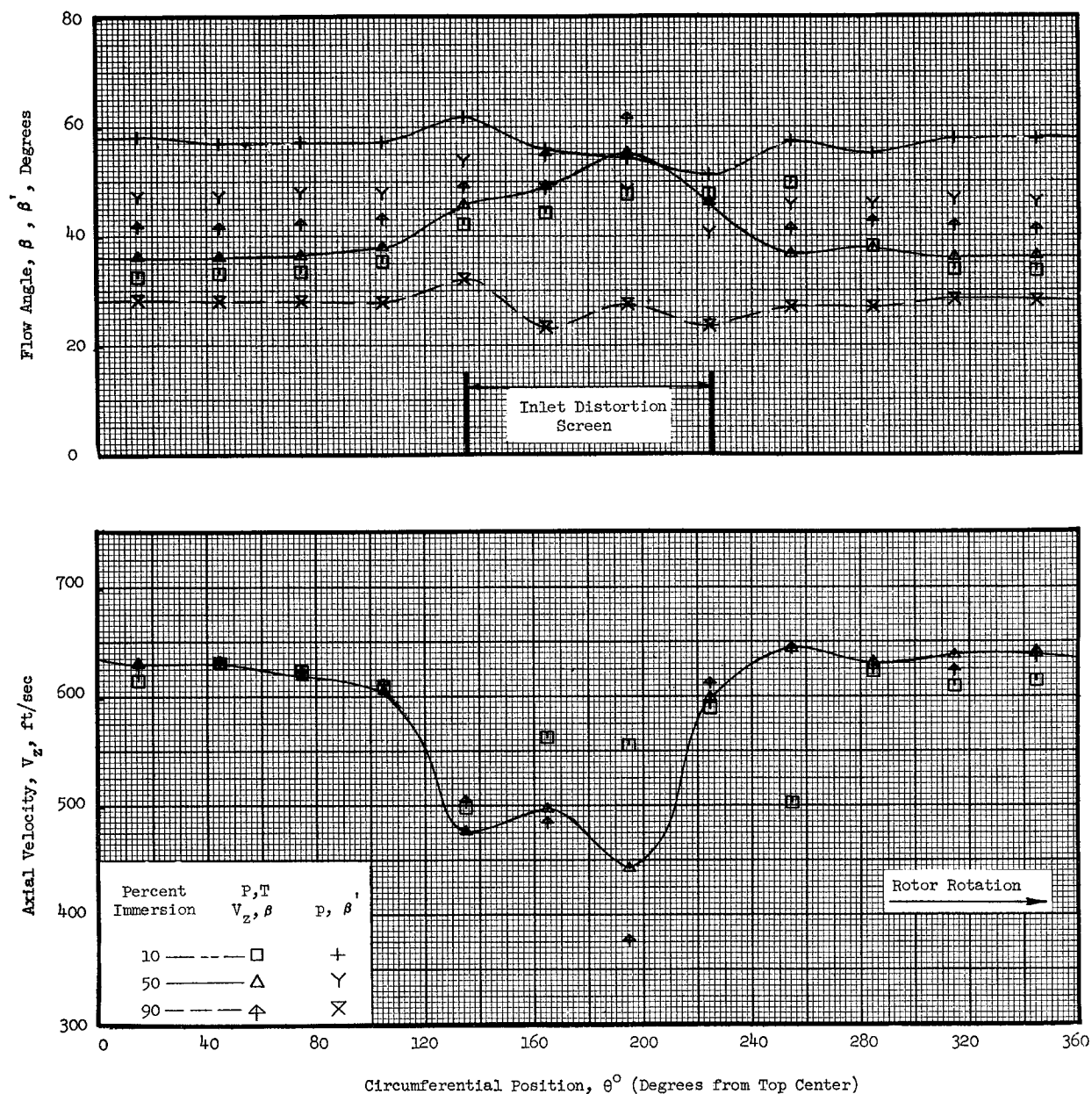


Figure 23 (b). Task II Stage Circumferential Distortion Profiles of Flow Conditions at 100% Speed Near Stall Without Inlet Guide Vanes and Without Casing Treatment Installed at Plane 1.51 (Concluded).

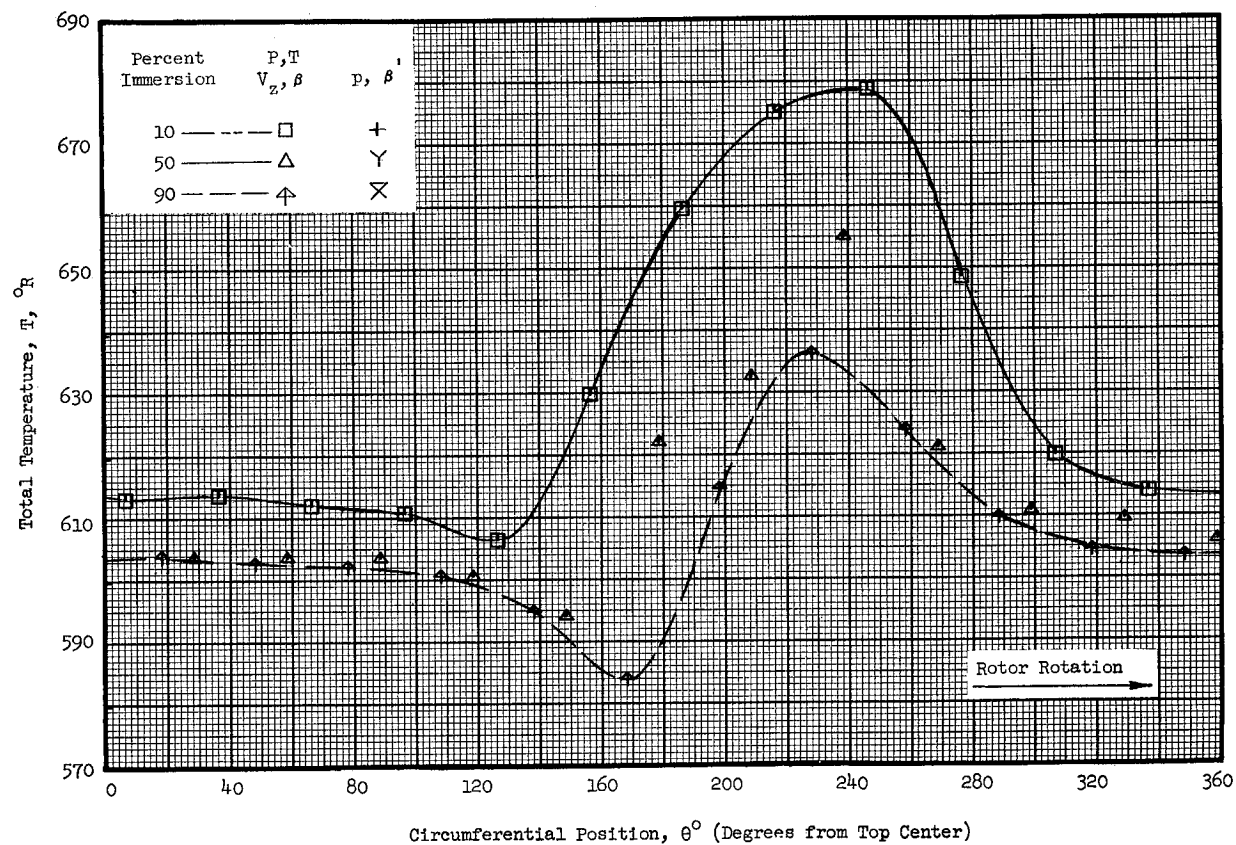
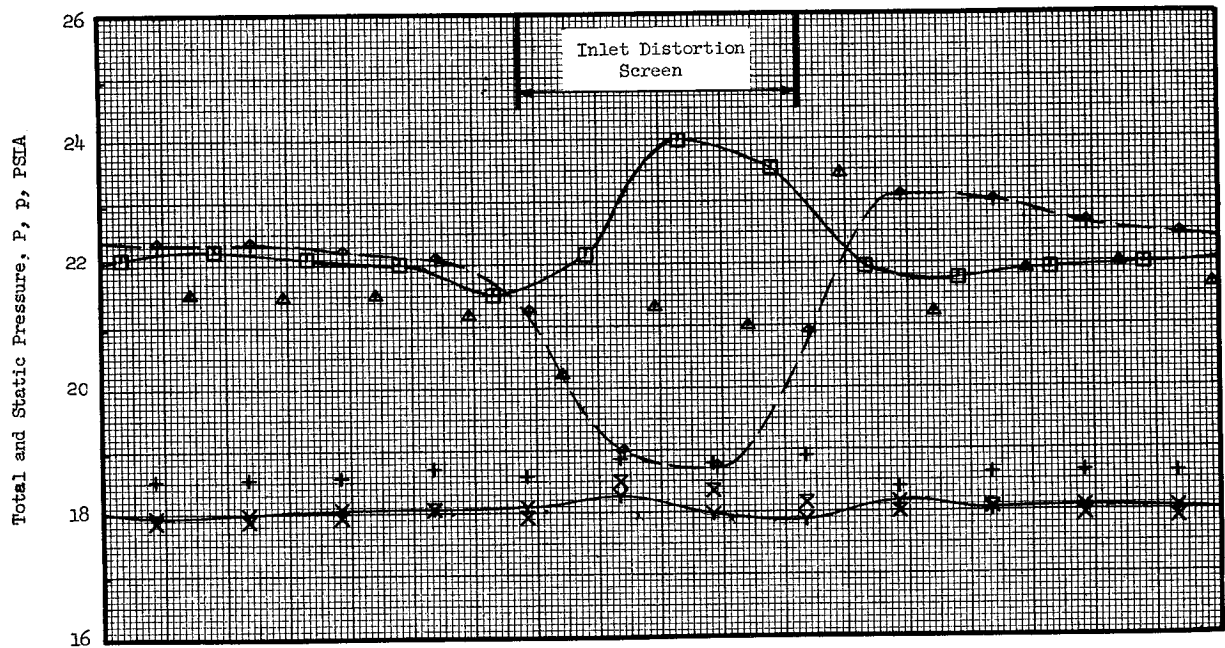


Figure 23 (c). Task II Stage Circumferential Distortion Profiles of Flow Conditions at 100% Speed Near Stall Without Inlet Guide Vanes and Without Casing Treatment Installed at Plane 2.20.

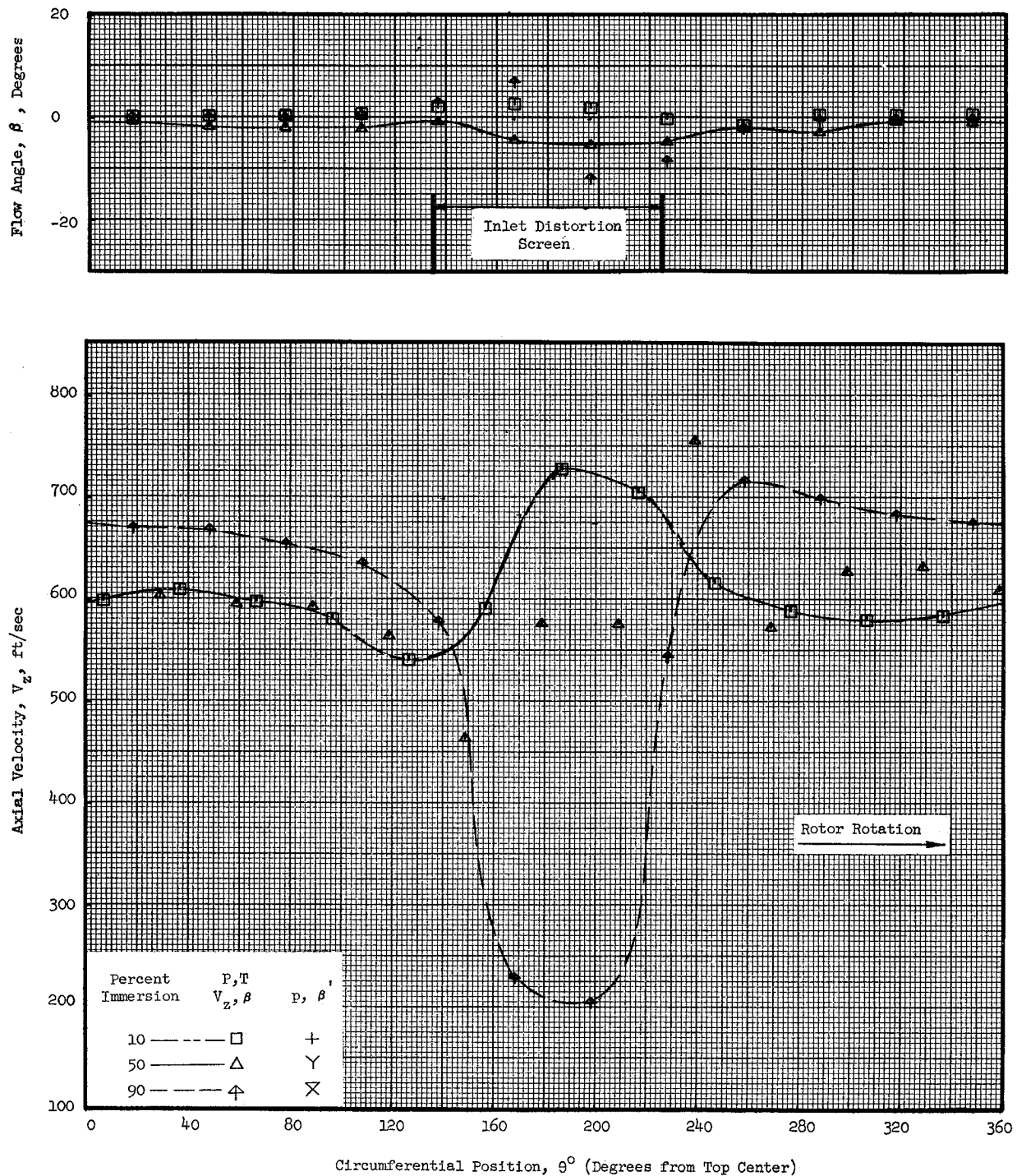


Figure 23 (c). Task II Stage Circumferential Distortion Profiles of Flow Conditions at 100% Speed Near Stall Without Inlet Guide Vanes and Without Casing Treatment Installed at Plane 2.20 (Concluded).

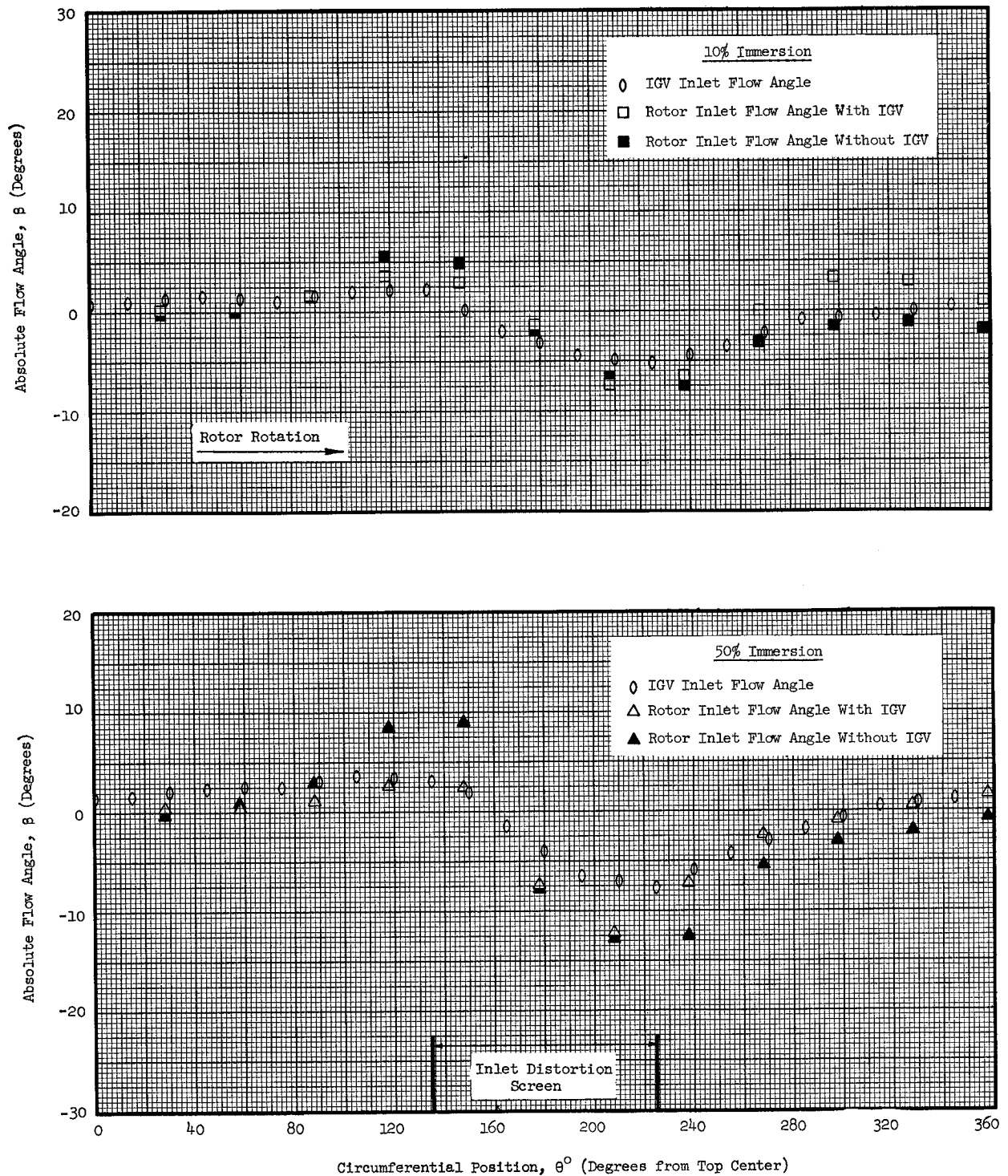


Figure 24. Task II Circumferential Distortion IGV Inlet and Rotor Inlet Flow Angles at 100% Speed Near Stall With and Without Inlet Guide Vanes.

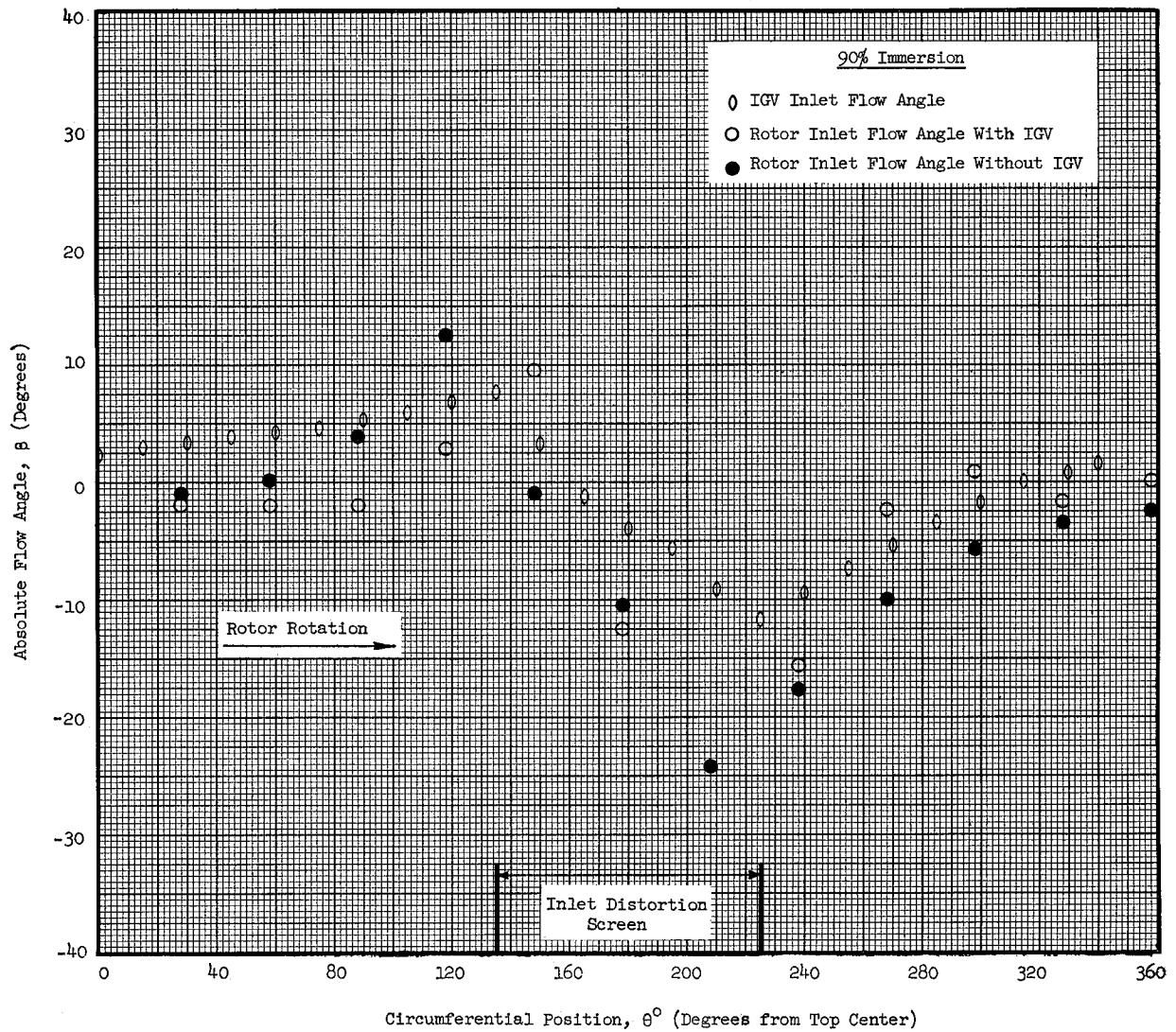


Figure 24. Task II Circumferential Distortion IGV Inlet and Rotor Inlet Flow Angles at 100% Speed Near Stall With and Without Inlet Guide Vanes (Concluded).

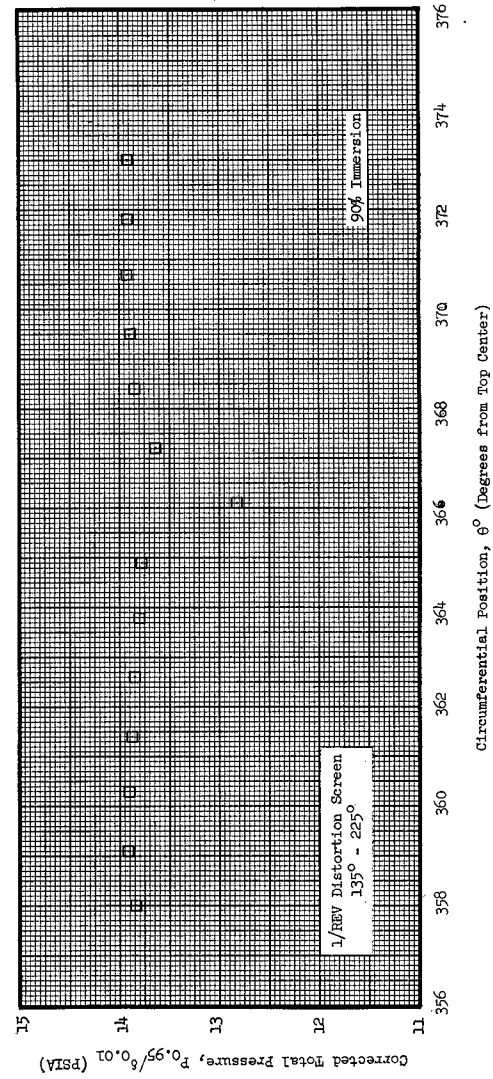
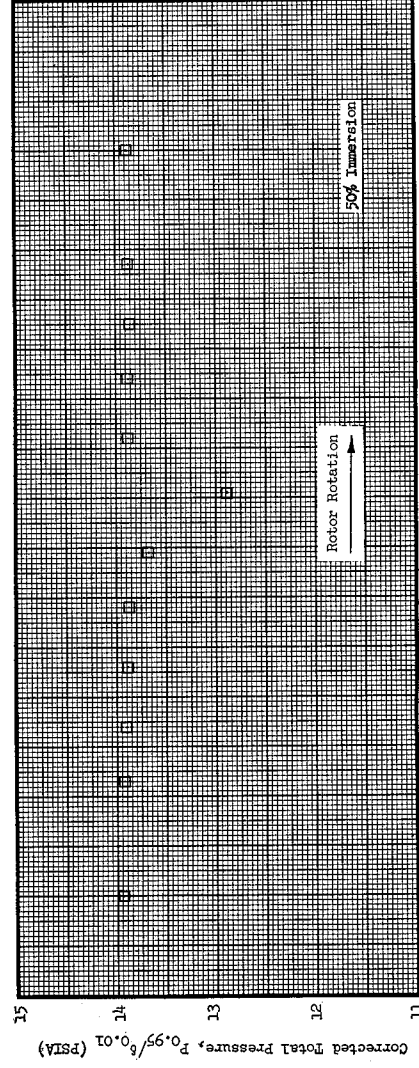
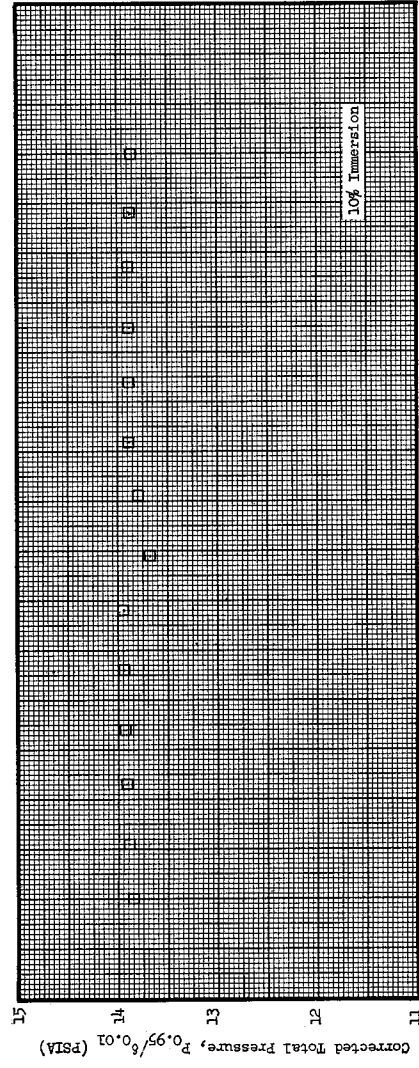


Figure 25 (a). Task II Circumferential Distortion Inlet Guide
Vane Wakes at 100% Speed, Near Stall; Undis-
torted Flow Region.

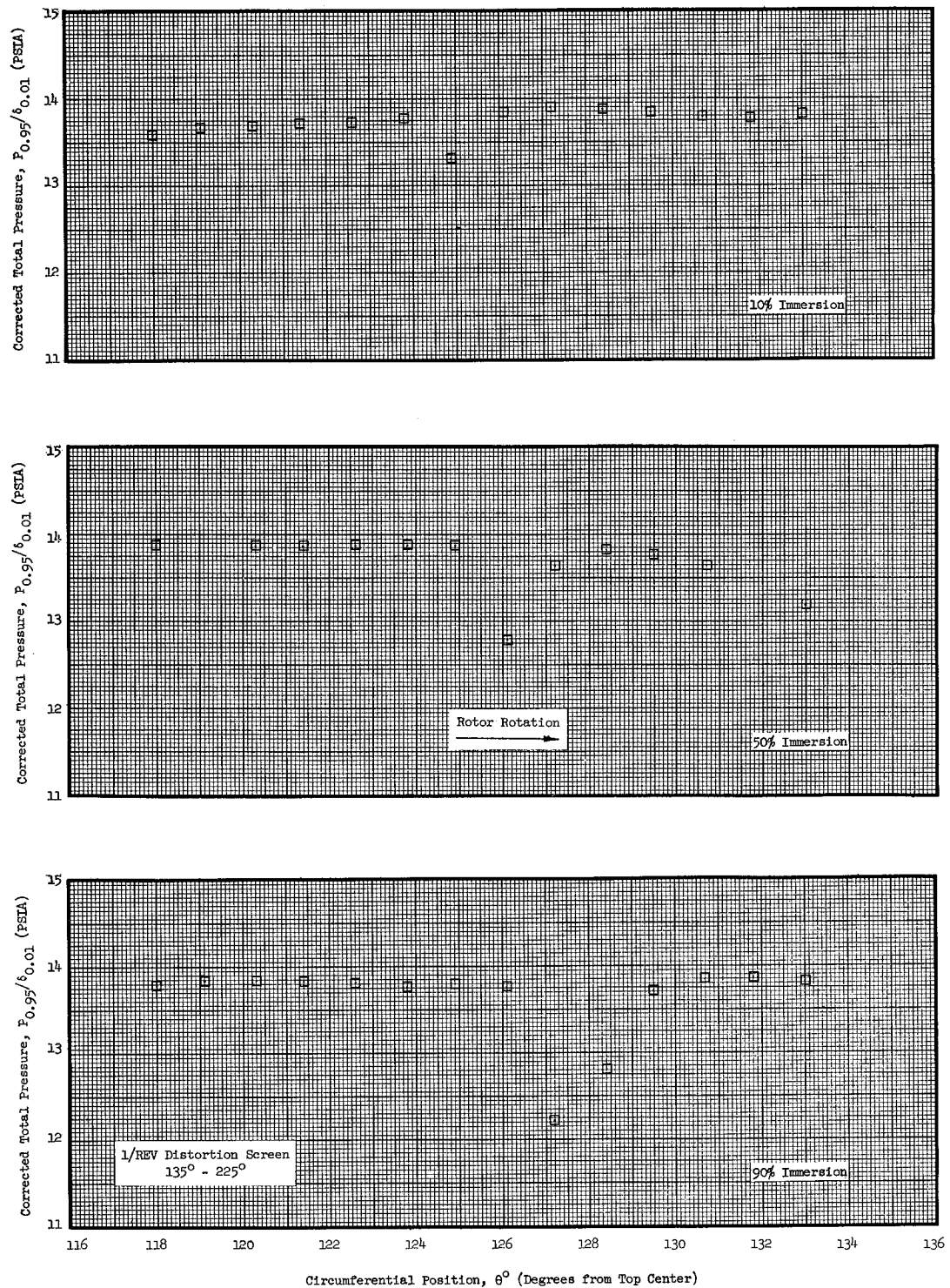


Figure 25 (b). Task II Circumferential Distortion Inlet Guide Vane Wakes at 100% Speed, Near Stall; Entering Distortion Screen Shadow.

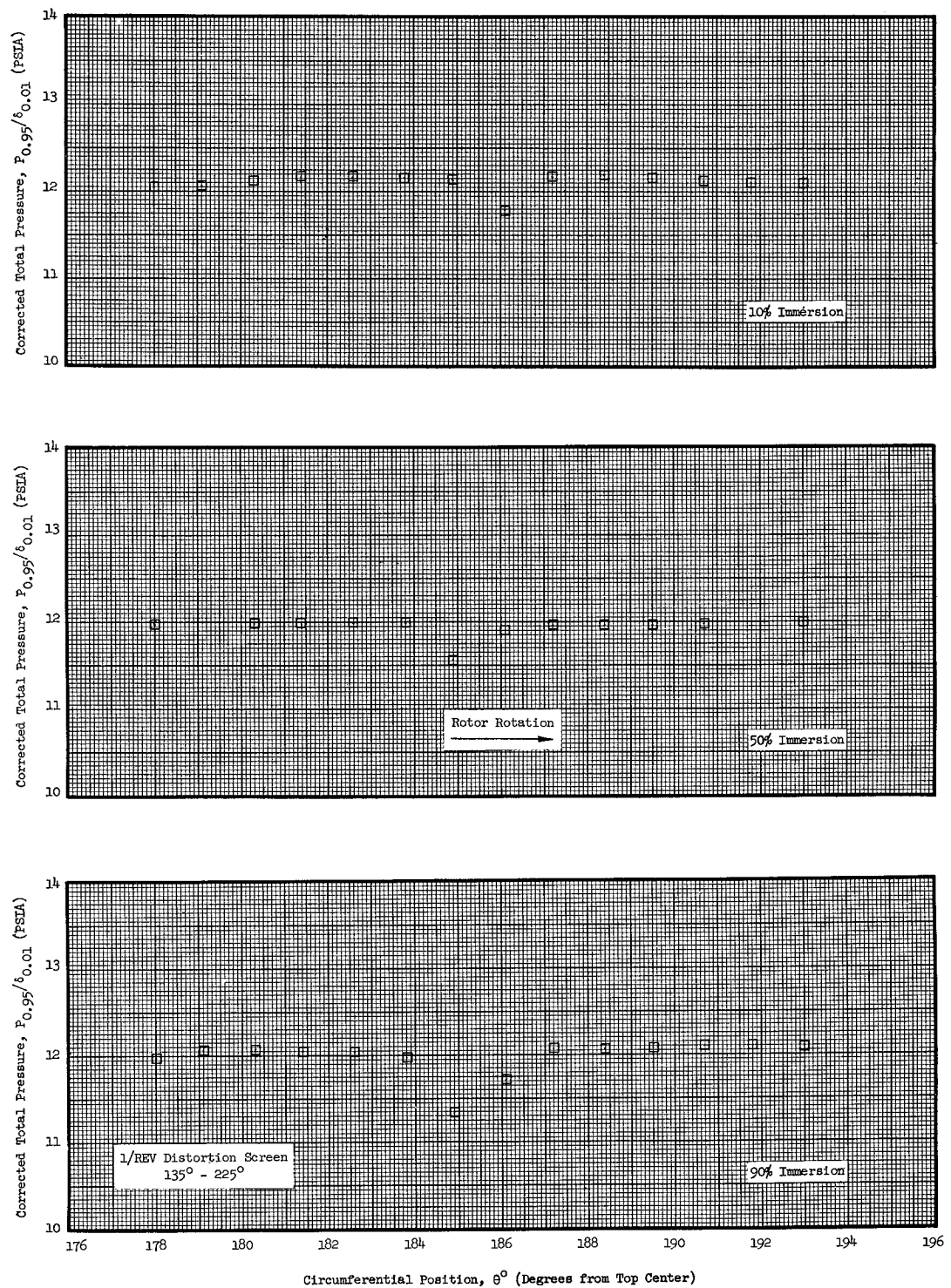


Figure 25 (c). Task II Circumferential Distortion Inlet Guide Vane Wakes at 100% Speed, Near Stall; Distorted Flow Region.

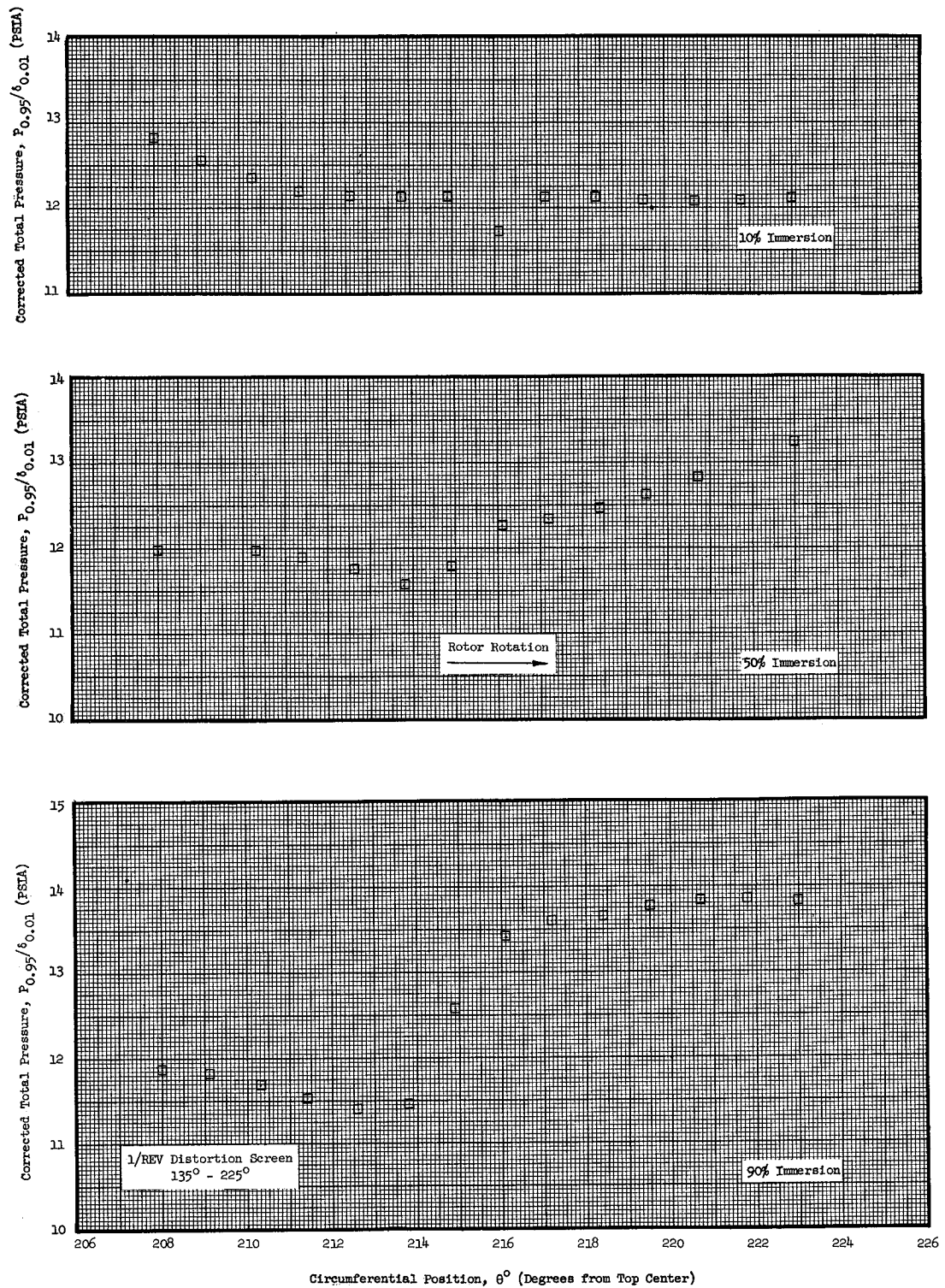


Figure 25 (d). Task II Circumferential Distortion Inlet Guide Vane Wakes at 100% Speed, Near Stall, Leaving Distortion Screen Shadow.

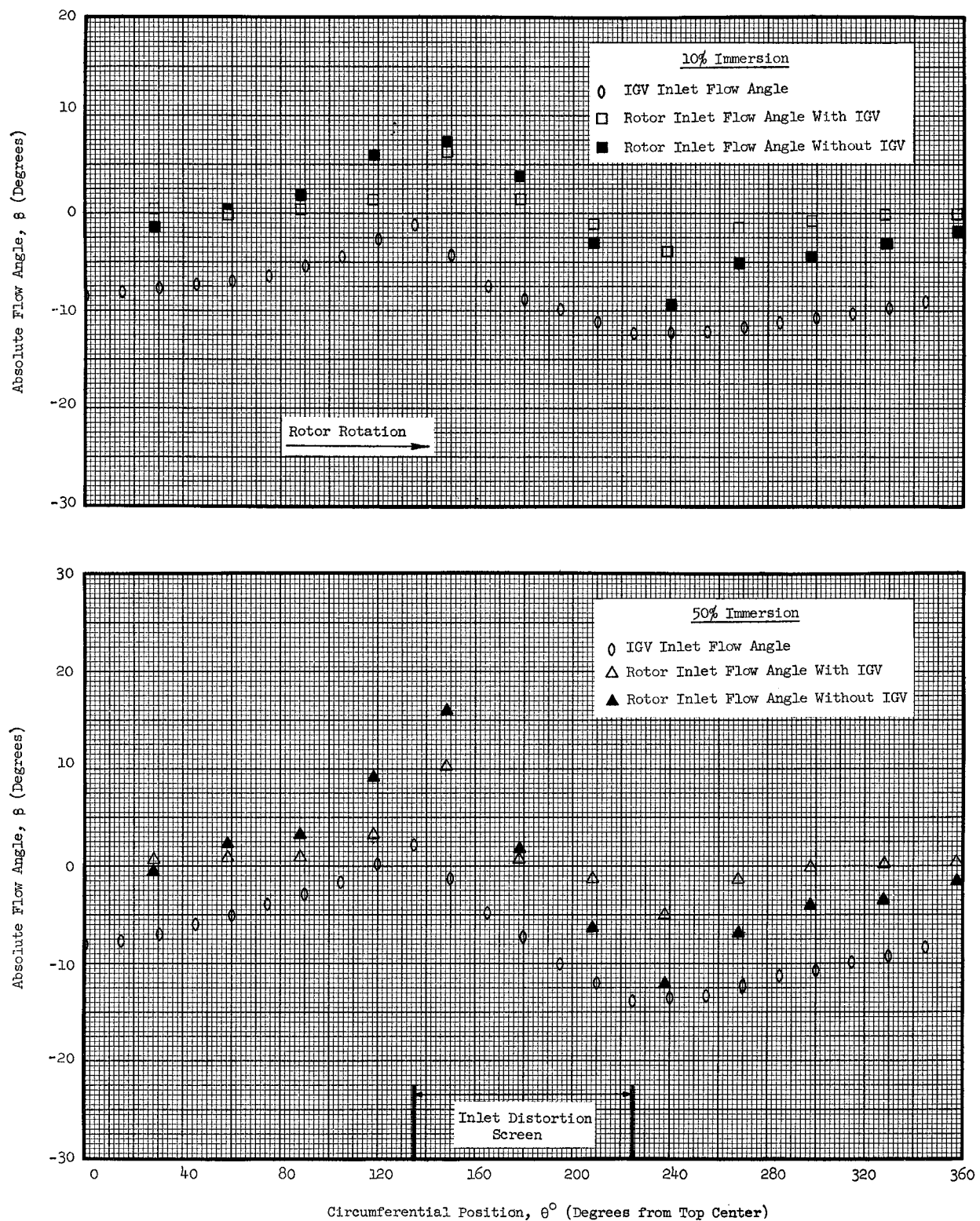


Figure 26. Task II Circumferential Distortion IGV Inlet and Rotor Inlet Flow Angles at 100% Speed Maximum Flow With and Without Inlet Guide Vanes.

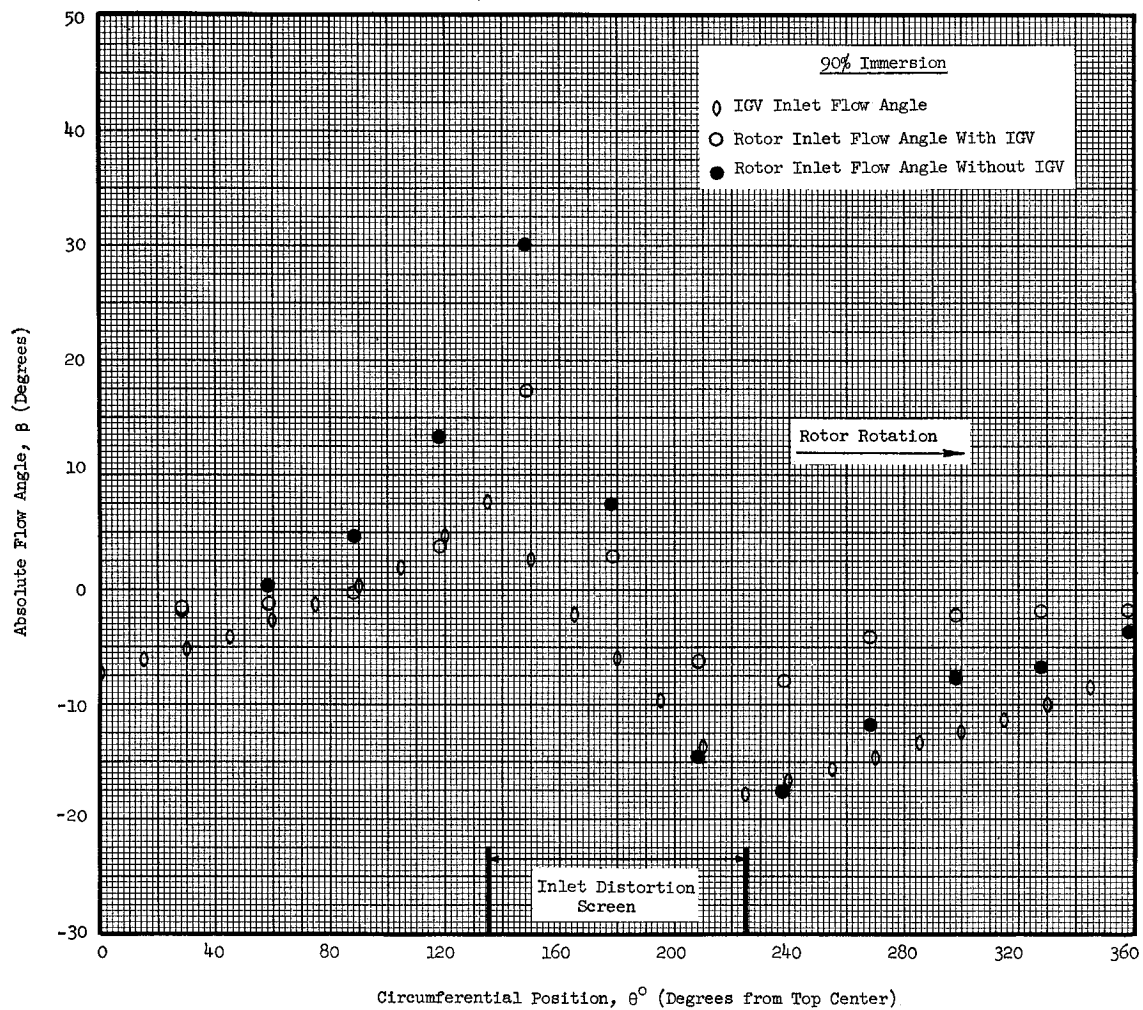


Figure 26. Task II Circumferential Distortion IGW Inlet and Rotor Inlet Flow Angles at 100% Speed Maximum Flow With and Without Inlet Guide Vanes (Concluded).

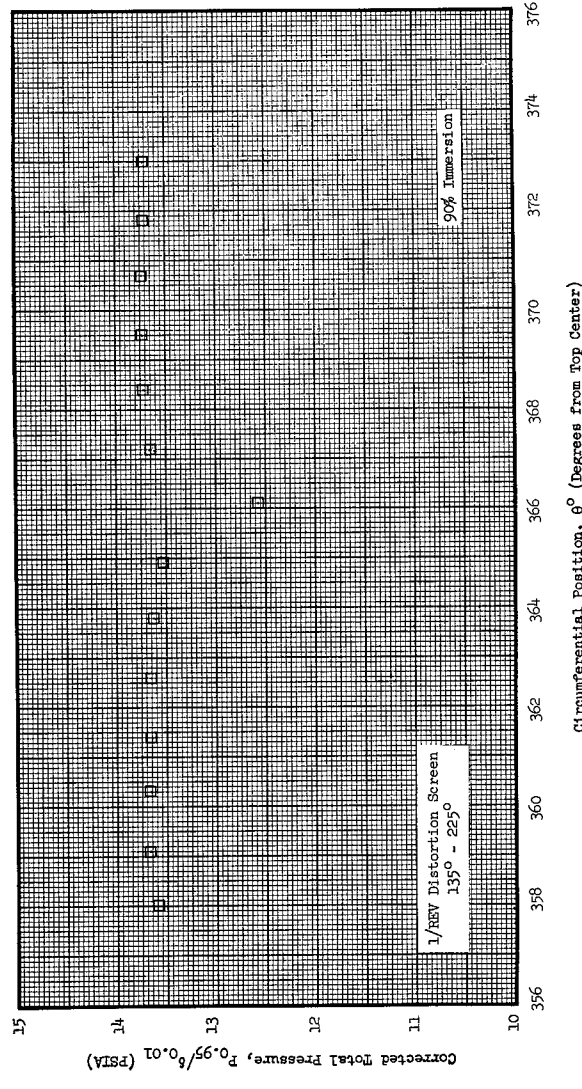
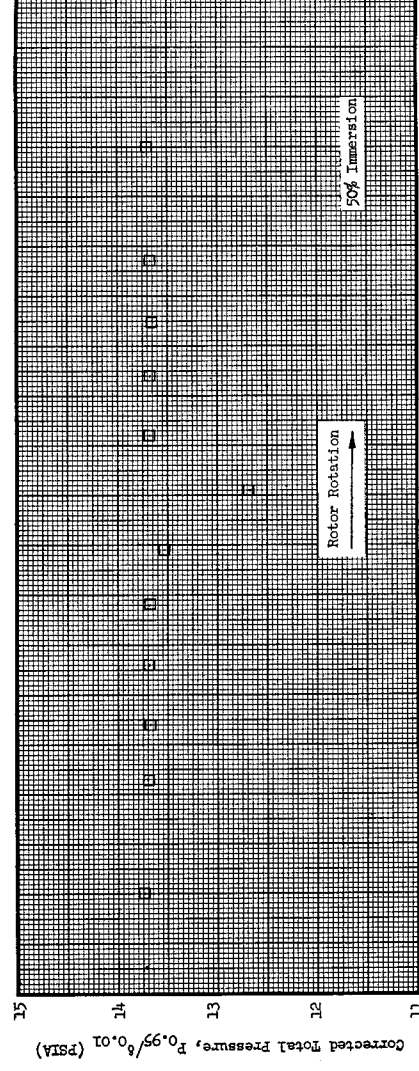
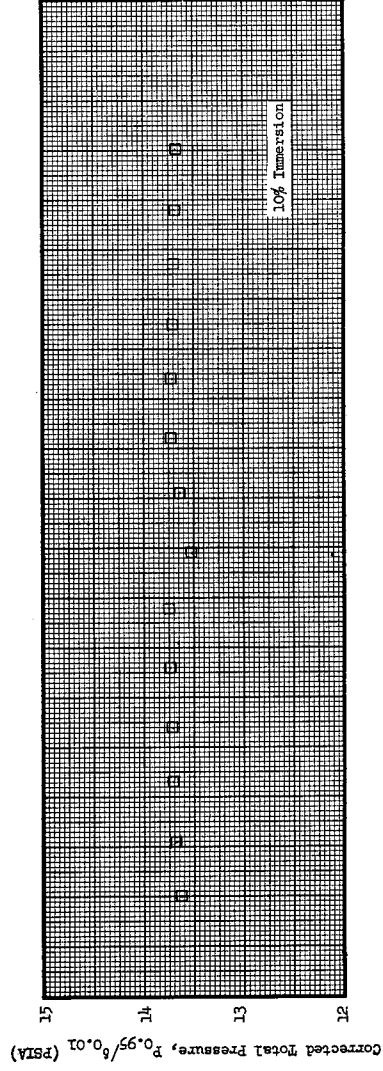


Figure 27 (a). Task II Circumferential Distortion Inlet Guide Vane Wake Survey at 100% Speed, Maximum Flow; Undistorted Flow Region.

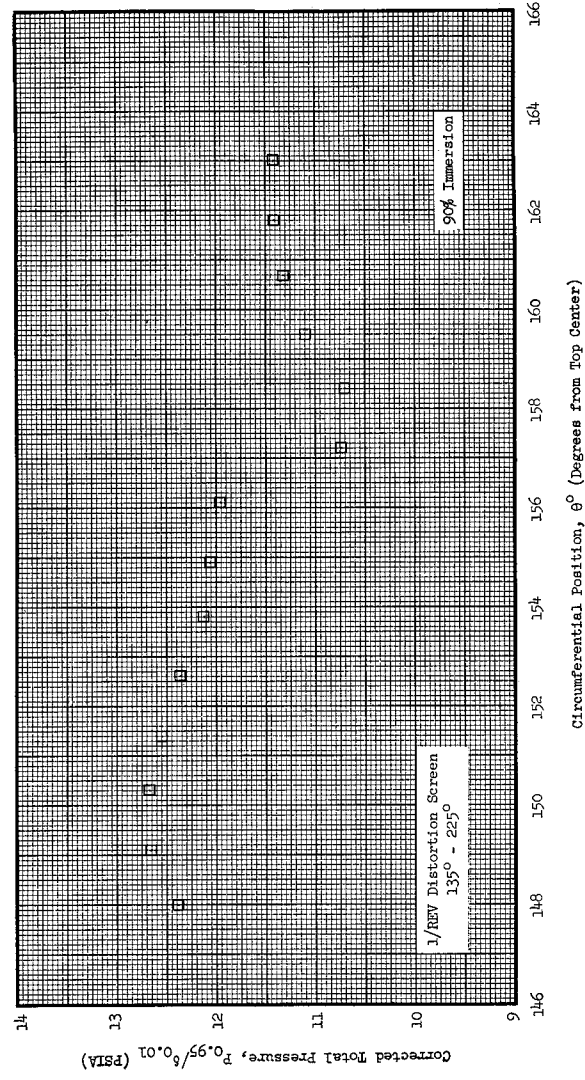
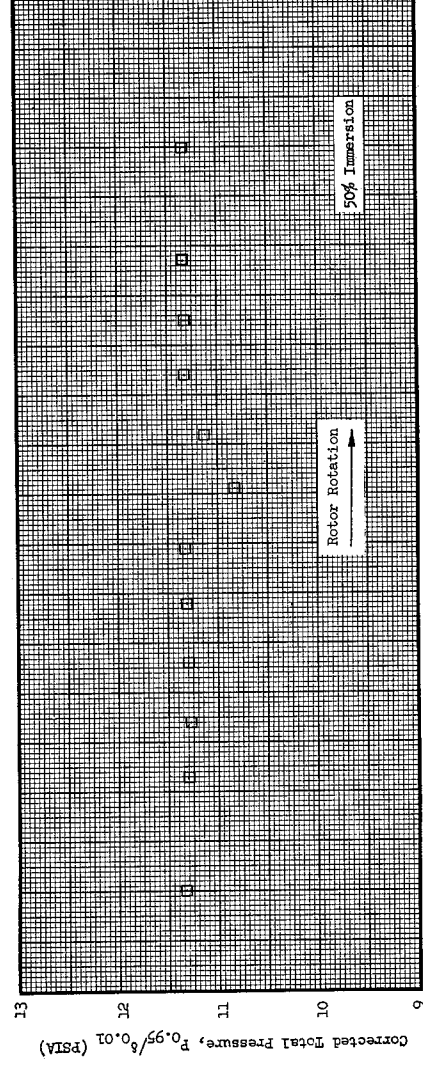
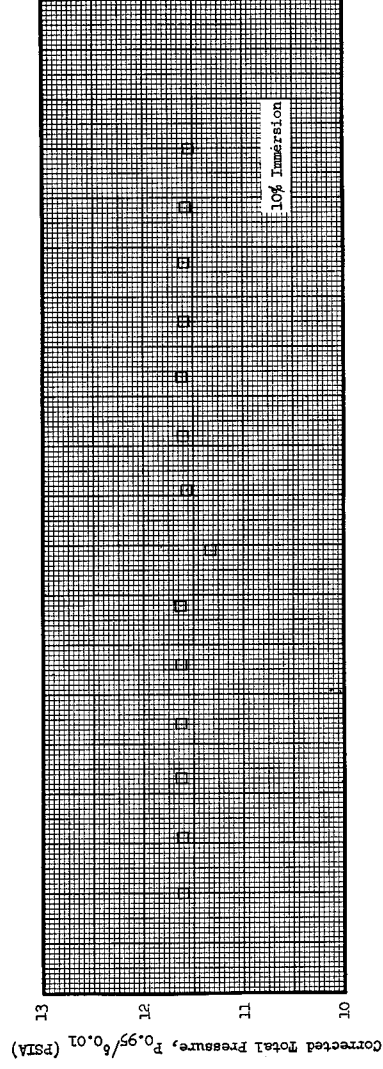


Figure 27 (b). Task II Circumferential Distortion Inlet Guide Vane Wake Survey at 100% Speed, Maximum Flow; Entering Distorted Flow Region.

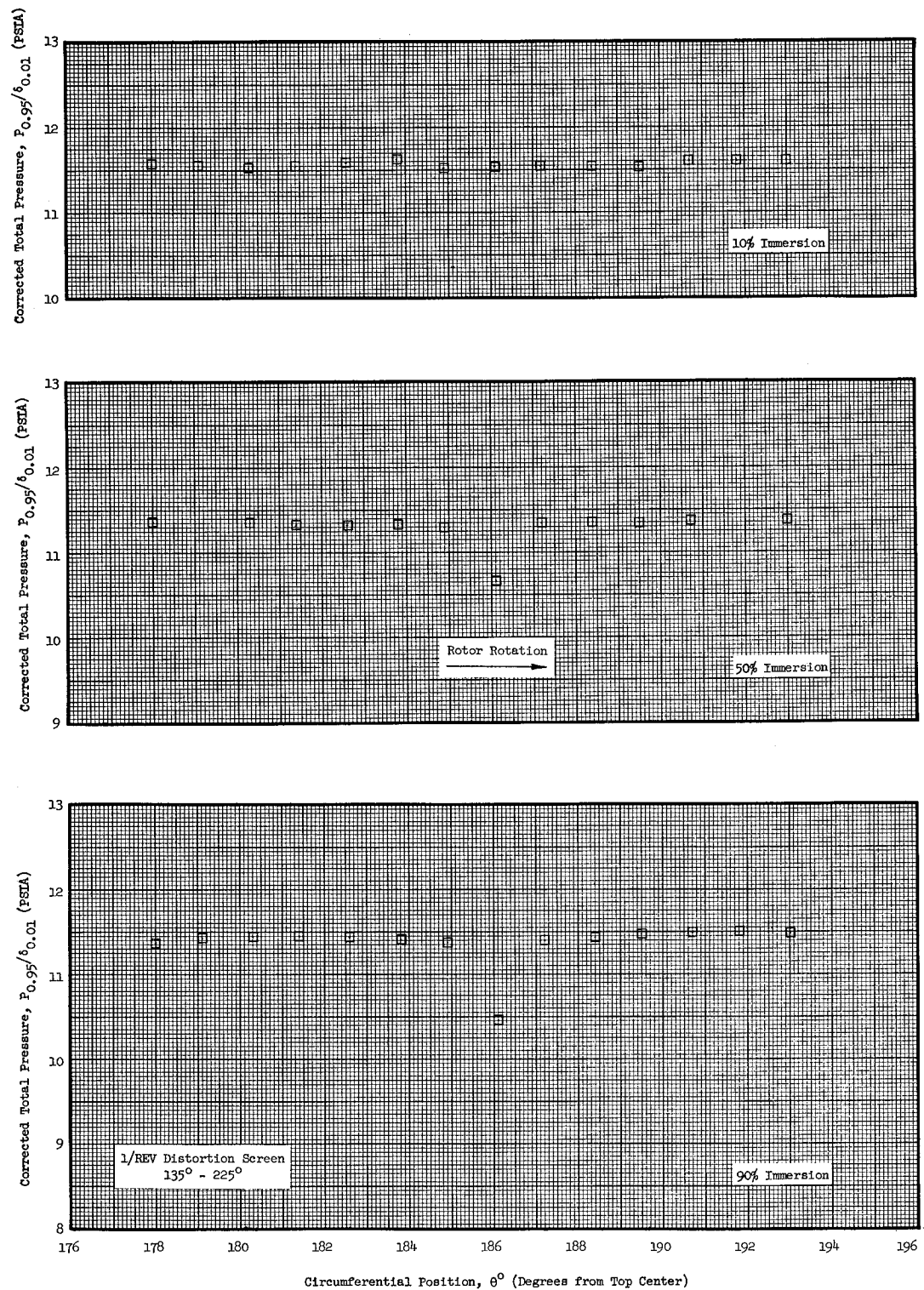


Figure 27 (c). Task II Circumferential Distortion Inlet Guide Vane Wake Survey at 100% Speed, Maximum Flow; Distorted Flow Region.

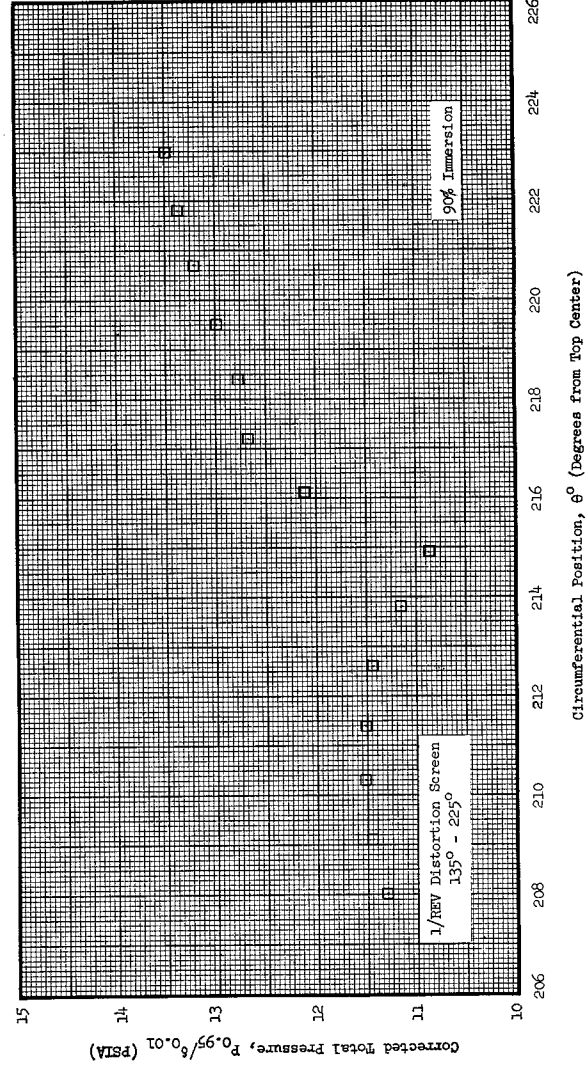
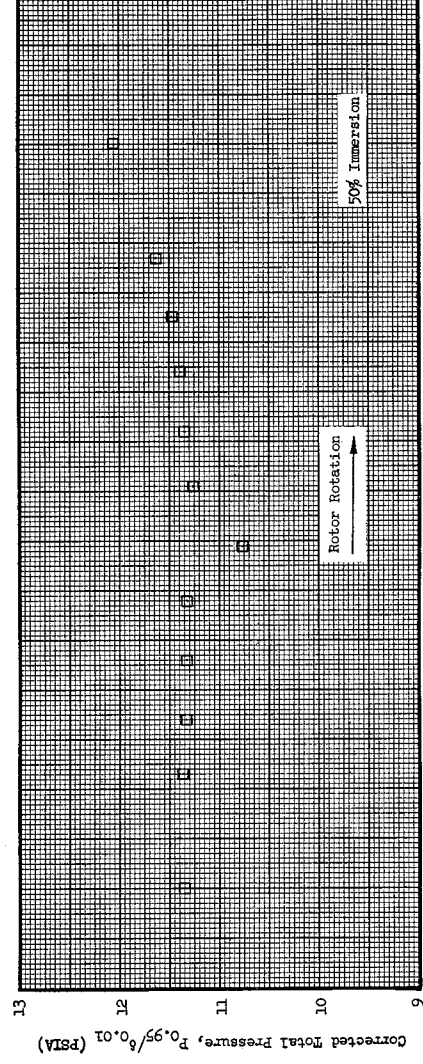
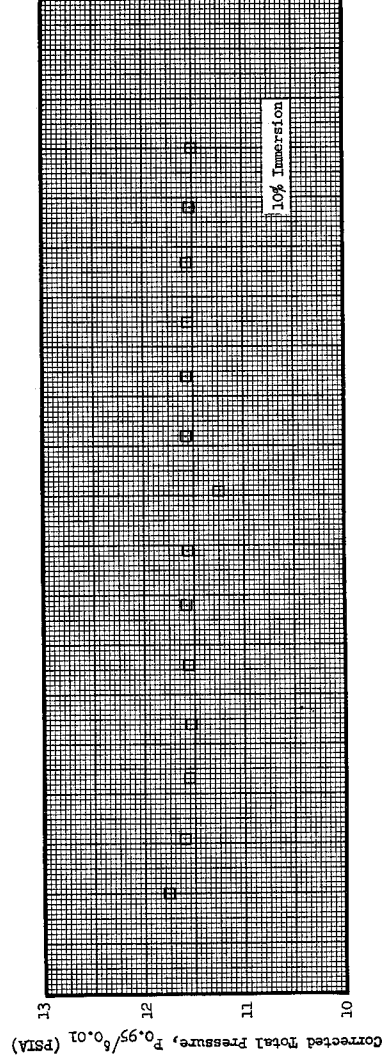


Figure 27 (d). Task II Circumferential Distortion Inlet Guide Vane Wake Survey at 100% Speed, Maximum Flow; Leaving Distorted Flow Region.